Advancements in Bacterial Diseases Affecting Channel Catfish (*Ictalurus punctatus*): Vaccine Development, Virulence Assessments, and Coinfection Interactions

By

Courtney Elizabeth Harrison

A dissertation submitted to the Graduate Faculty of
Auburn University
in partial fulfillment of the
requirements for the Degree of
Doctor of Philosophy

Auburn, Alabama
December 12, 2026

Keywords: Vaccination, channel catfish, *Flavobacterium covae*, yellow-pigmented bacteria, co-culture

Approved by

Timothy J. Bruce, Chair, Assistant Professor, School of Fisheries, Aquaculture and Aquatic Sciences
Mark R. Liles, Professor, Department of Biological Sciences
Anita M. Kelly, Extension Professor, School of Fisheries, Aquaculture and Aquatic Sciences
Benjamin R. LaFrentz, Research Molecular Biologist, USDA-ARS Aquatic Animal Health Research Unit
Matt J. Griffin, Research Professor, Pathobiology and Population Medicine, Aquaculture Research and Diagnostic Laboratory

Abstract

Columnaris disease, caused by columnaris-causing bacteria (CCB), is a constant threat to farmed fish species. Several types of columnaris vaccines have shown various levels of protection in multiple fish species; however, it is hypothesized that due to CCB host associations, development of a vaccine that targets specific host species could elicit a strong immune response and provide protection. The first study of this dissertation investigated rifampicin-resistant CCB strains as potential live-attenuated vaccine candidates in channel catfish (*Ictalurus punctatus*) and Nile tilapia (*Oreochromis niloticus*). Five *Flavobacterium covae* (ALG-00-530, FBCC-CC-12K, ML-17-22A, IPRS-15-49, and ALG-15-231) and two *Flavobacterium oreochromis* (Costa Rica 04-02-TN^T and R18-27) mutant strains demonstrated attenuation in channel catfish and Nile tilapia, respectively. Comparative genomic analysis of parent and mutant strains predicted deleterious *rpoB* mutations within 8/10 rifampicin-resistant mutant genomes. Other mutations affecting gene transcription, nutrient acquisition, and essential physiological pathways were also predicted as deleterious, suggesting attenuation is multifactorial. The second study assessed the efficacy of the five *F. covae* mutant isolates generated from the first study as live-attenuated vaccines in channel catfish. The vaccines were administered to fish via a static immersion for 30 minutes, then the fish were maintained for up to 8 weeks post-vaccination. Fish were then exposed to corresponding virulent parent strains and cumulative percent mortality and relative percent survival was determined. Two mutant strains (FBCC-CC-12K and ALG-15-231), exhibited variable protection; however,

serum IgM antibody titers did not correlate with protection observed in channel catfish, and vaccinated fish antibody titers were comparable to sham-vaccinated fish. Protein profiles revealed conserved antigenic patterns between the parent and mutant strains. This study demonstrated protective efficacy of *F. covae* mutants is strain-specific and trial dependent, with *F. covae* FBCC-CC-12K and ALG-15-231 mutants warranting further investigation and optimization as live-attenuated vaccines. The third study involved virulence screening of yellow-pigmented bacteria recovered from diseased farmed catfish. Whole genome sequencing of isolates revealed the identities of one *Chryseobacterium gleum*, four *C. mucoviscodosis,* one *C. cucumeris*, one *Empedobacter brevis*, and one *Flavobacterium saliperosum*. The *E. brevis* isolate demonstrated high mortality and clinical signs of disease following intraperitoneal injection in channel catfish. Koch's postulates were fulfilled in a replicated study, and the median lethal dose was estimated. A co-infection study with *E. brevis* and *F. covae* demonstrated significant mortality in the co-infection group compared to the single infection group of *F. covae*, but no significant difference in mortality between the co-infection group and single infection of *E. brevis*. This study demonstrated the exacerbated effect on mortality and disease following co-infection with *E. brevis* and *F. covae*. The final study assessed growth and proteomic responses of *F. covae* (Fc), virulent *Aeromonas hydrophila* (vAh), and *Edwardsiella ictaluri* (Ei) in co-culture. Growth metrics and secreted extracellular protein responses were assessed for three bacterial co-culture combinations. Growth metric analysis revealed cooperative growth in co-culture of Fc + Ei, while competitive growth was observed in co-cultures of vAh + Ei and Fc + vAh. Differential abundance of virulence-associated secreted proteins

provided insight into species-specific alterations in co-culture. Collectively, these studies advance the understanding of host-specific live-attenuated vaccine development against columnaris disease, identify other yellow-pigmented bacterial pathogens affecting farmed catfish, and provide insight to mechanisms that influence bacterial virulence during co-infection.

Artificial Intelligence (AI) Use Disclosure Statement

In the preparation of this dissertation, OpenAI ChatGPT and Codex were used as assistance tools during the development and refinement of R-based workflows used in Chapter V. Specifically, these tools assisted with development and troubleshooting of R code for analysis of bacterial co-culture growth metrics and performing statistical analyses, including two-way analysis of variance (ANOVA) and post hoc multiple comparisons. For the differential protein abundance, AI-assisted coding was used for development, troubleshooting, and refinement of workflow and data processing using the limma package. AI tools also assisted with development and troubleshooting of code used to conduct identification of virulence-associated proteins through sequence comparison with the Virulence Factor Database (VFDB) using Set A reference sequences and NCBI protein BLAST. Virulence-associated proteins were identified based on the resulting sequence comparison and predefined criteria, which were reviewed and evaluated by the author. AI tools were used with the technical implementation of these workflows and were not used as scientific interpretation or evaluation of data. The selection of statistical methods, data input, parameters and statistical criteria, execution, validation, interpretation of results, and conclusions presented in this dissertation were performed and reviewed by the author.

Digital Accessibility Use Disclosure Statement

In the preparation of this dissertation, Microsoft Word Accessibility Checker and Adobe Acrobat Pro Accessibility Checker were used to ensure this document complies with federal accessibility requirements. The author acknowledges full responsibility for the intellectual content of this work and has made a good faith effort to comply with digital accessibility requirements in publishing, wherein the nature of the content does not signify change in order to do so. Furthermore, all content has been reviewed and revised to meet these requirements prior to publication.

Acknowledgements

First, I would like to thank my advisor, Dr. Timothy Bruce, for his guidance, support, mentorship, patience, resources, and knowledge he has shared with me throughout my doctoral experience. I am extremely grateful for the opportunities he has provided for me. I would also like to thank the members of my graduate committee, including Dr. Benjamin LaFrentz, Dr. Anita Kelly, Dr. Mark Liles, and Dr. Matt Griffin, for their time, resources, encouragement, guidance, and support during my training.

A special thank you to Dr. Priscilla Barger for serving as the university reader for my dissertation. Also, Matt Paulson for helping me with the acquisition and transfer of channel catfish and Nile tilapia needed to perform experiments. Also, I would like to thank Dr. Cailtin Older, Dr. Melissa Boersma, Dr. Thomas Loch, Dr. Esteban Soto, and Dr. Eric Peatman for their research collaborations and guidance.

I would like to thank current and past members of the Bruce Fish Health Laboratory, including Allison Wise-Addison, Guillaume Cacot, Dr. Uthpala Padeniya, Dr. Abdulmalik Oladipupo, Ishini Mudalige, Aigeal Adeyemi, Dr. Crystal Lode, Dr. Krishna Singa, Dr. Daniela Carozza, Savannah Saegar, Syndey Staines, Gavin Southern, Brent Vuglar, Dr. Yoonhang Lee, Chandler Schnieder, Owen Ledford, Jamison Semla, Marie Tan, Feven Bekele, and John Williamson, for their support, encouragement, and friendship.

A heartfelt thank you to my family, Joe Harrison, Tammy Burton, Samantha, Matthew, and Magnolia Dolan, Sue Pauley, Jeff Burton, Trevor Burton, and Kim Vickers, for their unwavering support, encouragement, and love. Also, thank you to my very best

companions, Roby, Phoebe, and Sophie, for the countless hours supervising my progress and for endless cuddles.

Table of Contents

List of Tables

List of Figures

List of Abbreviations

μ	Instantaneous growth rate
μg	Microgram
μm	Micrometer
μ_{max}	Maximum specific growth rate
°C	Degree Celsius
A	Adenine
Å	Ångström
AGC	Automatic gain control
Ala	Alanine
ANI	Average nucleotide identity
ANOVA	Analysis of variance
APHIS	Animal and Plant Health Inspection Service
Arg	Arginine
ARS	Agricultural Research Service
Asn	Asparagine
Asp	Aspartic acid
ATCC	American Type Culture Collection
AUC	Area under the curve
BLASTN	Basic Local Alignment Search Tool, Nucleotide
bp	Base pairs
BUSCO	Benchmarking Universal Single-Copy Orthologs
BZ	Brazil
C	Cytosine
C.I.	Confidence interval
CA	California
$CaCl_2 \cdot 2H_2O$	Calcium chloride dihydrate

$CaCO_3$	Calcium carbonate
CCB	Columnaris-causing bacteria
CFU	Colony-forming unit
cm	Centimeter
Co	Co-culture
CPM	Cumulative percent mortality
Cys	Cysteine
d	Days
dDDH	Digital DNA-DNA hybridization
DEG	Differentially expressed genes
del	Deletion
df	Degrees of freedom
DI	Deionized
DNA	Deoxyribonucleic acid
DSMZ	Leibniz Institute DSMZ
DTT	Dithiothreitol
Ei	*Edwardsiella ictalrui*
ELISA	Enzyme-linked immunosorbent assay
ErpA	Essential respiratory protein A
FA	Formic acid
Fc	Flavobacterium covae
FCA	Freund's Complete Adjuvant
FDR	False discovery rate
g	Gravitational force
G	Guanine
g	Grams
GAG	Glycosaminoglycan
gDNA	Genomic DNA
GGDC	Genome-to-Genome Distance Calculator

Gln	Glutamine
Glu	Glutamic acid
Gly	Glycine
gyrB	DNA gyrase subunit B
h	Hour(s)
ha	Hectare
HCD	Higher-energy collisional dissociation
HCl	Hydrochloric acid
HRP	Horseradish peroxidase
HSD	Honestly Significant Difference
HSP	Heat shock protein
i.m.	intramuscular
i.p.	Intraperitoneal
IACUC	Institutional Animal Care and Use Committee
Ig	Immunoglobulin
IgG	Immunoglobulin G
IgM	Immunoglobulin M
IgT	Immunoglobulin T
Il-12b	Interleukin-12 beta
Il-17	Interleukin-17
Il-1b	Interleukin-1 beta
Il-8	Interleukin-8
Ile	Isoleucine
iNOS	Inducible nitric oxide
ins	Insertion
K	Carrying capacity
KCl	Potassium chloride
kDa	Kilodalton
KY	Kentucky

L	Liter
LD_{50}	Median lethal dose
Leu	Leucine
Lpp	Lipoprotein
LPS	Lipopolysaccharide
Lys	Lysine
m/z	Mass-to-charge
MA	Massachusetts
MAFFT	Multiple Alignment using Fast Fourier Transform
MALDI-TOF	Matrix-assisted laser desorption/ionization time-of-flight
Mb	Megabase
MD	Maryland
Met	Methionine
mg	Milligram
$MgCl_2 \cdot 6H_2O$	Magnesium chloride hexahydrate
MHC	Major histocompatibility
mL	Milliliter
MLPA	Multilocus phylogenetic analysis
mm	Millimeter
mM	Millimolar
MN	Minnesota
MreC	Rod-determining shape protein
MSA	Modified Shieh agar
MSB	Modified Shieh broth
MWCO	Molecular weight cutoff
NaCl	Sodium chloride
NASS	National Agriculture Statistics Service
NCBI	National Center for Biotechnology Information
NCBI	National Center for Biotechnology Information

NCoR	Nuclear receptor corepressors
NFDM	Non-fat dry milk
ng	Nanogram
nL	Nanoliter
NO	Nitric oxide
OD	Optical density
OMP	Outer membrane protein
ONT	Oxford Nanopore Technologies
PBS	Phosphate-buffered saline
PBST	Phosphate-buffered saline with Tween 20
PCR	Polymerase chain reaction
Phe	Phenylalanine
ppm	Parts per million
PRN	Protocol review number
Pro	Proline
PROVEAN	Protein Variation Effect Analyzer
RAST	Rapid Annotation using Subsystem Technology
RBL	Rhamnose-binding lectin
rDnaK	Recombinant DnaK
RF	Radio frequency
RFLP	Restriction fragment length polymorphism
rpm	Revolutions per minute
rpoB	RNA polymerase beta subunit
RPS	Relative percent survival
RRDR	Rifampicin-resistance determining region
rRNA	Ribosomal ribonucleic acid
RSLC	Rapid separation liquid chromatography
SDS-PAGE	Sodium dodecyl sulfate-polyacrylamide gel electrophoresis
SEM	Standard error of the mean

SEP	Secreted extracellular products
Ser	Serine
SNP	Single nucleotide polymorphism
STD	Standards
t	Test-statistic
T	Thymine
t_{10K}	Time to 10% carrying capacity
t_d	Doubling time
Thr	Threonine
TMB	3,3'5,5'-Tetramethylbenzidine
TYES	Tryptone yeast extract salts agar
TYGS	Type Strain Genome Server
Tyr	Tyrosine
U.S.	United States
USA	United States of America
USDA	United States Department of Agriculture
UV	Ultraviolet
V	Volts
v/v	Volume per volume
vAh	Virulent *Aeromonas hydrophila*
Val	Valine
WA	Washington
YPB	Yellow-pigmented bacteria

Chapter I

An Overview of Yellow-Pigmented Bacteria Affecting Channel Catfish (*Ictalurus punctatus*), with a Focus on Columnaris-Causing Bacteria

Published as: Harrison, C.E., LaFrentz, B.R., Shoemaker, C.A., Lange, M.D., Liles, M.R., Mohammed, H.H., Beck, B.H., Churchman, E.M., Peatman, E. and Bruce, T.J., 2025. An Overview of Vaccine Development Strategies for Columnaris-Causing Bacteria in Cultured Fish. Journal of Fish Diseases, p.e14155. https://doi.org/10.1111/jfd.14155

1.1. Abstract

Yellow-pigmented bacteria, including members of the families *Flavobacteriacea* and *Weeksellaceae*, are associated with disease in wild and cultured fish species. Columnaris disease, caused by columnaris-causing bacteria (CCB), belong to the phylum Bacteroidota and the family *Flavobacteriaceae*. CCB are gram-negative, yellow-pigmented bacteria that are presumed ubiquitous in freshwater habitats. Since the first report of the disease in 1922, growth and survival, pathogenesis, and transmission of these pathogens have been intensely researched, aiding in a greater understanding of host-pathogen interactions. Recent classification of *Flavobacterium columnare* into four distinct species based on genetic similarity, including *F. columnare*, *F. covae*, *F. davisii*, and *F. oreochromis*, along with their host associations is critical to understanding disease dynamics and prevention strategies. Outbreaks of the disease typically follow stressful events where CCB colonise external tissues, such as skin and gill. Additional yellow-

pigmented bacteria including *Chryseobacterium* spp., have been noted as emerging fish pathogens over the past few decades, and have been recovered from co-infections in diseased fish species. These closely-related bacteria can make diagnostics and prevention strategies difficult, as bacterial co-infections can make the primary and secondary bacterial species involved difficult to identify. However, bacterial secretome analysis has provided an avenue for characterization of growth and proteomic responses of bacterial species in co-culture, which in turn, could help identify virulence markers and immune targets for vaccination development. Vaccination against columnaris disease was practiced as early as the 1970's. Since then, many different vaccine types have been under development, including killed, live-attenuated, recombinant, and micro- and nano-particle vaccines. Among the different CCB vaccine types, immune responses and level of protection have been variable. However, some vaccines have been reported to offer moderate-significant protection in some fish species. This review synthesises the current knowledge of CCB taxonomy, genetic diversity, virulence, and immunity in various aquaculture species, with the goal of identifying knowledge gaps to be addressed for future CCB vaccine development. The development of an efficacious columnaris vaccine remains a challenge, with promising results in the laboratory that have yet to be reflected under production settings. This highlights the need for improved strategies tailored to the species of CCB most appropriate for the target host species.

1.2. Introduction

1.2.1. Historical Perspectives of Taxonomy and Genetic Diversity

Columnaris disease was first described by Davis (1922) and the etiological agent was reported as a motile (sinuous bending), rod-shaped bacterium with a tendency to form 'column-like masses'. This led to an original designation as *Bacillus columnaris*. Although large numbers of bacteria were visible in lesions of infected fish, Davis (1922) was unable to isolate the bacterium at the time. Ordal and Rucker (1944) first isolated the bacterium from a disease outbreak and classified it as belonging to the order *Myxobacteria* and renamed it *Chondrococcus columnaris*. Shortly thereafter, Garnjobst (1945) renamed the species *Cytophaga columnaris* due its inability to produce microcysts under pure culture conditions, and the species was reassigned to the genus *Flexibacter* as *Flexibacter columnaris* in 1974 (Leadbetter 1974).

Research on the genetic diversity of these bacteria began in the late 1980's with three defined groups of isolates described based on DNA homology (Song et al. 1988). In 1989, the species was officially described and validated as *Flexibacter columnaris* (Bernardet and Grimont 1989), and the deoxyribonucleic acid (DNA) homologies of isolates examined ranged from 76% to 100%, evidencing of genetic diversity. In 1996, the first 16S ribosomal ribonucleic acid (rRNA) gene sequences were obtained and analysis revealed intraspecific diversity among strains (Toyama et al. 1996). Based on DNA-rRNA hybridization, protein, and fatty acid profiling, the bacterium was re-classified as *Flavobacterium columnare* (Bernardet et al. 1996).

Restriction fragment length polymorphism (RFLP) analysis of 16S rRNA gene sequences and DNA–DNA hybridization led to the division of *F. columnare* into three genomovars, namely I, II, and III (Triyanto and Wakabayashi 1999). Genomovars are groups of bacterial isolates within a species that are phenotypically similar yet genotypically different (Rosselló et al. 1991; Ursing et al. 1995). The authors suggested the three genomovars may represent different species, although the isolates were phenotypically and biochemically similar (Triyanto and Wakabayashi 1999). RFLP was used to identify additional genomovars, designated as I-B and II-B (Olivares-Fuster et al. 2007).

Due to the widespread use, but lack of a formal protocol for genotyping *F. columnare* with RFLP, LaFrentz et al. (2014) standardised the assay. Through this research, the authors discovered the isolates designated as genomovar I-B by Olivares-Fuster et al. (2007) were indeed genomovar III isolates, and they formally described five *F. columnare* genomovars, I, II, II-B, III, and I/II based on restriction patterns (LaFrentz et al. 2014). LaFrentz et al. (2016) discovered that the primers used for amplification of the 16S rRNA gene for RFLP failed to generate amplicons for some isolates; therefore, a new reverse primer was generated which allowed for all *F. columnare* isolates to be assigned to genomovar. García et al. (2018) subsequently described a sixth genomovar, II-A.

From 2012 to 2016, when whole genome sequencing was beginning to be applied to fish pathogens, several genomes were published providing strong evidence for the potential of more than one bacterial species within *F. columnare*. In 2012, the first genome of *F. columnare* (American Type Culture Collection, ATCC 49512; genomovar I) was published by Tekedar et al. (2012) and in 2016 the first genome of a genomovar II isolate

(94–081) was sequenced (Kumru et al. 2016). These authors reported a two-way average nucleotide identity (ANI) of 90.71% between the genomovar I and II genomes, suggesting they may be classified as different species (Kumru et al. 2017). In 2018, the first genome of a genomovar III isolate was published and ANI's between this isolate and the genomovar I and II isolates also indicated the likelihood of the three genomovars representing different species (Criscuolo et al. 2018).

While these genome sequencing efforts were underway, two laboratories were simultaneously examining the genetic diversity of *F. columnare* using either comparative genome analyses (Kayansamruaj et al. 2017) or multilocus phylogenetic analysis (MLPA) (LaFrentz et al. 2018). Both research projects focused on determining if genomovar assignment reflected whole genome genetic diversity using higher resolution methods, and both reached similar conclusions. Kayansamruaj et al. (2017) revealed three or four clades of isolates depending on the locus used, and they suggested the need for amending the *F. columnare* species designation based on ANI values obtained from genome comparisons. Likewise, LaFrentz et al. (2018) characterised fifty *F. columnare* isolates from diverse geographic locations and fish hosts using MLPA. Results categorised isolates into four distinct genetic groups; however, the relationships between the previously described genomovars and newly characterised genetic groups did not accurately reflect the genetic diversity, as three of the genetic groups contained members from more than one genomovar. LaFrentz et al. (2018) also identified biological associations related to the genetic groups and proposed that isolates of *F. columnare* be assigned to genetic group rather than genomovar to facilitate a standard nomenclature.

The cumulative body of knowledge generated since the late 1980's provided a solid foundation of research to determine whether the four genetic groups of *F. columnare* were indeed unique species of bacteria. LaFrentz et al. (2022) conducted a polyphasic approach following the guidelines of Bernardet et al. (2002). The results demonstrated that although phenotypically similar, the four genetic groups of *F. columnare* exhibited sufficient differences in chemotaxonomic traits, matrix-assisted laser desorption/ionisation time-of-flight mass spectrometry (MALDI-TOF) peaks, and ANI/digital DNA–DNA hybridization calculations to justify reclassification. Isolates belonging to genetic group 1 retained the name *F. columnare*, while isolates of genetic groups 2, 3, and 4 were described as *F. covae*, *F. davisii*, and *F. oreochromis*, respectively (LaFrentz et al. 2022). This reclassification has been validated (Oren and Garrity 2022), and the term "columnaris-causing bacteria" (CCB) was coined by LaFrentz et al. (2024) to represent these four species that cause columnaris disease (Figure 1).

1.2.2. Authors Preface on Nomenclature

Taxonomic changes create a challenging task for authors when preparing review articles, because the species of CCB reported in publications prior to 2022 may not be fully known. For the purposes of this review, the authors use the umbrella term CCB to collectively refer to the four species. As the literature is discussed, the authors will use the scientific name as published and provide the new species classification if known.

Although past research may be unclear in terms of which species of bacteria were used, the fish health community has an opportunity for a clear future by identifying all

isolates of CCB to species in current and future research, and methods to do so have been previously published (LaFrentz et al. 2019; LaFrentz et al. 2022). Given the biology associated with the four species of CCB, the authors believe that this will advance and improve research to define host-pathogen-environment relationships, epidemiology, and guide efforts to develop effective control and prevention measures for columnaris disease.

1.2.3. Columnaris-Causing Bacteria

CCB are cultivated under laboratory conditions on low-nutrient media, such as cytophaga agar (Anacker and Ordal 1959), tryptone yeast extract salts agar (TYES; Holt et al. 1989), *F. columnare* growth medium (Farmer 2004), Hsu-Shotts medium (Bullock 1986), or modified Shieh medium (LaFrentz and Klesius 2009). The optimal incubation temperature for CCB ranges from 25°C to 30°C, wherein small colonies will be visible within 24 h, then grow to 3–4 mm in diameter after 48 h (Starliper and Schill 2011). Pale yellow colonies with rhizoid morphology that adhere to agar are characteristic of CCB (Starliper and Schill 2011). Other colony morphologies may occur, including round and smooth colonies (LaFrentz et al. 2012). When gram-stained, CCB are observed to be long and thin gram-negative bacilli (i.e., rods) between 0.3 and 0.5 mm in width and up to 14 mm in length (LaFrentz et al. 2022). Wet mount preparations of infected gill and skin tissue often reveal bacterial cells that form 'haystacks' or column-like masses.

These bacteria are believed to be ubiquitous within freshwater environments and have been observed to maintain viability within water for extended periods depending on the water chemistry (LaFrentz et al. 2012). Fijan (1969) demonstrated survival of *C. columnaris* (species unknown) in water with > 50 mg/L of $CaCO_3$ and high loads of organic

matter. *Flexibacter columnaris* (species unknown) was demonstrated to exhibit enhanced viability in formulated water containing specific concentrations of NaCl, KCl, $CaCl_2 \cdot 2H_2O$, and $MgCl_2 \cdot 6H_2O$, similar to its survival in tap water, compared to water formulations of the cations in distilled water (Chowdhury and Wakabayashi 1988). Nonetheless, *F. columnare* has demonstrated survival in distilled water for over five months (Kunttu et al. 2012), and up to 2 years in lake water (Kunttu 2010).

1.2.4. Columnaris Disease

Columnaris disease was first described by Davis (1922) between the summers of 1917 and 1918, when fish at the U.S. Fisheries Biological Station in Fairport, Iowa, started dying of an apparent bacterial infection. Davis (1922) described initial dirty-white or yellow lesions on the body of infected fish that eventually lead to mortality 24–72 h after the lesions were first observed. The disease appeared to be a consequence of injuries sustained by the fish where the infection began at the site of the injury. The disease has been reported in fish species on every continent except for Antarctica and affects many wild and cultured freshwater fish species worldwide. Fish of all ages may be susceptible, but infection is more prevalent in young fish. Columnaris disease was first reported in warmwater fish species from the Mississippi River (USA) including bluegill (*Lepomis macrochirus*), buffalofish (*Ictiobus bubalus* and *I. cyprinellus*), bullheads (*Ameiurus nebulosus* and *A. melas*), largemouth bass (*Micropterus salmoides*), carp (*Cyprinus carpio*), channel catfish (*Ictalurus punctatus*), crappies (*Pomoxis annularis* and *P. spheroids*), orangespotted sunfish (*L. humilis*), warmouth (*Chaenobryttus gulosus*), and

white bass (*Roccus chrysops*; Davis 1922). Ordal and Rucker (1944) isolated the pathogenic bacterium in pure culture following an epizootic in sockeye salmon (*Oncorhynchus nerka*) fingerlings in Washington (USA). The etiological agents of columnaris disease have also been recovered from body surface lesions and internal organs of adult Chinook salmon (*O. tshawytscha*), steelhead trout (*O. mykiss*), northern pikeminnow (*Ptychocheilus oregonensis*), suckers (*Catostomus*sp.), peamouth (*Mylocheilus caurinus*), and whitefish (*Prosopium* spp.), collected from the Columbia River of the Pacific Northwest (USA; Fish and Rucker 1945). It is generally assumed that most if not all freshwater fish are susceptible.

Columnaris disease outbreaks typically occur when water temperatures rise above 25°C and if fish become stressed due to handling, overcrowding, or reduced dissolved oxygen (Starliper and Schill 2011). However, outbreaks also occur at cooler temperatures (~ 15°C) in salmonid species. Other predisposing environmental factors contributing to pathogenesis include physical injury and poor water quality (Plumb and Hanson 2010). Abrasions on the skin/mucosa and external body injuries may predispose fish to CCB attachment and colonisation. The bacteria contain mucopolysaccharide and galactosamine on the surface, which aid in attachment and initial establishment of infection on the body surface of fish (Johnson and Chilton 1966; Thune et al. 1993). Another primary site of infection with CCB is gill tissues. Infection affinity for gill tissues begins at the tips of the lamellae and proceeds inward, with subsequent necrosis of the gill epithelium (Starliper and Schill 2011). The attachment of CCB on the body surface and fish gills may result in epithelial tissue damage, ulcerative skin lesions, and gill necrosis, which

can lead to problems with osmoregulation and decreased respiration that contribute to high morbidity and mortality that commonly reaches 60%–90% (LaFrentz et al. 2012; Starliper and Schill 2011).

CCB typically affect the external surfaces of fish, like the skin, mouth, gills, and fins (Declercq et al. 2013). Epidemics of columnaris disease may present in the form of either acute, sub-acute, or chronic (LaFrentz et al. 2012), where clinical signs are not typically present during acute infections. Diseased fish may exhibit lethargy and loss of appetite and may hang at the surface of the water column. Gross signs of the disease include depigmented skin lesions along the dorsal aspect of fish (i.e., saddleback), necrotic gill tissues, frayed fins, and greyish-white or yellow cutaneous foci on the skin, head, and body of infected fish (LaFrentz et al. 2012). It appears that CCB manifest similar clinical signs of disease regardless of host and bacterial species.

1.2.5. Pathogenesis

Because typical niduses for CCB are external tissues such as skin and gills, infected fish typically display external signs of disease and little to no internal pathology (Wakabayashi 1991). Extracellular proteases produced by CCB contribute to virulence (Johnson and Chilton 1966). Griffin (1991) characterised an enzyme of *C. columnaris* (species unknown) that degrades chondroitin A and C and hyaluronic acid, which is the complex polysaccharide of connective tissue. When tested in rainbow trout in vivo, chondroitin lyase activity in strains of *F. columnare* was significantly related to virulence (Suomalainen, Tiirola, et al. 2006). In contrast, a recent study showed that

chondroitin sulfate lyases of *F. columnare* are not required for virulence in rainbow trout and larval zebrafish (Thunes et al. 2022).

Other virulence factors, including the Type IX secretion system (T9SS), have been identified in CCB and contribute to pathogenicity (Li et al. 2017; Thunes et al. 2022). Recent experiments by Thunes et al. (2023) identified the role of secreted peptidases in *F. columnare* MS-FC-2 virulence via the construction of mutants lacking peptidase-encoding genes. Abdelhamed et al. (2021) reported that the denitrification genes *nasA*, *nirS*, *norB*, and *nosZ* of *F. columnare* 94–081 (now *F. covae*) contribute to growth in anaerobic conditions, and *nirS* is involved in virulence.

A positive correlation between the virulence of *F. columnare* (species unknown) and adherence to black molly (*Poecilia sphenops*) gill tissue was demonstrated, suggesting that adhesion to the gill tissue is important for pathogenesis (Decostere et al. 1999). The chemotactic responses of *F. columnare* genomovar I (some genomovar I isolates were incorrectly typed and isolates used were *F. columnare* and *F. davisii*) and genomovar II (now *F. covae*) isolates to channel catfish mucus were examined by the capillary tube method. Genomovar II isolates demonstrated higher chemotactic indices than genomovar I isolates, and such responses were variable depending on the concentration of chemoattractant(s) of individual fish mucus (Klesius et al. 2008). Further work by this group developed a culture-independent method for quantifying chemotaxis (LaFrentz and Klesius 2009), and the use of the method identified an important role of carbohydrate-binding receptors in chemotaxis (Klesius et al. 2010). Later, Peatman et al. (2013) reported that infection with *F. columnare* LV-359-01 (now *F. covae*) induced basal polarisation of

mucosal responses in channel catfish with differing susceptibility, which impacted the disease outcome.

1.2.6. Transmission

Transmission of CCB is horizontal through direct contact with infected fish or exposure to CCB within a water supply (Starliper and Schill 2011). Horizontal transmission of *F. columnare* ARS-1 (now *F. davisii*) was confirmed when channel catfish were challenged via intramuscular (i.m.) injection or immersion, resulting in infection of naïve channel catfish cohabitated in the same tank (Welker et al. 2005). This method of transmission has also been observed in wild salmon stocks, where feral *Catostomus* spp. residing in the Columbia River are thought to transmit *F. columnaris* (species unknown) to returning salmon (Wakabayashi 1991). Dead fish play an important role in the transmission and persistence of CCB in source water. Kunttu et al. (2009) demonstrated that transmission of *F. columnare* to healthy rainbow trout from dead rainbow trout was more efficient than from infected living fish, and the dead fish shed CCB at higher rates into water than the living fish. Similar results were observed with tilapia (Shoemaker and LaFrentz 2015). Furthermore, Kunttu et al. (2009) suggested that saprophytism, the process by which bacteria survive on dead or decaying organic matter, may be an important method of survival and transmission, as there is no cost to host death for CCB.

1.3. Virulence and Immunity to Columnaris Infection

1.3.1. Virulence

Virulence differences in isolates of CCB have been extensively researched for several decades. One of the first observations was a difference in virulence among strains of *C. columnaris* (species unknown). One strain of low virulence was shown to cause mass mortality under high water temperatures; however, infection was slow, and tissue damage occurred before observing mortalities (Rucker et al. 1954). Contrarily, another highly virulent *C. columnaris* strain (species unknown) produced extremely high mortality, reaching 100% within 12–24 h, and death ensued before any external disease manifestations appeared (Rucker et al. 1954). Likewise, and based on agglutinin-absorption tests and serological typing, strains of *C. columnaris* (species unknown) that were more virulent than others were not antigenically identical, which led to *C. columnaris* strains (species unknown) being classified into four serological groups, including Groups I, II, III, and IV (Anacker and Ordal 1959).

Random amplified polymorphic DNA (RAPD) was used to identify virulence markers in a collection of *F. columnare* isolates (species unknown) recovered from 6 different fish species. Results of RAPD segregated isolates based on cell size and fish species of origin; however, results of virulence studies suggested that virulence is strain-specific and variable (Thomas-Jinu and Goodwin 2004). Similarly, 30 Finnish *F. columnare* isolates and the *F. columnare* type strain NCIMB 2248^{T} were characterised using molecular methods (Suomalainen, Kunttu, et al. 2006) and were found to be affiliated with genomovar I, yet the isolates were subclassified into eight different groups using automated ribosomal

intergenic spacer analysis (ARISA). A closer look at virulence-related factors among the eight genetic groups revealed that chondroitin AC lyase was significantly associated with virulence, and mortality was increased at water temperatures of 25°C compared to 20°C in rainbow trout (Suomalainen, Tiirola, et al. 2005).

A pulsed-field gel electrophoresis (PFGE) approach was used to characterise more than 30 channel catfish *F. columnare* isolates (species unknown), and the results indicated two major groups (A and B) that exhibited virulence differences (Soto, et al. 2008). Isolates contained in group A caused significantly higher mortality than group B isolates when channel catfish were challenged by immersion. Later, Shoemaker et al. (2008) used single strand polymorphism analysis (SSCP) to assign channel catfish CCB isolates to genomovar and determined genomovar II isolates (now *F. covae*) were significantly more virulent in channel catfish fry than genomovar I isolates (some genomovar I isolates were incorrectly typed and isolates used were *F. columnare* and *F. davisii*). Shoemaker and LaFrentz (2015) reported no association between virulence and genomovar following immersion challenge of hybrid tilapia, *Oreochromis niloticus* (L.) *O. aureus* (Steindachner) with five genomovars (I, II, II-B, III, and I/II; now *F. columnare*, *F. covae*, and *F. davisii*).

Different species of CCB also display a difference in virulence depending on fish host species. Olivares-Fuster et al. (2007) discovered through multiple genotyping methods that there was a statistically significant association between *F. columnare* genomovar I isolates (now *F. columnare*) and threadfin shad (*Dorosoma pretenense*), and genomovar II *F. columnare* isolates (now *F. covae*) were primarily recovered from catfish

species (*Ictalurus* spp.). LaFrentz et al. (2018) revealed through MLPA that *F. columnare* genetic group 3 (now *F. davisii*) is mainly associated with *Ictaluridae* (37.5%) followed by *Cichlidae* (25.0%) and that genetic groups 1 (now *F. columnare*) and 4 (now *F. oreochromis*) are mostly recovered from *Salmonidae* (44.4%) and *Cichlidae* (97.3%), respectively.

Widespread geographic distribution of CCB species has been observed. LaFrentz et al. (2018) reported the recovery of *F. columnare* genetic group 1 isolates (now *F. columnare*) in North and South America, Asia, and Europe; genetic group 2 isolates (now *F. covae*) came primarily from North America and Asia; genetic group 3 isolates (now *F. davisii*) have been recovered in North America, Asia, and Africa; and genetic group 4 isolates (now *F. oreochromis*) have so far only been recovered in South America, Central America, and Asia.

1.3.2. Antigenicity and Immune Response

Early studies of Anacker and Ordal (1959) on *C. columnaris* (species unknown) suggested antigenic diversity among isolates using antiserum generated in rabbits; however, little work has been conducted in this area for CCB. Zhang et al. (2006) examined lipopolysaccharide (LPS) and total protein profiles of various CCB isolates (now *F. columnare*, *F. covae*, and *F. davisii*) using antiserum generated following immunisation of channel catfish. The results demonstrated antigenic variability in the protein profiles of the isolates, as expected due to the underlying genetic diversity. Some conserved protein antigens were identified among the isolates examined using two different antisera

generated against strains belonging to different genomovars I and II (now *F. columnare* and *F. covae*) (Zhang et al. 2006). Lipopolysaccharide (LPS) profiles were also found to differ between the isolates, but cross-reactivity was noted when the different antisera were used in western blot analysis. The results suggest antigenic and serologic diversity among isolates of CCB.

Fujihara and Nakatani (1971) demonstrated that coho salmon orally vaccinated with a heat-inactivated *C. columnaris* isolate (species unknown) produced measurable agglutinating antibody titers. In the same report (Fujihara and Nakatani 1971), rainbow trout survivors of a natural columnaris disease outbreak were shown to have agglutinating titers against *C. columnaris* (species unknown). The authors suggested a protective role of the adaptive immune response because the surviving fish were resistant to subsequent infection. Antigen-sensitised leukocytes were demonstrated in carp following bath immunisation with heat-inactivated whole cells of *F. columnaris* (species unknown; Liewes et al. 1982). Mucosal and humoral antibodies specific to the *F. columnare* type strain (ATCC 23463^{T}) were detected in parenterally immunised 66 g tilapia when Freund's complete adjuvant (FCA) was utilised with sonicated formalin-inactivated cells or whole cells (Grabowski et al. 2004). Cutaneous antibodies were detected in skin explants from channel catfish that were intraperitoneally (i.p.) immunised with live *F. columnare* isolate ARS-1 (now *F. davisii*) cells, although titers were low (Shoemaker, Xu, et al. 2005). Even though skin explant and serum anti-*F. columnare* (now *F. davisii*) ELISA optical density (OD) values were correlated, the authors concluded that the antibody detected was likely produced locally by antibody secreting cells in the skin explants. Western blot analysis

demonstrated catfish immunoglobulin (Ig) heavy chain presence and further showed the explant culture fluid detected specific antigens from sonicated *F. columnare* ARS-1 (now *F. davisii*; Shoemaker, Xu, et al. 2005). A recent study in rainbow trout identified mucosal immunoglobulin (Ig) IgT as the predominant Ig present in gills following infection with *F. columnare* isolate G4 (species unknown) and demonstrated IgT + B accumulation in survivors' suggesting a role in protective immunity (Tongsri et al. 2020). Leal et al. (2010) used oral, immersion, intraperitoneal and intramuscular (i.p. and i.m.) injection delivery of killed vaccines against *F. columnare* isolate BZ-1 (now *F. oreochromis*) in tilapia to evaluate humoral response and efficacy. They demonstrated injection (i.p. and i.m.) delivery elicited a strong antibody response, while oral vaccination did not induce humoral antibodies. Among all delivery methods, protection was not offered against virulent BZ-1 in Nile tilapia fingerlings (Leal et al. 2010). Shelby et al. (2008) generated anti-*F. columnare* (strain ALG-00-530; now *F. covae*) serum by immunising channel catfish with sonicated whole cells or purified LPS preparations. After antibody detection via enzyme-linked immunosorbent assay (ELISA) and western blot, antibody positive whole cell serum or LPS serum was i.p. delivered to juvenile catfish to assess the role of antibody in protection against columnaris disease. Delivery of complement-free (heat-inactivated) positive serum from either whole cell or LPS preparations resulted in increased survival upon i.p. challenge. Due to differing results between fish species and CCB species, much of the work warrants repeating to gain a better understanding of the humoral and cutaneous immune response to specific CCB species.

With the advent of molecular tools, global transcriptome profiling studies of fish tissues are increasing our understanding of the underlying mechanisms of infection and immunity to CCB. Sun et al. (2012) analysed the channel catfish gill transcriptome profile following immersion exposure to a genomovar II isolate of *F. columnare* (now *F. covae*). Results revealed a gene expressing a sugar binding protein called rhamnose-binding lectin (RBL) was highly expressed (> 100-fold). Subsequent research demonstrated saturation of RBLs with their natural binding partners (sugars L-rhamnose or D-galactose) lowered RBL expression and decreased mortality in a dosage-dependent manner following challenge with *F. columnare* (strain LV-359-01, now *F. covae*; Beck et al. 2012). Additionally, expression of RBL in gill tissue was positively correlated with susceptibility to *F. columnare* infection. Taken together, these results suggested that the host lectin mediated *F. columnare* binding to the surface mucosa. Investigators next asked if changes in feeding, as previously tied to susceptibility of catfish to *F. columnare*(strain ARS-1, now *F. davisii*; Shoemaker et al. 2003), impacted RBL expression. A significant upregulation of RBL transcripts was observed in the gill tissue of fasted fish (> 120-fold), and this led to increased mortality. When fasted fish were then fed to satiation, expression levels returned to that of fish continuously fed within 4 h after feeding, indicating a sensitive regulation of expression based on nutritional status. This remarkable co-regulation of a surface lectin by both infection and nutritional status led to a transcriptomic approach to investigate host gene expression in fasted versus fed and in catfish with differing susceptibilities to *F. columnare* isolate LV-359-01, now *F. covae* (Peatman et al. 2013), which indicated that beyond RBL, critical components of the

innate immune response governing host susceptibility to *F. covae* were perturbed by short-term feed deprivation (Peatman et al. 2013; Liu et al. 2013; Li et al. 2014). Both CCB susceptible and fasted (7 day) channel catfish were characterised by altered arginine metabolism pathways, critical for production of inducible nitric oxide synthase (iNOS) and its effector nitric oxide (NO), a potent antimicrobial molecule. iNOS expression, which was found to be extremely abundant in the fed catfish gill, was down-regulated greater than 17-fold following fasting. Evidence of immuno-nutritional co-regulation of lysozyme levels, major histocompatibility complex (MHC) class I/II profiles, mucin secretion, and the chemokine repertoire was also reported (Liu et al. 2013; Li et al. 2014). Tongsri et al. (2020) reported upregulation of Cathelicidin 1 and NOS2 in gill tissue of infected rainbow trout following *F. columnare* (strain G4, species unknown) infection providing further evidence of the importance of innate immune effectors in columnaris disease.

Zhang et al. (2024) used transcriptome profiling to examine the early immune response of catfish gill tissue following immersion exposure to virulent or attenuated *F. covae*. Differential gene expression was noted with 518 differentially expressed genes (DEG) found upon exposure to the attenuated strain versus 321 DEG upon exposure to the virulent strain. Exposure to the virulent strain appeared to suppress the early host response via induction of nuclear receptor corepressors (NCoR) that likely negatively impacted macrophage and T-cell signalling. In fish exposed to attenuated *F. covae*, the response was towards clearing NCoR and thus, induction of CC chemokines, proteases, iNOS, and Il-12b all suggesting an improved early immune response post vaccination (Zhang et al. 2024).

1.4. Other Yellow-Pigmented Bacteria Associated with Fish Disease

1.4.1. Flavobacterium spp.

Other yellow-pigmented bacteria within the Family *Flavobacteriacea* include well-known fish pathogens, including *F. psychrophilum*, the causative agent of bacterial coldwater disease and rainbow trout fry syndrome (Lorenzon, Dalsgaard, and Bernardet, 1997), and *F. branchiophilum*, the causative agent of bacterial gill disease (Bullock, 1990). Together with CCB, these species represent the major *Flavobacterium* spp. affecting both wild and cultured fish stocks worldwide (Shotts an Starliper, 1999; Bernardet and Bowman, 2006; Austin and Austin, 2016).

1.4.2. Chryseobacterium spp.

Within the past few decades, another yellow-pigmented bacterial genus emerged as a fish-associated pathogen, *Chryseobacterium*. The genus *Chryseobacterium* used to be a member of the Family *Flavobacteriacea*; however, due to ongoing readjustments to the structure of *Flavobacteriacea*, *Chryseobacterium* was moved to a new family, *Weeksellaceae* (Vandamme et al., 1994; García-López et al., 2019). Differences in the identity between *Flavobacterium* and *Chryseobacterium* were determined by phenotypic, biochemical, morphological, physiological, fatty acid profiling, and phylogenetic analysis (Bernardet, Nakagawa, and Holmes, 2002; reviewed in Loch and Faisal, 2015).

Just like *Flavobacterium*, *Chryseobacterium* species are ubiquitous in freshwater environments. However, *Chryseobacterium* pathogens in fish are considered opportunistic in nature, and disease and mortality typically follow stressful events such as poor water quality, stocking densities, and handling and transport (Bernardet et al., 2005). Many of the first disease-associated *Chryseobacterium* species were isolated from fish displaying signs of disease. For example, *C. scophthalmum* was isolated from a disease outbreak in farmed turbot (*Scophthalmus maximus*) that displayed gill hyperplasia, hemorrhage, necrosis, and ascites (Mudarris and Austin, 1989). The same authors then exposed juvenile turbot and juvenile rainbow trout to the same *C. scophthalmum* isolate via immersion and intraperitoneal injection and observed similar disease signs, and then bacterium was successfully re-isolated, fulfilling Koch's postulates. *C. piscicola* displayed moderate virulence in Atlantic salmon (Ilardi, Rintamäki, Bernardet, and Avendaño-Herrera, 2010), and *C. chaponense* was recovered from diseased Atlantic salmon from a co-infection with *F. psychrophilum* (Kämpfer, Fallschissel, and Avendaño_Herrera, 2011). Various freshwater fish species were experimentally infected via intraperitoneal injection with novel *Chryseobacterium* spp. isolates recovered from diseased freshwater fish in the Great Lakes region of the United States (Loch and Faisal, 2015). From this study, the authors revealed in a median lethal dose (LD_{50}) challenge using *Chryseobacterium* sp. T28 caused clinical signs of disease, and the LD_{50} exceeded 4.5×10^8 colony-forming units, suggesting its role as a facultative pathogen (Loch and Faisal, 2015). Likewise, undescribed *Chryseobacterium* spp. were recovered from columnaris-like diseased Nile tilapia (Dong et al., 2016). Upon experimental challenge in Nile tilapia fingerlings, the

Chryseobacterium spp. resulted in low virulence (0-20%), wherein the authors suggested they served as opportunistic pathogens (Dong et al., 2016). Recently, *C. siluri* was isolated from the liver of a moribund eastern catfish (*Silurus asotus*; Oh et al., 2020). Although *Chryseobacterium* spp. have been isolated from other fish species showing signs of disease, it is unknown if *Chryseobacterium* spp. have been recovered from channel catfish.

1.4.3. Empedobacter brevis

Another yellow-pigmented bacterium within the Family *Weeksellaceae* is *Empedobacter brevis*. Just like *Chryseobacterium* species, *E. brevis* was originally classified as *Flavobacterium breve* and belonged to the Family *Flavobacteriaceae* (Vandamme et al., 1994; García-López et al., 2019). Information on the pathogenicity of *E. brevis* in fish in scarce; however, *E. brevis* was identified in a mixed bacterial infection from the gills of diseased gilthead sea brim (*Sparus aurata* L.; Kapetanović et al., 2006). In the context of other yellow-pigmented bacteria affecting channel catfish, it is currently unknown if *E. brevis* is pathogenic to channel catfish.

1.5. Bacterial Co-Infections with Yellow-Pigmented Bacteria

1.5.1. Bacterial Co-Infection

Co-infections of microorganisms occur naturally and can sometimes occur with two different species of bacteria. In aquaculture, bacterial co-infections can alter disease progression and mortality; resulting in substantial mortality and exacerbated disease signs

compared to single bacterial pathogen infection (Kotob et al., 2016). Diagnostic investigations of bacterial co-infections can be challenging as it's often hard to distinguish between primary and secondary pathogens; likewise, proper treatment can be limiting for this same reason (Kotob et al., 2016). Bacteria in co-infections can compete with one another for host resources and bacterial loads of either organism can be suppressed or enhanced which can also alter pathogen-host interactions (Kotob et al., 2016). A review of bacterial co-infections in farmed catfish describes the necessity of understanding and identifying organisms involved in such complex interactions for proper diagnosis and treatment (Wise et al., 2021).

1.5.2. Co-Infections Involving Yellow-Pigmented Bacteria

Multiple bacterial co-infections involving *Flavobacterium* spp. and *Chryseobacterium* spp. have been reported or have been experimentally assess in the laboratory under controlled conditions. An investigation of a naturally occurring disease outbreak in striped catfish (*Pangasianodon hypophthalmus*) revealed a co-infection with *F. columnare* and *E. ictaluri* (Dong et al., 2015). Koch's postulates were fulfilled in experimental virulence trials with both bacterial species recovered from the natural disease outbreak (Dong et al., 2015). The virulence trials revealed markedly higher mortality in injection and immersion challenges in the co-infected groups compared to single pathogen infection groups (Dong et al., 2015). Additionally, the same histopathological manifestations were observed during the experimental trials that

mimicked those observed during the naturally occurring infection. This study demonstrated exacerbated mortality following co-infection with *E. ictaluri* and *F. columnare* (Dong et al., 2016). Another investigation of a naturally occurring disease outbreak in reared sturgeons (*Asipenser stellatus* and *Huso huso*) revealed a bacterial co-infection with *C. joostei* and *Aeromonas veronii* via 16S rDNA sequencing and phylogenetic assessment (Gholamhosseini et al., 2018). Although pathogenicity was not experimentally demonstrated in the laboratory, the naturally infected sturgeon species exhibited clinical signs of disease, such as unbalanced swimming, external wounds and petechia, pectoral fin rot, and internal hemorrhage (Gholamhosseini et al., 2018). Bruce et al., (2020) demonstrated similar disease signs observed in juvenile rainbow trout (*Oncorhynchus mykiss*) intramuscularly injected with either *Flavobacterium* or *Chryseobacterium* spp. isolates. Trout displayed focally extensive hemorrhaging on the dorsal aspect, unilateral exophthalmia, and ecchymotic hemorrhage and severe liver pallor following injection with *Flavobacterium* spp. and *Chryseobacterium* spp. isolates (Bruce et al., 2020). This underlines the challenges and complexity associated with closely related bacterial co-infections involving different bacterial species that can elicit the same disease signs.

1.5.3. Co-Infections Involving Yellow-Pigmented Bacteria in Channel Catfish

Wise et al. (2021) provided a diagnostic summary of bacterial co-infections in the Alabama and Mississippi catfish industries from 2016-2020. Within the summary, the number of disease diagnostic cases, bacterial species, and catfish species (channel catfish, hybrid catfish, and blue catfish) was indicated. Interestingly, 688/5,450 (12.6%) of

diagnostic cases between Alabama and Mississippi channel catfish involved a co-infection with *F. columnare* (likely *F. covae* based on our current knowledge; Wise et al. 2021; LaFrentz et al., 2024). This review highlights the prevalence of bacterial co-infections involving yellow-pigmented bacteria within the U.S. channel catfish industry.

In vivo bacterial co-infection disease dynamics in juvenile channel catfish were also investigated by the same authors (Wise et al., 2023; Wise et al., 2025). A co-infection with *F. covae* and *E. ictaluri* administered by immersion to channel catfish demonstrated significantly higher CPM in co-infection and *E. ictaluri* single-pathogen groups compared to *F. covae* single-pathogen groups, indicating the observed high mortality in co-infection groups was due to *E. ictaluri* (Wise et al., 2023). In another experimental bacterial co-infection study with *F. covae* and virulent *Aeromonas hydrophila*, significantly higher CPM was observed in juvenile channel catfish exposed to co-infection of *F. covae* and virulent *A. hydrophila*, compared to single-pathogen exposure of either bacteria (Wise et al., 2025). Disease signs were also exacerbated in co-infection groups compared to single-pathogen groups (Wise et al., 2025). Collectively, these findings highlight the prevalence and complex disease dynamics of bacterial co-infections within the U.S. channel catfish industry.

1.5.4. In vitro Approaches to Studying Bacterial Co-Culture Interactions

In vivo experimental studies of bacterial co-infections in channel catfish have provided essential information on host-pathogen interactions, mortality trends, signs of disease, and an indication of which species are primary or secondary in infection (Wise et

al., 2023; Wise et al., 2025). However, to gain a more comprehensive understanding of bacterial co-infections, it's crucial to also characterize bacterial-bacterial interactions *in vitro*. One approach to investigating such interactions is characterization of bacterial secretomes. A bacterial secretome is the comprehensive inventory of proteins that are released or secreted outside of the cell (Zubair et al., 2020). The secretome of bacterial pathogens can provide critical insight into pathogenesis and cell to cell communication, which in turn can provide important markers for diagnostics and vaccine development (Ranganathan and Garg, 2009; Zubair et al., 2020).

In the context of disease dynamics, studying the secretome of bacteria during co-infection track how one species supplies nutrients or modifies its environment in response to another species (Qiao et al., 2025; Ferreira, Antunes, and Sal-Man, 2025), and helps identify antagonistic or synergistic behaviors (Pallen et al., 2026). A study of a mixed bacterial cultures revealed *Pseudomonas aeruginosa* dominance when grown in co-culture with *Staphylococcus aureus*, wherein *P. aeruginosa* inhibited the growth of *S. aureus* (Kluge, Hoffman, Benndorf, Rapp, and Reichl, 2012). Another study demonstrated that different bacterial species acquire mutations that alter antagonistic effects of vesicle-enriched secretomes in co-culture (Warsi, Gedda, Edwards, and Andersson, 2023). These studies highlight the complexities of bacterial interactions in co-culture. Therefore, growth and secretome analyses of fish-associated bacterial pathogens could provide crucial insight into species-specific interactions during co-infection.

1.6. Types of Columnaris Vaccines

Several types of columnaris vaccines have been developed and have produced varying results (summarised in Table 1). A brief description of each vaccine type and preparation method, fish host, size or life stage, and level of protection offered to immunised fish will be discussed.

1.6.1. Inactivated/Killed Vaccines

Inactivated or "killed" vaccines contain microorganisms that have been killed through physical or chemical processes (e.g., heat, formalin, radiation). Another term frequently used is bacterin, which United States Department of Agriculture-Animal and Plant Health Inspection Service (USDA-APHIS) defines as "products containing whole, killed bacteria." Although inactivated/killed vaccines induce humoral immune responses, they cannot replicate within the host. Killed vaccines are the safest type of vaccine and can be administered with or without different types of adjuvants (Baxter 2007). The method to inactivate cells may impact the antigenicity of the bacterin. Bader et al. (1997) demonstrated that whole-cell lysates created with pressure and formalin inactivation shared four similar proteins. However, it was deduced that the formalin-killed preparation had a modification or inactivation of a shared 60 kda protein, which was not recognised when probed in a western blot with serum from channel catfish previously exposed to CCB (*F. columnare* strain BIOMED1, species unknown).

One of the first published reports of immunisation against columnaris disease was the use of heat-inactivated cells of *C. columnaris* (species unknown) with FCA that were

orally administered to juvenile coho salmon (*Oncorhynchus kisutch*; Fujihara and Nakatani 1971). Vaccinated salmon produced an average agglutinating antibody titre of 1:168, whereas agglutinating titres for control fish survivors were 1:17 (Fujihara and Nakatani 1971). Schachte Jr. and Mora (1973) injected channel catfish fingerlings subcutaneously and intramuscularly with heat-inactivated *C. columnaris* (species unknown), resulting in high antibody titres for both injection routes. Immersion immunisation of carp (*Cyprinus carpio* L.; 5 g) with a *F. columnaris* bacterin (strain M 15, species unknown) resulted in antigen-sensitised cells within the thymus, spleen, and mid-kidney at 28 days post-vaccination (Liewes et al. 1982).

An autogenous *F. columnaris* bacterin (species unknown) was used to immunise juvenile pond-reared channel catfish by immersion annually over a period of 5 years (Moore et al. 1990). The study revealed a reduction in mortality and a reduction in antibiotic treatment of immunised channel catfish compared to non-immunised fish. Vaccination of eel (*Anguilla japonica*) with formalin-inactivated cells of *C. columnaris* (species unknown) was achieved via immersion and injection. The immersion route of administration resulted in a 60% survival rate for eels, compared to a 20% survival in eels that were vaccinated by injection (Mano et al. 1996). A significant humoral response in Nile tilapia (*Oreochromis niloticus*) was detected within 2 weeks of immunisation with formalin-killed *F. columnare* (ATCC 23463^{T}) cells, but intraperitoneal injection with FCA was required to provide a robust response (Grabowski et al. 2004).

Guo et al. (2023) demonstrated an increased relative percent survival (RPS) juvenile grass carp (*Ctenopharyngodon idellus*) following vaccination with formalin-inactivated

genomovar II strain MU-04 of *F. columnare* (now either *F. covae* or *F. oreochromis*) supplemented with white oil. The authors also demonstrated aspects of cross-protection when using different strains and antigens. Thus, adjuvants or co-mixed compounds may be used with inactivated vaccines to enhance efficacy.

Previous studies have evaluated numerous approaches to employing biotechnology in CCB vaccine development, for example, bacterial ghosts. Bacterial ghosts are empty gram-negative bacterial envelopes produced by the controlled expression of the cloned lysis gene E and can be utilised for vaccine delivery (Langemann et al. 2010). Zhu et al. (2012) developed *F. columnare* (species unknown) G4cpN22 ghosts and found a high degree of protection in grass carp when i.p. injected and boosted. The RPS was 70.9 for the G4cpN22 vaccinated carp when challenged with the parent *F. columnare* isolate G4 (species unknown) that was isolated from a disease outbreak in cultured cyprinids.

Leal et al. (2010) immunised Nile tilapia fingerlings with a formalin-killed culture of *F. columnare* isolate BZ-1 (now *F. oreochromis*) by i.p. and i.m. injection, oral, and immersion routes. For all delivery routes of the killed vaccine, no positive RPS was reported (Leal et al. 2010). One potential reason for the lack of protection against columnaris disease is that the experimental challenge occurred 3 weeks at 26°C (~550°days) following immunisation, and peak antibody concentration in Nile tilapia mucus occurs after 6 weeks at 28°C (~1100°days; Grabowski et al. 2004), suggesting that protection may have been obtained if fish were challenged later post-immunisation (Leal et al. 2010).

Another approach to inactivated vaccine design is the ease of inclusion for polyvalent vaccine design, such as a *Streptococcus iniae* + *F. covae* bivalent vaccine tested in Asian seabass (*Lates calcarifer*) (Tumree et al. 2024). The study revealed that the monovalent *F. covae* (AQAHMFc) injectable vaccine induced a robust immune response, upregulated expression of immune-related genes, and provided the highest RPS (54.4) following exposure to virulent *F. covae* (Tumree et al. 2024).

1.6.2. Live-Attenuated Vaccines

Live-attenuated vaccines contain a weakened or less-virulent microorganism that is incapable of causing disease but can still replicate within the host. Live-attenuated vaccines offer the ability to stimulate humoral and cell-mediated immune responses. However, concerns regarding the safety of live-attenuated vaccines (i.e., reversion to virulence) exist, and safety evaluations and commercial licensing are rigorous and time-consuming. Currently, there are three licensed live-attenuated vaccines in the United States: *Arthrobacter* vaccine for use in salmonids, and *Edwardsiella ictaluri* and *F. columnare* vaccines for use in catfish (USDA-APHIS 2025). Attenuation can be achieved using several methods, including gene modification (Chen et al. 2020; Lan et al. 2007; Lawrence et al. 1997; Mohd-Aris et al. 2019; Moral et al. 1998; Vivas et al. 2004), transposon mutagenesis (Buchanan et al. 2005; Lawrence et al. 2001; Liu and Bi 2007; Norqvist et al. 1989), and creating antibiotic-resistant mutants (Bader et al. 2005; Hu et al. 2012; Klesius and Shoemaker 1999; Shoemaker et al. 2007).

A modified live vaccine, AQUAVAC-COL, using a virulent *F. columnare* isolate (confirmed as *F. columnare*) was developed by Shoemaker, Klesius, and Evans (2005). The vaccine was patented, licensed, and approved for use in channel catfish and largemouth bass. The vaccine was made by passing a virulent strain of *F. columnare* onto increasing concentrations of rifampicin. This attenuation method was first introduced by Schurig et al. (1991) when a rifampicin-resistant mutant of *Brucella abortus* was produced as a vaccine candidate against Brucellosis in cattle. The modified live *F. columnare* vaccine for columnaris disease protected channel catfish fry and largemouth bass fry via immersion bath under laboratory settings (Bebak et al. 2009; Shoemaker et al. 2011). However, due to inconsistency under production settings, AQUAVAC-COL is no longer available.

New rifampicin-resistant CCB vaccine candidates were developed by Olivares-Fuster and Arias (2011). The virulent wild-type isolates used for attenuation were genomovar II *F. columnare* isolates (now *F. covae*), which are now known to be the predominant CCB that impacts channel catfish (LaFrentz et al. 2024). Comparisons between the parent and mutant strains revealed that the mutants had distinctive mutations within their genome that translated into different protein profiles and lipopolysaccharides (Olivares-Fuster and Arias 2011; Cai and Arias 2021). Mohammed et al. (2013) tested the protective potential of these new rifampicin-resistant mutant strains of *F. columnare* (now *F. covae*) as vaccine candidates. When tested in vivo, the vaccine strain 17–23 provided greater protection to juvenile channel catfish, zebrafish (*Danio rerio*), and Nile tilapia than the vaccine strain utilised in the AQUAVAC-COL vaccine (Mohammed et al. 2013). A recent study highlighted potential benefits to vaccinating

channel catfish fingerlings during transfer to earthen ponds with the rifampicin-resistant *F. columnare* strain 17–23 (now *F. covae*; Malecki et al. 2021). Although there were no significant differences between the survival of vaccinated and control fish, vaccinated fish had significantly higher average weight at harvest and a significantly better feed conversion ratio compared to control fish. Additionally, economic analysis of rearing vaccinated fingerlings instead of non-vaccinated fish resulted in a net benefit of $1443/ha. These results present an attractive bioeconomic benefit to vaccinating channel catfish fingerlings with the 17–23 vaccine; however, further studies on survival of vaccinated and non-vaccinated fish in commercial settings are needed.

The live-attenuated vaccine strain 17–23 (now *F. covae*) was used to investigate the potential role of fish mucosal tissues in protection against columnaris disease in juvenile channel catfish (Zhang et al. 2017). Transcriptomic profiles were produced to compare vaccinated and nonvaccinated catfish fingerlings before and immediately following the challenge with a virulent *F. columnare* isolate BGFS-27 (now *F. covae*). In vaccinated fish, neuropeptides, hormones, complement factors, and proteases were expressed at 0 h post-challenge (Zhang et al. 2017). Following the challenge, these same elements fell to indiscernible levels 1-h post-challenge (Zhang et al. 2017). In unvaccinated fish, pro-inflammatory cytokines (e.g., IL-1b, IL-8, and IL-17) were expressed, whereas vaccinated fish showed expression in genes associated with collagen maturation and extracellular matrix remodelling (Zhang et al. 2017). Additionally, the vaccinated fish had significantly lower mortality compared to the unvaccinated fish (Mohammed et al. 2013). These

findings suggested that mucosal tissues (e.g., fish gill) play an important role in vaccine-induced protection against columnaris disease.

Research was conducted to determine the efficacy of vaccinating channel catfish eggs with the live attenuated strain used in the AQUAVAC-COL (confirmed as *F. columnare*) vaccine as well as a bivalent vaccine consisting of the AQUAVAC-COL vaccine strain and a live attenuated *Edwardsiella ictaluri* vaccine, AQUAVAC-ESC (Shoemaker et al. 2002) the commercially available vaccine was used as the *E. ictaluri* vaccine. The monovalent *F. columnare* vaccine protected catfish fry post-primary and booster vaccination at 109, 116, and 137 days, with RPS ranging from 50.0% to 76.8% (Shoemaker et al. 2007). The RPS following bivalent vaccination ranged from 33.0 to 59.7 in catfish challenged with *F. columnare* strain ALG-00-530 (now *F. covae*), and 44.5–66.7 in fish challenged with *E. ictaluri*, though these results were not statistically different. *In ovo* administration of the bivalent *F. columnare* and *E. ictaluri* vaccine provided protection to channel catfish fry against challenges with virulent strains (Shoemaker et al. 2007).

1.6.3. Recombinant Vaccines

Recombinant vaccine technology targets an immunogenic protein(s) or antigen(s) of a pathogen. Once the protein(s) is identified, the gene(s) encoding the protein is/are cloned, expressed, purified and finally tested as vaccines (Nascimento and Leite 2012). Recombinant vaccines can elicit humoral and cell-mediated immune responses, and because there is no live component, these vaccines are considered safe, stable, and easy to manufacture (Bedekar and Kole 2022). Studies investigating outer membrane protein

(OMPs) components in CCB found that some components could induce an immune response and protect against the pathogen in channel catfish and bluntnose black bream (*Megalobrama ambylcephala*; Hu et al. 2010). Initial studies used antisera to identify immunogenic OMPs in a virulent *F. columnare* strain G4 (species unknown; Liu et al. 2008; Liu et al. 2012; Luo, Fu, et al. 2016; Xie et al. 2005). Luo, Fu, et al. (2016) characterised immunogenic proteins of virulent *F. columnare* G4 (species unknown) and found that three proteins, including the gliding motility lipoprotein GldJ (GldJ), lipoprotein (Lip), and outer membrane efflux protein precursor (Omep), are major protective antigens and provided protection in grass carp (*Ctenopharyngodon idella*) against infection in an injection-challenge model. Later, Luo, Liu, et al. (2016) observed protection against infection and an increase in sera Ig expressions and cytokines using a recombinant fusion protein of 5 OMPs from the same isolate, G4. Computational models have also been used to discern immunogenic OMPs. Bhattacharya et al. (2020) identified three, 9 mer epitopes for *F. columnare* (ATCC 49512^{T}) OMPs that may be of interest for recombinant vaccine development.

The CCB heat shock protein (HSP) gene, DnaJ, was tested as an i.p. injected recombinant vaccine for juvenile channel catfish (Olivares-Fuster et al. 2010). Cloning and expression of DnaJ was completed utilising genomovar I and II isolates of *F. columnare* (now *F. columnare* and *F. covae*) and *F. covae* isolates (published as *F. columnare* genomovars I and II, respectively). Although HSPs are known to activate the immune system during infections in other animal models and provide protection (Zügel and Kaufmann 1999), the recombinant DnaJ vaccine delivered by i.p. injection did not

protect channel catfish against columnaris disease induced via bath immersion challenge. A recombinant protein vaccine based upon the DnaK protein (rDnaK) of *F. columnare* was developed by Lange et al. (2019) for protection against columnaris disease in juvenile channel catfish. Fish were immunised by bath immersion and challenged with *F. columnare* isolate LV-359-01 (now *F. covae*). DnaK was the dominant immunogen in the extracellular portion of *F. covae* in both catfish sera and skin explant. In experimental trials, the recombinant DnaK vaccine provided significant survival (> 30%) when compared to the non-immunised control fish as a bath immersion vaccine (Lange et al. 2019). The rDnaK-specific ELISA detected substantial levels of mucosal IgM antibodies in the skin of immunised catfish at 4- and 6-weeks post-immunisation and RNA sequencing (RNA-Seq) analysis of immunised fish showed an upregulation of several genes associated with B and T-cell differentiation and migration to mucosal tissues compared to control fish (Lange et al. 2019). In a following study, Lange et al. (2021) suggested that adding Montanide IMS 1312 VG adjuvant to the rDnaK vaccine may reduce the time required for bath immunisation. Recently, Sayed et al. (2023) surveyed several *F. covae* secreted extracellular products (SEP) as potential immunogens. The SEP cocktail included glycosaminoglycan (GAG) polysaccharide lyase, zinc-dependent metalloprotease, a DNA/RNA endonuclease G protein, an outer membrane protein beta-barrel domain, and a hypothetical protein (Sayed et al. 2023). The SEPs delivered via i.p. injection alone or with FCA (Seppic, Paris, France) showed protection in 40.5 g channel catfish against *F. covae* 3-weeks post injection (58%), while heat-inactivated SEPs did not yield significant survival compared to sham immunised (23.15%; Sayed et al. 2023). Though these are secreted

proteins directly from *F. covae*, they are a resource of potential recombinant subunit vaccine candidates.

1.6.4. Encapsulated Vaccines

Encapsulated vaccines utilise innovated technology to generate micro- or nanometre sized particles containing antigens that can also have adjuvant properties. This approach offers a variety of customisation to deliver safe, controlled, and targeted vaccination and immune response (Simonazzi et al. 2018). Continuous advances are being made within aquaculture to incorporate particle vaccines into practice (Ahmed et al. 2024; Tammas et al. 2024).

Cells of *F. columnare* isolate BZ-1 (now *F. oreochromis*) were encapsulated in alginate microparticles and used to immunise Nile tilapia fingerlings by oral, immersion, and i.p., and i.m. injection delivery. The killed bacterial cells were encapsulated following the method established by Rodrigues et al. (2006). However, all delivery methods failed to protect tilapia against infection with the virulent BZ-1 *F. oreochromis* isolate (Leal et al. 2010).

Kitiyodom, Yata, et al. (2019) hypothesised that an immersion formalin-inactivated CCB vaccine could be enhanced by nanoencapsulation while incorporating a mucoadhesive characteristic to the surface of a chitosan-complexed vaccine. Red tilapia (*Oreochromis* sp., 10 g) were challenged with a virulent *F. columnare* isolate (species unknown) at 30- and 60-days post-immunisation with the chitosan-complexed vaccine and a naked vaccine. The chitosan-complexed vaccine provided increased protection with

RPS of greater than 60% against the virulent *F. columnare* (species unknown) isolate and increased mucoadhesive affinity for fish gills by mimicking the mucoadhesive characteristic of live bacteria (Kitiyodom, Yata, et al. 2019). A further advanced biomimetic-mucoadhesive nanovaccine was also evaluated in 100 g red tilapia. The immersion vaccine was found to enhance humoral immunity and provide protection against genetic group 4 *F. columnare* isolate F-K17/1 (now *F. oreochromis*; Kitiyodom, Yata, et al. 2021; Kitiyodom, Trullas, et al. 2021). An *F. oreochromis* nanoencapsulated vaccine, EncapFlavoNP^{++}, provided significant protection in juvenile Asian sea bass (*Lates calcarifer*) reared in freshwater against columnaris disease by including a cationic surface for delivery of antigen to anionic sites in the skin mucosa of fish (Bunnoy et al. 2022). Bunnoy et al. (2023) also created a bivalent nanovaccine for *Francisella orientalis* and *F. oreochromis* and observed an enhancement to juvenile Nile tilapia serum IgM levels and protection against coinfection with both bacteria, in addition to single infections.

1.7. Conclusions and Future Directions

Yellow-pigmented bacteria, including columnaris-causing bacteria are widespread and possess attributes that allow them to persist in freshwater environments, making treatment and control difficult. An efficacious vaccine to prevent or reduce losses due to columnaris disease is needed. Multiple attempts to develop an effective vaccine have been made, and the protection afforded by killed vaccines has been variable, and the use of adjuvants may be needed to improve efficacy. Live-attenuated vaccines have shown promise in the laboratory and can elicit strong immune responses; however, more

research is needed regarding application and efficacy in production settings. Likewise, recent research developing recombinant and encapsulated vaccines has suggested protection against CCB in the laboratory. Advances in vaccine technology, coupled with knowledge of the four species of CCB having an affinity for different fish hosts, are likely to result in improvements in vaccine development for the prevention of columnaris disease.

1.8. Tables

Table 1.8.1. Types of developed CCB vaccines against columnaris disease in multiple fish species. O = oral, IP = intraperitoneal, IM = intramuscular, IMM = immersion, SC = sub-cutaneous, - = not reported.

Vaccine Type	Delivery Method	CCB Species/Strain	Fish Species	Avg. Weight/Age	Boosted	RPS/Survival Rate	Reference
Inactivated/killed	O, IP, & IM	*C. columnaris*[d]	*O. kisutch*	3 months	Yes	-	Fujihara & Nakatani, 1971
Inactivated/killed	IM & SC	*C. columnaris*[d]	*I. punctatus*	Unknown	No	-	Schachte & Mora, 1973
Inactivated/killed	IMM	M 15[d]	*C. carpio*	5 g	No	-	Liewes et al., 1982
Inactivated/killed	IMM	*F. columnaris*[d]	*I. punctatus*	2 g	No	-	Moore et al., 1990
Inactivated/killed	IMM	*C. columnaris*[d]	*A. japonica*	Unknown	No	60	Mano et al., 1996
Inactivated/killed	IP & IMM	ATCC 23463[T,a]	*O. niloticus*	66 g	Yes	-	Grabowski et al., 2004
Inactivated/killed	IP	MU-04[b or c]	*C. idellus*	15 g	Yes	55 –71	Guo et al., 2023
Inactivated/killed	IP, IM, IMM, & O	BZ-1[c]	*O. niloticus*	15 g	Yes	-	Leal et al., 2010
Inactivated/killed	IP & O	AQAHMFc[b]	*L. calcarifer*	12 g	Yes	54.4	Tumree et al., 2024
Recombinant	IP	G4[d]	*C. idellus*	45 g	Yes	70.9	Zhu et al., 2012
Live-attenuated	IMM	AQUAVAC-COL[a]	*M. salmoides*	7 dph	No	-	Bebak et al., 2009
Live-attenuated	IMM	17-23[b]	*I. punctatus*	27.5 g	No	-	Malecki et al., 2021
Live-attenuated	IMM	17-23[b]	*I. punctatus, D. rerio, & O. niloticus*	6 g, 0.5 g, & 9 g	No	37 & 90.0, 28.4, & 82.1 & 86.9	Mohammed et al., 2013
Live-attenuated	IMM	17-23[b]	*I. punctatus*	0.05 g	No	-	Zhang et al., 2017
Live-attenuated	IMM	AQUAVAC-COL [a]	*I. punctatus*	Eyed eggs	Yes	50 –76.8, & 33 –59.7	Shoemaker et al., 2007
Recombinant	IP	G4[d]	*C. idellus*	40 –60 g	No	64 –72	Zhang et al., 2016

Recombinant	IP	ALG-00-530[b]	*I. punctatus*	6 g	No	-	Olivares-Fuster et al., 2010
Recombinant	IMM	LV-359-01[b]	*I. punctatus*	5 g	No	>30	Lange et al., 2019
Recombinant	IMM	LV-359-01[b]	*I. punctatus*	5 g	No	37	Lange et al., 2021
Recombinant	IP	94-081[b]	*I. punctatus*	40 g	No	58.7 & 46.1	Sayed et al., 2023
Micro-/nano-particle	IP, IM, IMM, & O	BZ-1[c]	*O. niloticus*	16 g	Yes	-	Leal et al., 2010
Micro-/nano-particle	IMM	F-K17/1[c]	*Oreochromis sp.*	10 g	No	>60	Kitiyodom et al., 2019b
Micro-/nano-particle	IMM	F-K17/1[c]	*Oreochromis sp.*	100 g	No	>72	Kitiyodom et al., 2021a
Micro-/nano-particle	IMM	CC1802[c]	*L. calcarifer*	3 g	Yes	65.83 –72.50	Bunnoy et al., 2022
Micro-/nano-particle	IMM	NK01[c]	*O. niloticus*	10 g	Yes	55	Bunnoy et al., 2023

[a]*F. columnare,* [b]*F. covae*, [c]*F. oreochromis*, [d]CCB species unknown

1.9. Figures

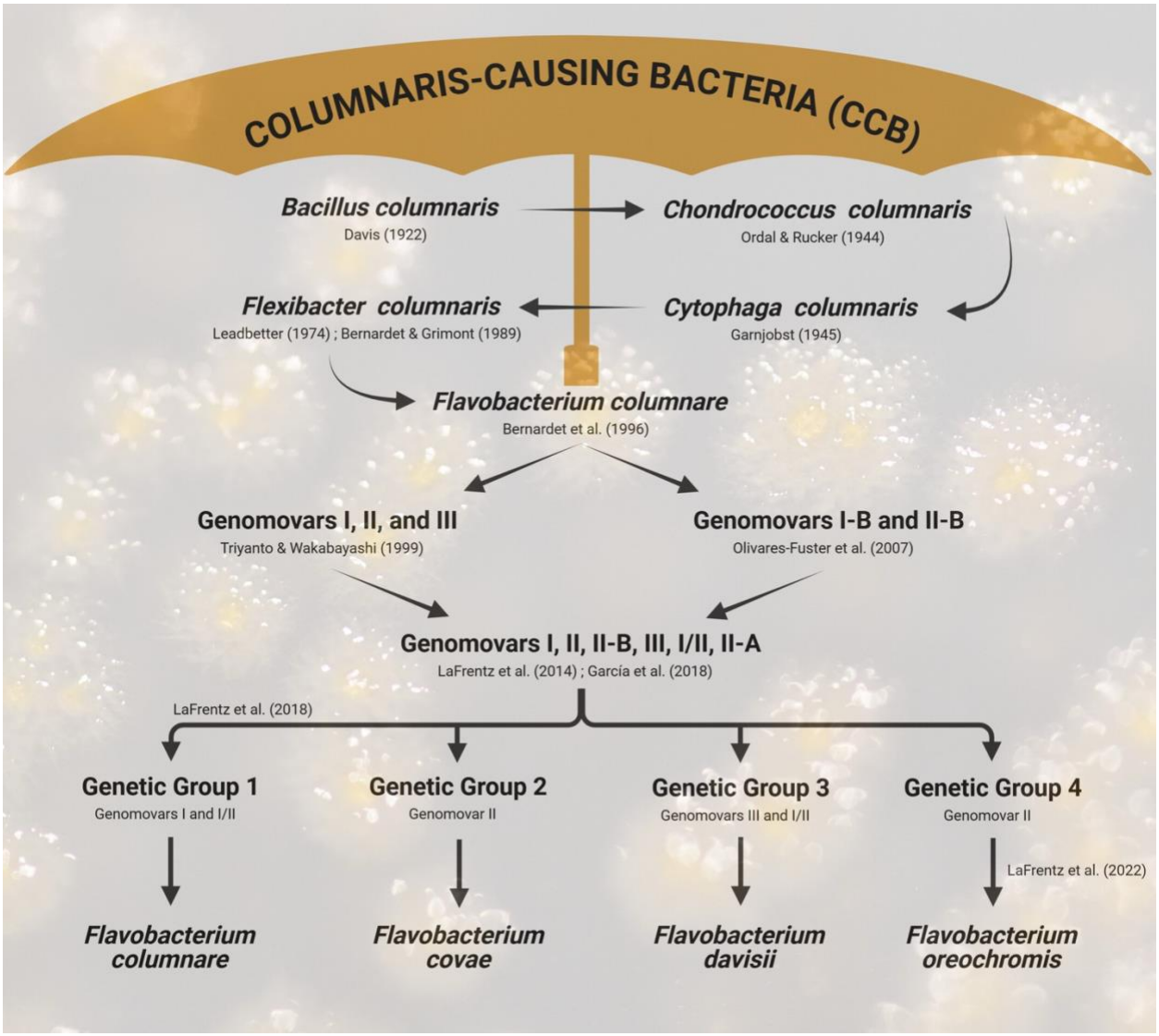

Figure 1.9.1. Schematic history of columnaris-causing bacteria taxonomy from 1922-present, with an emphasis on use of genomovar typing to decipher the genetic diversity.

1.10. References

Abdelhamed, H., S. W. Nho, A. Karsi, and M. L. Lawrence. 2021. The Role of Denitrification Genes in Anaerobic Growth and Virulence of *Flavobacterium columnare*. *Journal of Applied Microbiology,* 130, no. 4: 1062–1074. https://doi.org/10.1111/jam.14855.

Ahmed, M. T., M. S. Ali, T. Ahamed, S. Suraiya, and M. Haq. 2024. Exploring the Aspects of the Application of Nanotechnology System in Aquaculture: A Systematic Review. *Aquaculture International,* 32: 1–30. https://doi.org/10.1007/s10499-023-01370-7.

Anacker, R. L., and E. J. Ordal. 1959. Studies on the Myxobacterium *Chondrococcus columnaris*: I. Serological Typing. *Journal of Bacteriology,* 78: 25–32. https://doi.org/10.1128/jb.78.1.25-32.1959.

Austin, B. and Austin, D.A., 2016. Flavobacteria and Cytophagas. In *Bacterial Fish Pathogens: Disease of Farmed and Wild Fish* (pp. 397-465). Cham: Springer International Publishing.

Bader, J. A., P. H. Klesius, and S. Vinitnantharat. 1997. Comparison of Whole-Cell Antigens of Pressure- and Formalin-Killed *Flexibacter Columnaris* From Channel Catfish (*Ictalurus punctatus*). *American Journal of Veterinary Research,* 58, no. 9: 985–988. https://www.ncbi.nlm.nih.gov/pubmed/9285002.

Bader, J. A., C. A. Shoemaker, and P. H. Klesius. 2005. Production, Characterization and Evaluation of Virulence of an Adhesion Defective Mutant of Flavobacterium Columnare Produced by β-Lactam Selection. *Letters in Applied Microbiology,* 40: 123–127. https://doi.org/10.1111/j.1472-765X.2004.01641.x.

Baxter, D. 2007. Active and Passive Immunity, Vaccine Types, Excipients and Licensing. *Occupational Medicine,* 57: 552–556. https://doi.org/10.1093/occmed/kqm110.

Bebak, J., M. Matthews, and C. A. Shoemaker. 2009. Survival of Vaccinated, Feed Trained Largemouth Bass Fry (*Micropterus salmoides*) During Natural Exposure to *Flavobacterium columnare*. *Vaccine,* 27: 4297–4301. https://doi.org/10.1016/j.vaccine.2009.05.026.

Beck, B. H., B. D. Farmer, D. L. Straus, C. Li, and E. Peatman. 2012. Putative Roles for a Rhamnose Binding Lectin in *Flavobacterium columnare* Pathogenesis in Channel Catfish *Ictalurus punctatus*. *Fish & Shellfish Immunology,* 33: 1008–1015. https://doi.org/10.1016/j.fsi.2012.08.018.

Bedekar, M. K., and S. Kole. 2022. Vaccines for Veterinary Diseases. In *Fundamentals of Fish Vaccination*. Vaccine Design: Methods and Protocols, vol. 2, 147–173. Humana Press.

Bernardet, J.F. and Bowman, J.P., 2006. The Genus *Flavobacterium*. *The Prokaryotes*, *7*, pp.481-531. DOI: 10.1007/0-387-30747-8_17

Bernardet, J.F., Vancanneyt, M., Matte-Tailliez, O., Grisez, L., Tailliez, P., Bizet, C., Nowakowski, M., Kerouault, B. and Swings, J., 2005. Polyphasic Study of *Chryseobacterium* Strains Isolated from Diseased Aquatic Animals. *Systematic and Applied Microbiology*, 28(7), pp.640-660. https://doi.org/10.1016/j.syapm.2005.03.016

Bernardet, J. F., and P. A. Grimont. 1989. Deoxyribonucleic Acid Relatedness and Phenotypic Characterization of *Flexibacter Columnaris* sp. Nov., Nom. Rev., *Flexibacter Psychrophilus* sp. Nov., Nom. Rev., and *Flexibacter Maritimus* Wakabayashi, Hikida, and Masumura 1986. *International Journal of Systematic and Evolutionary Microbiology,* 39: 346–354. https://doi.org/10.1099/00207713-39-3-346.

Bernardet, J. F., Y. Nakagawa, B. Holmes, and Subcommittee On The Taxonomy Of Flavobacterium And Cytophaga-Like Bacteria Of The International Committee On Systematics Of Prokaryotes. 2002. Proposed Minimal Standards for Describing New Taxa of the Family Flavobacteriaceae and Emended Description of the Family. *International Journal of Systematic and Evolutionary Microbiology,* 52, no. 3: 1049–1070. https://doi.org/10.1099/ijs.0.02136-0.

Bernardet, J. F., P. Segers, M. Vancanneyt, F. Berthe, K. Kersters, and P. Vandamme. 1996. Cutting a Gordian Knot: Emended Classification and Description of the Genus Flavobacterium, Emended Description of the Family Flavobacteriaceae, and Proposal of *Flavobacterium hydatis* Nom. Nov. (Basonym, *Cytophaga*

aquatilis Strohl and Tait 1978). *International Journal of Systematic Bacteriology,* 46: 128–148. https://doi.org/10.1099/00207713-46-1-128.

Bhattacharya, M., R. C. Malick, N. Mondal, et al. 2020. Computational Characterization of Epitopic Region Within the Outer Membrane Protein Candidate in *Flavobacterium columnare* for Vaccine Development. *Journal of Biomolecular Structure and Dynamics,* 38 no. 2: 450–459. https://doi.org/10.1080/07391102.2019.1580222.

Bruce, T.J., Ma, J., Knupp, C., Loch, T.P., Faisal, M. and Cain, K.D., 2020. Cross-Potection of a Live-Attenuated *Flavobacterium psychrophilum* Immersion Vaccine Against Novel F*lavobacterium* spp. and *Chryseobacterium* spp. Strains. *Journal of Fish Diseases*, 43(8), pp.915-928. DOI: 10.1111/jfd.13201

Buchanan, J. T., J. A. Stannard, X. Lauth, et al. 2005. *Streptococcus iniae* Phosphoglucomutase is a Virulence Factor and a Target for Vaccine Development. *Infection and Immunity,* 73: 6935–6944. https://doi.org/10.1128/IAI.73.10.6935-6944.2005.

Bullock, G. L. 1986. *Columnaris Disease of Fishes*. Vol. 72. US Department of the Interior, Fish and Wildlife Service, Division of Fisheries and Wetlands Research.

Bullock, G.L., 1990. *Bacterial Gill Disease of Freshwater Fishes* (Vol. 84). US Department of the Interior, Fish and Wildlife Service.

Bunnoy, A., P. Thangsunan, P. Chokmangmeepisarn, et al. 2022. Mucoadhesive Cationic Lipid-Based Flavobacterium Oreochromis Nanoencapsulation Enhanced the Efficacy of Mucoadhesive Immersion Vaccination Against Columnaris Disease and Strengthened Immunity in Asian Sea Bass (*Lates Calcarifer*). *Fish & Shellfish Immunology,* 127: 633–646. https://doi.org/10.1016/j.fsi.2022.06.059.

Bunnoy, A., K. D. Thompson, P. Thangsunan, et al. 2023. Development of a Bivalent Mucoadhesive Nanovaccine to Prevent Francisellosis and Columnaris Diseases in Nile Tilapia (*Oreochromis niloticus*). *Fish & Shellfish Immunology,* 138: 108813. https://doi.org/10.1016/j.fsi.2023.108813.

Cai, W., and C. R. Arias. 2021. Deciphering the Molecular Basis for Attenuation of *Flavobacterium columnare* Strain Fc1723 Used as Modified Live Vaccine Against

Columnaris Disease. *Vaccines (Basel),* 9, no. 11: 1370. https://doi.org/10.3390/vaccines9111370.

Chen, Y., F. Wu, Z. Wang, J. Tang, S. Cai, and J. Jian. 2020. Construction and Evaluation of *Vibrio alginolyticus* ΔclpP Mutant, as a Safe Live Attenuated Vibriosis Vaccine. *Fish & Shellfish Immunology,* 98: 917–922. https://doi.org/10.1016/j.fsi.2019.11.054.

Chowdhury, B. R., and H. Wakabayashi. 1988. Effects of Sodium, Potassium, Calcium and Magnesium Ions on the Survival of *Flexibacter columnaris* in Water. *Fish Pathology,* 23: 231–235. https://doi.org/10.3147/jsfp.23.231.

Criscuolo, A., O. Chesneau, D. Clermont, and C. Bizet. 2018. Draft Genome Sequence of the Fish Pathogen *Flavobacterium Columnare* Genomovar III Strain PH-97028 (= CIP 109753). *Genome Announcements,* 6, no. 14: 10–1128. https://doi.org/10.1128/genomea.00222-18.

Davis, H. S. 1922. *A New Bacterial Disease of Fresh-Water Fishes*. US Government Printing Office. https://doi.org/10.5962/bhl.title.49773.

Declercq, A. M., F. Haesebrouck, W. Van den Broeck, P. Bossier, and A. Decostere. 2013. Columnaris Disease in Fish: A Review With Emphasis on Bacterium-Host Interactions. *Veterinary Research,* 44: 1–17. https://doi.org/10.1186/1297-9716-44-27.

Decostere, A., F. Haesebrouck, G. Charlier, and R. Ducatelle. 1999. The Association of *Flavobacterium columnare* Strains of High and Low Virulence With Gill Tissue of Black Mollies (*Poecilia sphenops*). *Veterinary Microbiology,* 67, no. 4: 287–298. https://doi.org/10.1016/s0378-1135(99)00050-4.

Dong, H.T., Nguyen, V.V., Phiwsaiya, K., Gangnonngiw, W., Withyachumnarnkul, B., Rodkhum, C. and Senapin, S., 2015. Concurrent Infections of *Flavobacterium columnare* and *Edwardsiella ictaluri* in Striped Catfish, *Pangasianodon hypophthalmus* in Thailand. *Aquaculture*, 448, pp.142-150. https://doi.org/10.1016/j.aquaculture.2015.05.046

Dong, H.T., Nguyen, V.V., Mata, W., Kayansamruaj, P., Senapin, S., Nilubol, D. and Rodkhum, C., 2016. Diversity of Non-*Flavobacterium columnare* Bacteria Associated with Columnaris-Like Diseased Fish. *The Thai Journal of Veterinary Medicine*, 46(2), pp.251-259.

Farmer, B. D. 2004. *Improved Methods for the Isolation and Characterization of Flavobacterium columnare*. Louisiana State University and Agricultural & Mechanical College.

Ferreira, R.B.R., Antunes, L.C.M. and Sal-Man, N., 2025. Pathogen-pathogen interactions during co-infections. *The ISME Journal*, 19(1), p.wraf104. https://doi.org/10.1093/ismejo/wraf104

Fijan, N. N. 1969. Drug Sensitivity of *Chondrococcus columnaris*. *Veterinarski Arhiv,* 39: 259–267.

Fish, F. F., and R. R. Rucker. 1945. Columnaris as a Disease of Cold-Water Fishes. *Transactions of the American Fisheries Society,* 73, no. 1: 32–36. https://doi.org/10.1577/1548-8659(1943)73[32:CAADOC]2.0.CO;2.

Fujihara, M. P., and R. E. Nakatani. 1971. Antibody Production and Immune Responses of Rainbow Trout and Coho Salmon to *Chondrococcus columnaris*. *Journal of the Fisheries Research Board of Canada,* 28: 1253–1258. https://doi.org/10.1139/f71-191.

García, J. C., B. R. LaFrentz, G. C. Waldbieser, F. S. Wong, and S. F. Chang. 2018. Characterization of Atypical *Flavobacterium columnare* and Identification of a New Genomovar. *Journal of Fish Diseases,* 41, no. 7: 1159–1164. https://doi.org/10.1111/jfd.12778.

García-López, M., Meier-Kolthoff, J.P., Tindall, B.J., Gronow, S., Woyke, T., Kyrpides, N.C., Hahnke, R.L. and Göker, M., 2019. Analysis of 1,000 Type-Strain Genomes Improves Taxonomic Classification of Bacteroidetes. *Frontiers in Microbiology*, 10, p.2083. https://doi.org/10.3389/fmicb.2019.02083

Garnjobst, L. 1945. *Cytophaga columnaris* (Davis) in Pure Culture: A Myxobacterium Pathogenic to Fish. *Journal of Bacteriology,* 49: 113–128. https://doi.org/10.1128/jb.49.2.113-128.1945.

Gholamhosseini, A., Taghadosi, V., Shiry, N., Akhlaghi, M., Sharifiyazdi, H., Soltanian, S. and Ahmadi, N., 2018, June. First Isolation and Identification of *Aeromonas veronii* and *Chryseobacterium joostei* from Reared Sturgeons in Fars Province, Iran. In *Veterinary Research Forum* (Vol. 9, No. 2, p. 113). https://doi.org/10.30466/VRF.2018.30826

Grabowski, L. D., S. E. LaPatra, and K. D. Cain. 2004. Systemic and Mucosal Antibody Response in Tilapia, *Oreochromis Niloticus* (L.), Following Immunization With *Flavobacterium Columnare*. *Journal of Fish Diseases,* 27, no. 10: 573–581. https://doi.org/10.1111/j.1365-2761.2004.00576.x.

Griffin, B. R. 1991. Characteristics of a Chondroitin AC Lyase Produced by *Cytophaga columnaris*. *Transactions of the American Fisheries Society,* 120: 391–395. https://doi.org/10.1577/1548-8659(1991)120%3C0391:COACAL%3E2.3.CO;2.

Guo, W., R. Han, W. Xu, et al. 2023. The Protective Effect of Inactivated *Flavobacterium columnare* Vaccine in Grass Carp (*Ctenopharyngodon idellus*). *Frontiers in Immunology,* 14: 1162975. https://doi.org/10.3389/fimmu.2023.1162975.

Holt, R. A., A. Amandi, J. S. Rohovec, and J. L. Fryer. 1989. Relation of Water Temperature to Bacterial Cold-Water Disease in Coho Salmon, Chinook Salmon, and Rainbow Trout. *Journal of Aquatic Animal Health,* 1: 94–101. https://doi.org/10.1577/1548-8667(1989)001%3C0094:ROWTTB%3E2.3.CO;2.

Hu, H. G., C. Z. Wang, and C. F. Chen. 2010. Immune Response of Bluntnose Black Bream to Outer Membrane Protein of Three Pathogenic Bacteria. *Feed Industry,* 31: 9–12.

Hu, Y. H., T. Deng, B. G. Sun, and L. Sun. 2012. Development and Efficacy of an Attenuated *Vibrio harveyi* Vaccine Candidate With Cross Protectivity Against *Vibrio alginolyticus*. *Fish & Shellfish Immunology,* 32: 1155–1161. https://doi.org/10.1016/j.fsi.2012.03.032.

Ilardi, P., Abad, J., Rintamäki, P., Bernardet, J.F. and Avendaño-Herrera, R., 2010. Phenotypic, Serological and Molecular Evidence of *Chryseobacterium piscicola* in Farmed Atlantic Salmon, *Salmo salar* L., in Finland. *Journal of Fish Diseases*, 33(2), pp.179-181. doi:10.1111/j.1365-2761.2009.01091.x

Johnson, J. L., and W. S. Chilton. 1966. Galactosamine Glycan of *Chondrococcus columnaris*. *Science,* 152: 1247–1248. https://doi.org/10.1126/science.152.3726.1247.

Kapetanović, D., Kurtović, B., Vardić, I., Teskeredžić, E. and Teskeredžić, Z., 2006. Gill Disease in a Gilthead Sea Bream (*Sparus aurata* L.). *Med. Weter*, 62, pp.1239-1241.

Kayansamruaj, P., H. T. Dong, I. Hirono, H. Kondo, S. Senapin, and C. Rodkhum. 2017. Comparative Genome Analysis of Fish Pathogen *Flavobacterium columnare* Reveals Extensive Sequence Diversity Within the Species. *Infection, Genetics and Evolution,* 54: 7–17. https://doi.org/10.1016/j.meegid.2017.06.012.

Kämpfer, P., Fallschissel, K. and Avendaño-Herrera, R., 2011. *Chryseobacterium chaponense* sp. nov., Isolated from Farmed Atlantic Salmon (*Salmo salar*). *International Journal of Systematic and Evolutionary Microbiology*, 61(3), pp.497-501. https://doi.org/10.1099/ijs.0.022004-0

Kitiyodom, S., C. Trullas, C. Rodkhum, et al. 2021. Modulation of the Mucosal Immune Response of Red Tilapia (Oreochromis sp.) Against Columnaris Disease Using a Biomimetic-Mucoadhesive Nanovaccine. *Fish & Shellfish Immunology,* 112: 81–91. https://doi.org/10.1016/j.fsi.2021.02.017.

Kitiyodom, S., T. Yata, K. D. Thompson, et al. 2021. Immersion Vaccination by a Biomimetic-Mucoadhesive Nanovaccine Induces Humoral Immune Response of Red Tilapia (*Oreochromis* sp.) Against *Flavobacterium columnare* Challenge. *Vaccines (Basel),* 9, no. 11: 1253. https://doi.org/10.3390/vaccines9111253.

Kitiyodom, S., T. Yata, J. Yostawornkul, et al. 2019. Enhanced Efficacy of Immersion Vaccination in Tilapia Against Columnaris Disease by Chitosan-Coated "Pathogen-Like" Mucoadhesive Nanovaccines. *Fish & Shellfish Immunology,* 95: 213–219. https://doi.org/10.1016/j.fsi.2019.09.064.

Klesius, P. H., J. W. Pridgeon, and M. Aksoy. 2010. Chemotactic Factors of *Flavobacterium columnare* to Skin Mucus of Healthy Channel Catfish (*Ictalurus punctatus*). *FEMS Microbiology Letters,* 310, no. 2: 145–151. https://doi.org/10.1111/j.1574-6968.2010.02060.x.

Klesius, P. H., and C. A. Shoemaker. 1999. Development and Use of Modified Live *Edwardsiella ictaluri* Vaccine Against Enteric Septicemia of Catfish. *Advances in Veterinary Medicine,* 41: 523–537. https://doi.org/10.1016/S0065-3519(99)80039-1.

Klesius, P. H., C. A. Shoemaker, and J. J. Evans. 2008. *Flavobacterium columnare* Chemotaxis to Channel Catfish Mucus. *FEMS Microbiology Letters,* 288, no. 2: 216–220. https://doi.org/10.1111/j.1574-6968.2008.01348.x.

Kluge, S., Hoffmann, M., Benndorf, D., Rapp, E. and Reichl, U., 2012. Proteomic Tracking and Analysis of a Bacterial Mixed Culture. *Proteomics*, 12(12), pp.1893-1901. https://doi.org/10.1002/pmic.201100362

Kumru, S., H. C. Tekedar, N. Gulsoy, G. C. Waldbieser, M. L. Lawrence, and A. Karsi. 2017. Comparative Analysis of the *Flavobacterium columnare* Genomovar I and II Genomes. *Frontiers in Microbiology,* 8: 1375. https://doi.org/10.3389/fmicb.2017.01375.

Kumru, S., H. C. Tekedar, G. C. Waldbieser, A. Karsi, and M. L. Lawrence. 2016. Genome Sequence of the Fish Pathogen *Flavobacterium Columnare* Genomovar II Strain 94–081. *Genome Announcements,* 4, no. 3: e00430. https://doi.org/10.1128/genomeA.00430-16.

Kunttu, H. 2010. *Characterizing the Bacterial Fish Pathogen Flavobacterium columnare, and Some Factors Affecting its Pathogenicity (No. 206)*. University of Jyväskylä.

Kunttu, H. M., L. R. Sundberg, K. Pulkkinen, and E. T. Valtonen. 2012. Environment May Be the Source of *Flavobacterium Columnare* Outbreaks at Fish Farms. *Environmental Microbiology Reports,* 4, no. 4: 398–402. https://doi.org/10.1111/j.1758-2229.2012.00342.x.

Kunttu, H. M., E. T. Valtonen, E. I. Jokinen, and L. R. Suomalainen. 2009. Saprophytism of a Fish Pathogen as a Transmission Strategy. *Epidemics,* 1, no. 2: 96–100. https://doi.org/10.1016/j.epidem.2009.04.003.

LaFrentz, B. R., J. C. García, H. T. Dong, et al. 2016. Optimized Reverse Primer for 16S-RFLP Analysis and Genomovar Assignment of *Flavobacterium columnare*. *Journal of Fish Diseases,* 40, no. 8: 1103–1108. https://doi.org/10.1111/jfd.12583.

LaFrentz, B. R., J. C. Garcia, and J. P. Shelley. 2019. Multiplex PCR for Genotyping of *Flavobacterium columnare*. *Journal of Fish Diseases,* 42: 1531–1542.

LaFrentz, B. R., J. C. García, G. C. Waldbieser, et al. 2018. Identification of Four Distinct Phylogenetic Groups in *Flavobacterium Columnare* With Fish Host Associations. *Frontiers in Microbiology,* 9: 452. https://doi.org/10.3389/fmicb.2018.00452.

LaFrentz, B. R., A. E. Goodwin, and C. A. Shoemaker. 2012. Book Chapter, 3. In *Columnaris Disease*. FHS Blue Book: Diagnostic Procedures for Finfish and Shellfish Pathogens; AFS-FHS (American Fisheries Society-Fish Health Section).

LaFrentz, B. R., L. H. Khoo, M. L. Lawrence, et al. 2024. *Flavobacterium covae* is the Predominant Species of Columnaris-Causing Bacteria Impacting the Channel Catfish Industry in the Southeastern United States. *Journal of Aquatic Animal Health,* 36, no. 1: 3–15. https://doi.org/10.1002/aah.10207.

LaFrentz, B. R., and P. H. Klesius. 2009. Development of a Culture Independent Method to Characterize the Chemotactic Response of *Flavobacterium columnare* to Fish Mucus. *Journal of Microbiological Methods,* 77: 37–40. https://doi.org/10.1016/j.mimet.2008.12.011.

LaFrentz, B. R., S. Králová, C. R. Burbick, et al. 2022. The Fish Pathogen *Flavobacterium columnare* Represents Four Distinct Species: *Flavobacterium columnare*, *Flavobacterium covae* sp. nov., *Flavobacterium davisii* sp. nov. and *Flavobacterium oreochromis* sp. nov., and Emended Description of *Flavobacterium columnare*. *Systematic and Applied Microbiology,* 45: 126293. https://doi.org/10.1016/j.syapm.2021.126293.

LaFrentz, B. R., G. C. Waldbieser, T. J. Welch, and C. A. Shoemaker. 2014. Intragenomic Heterogeneity in the 16S rRNA Genes of *Flavobacterium columnare* and Standard Protocol for Genomovar Assignment. *Journal of Fish Diseases,* 37: 657–669. https://doi.org/10.1111/jfd.12166.

Lan, M. Z., X. Peng, M. Y. Xiang, et al. 2007. Construction and Characterization of a Live, Attenuated esrB Mutant of *Edwardsiella tarda* and Its Potential as a Vaccine Against the Haemorrhagic Septicaemia in Turbot, *Scophthamus maximus* (L.). *Fish & Shellfish Immunology,* 23: 521–530. https://doi.org/10.1016/j.fsi.2006.11.002.

Lange, M. D., J. Abernathy, and B. D. Farmer. 2019. Evaluation of a Recombinant *Flavobacterium columnare* DnaK Protein Vaccine as a Means of Protection Against Columnaris Disease in Channel Catfish (*Ictalurus punctatus*). *Frontiers in Immunology,* 10: 1175. https://doi.org/10.3389/fimmu.2019.01175.

Lange, M. D., J. Abernathy, B. D. Farmer, and B. H. Beck. 2021. Use of an Immersion Adjuvant With a *Flavobacterium columnare* Recombinant Protein Vaccine in Channel Catfish. *Fish & Shellfish Immunology,* 117: 136–139. https://doi.org/10.1016/j.fsi.2021.07.025.

Langemann, T., V. J. Koller, A. Muhammad, P. Kudela, U. B. Mayr, and W. Lubitz. 2010. The Bacterial Ghost Platform System: Production and Applications. *Bioengineered Bugs,* 1, no. 5: 326–336. https://doi.org/10.4161/bbug.1.5.12540.

Lawrence, M. L., M. M. Banes, and M. L. Williams. 2001. Phenotype and Virulence of a Transposon-Derived Lipopolysaccharide O Side-Chain Mutant Strain of *Edwardsiella ictaluri*. *Journal of Aquatic Animal Health,* 13: 291–299.

Lawrence, M. L., R. K. Cooper, and R. L. Thune. 1997. Attenuation, Persistence, and Vaccine Potential of an *Edwardsiella ictaluri* purA Mutant. *Infection and Immunity,* 65: 4642–4651. https://doi.org/10.1128/iai.65.11.4642-4651.1997.

Leadbetter, E. R. 1974. The Genus *Flexibacter*. In *Bergey's Manual of Determinative Bacteriology*, edited by R. E. Buchanan and N. E. Gibbons, 8th ed., 105–107. Williams and Wilkins.

Leal, C. A. G., G. A. Carvalho-Castro, P. S. C. Sacchetin, C. O. Lopes, A. M. Moraes, and H. C. P. Figueiredo. 2010. Oral and Parenteral Vaccines Against *Flavobacterium columnare*: Evaluation of Humoral Immune Response by ELISA and *In Vivo* Efficiency in Nile Tilapia (*Oreochromis niloticus*). *Aquaculture International,* 18, no. 4: 657–666. https://doi.org/10.1007/s10499-009-9287-x.

Li, C., B. H. Beck, and E. Peatman. 2014. Nutritional Impacts on Gene Expression in the Surface Mucosa of Blue Catfish (*Ictalurus furcatus*). *Developmental and Comparative Immunology,* 44: 226–234. https://doi.org/10.1016/j.dci.2013.12.014.

Li, N., Y. Zhu, B. R. LaFrentz, et al. 2017. The Type IX Secretion System Is Required for Virulence of the Fish Pathogen *Flavobacterium columnare*. *Applied and Environmental Microbiology,* 83, no. 23: e01769-17. https://doi.org/10.1128/AEM.01769-17.

Liewes, E. W., R. H. VanDam, M. G. Vos-Mass, and R. Bootsma. 1982. Presence of Antigen Sensitized Leukocytes in Carp (*Cyprius carpio* L.) Following Bath Immunization Against *Flexibacter columnaris*. *Veterinary Immunology and Immunopathology,* 3: 603–609.

Liu, G. Y., P. Nie, J. Zhang, and N. Li. 2008. Proteomic Analysis of the Sarcosine-Insoluble Outer Membrane Fraction of *Flavobacterium columnare*. *Journal of Fish Diseases,* 31: 269–276. https://doi.org/10.1111/j.1365-2761.2007.00898.x.

Liu, L., C. Li, B. Su, B. H. Beck, and E. Peatman. 2013. Short-Term Feed Deprivation Alters Immune Status of Surface Mucosa in Channel Catfish (*Ictalurus punctatus*). *PLoS One,* 8, no. 9: e74581. https://doi.org/10.1371/journal.pone.0074581.

Liu, Y., and Z. Bi. 2007. Potential Use of a Transposon Tn916-Generated Mutant of *Aeromonas hydrophila* J-1 Defective in Some Exoproducts as a Live Attenuated Vaccine. *Preventive Veterinary Medicine,* 78: 79–84. https://doi.org/10.1016/j.prevetmed.2006.09.004.

Liu, Z. X., G. Y. Liu, N. Li, F. S. Xiao, H. X. Xie, and P. Nie. 2012. Identification of Immunogenic Proteins of *Flavobacterium columnare* by Two-Dimensional Electrophoresis Immunoblotting With Antibacterial Sera From Grass Carp, *Ctenopharyngodon idella* (Valenciennes). *Journal of Fish Diseases,* 35: 255–263. https://doi.org/10.1111/j.1365-2761.2011.01340.x.

Loch, T.P. and Faisal, M., 2015. Polyphasic Characterization Reveals the Presence of Novel Fish-Associated *Chryseobacterium* spp. in the Great Lakes of North America. *Diseases of Aquatic Organisms*, 113, pp.113-125. https://doi.org/10.3354/dao02819

Loch, T.P. and Faisal, M., 2015. Emerging Flavobacterial Infections in Fish: A Review. *Journal of Advanced Research*, 6(3), pp.283-300. https://doi.org/10.1016/j.jare.2014.10.009

Lorenzen, E., Dalsgaard, I. and Bernardet, J.F., 1997. Characterization of Isolates of *Flavobacterium psychrophilum* Associated with Coldwater Disease or Rainbow Trout Fry Syndrome I: Phenotypic and Genomic Studies. *Diseases of Aquatic Organisms*, 31, pp.197-208. https://doi.org/10.3354/dao

Luo, Z., J. Fu, N. Li, et al. 2016. Immunogenic Proteins and Their Vaccine Development Potential Evaluation in Outer Membrane Proteins (OMPs) of *Flavobacterium columnare*. *Aquaculture and Fisheries,* 1: 1–8. https://doi.org/10.1016/j.aaf.2016.10.002.

Luo, Z., Z. Liu, J. Fu, Q. Zhang, B. Huang, and P. Nie. 2016. Immunogenicity and Protective Role of Antigenic Regions From Five Outer Membrane Proteins of *Flavobacterium columnare* in Grass Carp *Ctenopharyngodon idella*. *Chinese Journal of Oceanology and Limnology,* 34: 1247–1257. https://doi.org/10.1007/s00343-016-5096-z.

Malecki, J. K., L. A. Roy, C. R. Arias, et al. 2021. Bioeconomic Analysis of *Flavobacterium columnare* Vaccine Pond Trials With Channel Catfish. *North American Journal of Aquaculture,* 83, no. 3: 207–217. https://doi.org/10.1002/naaq.10191.

Mano, N., T. Inui, D. Arai, H. Hirose, and Y. Y. Deguchi. 1996. Immune Response in the Skin of Eel Against *Cytophaga columnaris*. *Fish Pathology,* 31: 65–70.

Mohammed, H., O. Olivares-Fuster, S. LaFrentz, and C. R. Arias. 2013. New Attenuated Vaccine Against Columnaris Disease in Fish: Choosing the Right Parental Strain Is Critical for Vaccine Efficacy. *Vaccine,* 31: 5276–5280. https://doi.org/10.1016/j.vaccine.2013.08.052.

Mohd-Aris, A., M. Z. Saad, H. M. Daud, M. T. Yusof, and M. Y. Ina-Salwany. 2019. *Vibrio harveyi* Protease Deletion Mutant as a Live Attenuated Vaccine Candidate Against Vibriosis and Transcriptome Profiling Following Vaccination for *Epinephelus fuscoguttatus*. *Aquaculture International,* 27, no. 1: 125–140. https://doi.org/10.1007/s10499-018-0311-x.

Moore, A. A., M. E. Eimers, and M. A. Cardella. 1990. Attempts to Control *Flexibacter columnaris* Epizootics in Pond-Reared Channel Catfish by Vaccination. *Journal of Aquatic Animal Health,* 2: 109–111.

Moral, C. H., E. F. del Castillo, P. L. Fierro, et al. 1998. Molecular Characterization of the *Aeromonas Hydrophila aroA* Gene and Potential Use of an Auxotrophic *aroA* Mutant as a Live Attenuated Vaccine. *Infection and Immunity,* 66: 1813.

Mudarris, M. and Austin, B. 1989. Systemic Disease in Turbot *Scophthalmus maximus* Caused by a Previously Unrecognised *Cytophaga* Like Bacterium. *Diseases of Aquatic Organisms*, 6, pp.161-166.

Nascimento, I. P., and L. C. C. Leite. 2012. Recombinant Vaccines and the Development of New Vaccine Strategies. *Brazilian Journal of Medical and Biological Research,* 45, no. 12: 1102–1111. https://doi.org/10.1590/s0100-879x2012007500142.

Norqvist, A., Å. Hagström, and H. A. N. S. Wolf-Watz. 1989. Protection of Rainbow Trout Against Vibriosis and Furunculosis by the Use of Attenuated Strains of *Vibrio anguillarum*. *Applied and Environmental Microbiology,* 55: 1400–1405. https://doi.org/10.1128/aem.55.6.1400-1405.1989.

Oh, W.T., Jun, J.W., Giri, S.S., Yun, S., Kim, H.J., Kim, S.G., Kim, S.W., Han, S.J., Kwon, J. and Park, S.C., 2020. Isolation of *Chryseobacterium siluri* sp. nov., from Liver of Diseased Catfish (*Silurus asotus*). *Heliyon*, 6(2). https://doi.org/10.1016/j.heliyon.2020.e03454

Olivares-Fuster, O., and C. R. Arias. 2011. Development and Characterization of Rifampicin- Resistant Mutants From High Virulent Strains of *Flavobacterium columnare*. *Journal of Fish Diseases,* 34: 385–394. https://doi.org/10.1111/j.1365-2761.2011.01253.x.

Olivares-Fuster, O., J. L. Baker, J. S. Terhune, C. A. Shoemaker, P. H. Klesius, and C. R. Arias. 2007. Host-Specific Association Between *Flavobacterium columnare* Genomovars and Fish Species. *Systematic and Applied Microbiology,* 30, no. 8: 624–633. https://doi.org/10.1016/j.syapm.2007.07.003.

Olivares-Fuster, O., J. S. Terhune, C. A. Shoemaker, and C. R. Arias. 2010. Cloning, Expression, and Immunogenicity of *Flavobacterium columnare* Heat Shock Protein DnaJ. *Journal of Aquatic Animal Health,* 22: 78–86.

Ordal, E. J., and R. R. Rucker. 1944. Pathogenic Myxobacteria. *Proceedings of the Society for Experimental Biology and Medicine,* 56, no.1: 15–18. https://doi.org/10.3181/00379727-56-14572.

Oren, A., and G. Garrity. 2022. Valid Publication of New Names and New Combinations Effectively Published Outside the IJSEM. *International Journal of Systematic and Evolutionary Microbiology,* 72, no. 5: 5331. https://doi.org/10.1099/ijsem.0.005096.

Pallen, S., Madhavan, A., Subhashree, S., MR, V., Lal, P.B., Mukhopadhyay, C., Herai, R., Ghosh Dastidar, S. and Ghosh Dastidar, R. 2026. Secretion systems shaping host–pathogen interactions in *Burkholderia* species. *Applied Microbiology and Biotechnology*. https://doi.org/10.1007/s00253-026-13833-x

Peatman, E., C. Li, B. C. Peterson, D. L. Straus, B. D. Farmer, and B. H. Beck. 2013. Basal Polarization of the Mucosal Compartment in *Flavobacterium columnare* Susceptible and Resistant Channel Catfish (*Ictalurus punctatus*). *Molecular Immunology,* 56: 317–327. https://doi.org/10.1016/j.molimm.2013.04.014.

Plumb, J. A., and L. A. Hanson. 2010. *Health Maintenance and Principal Microbial Diseases of Cultured Fishes*. John Wiley & Sons. https://doi.org/10.1002/9780470958353.

Qiao, S., Wang, T., Sun, J., Han, J., Dai, H., Du, M., Yang, L., Guo, C.J., Liu, C., Liu, S.J. and Liu, H., 2025. Cross-feeding-based rational design of a probiotic combination of *Bacterides xylanisolvens* and *Clostridium butyricum* therapy for metabolic diseases. *Gut Microbes*, 17(1), p.2489765. https://doi.org/10.1080/19490976.2025.2489765

Ranganathan, S. and Garg, G. 2009. Secretome: clues into pathogen infection and clinical applications. *Genome Medicine*, 1(11), p.113. https://doi.org/10.1186/gm113

Rodrigues, A. P., D. Hirsch, H. C. P. Figueiredo, P. V. R. Logato, and A. M. Moraes. 2006. Production and Characterisation of Alginate Microparticles Incorporating *Aeromonas hydrophila* Designed for Fish Oral Vaccination. *Process Biochemistry,* 41: 638–643. https://doi.org/10.1016/j.procbio.2005.08.010.

Rosselló, R., E. Garcia-Valdes, J. Lalucat, and J. Ursing. 1991. Genotypic and Phenotypic Diversity of *Pseudomonas stutzeri*. *Systematic and Applied Microbiology,* 14:150–157. https://doi.org/10.1016/S0723-2020(11)80294-8.

Rucker, R. R., B. J. Earp, and E. J. Ordal. 1954. Infectious Diseases of Pacific Salmon. *Transactions of the American Fisheries Society,* 83: 297–312. https://doi.org/10.1577/1548-8659(1953)83%5b297:idops%5d2.0.co;2.

Sayed, M., L. Narayanan, M. Essa, M. Lawrence, A. Karsi, and H. Abdelhamed. 2023. Secreted Extracellular Products of *Flavobacterium covae* as Potential Immunogenic Factors for Protection Against Columnaris Disease in Channel Catfish (*Ictalurus punctatus*). *Pathogens,* 12, no. 6: 808. https://doi.org/10.3390/pathogens12060808.

Schachte, J. H., Jr., and E. C. Mora. 1973. Production of Agglutinating Antibodies in the Channel Catfish (*Ictalurus punctatus*) Against *Chondrococcus columnaris*. *Journal of the Fisheries Board of Canada,* 30: 116–118. https://doi.org/10.1139/f73-017.

Schurig, G. G., R. M. Roop II, T. Bagchi, S. Boyle, D. Buhrman, and N. Sriranganathan. 1991. Biological Properties of RB51; A Stable Rough Strain of *Brucella abortus*. *Veterinary Microbiology,* 28: 171–188. https://doi.org/10.1016/0378-1135(91)90091-S.

Shelby, R. A., C. A. Shoemaker, and P. H. Klesius. 2008. Passive Immunization of Channel Catfish *Ictalurus Punctatus* With Anti-*Flavobacterium columnare* Sera. *Diseases of Aquatic Organisms,* 77: 143–147. https://doi.org/10.3354/dao01828.

Shoemaker, C. A., P. H. Klesius, J. D. Drennan, and J. J. Evans. 2011. Efficacy of a Modified Live *Flavobacterium columnare* Vaccine in Fish. *Fish & Shellfish Immunology,* 30: 304–308. https://doi.org/10.1016/j.fsi.2010.11.001.

Shoemaker, C. A., P. H. Klesius, and J. J. Evans. 2002. *In Ovo* Methods for Utilizing the Modified Live *Edwardsiella ictaluri* Vaccine Against Enteric Septicemia in Channel Catfish. *Aquaculture,* 203: 221–227. https://doi.org/10.1016/S0044-8486(01)00631-7.

Shoemaker, C. A., P. H. Klesius, and J. J. Evans. 2005. *U.S. Patent No. 6,881,412*. U.S. Patent and Trademark Office.

Shoemaker, C. A., P. H. Klesius, and J. J. Evans. 2007. Immunization of Eyed Channel Catfish, *Ictalurus punctatus*, Eggs With Monovalent *Flavobacterium columnare* Vaccine and Bivalent *F. columnare* and *Edwardsiella ictaluri* Vaccine. *Vaccine,* 25: 1126–1131. https://doi.org/10.1016/j.vaccine.2006.09.055.

Shoemaker, C. A., P. H. Klesius, C. Lim, and M. Yildirim. 2003. Feed Deprivation of Channel Catfish, *Ictalurus punctatus*, (Rafinesque), Influenced Organosomatic Indices, Chemical Composition and Susceptibility to *Flavobacterium columnare*. *Journal of Fish Diseases,* 26: 553–561.

Shoemaker, C. A., and B. R. LaFrentz. 2015. Lack of Association Between *Flavobacterium columnare* Genomovar and Virulence in Hybrid Tilapia *Oreochromis niloticus* (L.) × *Oreochromis aureus* (Steindachner). *Journal of Fish Diseases,* 38: 491–498. https://doi.org/10.1111/jfd.12262.

Shoemaker, C. A., O. Olivares-Fuster, C. R. Arias, and P. H. Klesius. 2008. *Flavobacterium columnare* Genomovar Influences Mortality in Channel Catfish *Ictalurus punctatus*. *Veterinary Microbiology,* 127: 353–359. https://doi.org/10.1016/j.vetmic.2007.09.003.

Shoemaker, C. A., D. H. Xu, R. A. Shelby, and P. H. Klesius. 2005. Detection of Cutaneous Antibodies Against *Flavobacterium columnare* in Channel Catfish, *Ictalurus punctatus* (Rafinesque). *Aquaculture Research,* 36: 813–818. https://doi.org/10.1111/j.1365-2109.2004.01291.x.

Simonazzi, A., A. G. Cid, M. Villegas, A. I. Romero, S. D. Palma, and J. M. Bermúdez. 2018. Drug Targeting and Stimuli Sensitive Drug Delivery Systems. In *Nanotechnology*

Applications in Drug Controlled Release, 81–116. William Andrew Publishing. https://doi.org/10.1016/b978-0-12-813689-8.00003-3.

Song, Y. L., J. L. Fryer, and J. S. Rohovec. 1988. Comparison of Gliding Bacteria Isolated From Fish in North America and Other Areas of the Pacific Rim. *Fish Pathology,* 23, no. 3: 197–202. https://doi.org/10.3147/jsfp.23.197.

Soto, E., M. J. Mauel, A. Karsi, and M. L. Lawrence. 2008. Genetic and Virulence Characterization of *Flavobacterium columnare* From Channel Catfish (*Ictalurus punctatus*). *Journal of Applied Microbiology,* 104, no. 5: 1302–1310. https://doi.org/10.1111/j.1365-2672.2007.03632.x.

Starliper, C. E., and W. B. Schill. 2011. Flavobacterial Diseases: Columnaris Disease, Coldwater Disease and Bacterial Gill Disease. In *Volume 3: Viral, Bacterial and Fungal Infections*, edited by D. a. D. Fish, 606–631. CABI. https://doi.org/10.1079/9781845935542.0606.

Sun, F., E. Peatman, C. Li, et al. 2012. Transcriptomic Signatures of Attachment, NF-kB Suppression and IFN Stimulation in the Catfish Gill Following Columnaris Bacterial Infection. *Developmental and Comparative Immunology,* 38: 169–180.

Suomalainen, L.-R., H. Kunttu, E. T. Valtonen, V. Hirela-Koski, and M. Tiirola. 2006. Molecular Diversity and Growth Features of *Flavobacterium columnare* Strains Isolated in Finland. *Diseases of Aquatic Organisms,* 70: 55–61. https://doi.org/10.3354/dao070055.

Suomalainen, L. R., M. Tiirola, and E. T. Valtonen. 2006. Chondroitin AC Lyase Activity Is Related to Virulence of Fish Pathogenic *Flavobacterium columnare*. *Journal of Fish Diseases,* 29: 757–763. https://doi.org/10.1111/j.1365-2761.2006.00771.x.

Suomalainen, L. R., M. A. Tiirola, and E. T. Valtonen. 2005. Influence of Rearing Conditions on *Flavobacterium columnare* Infection of Rainbow Trout, *Oncorhynchus mykiss* (Walbaum). *Journal of Fish Diseases,* 28, no. 5: 271–277. https://doi.org/10.1111/j.1365-2761.2005.00631.x.

Tammas, I., K. Bitchava, and A. I. Gelasakis. 2024. Transforming Aquaculture Through Vaccination: A Review on Recent Developments and Milestones. *Vaccine,* 12, no. 7: 732. https://doi.org/10.3390/vaccines12070732.

Tekedar, H. C., A. Karsi, A. F. Gillaspy, et al. 2012. Genome Sequence of the Fish Pathogen *Flavobacterium columnare* ATCC 49512. *Journal of Bacteriology,* 194, no. 10: 2763–2764. https://doi.org/10.1128/JB.00281-12.

Thomas-Jinu, S., and A. E. Goodwin. 2004. Morphological and Genetic Characteristics of *Flavobacterium columnare* Isolates: Correlations With Virulence in Fish. *Journal of Fish Diseases,* 27: 29–35. https://doi.org/10.1046/j.1365-2761.2003.00507.x.

Thune, R. L., L. A. Stanley, and R. K. Cooper. 1993. Pathogenesis of Gram-Negative Bacterial Infections in Warmwater Fish. *Annual Review of Fish Diseases,* 3: 37–68. https://doi.org/10.1016/0959-8030(93)90028-A.

Thunes, N. C., R. A. Conrad, H. H. Mohammed, et al. 2022. Type IX Secretion System Effectors and Virulence of the Model *Flavobacterium columnare* Strain MS-FC-4. *Applied and Environmental Microbiology,* 88, no. 3: e01705–e01721. https://doi.org/10.1128/aem.01705-21.

Thunes, N. C., H. H. Mohammed, J. P. Evenhuis, et al. 2023. Secreted Peptidases Contribute to Virulence of Fish Pathogen *Flavobacterium columnare*. *Frontiers in Cellular and Infection Microbiology,* 13: 1093393. https://doi.org/10.3389/fcimb.2023.1093393.

Tongsri, P., K. Meng, X. Liu, et al. 2020. The Predominant Role of Mucosal Immunoglobulin IgT in the Gills of Rainbow Trout (*Oncorhynchus mykiss*) After Infection With *Flavobacterium columnare*. *Fish & Shellfish Immunology,* 99: 654–662. https://doi.org/10.1016/j.fsi.2020.01.044.

Toyama, T., K. Kita-Tsukamoto, and H. Wakabayashi. 1996. Identification of *Flexibacter maritimus*, *Flavobacterium branchiophilum* and *Cytophaga columnaris* by PCR Targeted 16S Ribosomal DNA. *Fish Pathology,* 31: 25–31. https://doi.org/10.3147/jsfp.31.25.

Triyanto, and H. Wakabayashi. 1999. Genotypic Diversity of Strains of *Flavobacterium columnare* From Diseased Fishes. *Fish Pathology,* 34: 65–71

Tumree, P., A. Bunnoy, X. Tang, and P. Srisapoome. 2024. Efficacy of Whole-Cell-Based Monovalent and Bivalent Vaccines Against *Streptococcus iniae* and *Flavobacterium covae* in Fingerling Asian Seabass (*Lates calcarifer*). *Fish & Shellfish Immunology,* 144: 109269. https://doi.org/10.1016/j.fsi.2023.109269.

United States Department of Agriculture Animal and Plant Health Inspection Service. 2025. Licensed Veterinary Biological Product Information-Currently Licensed Biologics for Aquatic Animals. https://www.aphis.usda.gov/veterinary-biologics/licensed-products.

Ursing, J. B., R. A. Rossello-Mora, E. Garcia-Valdes, and J. Lalucat. 1995. Taxonomic Note: A Pragmatic Approach to the Nomenclature of Phenotypically Similar Genomic Groups. *International Journal of Systematic and Evolutionary Microbiology,* 45: 604. https://doi.org/10.1099/00207713-45-3-604.

Vandamme, P., Bernardet, J.F., Segers, P., Kersters, K. and Holmes, B., 1994. New Perspectives in the Classification of the Flavobacteria: Description of *Chryseobacterium* gen. nov., *Bergeyella* gen. nov., and *Empedobacter* nom. rev. *International Journal of Systematic and Evolutionary Microbiology*, 44(4), pp.827-831. https://doi.org/10.1099/00207713-44-4-827

Vivas, J., J. Riaño, B. Carracedo, et al. 2004. The Auxotrophic *aroA* Mutant of *Aeromonas hydrophila* as a Live Attenuated Vaccine Against *A. salmonicida* Infections in Rainbow Trout (*Oncorhynchus mykiss*). *Fish & Shellfish Immunology,* 16: 193–206. https://doi.org/10.1016/S1050-4648(03)00078-0.

Wakabayashi, H. 1991. Effect of Environmental Conditions on the Infectivity of *Flexibacter columnaris* to Fish. *Journal of Fish Diseases,* 14: 279–290. https://doi.org/10.1111/j.1365-2761.1991.tb00825.x.

Warsi, O.M., Gedda, L., Edwards, K. and Andersson, D.I., 2023. Vesicle-Enriched Secretomes Alter Bacterial Competitive Abilities and are Drivers of Evolution in Microbial Communities. *FEMS Microbiology Ecology*, 99(12), p.fiad141. https://doi.org/10.1093/femsec/fiad141

Wise, A.L., LaFrentz, B.R., Kelly, A.M., Khoo, L.H., Xu, T., Liles, M.R. and Bruce, T.J., 2021. A Review of Bacterial Co-Infections in Farmed Catfish: Components, Diagnostics, and Treatment Directions. *Animals*, 11(11), p.3240. https://doi.org/10.3390/ani11113240

Wise, A.L., LaFrentz, B.R., Kelly, A.M., Liles, M.R., Griffin, M.J., Beck, B.H. and Bruce, T.J., 2023. The Infection Dynamics of Experimental *Edwardsiella ictaluri* and *Flavobacterium covae* Coinfection in Channel Catfish (*Ictalurus punctatus*). *Pathogens*, 12(3), p.462. https://doi.org/10.3390/pathogens12030462

Welker, T. L., C. A. Shoemaker, C. R. Arias, and P. H. Klesius. 2005. Transmission and Detection of *Flavobacterium columnare* in Channel Catfish *Ictalurus punctatus*. *Diseases of Aquatic Organisms,* 63: 129–138. https://doi.org/10.3354/dao063129.

Wise, A.L., LaFrentz, B.R., Kelly, A.M., Liles, M.R., Griffin, M.J., Beck, B.H. and Bruce, T.J., 2025. Coinfection of Channel Catfish (*Ictalurus punctatus*) with Virulent *Aeromonas hydrophila* and *Flavobacterium covae* Exacerbates Mortality. *Journal of Fish Diseases*, 48(8), p.e13912. DOI: 10.1111/jfd.13912

Xie, H. X., P. Nie, M. X. Chang, Y. Liu, and W. J. Yao. 2005. Gene Cloning and Functional Analysis of Glycosaminoglycan-Degrading Enzyme Chondroitin AC Lyase From *Flavobacterium columnare* G4. *Archives of Microbiology,* 184: 49–55. https://doi.org/10.1007/s00203-005-0009-0.

Zubair, M., Khan, F.A., Menghwar, H., Faisal, M., Ashraf, M., Rasheed, M.A., Marawan, M.A., Dawood, A., Chen, Y., Chen, H. and Guo, A., 2020. Progresses on Bacterial Secretomes Enlighten Research on Mycoplasma Secretome. *Microbial Pathogenesis*, 144, p.104160. https://doi.org/10.1016/j.micpath.2020.104160

Zhang, D., W. Thongda, C. Li, et al. 2017. More Than Just Antibodies: Protective Mechanisms of a Mucosal Vaccine Against Fish Pathogen *Flavobacterium columnare*. *Fish & Shellfish Immunology,* 71: 160–170. https://doi.org/10.1016/j.fsi.2017.10.001.

Zhang, D., G. Zhou, W. Thongda, et al. 2024. Early Divergent Responses to Virulent and Attenuated Vaccine Isolates of *Flavobacterium covae* sp. nov. in Channel

Catfish, *Ictalurus punctatus*. *Fish & Shellfish Immunology,* 144: 109248. https://doi.org/10.1016/j.fsi.2023.109248.

Zhang, Y., C. R. Arias, C. A. Shoemaker, and P. H. Klesius. 2006. Comparison of Lipopolysaccharide and Protein Profiles Between *Flavobacterium columnare* Strains From Different Genomovars. *Journal of Fish Diseases,* 29: 657–663. https://doi.org/10.1111/j.1365-2761.2006.00760.x 2006.

Zhang, Y., P. Nie, and L. Lin. 2016. Complete Genome Sequence of the Fish Pathogen *Flavobacterium columnare* Pf1. *Genome Announcements,* 4: e00900. https://doi.org/10.1128/genomeA.00900-16.

Zhu, W., G. Yang, Y. Zhang, J. Yuan, and L. An. 2012. Generation of Biotechnology-Derived *Flavobacterium columnare* Ghosts by PhiX174 Gene E-Mediated Inactivation and the Potential as Vaccine Candidates Against Infection in Grass Carp. *Journal of Biomedicine and Biotechnology,* 2012: 760730. https://doi.org/10.1155/2012/760730.

Zügel, U., and S. H. Kaufmann. 1999. Role of Heat Shock Proteins in Protection From and Pathogenesis of Infectious Diseases. *Clinical Microbiology Reviews,* 12: 19–39. https://doi.org/10.1128/CMR.12.1.19.

Chapter II

Development and Evaluation of Rifampicin-Attenuated Flavobacterium spp. Mutants as Vaccine Candidates Against Columnaris Disease

2.1 Abstract

Columnaris disease, caused by columnaris-causing bacteria (CCB) including *Flavobacterium columnare*, *F. covae*, *F. davisii*, and *F. oreochromis*, remains a major disease issue for channel catfish (*Ictalurus punctatus*) and Nile tilapia (*Oreochromis niloticus*) aquaculture. In this study, rifampicin-resistant mutants were generated from ten virulent CCB parent strains and evaluated for attenuation in channel catfish and Nile tilapia via immersion challenge. Comparisons in mean cumulative percent mortality (CPM) was assessed for each parent and mutant strain across of range of volume-dependent doses in across two separate laboratories. Most mutant isolates exhibited reduced virulence compared to their corresponding parent strains. *F. covae* mutant isolates ALG-00-530, FBCC-CC-12K, ML-17-22A, IPRS-15-49, and ALG-15-231, and *F. oreochromis* R18-27 demonstrated reduced or no virulence compared to their parent strain. *F. davisii* parent strain doses of TN-3-2012 and ARS-15-12 resulted in low CPM, however, their corresponding mutant strain doses resulted in 0% CPM. Comparative genomic analysis revealed that mutations within the DNA-directed RNA polymerase beta subunit gene (*rpoB*) were present in all mutant strains except for *F. davisii* TN-30-2012 and *F. oreochromis* BZ-

1-02. However, additional mutations affecting stress response, nutrient acquisition, cell structure, and regulatory pathways were also identified via genome analysis, suggesting attenuation is multifactorial. Overall, rifampicin resistance effectively generated attenuated CCB strains across two fish species, supporting their potential as live-attenuated vaccine candidates for the control of columnaris disease in production aquaculture.

2.2. Introduction

Columnaris disease is one of the leading causes of disease-related losses in the southeastern United States aquaculture sector (Peterman & Posadas, 2019; Abdelrahman et al., 2023). LaFrentz et al. (2022) revealed that the disease is caused by four distinct *Flavobacterium* species, also known as columnaris-causing bacteria (CCB), including *F. columnare*, *F. covae*, *F. davisii*, and *F. oreochromis*. Notably, each CCB species is associated with virulence in specific host species (LaFrentz et al., 2018, 2024), underscoring the biological relevance of CCB diversity and its role in understanding pathogenesis. CCB are gram-negative, yellow-pigmented bacteria that infect external tissues of fish, like skin and gills (Wakabayashi, 1991). Outbreaks of columnaris disease typically occur at elevated water temperatures (above 25°C) and when fish are stressed (Starliper and Schill, 2011). Since CCB are believed to be ubiquitous in freshwater environments, the best approach is to incorporate proactive and preventive therapies to prevent columnaris disease. Several antimicrobials have been approved for use in aquaculture production to treat columnaris disease; however, there are growing concerns

about antimicrobial resistance. As such, alternative strategies are being strongly considered as best practices in production.

Vaccination against columnaris disease has been extensively studied and efforts to develop an efficacious vaccine at the production level are a high priority. Many different types of columnaris vaccines have been tested, including killed, live-attenuated, recombinant, and encapsulated vaccines (Harrison et al., 2025). Killed vaccines are considered safe and are easy to produce, however they typically require an adjuvant to produce a robust immune response, and the method used to kill the pathogen could affect immunogenicity (Baxter, 2007; Bader et al., 1997). In contrast, recombinant vaccines offer highly specific and targeted immunity but require careful antigen selection to achieve strong immunity (Nascimento and Leite, 2012). Whereas encapsulated vaccines can enhance delivery and mucosal uptake, but they can be complex to formulate and have shown variable efficacy (Ahmed et al., 2024; Tammas et al., 2024; Kitiyodom et al., 2019; Kitiyodom et al., 2021).

Among the different types of vaccines, live-attenuated vaccines offer the ability to provide greater humoral and cell-mediated responses and typically do not require adjuvants (Ma, Bruce, Jones, and Cain, 2019). These vaccines contain weakened microorganisms that can still infect the host but not cause disease. Live-attenuated vaccines also have the advantage over other types of vaccines by replicating within the host, being easier to deliver (e.g., immersion or oral), being cheaper to manufacture, and are scalable for commercial settings (Shoemaker, Klesius, Evans, and Arias, 2009). However, there are concerns regarding the risk of reversion to virulence which can make

safety evaluation and licensing rigorous and time-consuming. Therefore, understanding the mechanisms of attenuation is imperative for vaccine development and safety testing.

There are several different methods used to attenuate a microorganism, such as serial passage on media, chemical or physical mutagenesis, passage in an unsusceptible host, the use of an environmental bacterium that mimics the target pathogen's antigenic structure, and genetic engineering by manipulation of metabolic pathway(s) or virulence gene(s) (Shoemaker, Klesius, Evans, and Arias, 2009). For gram-negative bacteria, the creation of rifampicin-resistant mutants has led to efficacious vaccine candidates against *Brucella abortus* and *Francisella tularensis* (Schurig et al., 1991; Bhatnagar et al., 1994). Rifampicin is a broad-spectrum antibiotic that inhibits bacterial RNA polymerase by binding to the beta subunit encoded by the *rpoB* gene. Resistance occurs when mutations within the *rpoB* gene prevent rifampicin from binding to RNA polymerase (Goldstein, 2014). Attenuation of a bacterium with rifampicin is achieved by serial passage on growth media supplemented with increasing concentrations of rifampicin (Schurig et al., 1991). The development of rifampicin-attenuated or “rough” strains of gram-negative bacteria (i.e., lacking the O-antigen chain in the lipopolysaccharides; an important virulence factor) results in a weakened or non-virulent strain (Schurig et al., 1991; Klesius and Shoemaker, 1999; Arias et al., 2003; Zhang et al., 2006).

In aquaculture specifically, the use of rifampicin attenuation has proven to be quite effective in producing vaccines against gram-negative bacterial fish pathogens like *F. psychrophilum* (LaFrentz, LaPatra, Call, and Cain, 2008) and *Edwardsiella ictaluri* (Wise, Greenway, Byars, Griffin, and Khoo, 2015). There is a live-attenuated vaccine for

columnaris disease that was derived from a rifampicin-resistant *F. columnare* isolate and is licensed for use in channel catfish (*Ictalurus punctatus*) and largemouth bass (*Micropterus salmoides*; Shoemaker, Klesius, and Evans, 2005). However, its efficacy at the production level has been questionable and is no longer being produced (Kirkland, 2010; Bebak and Wagner, 2012). One possible explanation for inconsistent efficacy could be that it was made using an *F. columnare* isolate, which is not prominent in the U.S. channel catfish industry (LaFrentz et al., 2024). A previous study also demonstrated that vaccination of channel catfish using a rifampicin-resistant *F. covae* mutant provided greater protection than vaccination with a *F. columnare* isolate (Mohammed, Olivares-Fuster, LaFrentz, and Arias, 2013). Therefore, given the variability in protection, a larger study evaluating multiple CCB species and strains is warranted.

With the resolution of four distinct CCB species causing columnaris disease and having specific host species associations, the overarching goal is to identify promising live-attenuated CCB vaccine candidates for channel catfish and Nile tilapia. It is hypothesized that by generating a live-attenuated strain that is associated with virulence in the targeted host species, immunization may elicit a protective immune response against the virulent parent strain. To accomplish this, virulent strains of CCB will be used to develop rifampicin-attenuated mutants and confirm attenuation *in vivo*. To understand the mechanism of attenuation, comparative genome analysis between parent and mutant strains can help identify mutations potentially leading to attenuation and possible trends among CCB species.

2.3. Materials and Methods

2.3.1. Development of Rifampicin-Resistant Mutants

CCB parent strains, including five *F. covae*, two *F. davisii*, and three *F. oreochromis,* were selected based on their demonstrated virulence in either channel catfish or Nile tilapia and belong to the species most associated with catfish and tilapia aquaculture (Table 2.7.1). Frozen glycerol stock CCB parent isolates were revived on modified Shieh agar plates (MSA; LaFrentz and Klesius, 2009) and incubated for 48 h at 28 °C. Single colonies were picked and transferred to MSA plate containing 0.01 µg mL^{-1} of rifampicin (Thermo Fisher Scientific, Waltham, MA) and grown for 48 h at 28 °C. After 48 h of incubation, individual colonies were transferred to another MSA plate containing a higher rifampicin concentration (0.05 µg mL^{-1}) and the procedure was continued until reaching a final concentration of 500 µg mL^{-1}. Pure, rifampicin-resistant isolates were supplemented with 20% v/v glycerol and cryopreserved at -80 °C for storage.

2.3.2. Bacterial Preparation for Immersion Challenges

Parent and rifampicin-resistant mutants were revived from cryostock onto MSA and incubated for 48 h at 28 °C. Next, a single colony was picked and subcultured onto a fresh MSA plate and grown for an additional 24 h at 28 °C. Between 3-5 colonies were transferred to multiple 50 mL conical tubes containing 12 mL of modified Shieh broth (MSB) and incubated at 28 °C for 12 h at 175 rpm. Cultures were expanded by inoculating 30 mL of the 12-h culture into 1.2 L of MSB and incubated for an additional 12-16 h following the same incubation conditions. The optical density was read at 540 nm and adjusted to ~0.700,

which corresponded to approximately 10^6 CFU mL^{-1} and was previously associated with at least 50% CPM in pilot immersion challenges, depending on strain-specific virulence. A 1 mL sample of each bacterial culture was used to perform ten-fold serial dilutions to determine the concentration.

2.3.3. In vivo Attenuation Confirmation

Juvenile channel catfish (Delta Select strain) and Nile tilapia (~5-20 g) were transferred to individual tanks containing 38 L supplied with flow-through dechlorinated municipal water at 28°C and aeration. Tanks were randomized and assigned to 1 of 2 treatments (parent or mutant strain) and dose (by volume; 50, 100, 150, or 200 mL, for *F. covae* isolates, 50, 100, 200, or 400 mL for *F. davisii* isolates TN-3-2012 and ARS-15-12 and *F. oreochromis* isolate Costa Rica FC-04-TN^T, and 25, 50, and 100 mL for *F. oreochromis* R18-27), with each tank holding 25 fish with two replicate tanks per dose. *F. oreochromis* parent strain BZ-1-02 required a larger volume (500 mL) to elicit sufficient mortality to assess attenuation of the mutant strain, so only one dose was used. Doses for each fish species were determined in pilot challenges with the virulent parent strain, and range of doses was determined to observe dose-dependent mortality. One mock control tank was used for each parent/mutant pair. Prior to immersion, the water volume in each tank was lowered to 10 L and water flow was stopped for the duration of the 30-minute immersion. Bacterial concentration for each pair of parent and mutant strains for each attenuation confirmation immersion study is summarized in Table 2.6.2. Following the 30-minute immersion, water flow was restored and adjusted to 0.4 L min^{-1} and water volume adjusted

to 38 L. Water temperature was adjusted to 28.0 ± 1.0 °C and dissolved oxygen was around 8.3 ± 0.1 mg L^{-1}. Fish were offered food twice per day, and any uneaten food was removed from tanks. Each study lasted for approximately 7 days post-challenge, or until mortality ceased for 2 consecutive days, and cumulative percent mortality (CPM) was recorded. Additionally, 20% of daily tank mortalities were subjected to necropsy and bacterial cultures of the gills and posterior kidney were plated onto MSA for bacterial re-isolation and confirmation.

Select isolates, including *F. covae* ALG-00-530, *F. davisii* TN-3-2012, and *F. oreochromis* R18-27 parent and mutant strains were also tested for attenuation at the United States Department of Agriculture-Agriculture Research Services (USDA-ARS) Aquatic Animal Health Research Unit (AAHRU) in Auburn, AL, USA. Four doses of ALG-00-530 parent and mutant strains were tested without replication (38, 50, 100, and 200 mL), then, a second trial tested three doses of ALG-00-530 parent and mutant strains in two replicated tanks (Table 2.7.3). *F. davisii* parent and mutant strains of TN-3-2012 were tested with doses of 40, 75, 150, and 300 mL, and *F. oreochromis* parent and mutant strains were assessed using doses of 35, 70 140 and 280 mL. The average size of channel catfish was 2.2 ± 0.3 g and 2.4 ± 0.3 g, while the average size of Nile tilapia was 26.7 ± 1.5 and 27.4 ± 1.9 g. The experimental design involved two replicate tanks per parent and strain dose, with 25 fish per tank. Parent and mutant strains were administered via a constant flow immersion bath. Tanks holding 51 L of water were set to a flow rate of 0.5 L min^{-1}, then water was drained to 13 L. Bacteria was added to the 13 L of tank water, then the tanks were allowed to fill to the full 51 L volume. Fish were monitored and offered a

commercial diet twice daily. Mortalities were recorded to determine CPM of individual tanks, and necropsy of 20% of daily tank mortality was performed. Bacterial cultures of gill and posterior kidney were taken for bacterial re-isolation.

2.3.4. Bacterial DNA Extraction and PCR Confirmation

Bacterial isolates obtained from mortalities were purified and inoculated in MSB, pelleted, and stored at -20 °C. Bacterial DNA extraction was carried out with the Zymo Quick-DNA Fungal/Bacterial Miniprep Kit (Zymo Research, Irvine, CA, USA) according to the manufacturer's instructions. DNA concentrations were measured using a Nanodrop One^{c} (Thermo Fisher Scientific) and diluted to 5 ng mL^{-1}. Identification of bacteria re-isolated from mortalities was achieved using the CCB multiplex PCR protocol outlined by LaFrentz, Garcia, and Shelley (2019). The positive controls used were *F. columnare* IA-S-4, *F. covae* AL-02-36^{T}, *F. davisii* 90-106^{T}, and *F. oreochromis* Costa Rica 04-02-TN^{T}. Each PCR reaction (25 μL) consisted of 12.5 μL of 2X DreamTaq Hot Start Green PCR Master Mix (Thermo Fisher Scientific), 2.0 μL of primer mix, 5.5 μL of nuclease-free water, and 5.0 μL of DNA template. Amplification consisted of an initial denaturation at 95 °C of 5 minutes, followed by 40 cycles of 94 °C for 30 seconds, 56 °C for 20 seconds, and 72 °C for 1 minute, concluding with a final extension at 72 °C for 10 minutes. PCR products were separated on a 2% agarose gel at 75V for 1 h. Amplicon sizes of positive controls are 415, 320, 894, and 659 base pairs (bp), corresponding to *F. columnare*, *F. covae*, *F. davisii*, and *F. oreochromis*, respectively.

2.3.5. Whole Genome Sequencing of Parent and Mutant Isolates

All parent (n=10) and mutant (n=10) CCBs were revived onto MSA and incubated for 48 hours at 28 °C. Using a 10 μL inoculation loop, a "mass" of the 48-h culture was inoculated into 10 mL of MSB and incubated overnight at 28 °C and 175 rpm. Genomic DNA (gDNA) was extracted using the DNeasy PowerSoil Pro Kit (Qiagen, Hilden, Germany) following the manufacturer's protocol except for the homogenizing step, where samples were homogenized at 1,500 rpm for 5 minutes. Eluted DNA was quantified using the Qubit 3 (Thermo Fisher Scientific) and stored at 4 °C until library preparation.

Hybrid genomes of each parent and mutant strain were generated using a combination of long-read (Oxford Nanopore Technologies; ONT) and short-read (Illumina) sequencing technologies. Libraries for ONT were prepared using the rapid sequencing DNA v14 barcoding kit (SQK-RBK114.24) and sequenced on R10.4.1 flow cells. ONT reads were basecalled using the dna_r10.4.1_e8.2_sup@v3.5.1 model and filtered using NanoFilt (Version 2.8.0) with a minimum Phred quality score of 10 and minimum read length of 1,000 bp. Long-read assemblies were generated using Canu (Version 2.2). Illumina reads were adapter and quality-trimmed using Trimmomatic (Version 0.39). Trimmed Illumina reads were aligned to the ONT draft assemblies, and short-read-guided polishing was performed using Polypolish (Version 0.6.0) to correct errors and improve consensus accuracy. Quality assessment of individual parent and mutant genome assemblies was done using BUSCO (Benchmarking Universal Single-Copy Orthologs; Version 5.8.0; Seppey, Manni, and Zdobnov, 2019) and the flavobacteriales_odb10 dataset. Gene

prediction was performed using Prodigal for prokaryotic genomes (Version 2.6.3; Hyatt et al., 2010).

2.3.6. Annotation and Predicted Effectors

Parent and mutant genomes were annotated using the Rapid Annotation using Subsystem Technology for prokaryotic bacteria (RAST; Aziz et al., 2008). Annotated genomes were exported in GenBank format and uploaded to the Galaxy platform for comparative genomic analysis. Single nucleotide polymorphisms (SNPs) and small insertion/deletion variants were identified using Snippy (Version 4.6.0; Seemann, T., 2015), using default parameters and the annotated parent strain genome used as the reference for each corresponding mutant strain. Mutations identified by Snippy were functionally annotated using SnpEFF (Version 5.2; Cingolani et al., 2012). A custom SnpEFF database was constructed for each parent strain using the corresponding annotated GenBank file to ensure accurate prediction of mutation effects. Variants were classified based on predicted functional impact (e.g., synonymous, missense, nonsense, frameshift, insertion, and deletion). Variants predicted to result in amino acid substitutions (missense SNPs), as well as coding insertions and deletions, were further evaluated using the PROVEAN web server function (Protein Variation Effect Analyzer, Version 1.1.3; Choi, Sims, Murphy, Miller, and Chan, 2012; Choi and Chan, 2015) to predict their potential effect on protein function. For PROVEAN analysis, variants having a default threshold of a score equal to or below -2.5 (set to maximize the minimum of sensitivity and specificity; Choi et al., 2012) were

considered deleterious. Only non-synonymous variants located within coding regions were included in PROVEAN analysis.

2.3.7. Alignment of rpoB Genes

Protein sequences of the *rpoB* gene from *Flavobacterium covae*, *F. davisii*, and *F. oreochromis* were aligned using MAFFT in Geneious (version 2026.0.2, Katoh, Misawa, Kuma, and Miyata, 2002; Katoh and Standley, 2013). The *Escherichia coli* type strain (K-12 MG1655) *rpoB* sequence (NP_418414.1) was included as a reference for amino acid numbering. Alignment quality was assessed by visual inspection, and mutation positions were interpreted relative to the *E. coli* sequence numbering. The rifampicin-resistance determining region (RRDR) was defined based on its location in *E. coli*.

2.3.8. Statistical Analyses

Cumulative percent mortality data from attenuation confirmation trials were analyzed using GraphPad Prism (version 11.0.0). Differences in mean CPM between parent and mutant strains at each dose was assessed using independent, unpaired Welch's t-test. Significance was defined as $P < 0.05$.

2.4. Results

2.4.1. Rifampicin-Resistant Mutants and Attenuation Confirmation

The number of passages on increasing concentrations of rifampicin to reach resistance to 500 μg mL^{-1} was variable for each strain. For instance, *F. covae* ALG-00-530

mutant reached resistance to the target concentration of rifampicin in 31 passages, while another strain of *F. covae*, ML-17-22A, reached resistance to the same concentration after 75 passages (Table 2.7.1). This variability was noted among all three CCB species (*F. covae, F. davisii*, and *F. oreochromis*) and strains used in this study. Collectively, all ten CCB strains achieved resistance to 500 μg mL^{-1} of rifampicin.

Attenuation confirmation experiments at Auburn University and USDA-ARS AAHRU demonstrated that most rifampicin-resistant mutants exhibited reduced virulence compared to their corresponding parent strains in channel catfish and Nile tilapia. At Auburn University, all *F. covae* parent isolates caused moderate to high mortality, whereas mutants showed little to no mortality across tested doses in channel catfish (Table 2.7.2). The ALG-00-530 parent strain (4 doses ranging from $2.9 \times 10^5 – 1.1 \times 10^6$) produced 22-32% CPM, while the mutant strain doses ($2.4 \times 10^6 – 9.6 \times 10^6$) resulted in 0% CPM at all doses. The FBCC-CC-12K parent strain (doses ranging from $1.8 \times 10^6 – 7.2 \times 10^6$) caused 90-100% CPM, whereas the mutant strain ($5.5 \times 10^6 – 2.2 \times 10^7$) resulted in 0-2.5% CPM. A significant difference in CPM was observed at dose 2 (100 mL; $P = 0.034$). Although doses 3 and 4 (150-200 mL) resulted in 100% CPM from the parent strain, the same doses with the mutant strain resulted in 0% CPM. However, due to the lack of variation in CPM between replicate tanks in both groups, a t-test could not be run. Similarly, IPRS-15-49 parent strain ($1.1 \times 10^5 – 4.4 \times 10^5$) caused between 92.5-100% CPM, while the mutant resulted in 0% CPM at all doses (doses ranged between $1.2 \times 10^6 – 4.6 \times 10^6$). ML-17-22A parent strain produced 60-100% CPM in doses ranging from $4.7 \times 10^4 – 1.9 \times 10^5$, whereas the mutant caused 0% CPM across doses $3.9 \times 10^6 – 1.5 \times 10^7$. The ALG-15-231 parent strain resulted

in 70-100% CPM ($1.4 \times 10^6 – 5.4 \times 10^6$), while the mutant strain caused 0-2.5% CPM ($3.2 \times 10^5 – 1.3 \times 10^6$). Statistically significant differences in CPM at dose 1 (50 mL; $P = 0.024$) and dose 4 (200 mL; $P = 0.016$) were observed.

During examination of mortalities, fish exhibited typical signs of columnaris disease, including necrotic gills, frayed fins, and saddleback lesions. Attempts were made to re-isolate *F. covae* from gill and kidney tissue of mortalities, however, not all suspected *F. covae* isolates were able to be purified for bacterial extraction. Pure bacterial isolates recovered from ALG-00-530 (6/6), FBCC-CC-12K (15/15), ML-17-22A (2/8), IPRS-15-49 (9/9), and ALG-15-231 (10/10) attenuation confirmation challenges were confirmed as *F. covae* by PCR.

In Nile tilapia, *F. davisii* isolates exhibited low virulence. TN-3-2012 parent strain (doses ranging from $2.2 \times 10^6 – 1.8 \times 10^7$) caused 0-10.4% CPM, while the mutant strain ($5.7 \times 10^6 – 4.6 \times 10^7$) caused 0% CPM at all doses. ARS-15-12 parent strain produced minimal mortality (0-2% CPM) across all tested doses ($1.5 \times 10^6 – 1.2 \times 10^7$), while the mutant strain resulted in 0% CPM across all tested doses ($1.2 \times 10^5 – 9.2 \times 10^5$). Only 1 bacterial isolate was recovered from mortalities from TN-3-2012 and was confirmed as *F. davisii*. Bacterial isolates were not recovered from the ARS-15-12 parent strain mortality.

All *F. oreochromis* parent strains caused moderate to high mortality in Nile tilapia, while mutants showed reduced virulence. The Costa Rica 04-02-TN^T parent strain caused 29.1-100% CPM in doses ranging from $1.7 \times 10^5 – 1.3 \times 10^6$, whereas the mutant strain caused 0-8.3% CPM from doses $2.5 \times 10^6 – 2.0 \times 10^7$. Significant differences in CPM were observed st dose 2 (100 mL; $P = 0.031$), and dose 4 (400 mL; $P = 0.029$). The R18-27 parent

strain (doses ranging from $1.6 \times 10^5 – 6.5 \times 10^5$) resulted in 72.5-100% CPM, while the mutant strain (doses ranging from $1.5 \times 10^6 – 5.8 \times 10^6$) caused 0% CPM at all doses. The parent and mutant dose of 50 mL showed significant difference in CPM ($P = 0.016$). In contrast, BZ-1-02 parent strain (dose of 6.4×10^8) produced 62% CPM, and the mutant strain (1.1×10^7) resulted in 42% CPM. Re-isolated bacteria were confirmed by PCR as *F. oreochromis* in mortalities from R18-27 (5/8). Attempts to re-isolate bacteria from mortalities in challenges with Costa Rica 04-02-TN^T and BZ-1-02 were unsuccessful, as pure colonies were not recovered.

Attenuation confirmation trials performed at USDA-ARS AAHRU complimented the mortality data that was observed from trials performed at Auburn University. In the first trial testing ALG-00-530 parent (doses ranging from $3.53 \times 10^6 – 1.86 \times 10^7$) and mutant strains ($4.59 \times 10^6 – 2.42 \times 10^7$), the parent strain exhibited dose-dependent mortality ranging from 4% - 100% CPM, while the highest dose of the mutant strain resulted in 8% CPM (Table 2.7.3). In the second trial with ALG-00-530 parent and mutant strains, higher doses of each strain were tested ($6.46 \times 10^6 – 2.58 \times 10^7$ for the parent strain and $9.0 \times 10^6 – 3.6 \times 10^7$ for the mutant strain; Table 2.7.3). The parent strain displayed dose-dependent mortality (42% - 100% CPM), and the highest dose of the mutant strain resulted in 34% CPM, while the two lower doses resulted in 0% CPM.

Attenuation of *F. davisii* TN-3-2012 was tested in Nile tilapia, wherein a similar trend in mortality was seen in the attenuation trial at Auburn University. The parent strain doses (4 doses, ranging from $3.32 \times 10^6 – 2.49 \times 10^7$) resulted in low mortality (0% - 6% CPM). The mutant strain (4 doses, ranging from $1.02 \times 10^6 – 7.62 \times 10^7$) did not cause mortality (0%

CPM). Parent and mutant strain of *F. oreochromis* R18-27 were also tested at USDA-ARS AAHRU. The doses for each strain ranged from $2.53 \times 10^6 – 2.02 \times 10^7$ (parent strain), and $4.07 \times 10^6 – 3.25 \times 10^7$ (mutant strain). The parent strain resulted in 20% - 96% CPM, and the mutant strain resulted in 0% - 6% CPM (Table 2.7.3). A significant difference in CPM was observed at the highest dose (dose 4; 280 mL; $P = 0.009$).

2.4.2. Whole Genome Sequencing

Whole genome sequencing and hybrid assembly were performed for all CCB parent and corresponding mutant strains. Assembly information is summarized in Table 2.7.4. Genome sizes ranged from 3.30-3.59 Mb. For most parent-mutant pairs, genome length was highly comparable, with only minor differences between strains. Assembly contiguity varied among isolates, with most genomes being fragmented and having between 2-15 contigs (Table 2.7.4). However, complete circularized genomes were obtained for four isolates, including *F. covae* FBCC-CC-12K (parent and mutant), *F. covae* IPRS-15-49 mutant, and *F. oreochromis* Costa Rica 04-02-TN^T parent. Of note, BZ-1-02 mutant isolate required additional sequencing and hybrid assembly. Initial hybrid assembly produced a genome approximately 6.86 Mb in size, which is nearly double the genome length of all other isolates. Due to this discrepancy, BZ-1-02 was submitted to Plasmidsaurus (Louisville, KY, USA) for hybrid bacterial whole genome sequencing (ONT + Illumina) and genome assembly. The finalized hybrid assembly resolved the genome to 3.58 Mb consisting of 3 contigs. BUSCO completeness score for individual genomes was determined and recorded in Table 2.7.4. All but one parent and mutant pair had an

identical BUSCO score, although *F. covae* ALG-15-231 scores differed only by 0.1%. The range of completeness for all genomes was 99.5-99.7%, indicating all were high-quality assemblies.

2.4.2. Annotation, Mutation Identification, and Predicted Protein Effect

Parent and mutant genomes were annotated using RAST. Annotated parent genomes were used as references for mutation identification within their corresponding mutant strain. Variant analysis focused on non-synonymous coding region mutations. Comparative genomic analysis identified SNPs, insertions, deletions, and complex nucleotide substitutions across isolates (Table 2.7.5). The BZ-1-02 mutant was excluded from variant analysis due to a high number of mutations (>8,000) identified in its parent strain, suggesting possible sequencing artifacts that inflated the mutation count. Across nearly all rifampicin-resistant mutants, mutations in the DNA-directed RNA polymerase beta subunit (*rpoB*) were identified (Figure 2.8.1). Deleterious mutations within the DNA-directed RNA polymerase beta subunit in *F. covae* isolates included Gln473Lys (ALG-00-530), LeuSer471SerPro and Gly496Arg (FBCC-CC-12K), Pro495Ser, Asp476Gly, and Val143Gly (ML-17-22A), Asp476Asn and Gly494Glu (IPRS-15-49), Gln145Arg, Met475Ile, and Gln726Lys (ALG-15-231). Only one *F. davisii* isolate, ARS-15-12, contained a deleterious insertion of GlnPhe between Phe474 and Met475 (PROVEAN score of -10.7). Interestingly, *F. davisii* mutant TN-3-2012 contained two mutations (Lys473Gln and Ser496Gly) that PROVEAN predicted as having a neutral protein effect (3.892 and 6.000, respectively). *F. oreochromis* isolates Costa Rica 04-02-TN^{T} and R18-27 demonstrated

Gln473Arg and Ala482Glu, respectively. Most mutations clustered within the positions ~471-496 of the region within *rpoB* (Figure 2.8.2), although some amino acid substitutions occurred outside of this region (Val143Gly in ML-17-22A, Gln145Arg in ALG-15-231, and Ala482Glu in R18-27 (Figure 2.8.1).

Additional deleterious variants were detected in other genes across mutant isolates (Table 2.7.5). Among *F. covae* mutants, ALG-00-530 contained a single SNP resulting in a Pro7Thr substitution in a hypothetical protein. FBCC-CC-12K contained two additional SNPs, including Pro218Leu in the chaperone protein DnaJ and Pro267Leu in UDP-N-acetylglucosamine 2-epimerase. ML-17-22A contained two SNPs affecting butyryl-CoA dehydrogenase (Gly339Asp) and a Kup system potassium uptake protein (Gly17Arg). ALG-15-231 mutant also contained a SNP affecting the Kup system potassium uptake protein (Ala113Thr), along with SNPs affecting an AcrR family transcriptional regulator (Tyr38His) and a hypothetical protein (Pro38Ser). A single SNP was also detected in IPRS-15-49 resulting in a Glu110Lys substitution in the rod shape-determining protein MreC.

For *F. davisii* mutants, TN-3-2012 contained a Phe73Cys substitution in a putative acyltransferase and a complex mutation resulting in Gly312Asp in a serine hydroxymethyltransferase. ARS-15-12 mutant contained a Cys52Tyr SNP affecting a citrate synthase. *F. oreochromis* mutant R18-27 contained multiple mutations, including Asp558Asn in glutamine-fructose-6-phosphate aminotransferase, substitutions in three separate hypothetical proteins (Ser40Tyr, Val27Asp, and Leu21Ser), and Leu98Phe in a two-component system response regulator protein. Additionally, a deletion resulted in the

loss of 11 amino acids at Ile426-Asn436 in an outer membrane TonB-dependent transporter.

2.5. Discussion

The present study demonstrates that serial passage on increasing concentrations of rifampicin is an effective strategy for generating attenuated mutants across multiple columnaris-causing bacterial species, including *F. covae*, *F. davisii*, and *F. oreochromis*. Variability in the number of passages required to achieve resistance at 500 μg mL^{-1} was observed across all CCB species and strains (Table 2.7.1). These differences may reflect strain-specific variation in fitness costs associated with resistance-conferring mutations under the same selective pressure (Billington, McHugh, and Gillespie, 1999; Miriam, Mengistu, Hoffner, and Andersson, 2004; Maughan, Galeano, and Nicholson, 2004; LaFrentz, LaPatra, Call, and Cain, 2008; Sun et al., 2019; Cutugno et al., 2020). Likewise, variability in the number of passages required to achieve resistance could also be a result of the stochastic nature of the mutation/selection process. Although the pleiotropic nature of phenotypes was not thoroughly investigated in the current study, the variability in the number of passages required to achieve rifampicin resistance, *rpoB* gene mutations, and virulence highlight the complexity of rifampicin resistance among CCB.

Across most isolates, rifampicin-resistant mutants exhibited a significant loss in virulence relative to their corresponding parent strains (Tables 2.7.2 and 2.7.3). This method of attenuation via rifampicin-resistance has been demonstrated with other fish-pathogenic bacteria, including other strains of CCB (Shoemaker, Klesius, and Evans, 2005;

Shoemaker, Klesius, Drennan, and Evans, 2011; Olivares-Fuster and Arias, 2011), other Flavobacteria, including *F. psychrophilum* (LaFrentz, LaPatra, Call, and Cain, 2008), and *Edwardsiella ictaluri* (Klesius and Shoemaker, 1999; Wise, Greenway, Byars, Griffin, and Khoo, 2015). Herein, the production of multiple rifampicin-resistant CCB supports the continued use of this approach for development of live-attenuated vaccines in aquaculture.

The strong attenuation observed in many of the CCB mutants is consistent with previous studies demonstrating that rifampicin-resistant mutants exhibit reduced or loss of virulence. However, some parent strains (*F. davisii* TN-3-2012 and ARS-15-12) displayed low CPM across tested doses (Tables 2.7.2 and 2.7.3), which limited the ability to fully assess attenuation in their corresponding mutant strains. However, our study standardized the dose volume between parent and mutant strains to test attenuation. Despite fish receiving mutant doses that were comparable to or higher than that of the parent strains (based on bacterial concentration), catfish and tilapia exposed to mutant strains experienced negligible mortality. In contrast, catfish and tilapia exposed to parent strains experienced high levels of mortality, often reaching 100% CPM. Together, these findings provide strong evidence that the observed reduction in virulence observed from exposing fish to mutant strains reflects attenuation.

In contrast, the *F. oreochromis* BZ-1-02 mutant strain displayed reduced, but not fully attenuated virulence compared to other isolates (42% CPM; Table 2.7.2). One possible explanation for the reduced virulence observed is that rifampicin resistance in BZ-1-02 imposed only a partial fitness cost, allowing the mutant strain to retain sufficient

transcriptional function to infect the host and cause mortality. Alternatively, the fitness effects associated with rifampicin resistance may have been less severe, or compensatory mutations may have mitigated these effects, as has been reported in other bacteria (Reynolds, 2000; Hall, Iles, and MacLean, 2011; Brandis, Wrande, Liljas, and Hughes, 2012; Hughes and Brandis, 2013). However, because mutations could not be compared between the parent and mutant strains for this isolate, this explanation remains speculative. Although reduced virulence was confirmed *in vivo*, achieving measurable mortality required substantially higher culture volumes (500 mL), making repeated trials impractical within the scope of the current study. Given both the incomplete attenuation and the challenges associated with reproducible challenge conditions, BZ-1-02 mutant was not prioritized for further investigation.

Comparative genomic analysis revealed that nearly all rifampicin-resistant mutants harbored mutations within the DNA-directed RNA polymerase beta subunit (*rpoB*; Figure 2.8.1), with many mutations clustering within amino acid positions 471-496 (Figure 2.8.2). Alignment of *Flavobacterium covae*, *F. davisii*, and *F. oreochromis rpoB* genes with the type strain *Escherichia coli rpoB* gene (NCBI reference sequence: NP_418414.1) demonstrated that this region corresponds to the rifampicin resistance-determining region (RRDR), specifically cluster I (positions 507-533 in *E. coli*), a highly conserved region where mutations disrupt rifampicin binding to RNA polymerase (Jin and Gross, 1988; Goldstein, 2014). The clustering of mutations observed across multiple CCB species is therefore consistent with established patterns of rifampicin resistance in diverse bacterial taxa, including *Mycobacterium tuberculosis*, where independent mutations arise within the

same functional region of *rpoB* (Thirumurugan et al, 2015). Similarly, Cai and Arias (2021), identified mutations within the RRDR cluster I of a rifampicin-resistant *F. covae* mutant (FC1723), further supporting that this region potentially represents a conserved target of rifampicin selection across *Flavobacterium* species.

Although mutations within the *rpoB* gene were identified across multiple rifampicin-resistant mutants, these mutations alone may not fully explain attenuation. Notably, *F. davisii* TN-3-2012 mutant harbored two SNPs within the *rpoB* gene that were predicted to have a neutral functional effect, yet it exhibited no mortality under experimental conditions. The protein function prediction tool used in this study, PROVEAN, bases predictions on sequence homology and evolutionary conservation, and therefore may classify mutations as neural if they do not substantially disrupt conserved protein features (Choi and Chan, 2015). Rifampicin resistance occurs from mutations in the beta subunit of RNA polymerase that alter the structure of the drug binding site and reduce rifampicin binding without necessarily impairing transcriptional activity (Wehrli, 1983; Jin and Gross, 1988; Goldstein, 2014). As a result, mutations within *rpoB* may be predicted as functionally neutral despite conferring resistance, as they preserve RNA polymerase function while reducing antibiotic binding. These observations indicate that disruption of rifampicin binding through *rpoB* mutation may not necessarily correlate with reduced virulence, and that additional factors likely contribute to attenuation.

In addition to conferring rifampicin resistance, mutations in *rpoB* can have pleiotropic effects due to the central role of RNA polymerase in regulating global gene expression (Goldstein, 2014). In a study investigating the mechanisms of rifampicin

attenuation in *F. psychrophilum*, Gliniewicz et al. (2015) demonstrated that strains passaged in the absence of rifampicin also accumulated mutations and exhibited partial attenuation relative to the parent strain, despite lacking antibiotic selection pressure. Similarly, Cai and Arias (2021) reported that attenuation in rifampicin-resistant *F. covae* mutants was associated with the accumulation of multiple mutations acquired during serial passage, with evidence suggesting a synergistic effect of these mutations rather than a single causal change. Another study demonstrated that attenuation of a virulent swine isolate of *Brachyspira hampsonii* was achieved by 100 serial passages in the laboratory (Perez et al., 2018). Conversely, serial passage of a virulent strain of *Streptococcus pneumoniae* resulted in mutational changes in the genome of the mutant strain, however, median lethal dose challenges in a mouse model showed no significant reduction in virulence between the parent and mutant strains (Pandya, Sinha, Luxon, Watson, and Niesel, 2009). These findings support the hypothesis that mutations may arise from the process of serial passage itself, in addition to antibiotic-driven selection. This is consistent with the present study, where multiple mutations outside of *rpoB* were identified across multiple mutants, suggesting that cumulative genomic changes may contribute to reduced virulence and attenuation. Several mutations affecting bacterial virulence and fitness were identified. Notably, a predicted deleterious SNP in the chaperone protein DnaJ of *F. covae* mutant FBCC-CC-12K may explain the reduced virulence observed. DnaJ, a co-chaperone with DnaK, supports protein folding and stress recovery (Zügel and Kaufmann, 1999). In fish, disruption of these stress response proteins can impair pathogen fitness (Jeyachadran et al., 2023). Here, the DnaJ SNP likely impaired chaperone function,

compromising stress tolerance and protein stability, thus reducing virulence. Beyond mutations affecting stress response, other mutations affecting bacterial nutrient acquisition may also contribute to attenuation. Iron uptake is essential for bacterial survival and virulence in host environments (Payne, 1993; Woolridge and Williams, 1993; Braun, 1995; Wycoff et al., 2007). Gram-negative bacteria capture iron via outer membrane receptors and transport it through the TonB system (Andrews, Robinson, and Rodríguez-Quiñones, 2003). In this study, the *F. oreochromis* R18-27 mutant had a predicted deletion in its TonB-dependent transporter, likely causing reduced virulence in Nile tilapia. Supporting this, Beck et al. (2015) reported that a highly virulent strain of *F. columnare* exhibited significantly greater expression of the TonB-dependent receptor (~111x) and ferroxidase (~12x) compared to the low-virulent strain, highlighting the importance of iron acquisition in pathogenicity of CCB. Similarly, Álvarez, Álvarez, Menéndez, and Guijarro (2008) found that a TonB mutation in *F. psychrophilum* grown in iron-depleted media attenuated the pathogen and protected rainbow trout (*Oncorhynchus mykiss*) against a virulent strain. Thus, the mutation in the TonB-dependent transporter within R18-27 in this study could also contribute to the attenuation seen in Nile tilapia, and in combination with rifampicin resistance, provide an additional layer of attenuation.

While disruption of iron acquisition pathways likely contributed to attenuation, additional mutations affecting bacterial structure and physiology may also play a role. A predicted deleterious mutation in the rod shape-determining protein MreC was found in mutant strain IPRS-15-49. A rifampicin-attenuated *F. psychrophilum* strain with a MreC mutation was hypothesized as contributing to its reduced virulence

(Gliniewicz et al., 2015). Likewise, the role of MreC in *Salmonella* had also been linked to virulence (Bulmer et al., 2012). This supports the hypothesis that a deleterious mutation in MreC could likely contribute to attenuation. Additionally, a mutation in the polysaccharide envelope synthesis enzyme UDP-N-acetylglucosamine-2-epimerase was identified in FBCC-CC-12K, which has also been linked to virulence in Flavobacteria (Tekedar et al., 2017). These mutations potentially contribute to attenuation of CCB strains in this study by compromising cell envelope integrity and activating stress-response pathways that suppress virulence. Many mutations were identified across CCB species. While some are directly linked to virulence, others may contribute to attenuation indirectly by negatively affecting gene expression, transcription, nutrient acquisition, physiological and metabolic pathways, and antibiotic resistance. For example, predicted deleterious mutations were found in regulatory proteins, such as the two-component system response regulator (Xie et al., 2022) and AcrR family transcriptional regulator (Deng et al., 2013). Deleterious mutations were also identified in enzymes involved in essential pathways, including butyryl-CoA dehydrogenase (Kim et al., 2023), serine hydroxymethyltransferase (Schirch and Szebenyi, 2005), citrate synthase (Wiegand and Remington, 1986), glutamine-fructose-6-phosphate aminotransferase (Milewski, 2002), and the Kup potassium uptake protein (Trchounian and Kobayashi, 1999). Collectively, these findings suggest that attenuation in rifampicin-resistant CCB mutants is multifactorial and is likely driven by cumulative impacts on multiple regulatory and physiological pathways.

Findings from this study demonstrate that rifampicin resistance is an effective, yet complex and multifactorial process. Although some of the generated rifampicin-resistant

mutants did not show a difference in mean CPM (BZ-1-02 and ARS-15-12), all others exhibited significantly reduced virulence compared to their parent strains, supporting their potential as live-attenuated vaccine candidates. Comparative genomic analysis revealed that while mutations within the *rpoB* gene confer rifampicin resistance, attenuation is likely multifactorial and influenced by additional mutations compensatory to *rpoB* mutations, or by the accumulation of mutations through serial passage. Mutations identified in rifampicin-resistant strains were predicted to affect stress response, nutrient acquisition, cellular structure, and regulatory pathways, all which can influence bacterial virulence. These findings highlight the complexity of attenuation mechanisms and underscore the importance of considering whole-genome changes rather than single-gene effects when evaluating vaccine candidates. Future work should investigate the genetic basis of attenuation through targeted mutagenesis to distinguish causal mutations from secondary effects. Further studies should evaluate the protective efficacy and duration of immunity conferred by the generated mutants in vaccination trials with channel catfish and Nile tilapia. Characterization of host immune responses will be critical for understanding the mechanisms of protection and optimizing vaccine efficacy. The stability of attenuation should also be assessed to evaluate the potential for reversion to virulence.

2.7. Tables

Table 2.7.1. Columnaris-causing bacteria parent species, isolate, fish host species, location of origin, and references of virulence. The passage number indicates the number of sequential passages on modified Shieh agar containing increasing concentration of rifampicin. NA = not available.

Species	Isolate	Passage #	Fish Host	Location/Date	References
F. covae	ALG-00-530	31	Channel catfish	Alabama, 2000	(Shoemaker et al., 2008; LaFrentz et al., 2018, 2022, 2024)
	FBCC-CC-12K	64	Channel catfish	Florida, 2013	(LaFrentz et al., 2018, 2024)
	ML-17-22A	75	Channel catfish	Alabama, 2017	(LaFrentz et al., 2024)
	IPRS-15-49	49	Channel catfish	Alabama, 2015	(LaFrentz et al., 2024)
	ALG-15-231	53	Hybrid catfish	Alabama, 2015	(LaFrentz et al., 2024)
F. davisii	TN-3-2012	51	Nile tilapia	Alabama, 2012	(Xu et al., 2014; Shoemaker et al., 2014)
	ARS-15-12	48	Nile tilapia	Florida, 2015	NA
F. oreochromis	Costa Rica 04-02-TN^{T}	58	Tilapia	Costa Rica, 2004	(LaFrentz et al., 2024)
	BZ-1-02	46	Nile tilapia	Brazil, 2002	(LaFrentz et al., 2024)
	R18-27	66	Nile tilapia	Brazil, 2018	(LaFrentz et al., 2024)

Table 2.7.2. Mean cumulative percent mortality (CPM) ± standard error of the mean (SEM) of channel catfish (*I. punctatus*) and Nile tilapia (*O. niloticus*) following immersion challenge with parent and mutant CCB isolates at multiple doses at Auburn University. "CFU" indicates colony-forming unit.

CCB Species	Parent Isolate	Fish Species	Average Fish Size	Parent Dose (CFU mL^{-1})	Parent Dose (mL)	CPM ± SEM	Mutant Dose (CFU mL^{-1})	Mutant Dose (mL)	CPM ± SEM	*P*-value
F. covae	ALG-00-530	*I. punctatus*	22 ± 1.5 g	1.1×10^6	200	32.0 ± 4.0[a]	9.6×10^6	200	0.0 ± 0.0[a]	0.079
				8.7×10^5	150	22.0 ± 2.0[a]	7.2×10^6	150	0.0 ± 0.0[a]	0.057
				5.8×10^5	100	24.0 ± 20.0[a]	4.8×10^6	100	0.0 ± 0.0[a]	0.442
				2.9×10^5	50	28.0 ± 0.0	2.4×10^6	50	0.0 ± 0.0	NA
	FBCC-CC-12K		8 ± 0.3 g	7.2×10^6	200	100.0 ± 0.0	2.2×10^7	200	0.0 ± 0.0	NA
				5.4×10^6	150	100.0 ± 0.0	1.7×10^7	150	0.0 ± 0.0	NA
				3.6×10^6	100	100.0 ± 0.0[a]	1.1×10^7	100	2.5 ± 5.0[b]	0.034
				1.8×10^6	50	90.0 ± 10.0[a]	5.5×10^6	50	0.0 ± 0.0[a]	0.070
	ML-17-22A		22 ± 1.5 g	1.9×10^5	200	100.0 ± 0.0	1.5×10^7	200	0.0 ± 0.0	NA
				1.4×10^5	150	100.0 ± 0.0	1.1×10^7	150	0.0 ± 0.0	NA
				9.5×10^4	100	100.0 ± 0.0	7.9×10^6	100	0.0 ± 0.0	NA
				4.7×10^4	50	60.0 ± 5.0[a]	3.9×10^6	50	0.0 ± 0.0[a]	0.053
	IPRS-15-49		8 ± 0.3 g	4.4×10^5	200	100.0 ± 0.0	4.6×10^6	200	0.0 ± 0.0	NA
				3.3×10^5	150	100.0 ± 0.0[a]	3.5×10^6	150	0.0 ± 0.0[a]	0.052
				2.2×10^5	100	92.5 ± 7.5	2.3×10^6	100	0.0 ± 0.0	NA
				1.1×10^5	50	100.0 ± 0.0	1.2×10^6	50	0.0 ± 0.0	NA
	ALG-15-231		8 ± 0.3 g	5.4×10^6	200	97.5 ± 2.5[a]	1.3×10^6	200	0.0 ± 0.0[b]	0.016
				4.1×10^6	150	100.0 ± 0.0	9.5×10^5	150	0.0 ± 0.0	NA
				2.7×10^6	100	100.0 ± 0.0	6.3×10^5	100	0.0 ± 0.0	NA

				1.4×10^6	50	70.0 ± 0.0[a]	3.2×10^6	50	2.5 ± 2.5[b]	0.024
F. davisii	TN-3-2012	*O. niloticus*	5 ± 0.3 g	1.8×10^7	400	10.4 ± 2.1[a]	4.6×10^7	400	0.0 ± 0.0[a]	0.127
				9.0×10^6	200	4.1 ± 0.0	2.3×10^7	200	0.0 ± 0.0	NA
				4.5×10^6	100	2.1 ± 2.1[a]	1.1×10^7	100	0.0 ± 0.0[a]	0.500
				2.2×10^6	50	0.0 ± 0.0	5.7×10^6	50	0.0 ± 0.0	NA
	ARS-15-12		6 ± 0.1 g	1.2×10^7	400	0.0 ± 0.0	9.2×10^5	400	0.0 ± 0.0	NA
				6.0×10^6	200	2.0 ± 2.0[a]	4.6×10^5	200	0.0 ± 0.0[a]	0.500
				3.0×10^6	100	0.0 ± 0.0	2.3×10^5	100	0.0 ± 0.0	NA
				1.5×10^6	50	0.0 ± 0.0	1.2×10^5	50	0.0 ± 0.0	NA
F. oreochromis	Costa Rica 04-02-TN[T]		5 ± 0.3 g	1.3×10^6	400	100.0 ± 0.0[a]	2.0×10^7	400	8.3 ± 4.2[b]	0.029
				6.0×10^5	200	87.5 ± 12.5[a]	1.0×10^7	200	2.1 ± 2.1[a]	0.085
				3.4×10^5	100	43.7 ± 2.1[a]	5.0×10^6	100	4.2 ± 4.2[b]	0.031
				1.7×10^5	50	29.1 ± 0.0	2.5×10^6	50	0.0 ± 0.0	NA
	BZ-1-02		3 ± 0.6 g	6.4×10^8	500	62.0 ± 23.3[a]	1.1×10^7	500	42.0 ± 29.5[a]	0.597
	R18-27		5 ± 0.3 g	6.5×10^5	100	100.0 ± 0.0	5.8×10^6	100	0.0 ± 0.0	NA
				3.3×10^5	50	97.5 ± 2.5[a]	2.9×10^6	50	0.0 ± 0.0[b]	0.016
				1.6×10^5	25	72.5 ± 27.5[a]	1.5×10^6	25	0.0 ± 0.0[b]	0.231

Table 2.7.3. Mean cumulative percent mortality (CPM) ± standard error of the mean (SEM) of channel catfish (*I. punctatus*) and Nile tilapia (*O. niloticus*) following immersion challenge with parent and mutant CCB isolates at multiple doses at USDA ARS Aquatic Animal Health Research Unit. "CFU" indicates colony-forming unit.

CCB Species	Parent Isolate	Fish Species	Average Fish Size	Parent Dose (CFU mL^{-1})	Parent Dose (mL)	CPM ± SEM	Mutant Dose (CFU mL^{-1})	Mutant Dose (mL)	CPM ± SEM	*P*-value
F. covae	ALG-00-530	*I. punctatus*	2.2 g ± 0.3 g	1.86×10^7	200	100.0	2.42×10^7	200	8.0	NA
				9.30×10^6	100	54.2	1.21×10^7	100	0.0	NA
				4.65×10^6	50	16.0	6.04×10^6	50	0.0	NA
				3.53×10^6	38	4.0	4.59×10^6	38	0.0	NA
			2.4 g ± 0.3 g	2.58×10^7	300	100.0 ± 0.0[a]	3.60×10^7	300	34.0 ± 2.8[b]	0.019
				1.29×10^7	150	88.0 ± 17.0[a]	1.80×10^7	150	0.0 ± 0.0[a]	0.086
				6.46×10^6	75	42.0 ± 8.5[a]	9.00×10^6	75	0.0 ± 0.0[a]	0.090
F. davisii	TN-3-2012	*O. niloticus*	26.7 g ± 1.5 g	2.49×10^7	300	6.0 ± 2.8[a]	7.62×10^7	300	0.0 ± 0.0[a]	0.205
				1.25×10^7	150	4.0 ± 0.0	3.81×10^7	150	0.0 ± 0.0	NA
				6.23×10^6	75	0.0 ± 0.0	1.90×10^7	75	0.0 ± 0.0	NA
				3.32×10^6	40	0.0 ± 0.0	1.02×10^6	40	0.0 ± 0.0	NA
F. oreochromis	R18-27		27.4 g ± 1.9 g	2.02×10^7	280	96.0 ± 5.7[a]	3.25×10^7	280	6.0 ± 2.8[b]	0.009
				1.01×10^7	140	36.0 ± 0.0	1.63×10^7	140	0.0 ± 0.0	NA
				5.06×10^6	70	22.0 ± 8.5[a]	8.13×10^6	70	0.0 ± 0.0[a]	0.170
				2.53×10^6	35	20.0 ± 5.7[a]	4.07×10^6	35	0.0 ± 0.0[a]	0.126

Table 2.7.4. Summary of long-read (Oxford Nanopore Technologies) and short-read (Illumina) hybrid genome assemblies of CCB parent and mutant strains.

Isolate	Strain	Genome Length (bp)	Genome Length (Mb)	# Contigs	Circularized	BUSCO Completeness Score
ALG-00-530	Parent	3535291	3.54	2	No	99.6 %
ALG-00-530	Mutant	3511128	3.51	2	No	99.6 %
FBCC-CC-12K	Parent	3301659	3.30	1	Yes	99.5 %
FBCC-CC-12K	Mutant	3301578	3.30	1	Yes	99.5 %
ML-17-22A	Parent	3414174	3.41	4	No	99.6 %
ML-17-22A	Mutant	3474438	3.47	4	No	99.6 %
IPRS-15-49	Parent	3561397	3.56	3	No	99.6 %
IPRS-15-49	Mutant	3507344	3.51	1	Yes	99.6 %
ALG-15-231	Parent	3470763	3.47	2	No	99.6 %
ALG-15-231	Mutant	3512794	3.51	15	No	99.5 %
TN-3-2012	Parent	3458913	3.46	3	No	99.7 %
TN-3-2012	Mutant	3438048	3.44	2	No	99.7 %
ARS-15-12	Parent	3473845	3.47	3	No	99.7 %
ARS-15-12	Mutant	3516922	3.52	7	No	99.7 %
Costa Rica 04-02-TN	Parent	3552508	3.55	1	Yes	99.7 %
Costa Rica 04-02-TN	Mutant	3592973	3.59	3	No	99.7 %
BZ-1-02	Parent	3396638	3.40	2	No	99.7 %
BZ-1-02	Mutant	3580659	3.58	3	No	99.7 %
R18-27	Parent	3406504	3.41	3	No	99.7 %
R18-27	Mutant	3409843	3.41	3	No	99.7 %

Table 2.7.5. Predicted deleterious variants identified in rifampicin-resistant mutants of columnaris-causing bacteria (CCB) compared to their corresponding parent strains. Variants predicted as deleterious (PROVEAN score < -2.5) are presented here. SNP = single nucleotide polymorphism.

Species	Strain	Contig	Position	Variant Type	Nucleotide Change	Amino Acid Change	Annotation
F. covae	ALG-00-530	tig00000004	244992	SNP	C > A	Gln473Lys	DNA-directed RNA polymerase beta subunit
	ALG-00-530	tig00000004	1222836	SNP	C > A	Pro7Thr	Hypothetical protein
	FBCC-CC-12K	FBCC-CC-12K_P	787279	Complex	TAT > CAC	LeuSer471SerPro	DNA-directed RNA polymerase beta subunit
	FBCC-CC-12K	FBCC-CC-12K_P	787353	SNP	G > A	Gly496Arg	DNA-directed RNA polymerase beta subunit
	FBCC-CC-12K	FBCC-CC-12K_P	1111039	SNP	C > T	Pro218Leu	Chaperone protein DnaJ
	FBCC-CC-12K	FBCC-CC-12K_P	2364672	SNP	G > A	Pro267Leu	UDP-N-acetylglucosamine 2-epimerase
	ML-17-22A	tig00000008	538550	SNP	G > A	Pro495Ser	DNA-directed RNA polymerase beta subunit
	ML-17-22A	tig00000008	538606	SNP	T > C	Asp476Gly	DNA-directed RNA polymerase beta subunit
	ML-17-22A	tig00000008	539605	SNP	A > C	Val143Gly	DNA-directed RNA polymerase beta subunit
	ML-17-22A	tig00000004	684554	SNP	G > A	Gly339Asp	Butyryl-CoA dehydrogenase

	ML-17-22A	tig00000004	316530	SNP	G > A	Gly17Arg	Kup system potassium uptake protein
	IPRS-15-49	tig00000005	171888	SNP	G > A	Asp476Asn	DNA-directed RNA polymerase beta subunit
	IPRS-15-49	tig00000005	171943	SNP	G > A	Gly494Glu	DNA-directed RNA polymerase beta subunit
	IPRS-15-49	tig00000008	1339352	SNP	C > T	Glu110Lys	Rod shape-determining protein MreC
	ALG-15-231	tig00000003	817689	SNP	G > A	Ala113Thr	Kup system potassium uptake protein
	ALG-15-231	tig00000003	2286164	SNP	A > G	Tyr38His	Transcriptional regulator, AcrR family
	ALG-15-231	tig00000003	3094109	SNP	G > A	Pro38Ser	Hypothetical protein
	ALG-15-231	tig00000004	175610	SNP	A > G	Gln145Arg	DNA-directed RNA polymerase beta subunit
	ALG-15-231	tig00000004	176601	SNP	G > A	Met475Ile	DNA-directed RNA polymerase beta subunit
	ALG-15-231	tig00000004	177352	SNP	C > A	Gln726Lys	DNA-directed RNA polymerase beta subunit
F. davisii	TN-3-2012	tig00000005	435791	SNP	A > C	Phe73Cys	Putative acyltransferase
	TN-3-2012	tig00000003	311635	Complex	AC > GT	Gly312Asp	Serine hydroxymethyltransferase

	ARS-15-12	tig00000003	389506	Insertion	C > CTCAGTT	Phe474_Met475insGlnPhe	DNA-directed RNA polymerase beta subunit
	ARS-15-12	tig00000004	1130165	SNP	C > T	Cys52Tyr	Citrate synthase
F. oreochromis	Costa Rica 04-02-TN^{T}	Costa Rica 04-02-TN^{T}_P	2964561	SNP	A > G	Gln473Arg	DNA-directed RNA polymerase beta subunit
	R18-27	tig00000003	1339207	SNP	G > A	Asp558Asn	Glutamine—fructose-6-phosphate aminotransferase
	R18-27	tig00000005	318421	Complex	CTC > TTA	Ser40Tyr	Hypothetical protein
	R18-27	tig00000005	383949	SNP	T > A	Val27Asp	Hypothetical protein
	R18-27	tig00000005	384047	SNP	T > C	Leu21Ser	Hypothetical protein
	R18-27	tig00000005	552047	SNP	T > G	Leu98Phe	Two-component system response regulator protein
	R18-27	tig00000002	542007	SNP	G > T	Ala482Glu	DNA-directed RNA polymerase beta subunit
	R18-27	tig00000002	563279	Deletion	CATTTCTTGCCCAAATAGGATAAATAGGTGCAAT > C	Ile426_Asn436del	Outer membrane TonB-dependent transporter

2.8. Figures

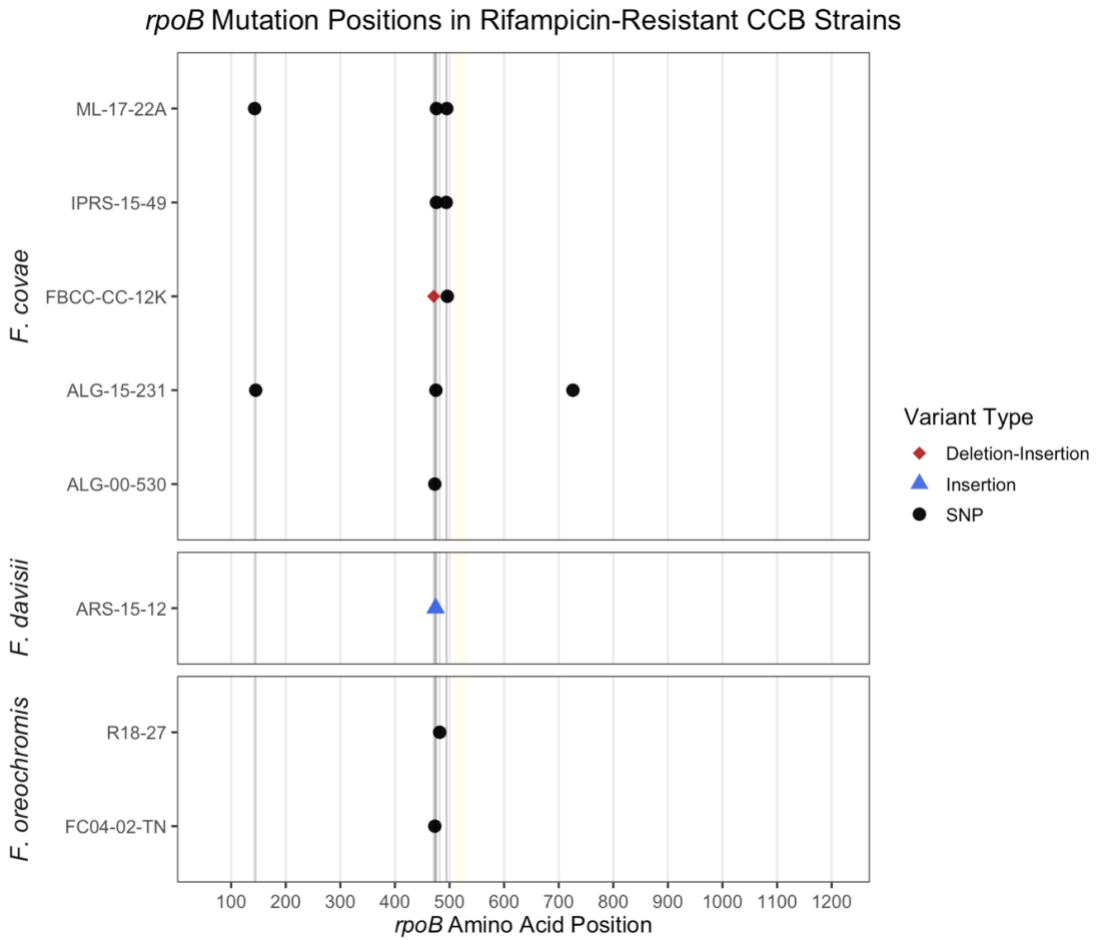

Figure 2.8.1. Amino acid positions of mutations in the *rpoB* gene of rifampicin-resistant columnaris-causing bacterial (CCB) isolates.

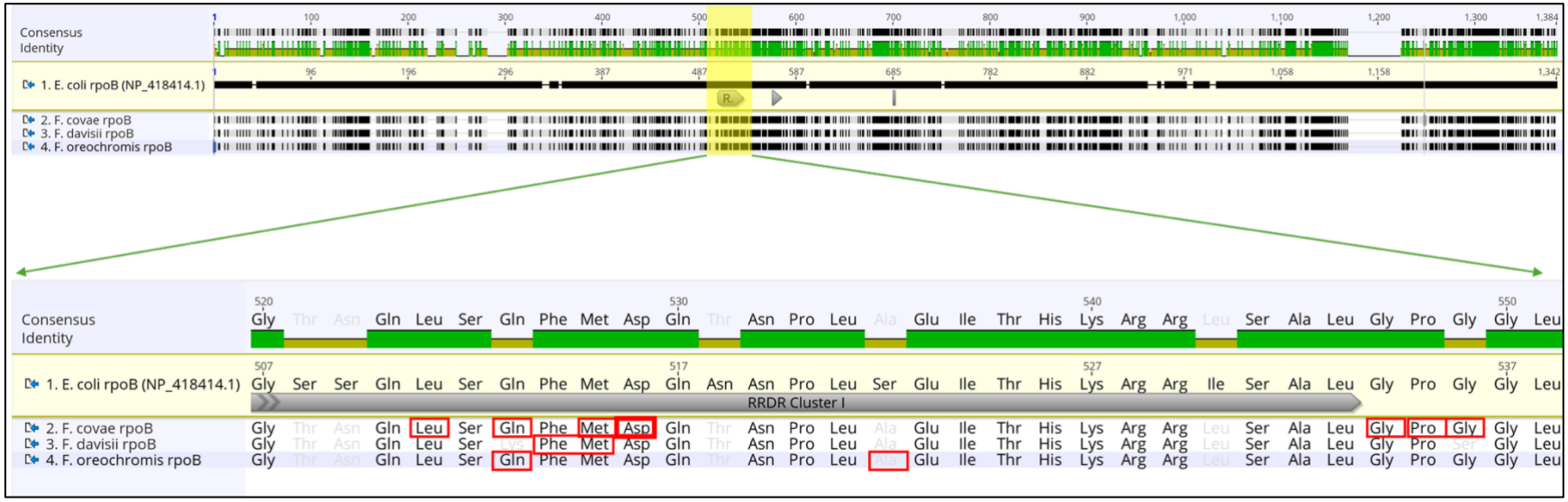

Figure 2.8.2. MAFFT Alignment of *rpoB* gene sequences of *Escherichia coli* (K-12 substr. MG1655), *Flavobacterium covae*, *F. davisii*, and *F. oreochromis*. The rifampicin-resistance determining region (RRDR) in *E. coli* is highlighted in yellow. Red-outlined boxes depict mutations identified within and near the RRDR cluster I (amino acid positions 507-533) of rifampicin-resistant CCB mutants. Figure created using Geneious Prime (2026.0.2).

2.9. References

Abdelrahman, H.A., Hemstreet, W.G., Roy, L.A., Hanson, T.R., Beck, B.H. and Kelly, A.M. 2023. Epidemiology and Economic Impact of Disease-Related Losses on Commercial Catfish Farms: A Seven-Year Case Study from Alabama, USA. *Aquaculture*, *566*, p.739206. https://doi.org/10.1016/j.aquaculture.2022.739206

Ahmed, M. T., M. S. Ali, T. Ahamed, S. Suraiya, and M. Haq. 2024. Exploring the Aspects of the Application of Nanotechnology System in Aquaculture: A Systematic Review. *Aquaculture International,* 32: 1–30. https://doi.org/10.1007/s10499-023-01370-7.

Alvarez, B., Alvarez, J., Menendez, A. and Guijarro, J.A. 2008. A Mutant in One of Two *exbD* Loci of a TonB System in *Flavobacterium psychrophilum* Shows Attenuated Virulence and Confers Protection Against Cold Water Disease. *Microbiology*, 154(4), pp.1144-1151. https://doi.org/10.1099/mic.0.2007/010900-0

Andrews, S.C., Robinson, A.K. and Rodríguez-Quiñones, F. 2003. Bacterial Iron Homeostasis. *FEMS Microbiology Reviews*, 27(2-3), pp.215-237. https://doi.org/10.1016/s0168-6445(03)00055-x

Aziz, R.K., Bartels, D., Best, A.A., DeJongh, M., Disz, T., Edwards, R.A., Formsma, K., Gerdes, S., Glass, E.M., Kubal, M. and Meyer, F. 2008. The RAST Server: Rapid Annotations Using Subsystems Technology. *BMC Genomics*, 9(1), p.75. https://doi.org/10.1186/1471-2164-9-75

Bader, J. A., P. H. Klesius, and S. Vinitnantharat. 1997. Comparison of Whole-Cell Antigens of Pressure- and Formalin-Killed *Flexibacter Columnaris* from Channel Catfish (*Ictalurus punctatus*). *American Journal of Veterinary Research,* 58, no. 9: 985–988. https://www.ncbi.nlm.nih.gov/pubmed/9285002.

Baxter, D. 2007. Active and Passive Immunity, Vaccine Types, Excipients and Licensing. *Occupational Medicine,* 57: 552–556. https://doi.org/10.1093/occmed/kqm110.

Bebak, J. and Wagner, B. 2012. Use of Vaccination Against Enteric Septicemia of Catfish and Columnaris Disease by the US Catfish Industry. *Journal of Aquatic Animal Health*, 24(1), pp.30-36. https://doi.org/10.1080/08997659.2012.667048

Beck, B.H., Li, C.H.A.O., Farmer, B.D., Barnett, L.M., Lange, M.D. and Peatman, E.R.I.C. 2016. A Comparison of High-and Low-Virulence *Flavobacterium columnare* Strains Reveals Differences in Iron Acquisition Components and Responses to Iron Restriction. *Journal of Fish Diseases*, 39(3), pp.259-268. https://doi.org/10.1111/jfd.12343

Bhatnagar, N., Getachew, E., Straley, S., Williams, J., Meltzer, M. and Fortier, A. 1994. Reduced Virulence Of Rifampicin-Resistant Mutants Of *Francisella tularensis* [X]. *Journal of Infectious Diseases*, 170(4), pp.841-847. https://doi.org/10.1093/infdis/170.4.841

Billington, O.J., McHugh, T.D. and Gillespie, S.H. 1999. Physiological Cost of Rifampin Resistance Induced *In Vitro* in *Mycobacterium tuberculosis*. *Antimicrobial Agents and Chemotherapy*, 43(8), pp.1866-1869. https://doi.org/10.1128/aac.43.8.1866

Brandis, G., Wrande, M., Liljas, L. and Hughes, D., 2012. Fitness-Compensatory Mutations in Rifampicin-Resistant RNA Polymerase. *Molecular Microbiology*, 85(1), pp.142-151. https://doi.org/10.1111/j.1365-2958.2012.08099.x

Braun, V., 1995. Energy-Coupled Transport and Signal Transduction Through the Gram-Negative Outer Membrane Via TonB-ExbB-ExbD-Dependent Receptor Proteins. *FEMS Microbiology Reviews*, 16(4), pp.295-307. https://doi.org/10.1016/0168-6445(95)00003-u

Bulmer, D.M., Kharraz, L., Grant, A.J., Dean, P., Morgan, F.J., Karavolos, M.H., Doble, A.C., McGhie, E.J., Koronakis, V., Daniel, R.A. and Mastroeni, P. 2012. The Bacterial Cytoskeleton Modulates Motility, Type 3 Secretion, and Colonization in *Salmonella*. *PLoS Pathogens*, 8(1), p.e1002500. https://doi.org/10.1371/journal.ppat.1002500

Cai, W. and Arias, C.R. 2021. Deciphering the Molecular Basis for Attenuation of *Flavobacterium columnare* Strain fc1723 Used As Modified Live Vaccine Against Columnaris Disease. *Vaccines*, 9(11), p.1370. https://doi.org/10.3390/vaccines9111370

Choi, Y. and Chan, A.P. 2015. PROVEAN Web Server: A Tool to Predict the Functional Effect of Amino Acid Substitutions and Indels. *Bioinformatics*, 31(16), pp.2745-2747. https://doi.org/10.1093/bioinformatics/btv195

Choi, Y., Sims, G.E., Murphy, S., Miller, J.R. and Chan, A.P. 2012. Predicting the Functional Effect of Amino Acid Substitutions and Indels. https://doi.org/10.1371/journal.pone.0046688

Cingolani, P., Platts, A., Wang, L.L., Coon, M., Nguyen, T., Wang, L., Land, S.J., Lu, X. and Ruden, D.M. 2012. A Program for Annotating and Predicting the Effects of Single Nucleotide Polymorphisms, SnpEff: SNPs in the Genome of *Drosophila melanogaster* Strain w1118; iso-2; iso-3. *Fly*, 6(2), pp.80-92. https://doi.org/10.4161/fly.19695

Cutugno, L., Mc Cafferty, J., Pané-Farré, J., O'Byrne, C. and Boyd, A. 2020. *rpoB* Mutations Conferring Rifampicin-Resistance Affect Growth, Stress Response and Motility in *Vibrio vulnificus*. *Microbiology*, 166(12), pp.1160-1170. https://doi.org/10.1099/mic.0.000991

Deng, W., Li, C. and Xie, J. 2013. The Underlying Mechanism of Bacterial TetR/AcrR Family Transcriptional Repressors. *Cellular Signalling*, 25(7), pp.1608-1613. https://doi.org/10.1016/j.cellsig.2013.04.003

Gliniewicz, K., Wildung, M., Orfe, L.H., Wiens, G.D., Cain, K.D., Lahmers, K.K., Snekvik, K.R. and Call, D.R. 2015. Potential Mechanisms of Attenuation for Rifampicin-Passaged Strains of *Flavobacterium psychrophilum*. *BMC Microbiology*, 15(1), p.179. https://doi.org/10.1186/s12866-015-0518-1

Goldstein, B.P. 2014. Resistance to Rifampicin: A Review. *The Journal of Antibiotics*, 67(9), pp.625-630. https://doi.org/10.1038/ja.2014.107

Hall, A.R., Iles, J.C. and MacLean, R.C. 2011. The Fitness Cost of Rifampicin Resistance in *Pseudomonas aeruginosa* Depends on Demand for RNA Polymerase. *Genetics*, 187(3), pp.817-822. https://doi.org/10.1534/genetics.110.124628

Harrison, C.E., LaFrentz, B.R., Shoemaker, C.A., Lange, M.D., Liles, M.R., Mohammed, H.H., Beck, B.H., Churchman, E.M., Peatman, E. and Bruce, T.J. 2025. An Overview

of Vaccine Development Strategies for Columnaris-Causing Bacteria in Cultured Fish. *Journal of Fish Diseases*, 48(8), p.e14155. https://doi.org/10.1111/jfd.14155

Hughes, D. and Brandis, G. 2013. Rifampicin Resistance: Fitness Costs and the Significance of Compensatory Evolution. *Antibiotics*, 2(2), pp.206-216. https://doi.org/10.3390/antibiotics2020206

Hyatt, D., Chen, G.L., LoCascio, P.F., Land, M.L., Larimer, F.W. and Hauser, L.J. 2010. Prodigal: Prokaryotic Gene Recognition and Translation Initiation Site Identification. *BMC Bioinformatics*, 11(1), p.119. https://doi.org/10.1186/1471-2105-11-119

Jeyachandran, S., Chellapandian, H., Park, K. and Kwak, I.S. 2023. A Review on the Involvement of Heat Shock Proteins (Extrinsic Chaperones) in Response to Stress Conditions in Aquatic Organisms. *Antioxidants*, 12(7), p.1444. https://doi.org/10.3390/antiox12071444

Jin, D.J. and Gross, C.A. 1988. Mapping and Sequencing of Mutations in the *Escherichia coli rpoB* Gene that Lead to Rifampicin Resistance. *Journal of Molecular Biology*, 202(1), pp.45-58. https://doi.org/10.1016/0022-2836(88)90517-7

Katoh, K., Misawa, K., Kuma, K.I. and Miyata, T. 2002. MAFFT: A Novel Method for Rapid Multiple Sequence Alignment Based on Fast Fourier Transform. *Nucleic Acids Research*, 30(14), pp.3059-3066. https://doi.org/10.1093/nar/gkf436

Katoh, K. and Standley, D.M. 2013. MAFFT Multiple Sequence Alignment Software Version 7: Improvements in Performance and Usability. *Molecular Biology and Evolution*, 30(4), pp.772-780. https://doi.org/10.1093/molbev/mst010

Kitiyodom, S., T. Yata, J. Yostawornkul, et al. 2019. Enhanced Efficacy of Immersion Vaccination in Tilapia Against Columnaris Disease by Chitosan-Coated "Pathogen-Like" Mucoadhesive Nanovaccines. *Fish & Shellfish Immunology,* 95: 213–219. https://doi.org/10.1016/j.fsi.2019.09.064.

Kitiyodom, S., T. Yata, K. D. Thompson, et al. 2021. Immersion Vaccination by a Biomimetic-Mucoadhesive Nanovaccine Induces Humoral Immune Response of Red Tilapia (*Oreochromis* sp.) Against *Flavobacterium columnare* Challenge. *Vaccines (Basel)* 9, no. 11: 1253. https://doi.org/10.3390/vaccines9111253.

Kim, M., Cha, I.T., Lee, K.E., Li, M. and Park, S.J. 2023. Pangenome Analysis Provides Insights into the Genetic Diversity, Metabolic Versatility, and Evolution of the Genus *Flavobacterium*. *Microbiology Spectrum*, 11(5), pp.e01003-23. https://doi.org/10.1128/spectrum.01003-23

Kirkland, S. 2010. *Evaluation of the Live-Attenuated Vaccine AquaVac-COL® on Hybrid Channel x Blue Catfish Fingerlings in Earthen Ponds*. Auburn University.

Klesius, P.H. and Shoemaker, C.A. 1999. Development and Use of Modified Live *Edwardsiella ictaluri* Vaccine Against Enteric Septicemia of Catfish. In *Advances in Veterinary Medicine* (Vol. 41, pp. 523-537). Academic Press. https://doi.org/10.1016/s0065-3519(99)80039-1

LaFrentz, B.R. and Klesius, P.H. 2009. Development of a Culture Independent Method to Characterize the Chemotactic Response of *Flavobacterium columnare* to Fish Mucus. *Journal of Microbiological Methods*, 77(1), pp.37-40. https://doi.org/10.1016/j.mimet.2008.12.011

LaFrentz, B.R., García, J.C. and Shelley, J.P. 2019. Multiplex PCR for Genotyping *Flavobacterium columnare*. *Journal of Fish Diseases*, 42(11), pp.1531-1542. https://doi.org/10.1111/jfd.13068

LaFrentz, B.R., Khoo, L.H., Lawrence, M.L., Petrie-Hanson, L., Hanson, L.A., Baumgartner, W.A., Hemstreet, W.G., Kelly, A.M., García, J.C., Shelley, J.P. and Johnston, A.E. 2024. *Flavobacterium covae* is the Predominant Species of Columnaris-Causing Bacteria Impacting the Channel Catfish Industry in the Southeastern United States. *Journal of Aquatic Animal Health*, 36(1), pp.3-15. https://doi.org/10.1002/aah.10207

LaFrentz, B.R., Králová, S., Burbick, C.R., Alexander, T.L., Phillips, C.W., Griffin, M.J., Waldbieser, G.C., García, J.C., de Alexandre Sebastião, F., Soto, E. and Loch, T.P. 2022. The Fish Pathogen *Flavobacterium columnare* Represents Four Distinct Species: *Flavobacterium columnare*, *Flavobacterium covae* sp. nov., *Flavobacterium davisii* sp. nov. and *Flavobacterium oreochromis* sp. nov., and Emended Description of *Flavobacterium columnare*. *Systematic and Applied Microbiology*, 45(2), p.126293. https://doi.org/10.1016/j.syapm.2021.126293

LaFrentz, B.R., LaPatra, S.E., Call, D.R. and Cain, K.D. 2008. Isolation of Rifampicin Resistant *Flavobacterium psychrophilum* Strains and Their Potential as Live Attenuated Vaccine Candidates. *Vaccine*, 26(44), pp.5582-5589. https://doi.org/10.1016/j.vaccine.2008.07.083

Ma, J., Bruce, T.J., Jones, E.M. and Cain, K.D. 2019. A Review of Fish Vaccine Development Strategies: Conventional Methods and Modern Biotechnological Approaches. *Microorganisms*, 7(11), p.569. https://doi.org/10.3390/microorganisms7110569

Mariam, D.H., Mengistu, Y., Hoffner, S.E. and Andersson, D.I. 2004. Effect of *rpoB* Mutations Conferring Rifampin Resistance on Fitness of *Mycobacterium tuberculosis*. *Antimicrobial Agents and Chemotherapy*, 48(4), pp.1289-1294. https://doi.org/10.1128/aac.48.4.1289-1294.2004

Maughan, H., Galeano, B. and Nicholson, W.L. 2004. Novel *rpoB* Mutations Conferring Rifampin Resistance on *Bacillus subtilis*: Global Effects on Growth, Competence, Sporulation, and Germination. *Journal of Bacteriology*, 186(8), pp.2481-2486. https://doi.org/10.1128/jb.186.8.2481-2486.2004

Milewski, S. 2002. Glucosamine-6-Phosphate Yynthase—the Multi-Facets Enzyme. *Biochimica et Biophysica Acta (BBA)-Protein Structure and Molecular Enzymology*, 1597(2), pp.173-192. https://doi.org/10.1016/s0167-4838(02)00318-7

Mohammed, H., Olivares-Fuster, O., LaFrentz, S. and Arias, C.R. 2013. New Attenuated Vaccine Against Columnaris Disease in Fish: Choosing the Right Parental Strain is Critical for Vaccine Efficacy. *Vaccine*, 31(45), pp.5276-5280. https://doi.org/10.1016/j.vaccine.2013.08.052

Nascimento, I. P., and L. C. C. Leite. 2012. Recombinant Vaccines and the Development of New Vaccine Strategies. *Brazilian Journal of Medical and Biological* Research 45, no. 12: 1102–1111. https://doi.org/10.1590/s0100-879x2012007500142.

Olivares-Fuster, O. and Arias, C.R. 2011. Development and Characterization of Rifampicin-Resistant Mutants from High Virulent Strains of *Flavobacterium columnare*. *Journal of Fish Diseases*, 34(5), pp.385-394. https://doi.org/10.1111/j.1365-2761.2011.01253.x

Pandya, U., Sinha, M., Luxon, B.A., Watson, D.A. and Niesel, D.W. 2009. Global Transcription Profiling and Virulence Potential of *Streptococcus pneumoniae* After Serial Passage. *Gene*, 443(1-2), pp.22-31. https://doi.org/10.1016/j.gene.2009.04.014

Payne, S.M. 1993. Iron Acquisition in Microbial Pathogenesis. *Trends in Microbiology*, 1(2), pp.66-69. https://doi.org/10.1016/0966-842x(93)90036-q

Perez, J.B.D., Fernando, C., Nosach, R.V., Huang, Y., Harding, J.C. and Hill, J.E. 2018. *In Vitro* Attenuation of a Virulent Swine Isolate of *Brachyspira hampsonii*. *Pathogens and Disease*, 76(1), p.ftx116. https://doi.org/10.1093/femspd/ftx116

Peterman, M.A. and Posadas, B.C. 2019. Direct Economic Impact of Fish Diseases on the East Mississippi Catfish Industry. *North American Journal of Aquaculture*, 81(3), pp.222-229. https://doi.org/10.1002/naaq.10090

Reynolds, M.G. 2000. Compensatory Cvolution in Rifampin-Resistant *Escherichia coli*. *Genetics*, 156(4), pp.1471-1481. https://doi.org/10.1093/genetics/156.4.1471

Seppey, M., Manni, M. and Zdobnov, E.M. 2019. BUSCO: Assessing Genome Assembly and Annotation Completeness. In *Gene Prediction: Methods and Protocols* (pp. 227-245). New York, NY: Springer New York. https://doi.org/10.1007/978-1-4939-9173-0_14

Schirch, V. and Szebenyi, D.M., 2005. Serine Hydroxymethyltransferase Revisited. *Current Opinion in Chemical Biology*, *9*(5), pp.482-487. https://doi.org/10.1016/j.cbpa.2005.08.017

Schurig, G.G., Roop II, R.M., Bagchi, T., Boyle, S., Buhrman, D. and Sriranganathan, N. 1991. Biological Properties of RB51; A Stable Rough Strain of *Brucella abortus*. *Veterinary Microbiology*, 28(2), pp.171-188. https://doi.org/10.1016/0378-1135(91)90091-s

Seemann, T. 2015. Snippy: Rapid Haploid Variant Calling and Core SNP Phylogeny. *GitHub*. *Available at: GitHub. com/tseemann/snippy*.

Shoemaker, C.A., Klesius, P.H. and Evans, J.J. US Department of Agriculture USDA, 2005. Modified Live *Flavobacterium columnare* Against Columnaris Disease in Fish. U.S. Patent 6,881,412. https://doi.org/10.1016/j.fsi.2010.11.001

Shoemaker, C.A., Klesius, P.H., Evans, J.J. and Arias, C.R. 2009. Use of Modified Live Vaccines in Aquaculture. *Journal of the World Aquaculture Society*, 40(5), pp.573-585. https://doi.org/10.1111/j.1749-7345.2009.00279.x

Shoemaker, C.A., Klesius, P.H., Drennan, J.D. and Evans, J.J. 2011. Efficacy of a Modified Live *Flavobacterium columnare* Vaccine in Fish. *Fish & Shellfish Immunology*, 30(1), pp.304-308. https://doi.org/10.1016/j.fsi.2010.11.001

Shoemaker, C.A. and LaFrentz, B.R. 2015. Lack of Association Between *Flavobacterium columnare* Genomovar and Virulence in Hybrid Tilapia *Oreochromis niloticus* (L.)× *Oreochromis aureus* (Steindachner). *Journal of Fish Diseases*, 38(5), pp.491-498. https://doi.org/10.1111/jfd.12262

Starliper, C.E. and Schill, W.B. 2011. Flavobacterial Diseases: Columnaris Disease, Coldwater Disease and Bacterial Gill Disease. In *Fish Diseases and Disorders. Volume 3: Viral, Bacterial and Fungal Infections* (pp. 606-631). Wallingford UK: CABI. https://doi.org/10.1079/9781845935542.0606

Sun, J., Zhu, D., Xu, J., Jia, R., Chen, S., Liu, M., Zhao, X., Yang, Q., Wu, Y., Zhang, S. and Liu, Y. 2019. Rifampin Resistance and its Fitness Cost in *Riemerella anatipestifer*. *BMC Microbiology*, 19(1), p.107. https://doi.org/10.1186/s12866-019-1478-7

Tammas, I., K. Bitchava, and A. I. Gelasakis. 2024. Transforming Aquaculture Through Vaccination: A Review on Recent Developments and Milestones. *Vaccine*, 12, no. 7: 732. https://doi.org/10.3390/vaccines12070732.

Tekedar, H.C., Karsi, A., Reddy, J.S., Nho, S.W., Kalindamar, S. and Lawrence, M.L. 2017. Comparative Genomics and Transcriptional Analysis of *Flavobacterium columnare* Strain ATCC 49512. *Frontiers in Microbiology*, 8, p.588. https://doi.org/10.3389/fmicb.2017.00588

Thirumurugan, R., Kathirvel, M., Vallayyachari, K., Surendar, K., Samrot, A.V. and Muthaiah, M. 2015. Molecular Analysis of *rpoB* Gene Mutations in Rifampicin Resistant

Mycobacterium tuberculosis Isolates by Multiple Allele Specific Polymerase Chain Reaction in Puducherry, South India. *Journal of Infection and Public Health*, 8(6), pp.619-625. https://doi.org/10.1016/j.jiph.2015.05.003

Trchounian, A. and Kobayashi, H. 1999. Kup is the Major K+ Uptake System in *Escherichia coli* Upon Hyper-Osmotic Stress at a Low pH. *FEBS Letters*, 447(2-3), pp.144-148. https://doi.org/10.1016/s0014-5793(99)00288-4

Wakabayashi, H. 1991. Effect of Environmental Conditions on the Infectivity of *Flexibacter columnaris* to Fish. *Journal of Fish Diseases*, 14(3), pp.279-290. https://doi.org/10.1111/j.1365-2761.1991.tb00825.x

Wehrli, W. 1983. Rifampin: Mechanisms of Action and Resistance. *Reviews of Infectious Diseases*, 5 (Supplement_3), pp.S407-S411. https://doi.org/10.1093/clinids/5.supplement_3.s407

Wiegand, G. and Remington, S.J. 1986. Citrate Synthase: Structure, Control, and Mechanism. *Annual Review of Biophysics and Biophysical Chemistry*, 15(1), pp.97-117. https://doi.org/10.1146/annurev.bb.15.060186.000525

Wise, D.J., Greenway, T.E., Byars, T.S., Griffin, M.J. and Khoo, L.H. 2015. Oral Vaccination of Channel Catfish Against Enteric Septicemia of Catfish Using a Live Attenuated *Edwardsiella ictaluri* Isolate. *Journal of Aquatic Animal Health*, 27(2), pp.135-143. https://doi.org/10.1080/08997659.2015.1032440

Wooldridge, K.G. and Williams, P.H. 1993. Iron Uptake Mechanisms of Pathogenic Bacteria. *FEMS Microbiology Reviews*, 12(4), pp.325-348. https://doi.org/10.1111/j.1574-6976.1993.tb00026.x

Wyckoff, E.E., Mey, A.R. and Payne, S.M. 2007. Iron Acquisition in *Vibrio cholerae*. *Biometals*, 20(3), pp.405-416. https://doi.org/10.1007/s10534-006-9073-4

Xie, Y., Li, J., Ding, Y., Shao, X., Sun, Y., Xie, F., Liu, S., Tang, S. and Deng, X. 2022. An Atlas of Bacterial Two-Component Systems Reveals Function and Plasticity in Signal Transduction. *Cell Reports*, 41(3). https://doi.org/10.1016/j.celrep.2022.111502

Xu, D.H., Shoemaker, C.A. and LaFrentz, B.R. 2014. Enhanced Susceptibility of Hybrid Tilapia to *Flavobacterium columnare* After Parasitism by *Ichthyophthirius multifiliis*. *Aquaculture*, 430, pp.44-49. https://doi.org/10.1016/j.aquaculture.2014.03.041

Zhang, Y., Arias, C.R., Shoemaker, C.A. and Klesius, P.H. 2006. Comparison of Lipopolysaccharide and Protein Profiles Between *Flavobacterium columnare* Strains from Different Genomovars. *Journal of Fish Diseases*, 29(11), pp.657-663. https://doi.org/10.1111/j.1365-2761.2006.00760.x

Zügel, U. and Kaufmann, S.H. 1999. Role of Heat Shock Proteins in Protection From and Pathogenesis of Infectious Diseases. *Clinical Microbiology Reviews*, 12(1), pp.19-39. https://doi.org/10.1128/cmr.12.1.19

Chapter III

Efficacy of Rifampicin-Resistant *Flavobacterium covae* Mutants as Vaccines Against Columnaris Disease

3.1. Abstract

Columnaris disease remains a persistent challenge in channel catfish (*Ictalurus punctatus*) aquaculture. Recent taxonomic clarification has identified *Flavobacterium covae* as the predominant columnaris-causing bacteria (CCB) species associated with outbreaks in the southeastern United States aquaculture industry. Given that virulence is species-specific among CCB and the demonstrated success of rifampicin-resistant live-attenuated vaccines in catfish aquaculture, targeting the CCB species most associated with channel catfish production, *F. covae*, may improve protective efficacy. Five rifampicin-resistant *F. covae* mutants derived from virulent parent strains (ALG-00-530, FBCC-CC-12K, ML-17-22A, IPRS-15-49, and ALG-15-231) were evaluated for vaccination efficacy in channel catfish. Vaccination with mutant strains was administered via static immersion, and after the catfish were held for 28 – 48 days post-vaccination, they were exposed to the corresponding virulent parent strain. Vaccine efficacy was assessed using cumulative percent mortality (CPM) and relative percent survival (RPS). Serum IgM antibody titers of sham-vaccinated (control), and vaccinated channel catfish sera were measured by indirect enzyme-linked immunosorbent assay (ELISA), and antigenic profiling

was examined by sodium dodecyl sulfate-polyacrylamide gel electrophoresis (SDS-PAGE) and Western blotting. ALG-00-530, ML-17-22A, and IPRS-15-49 mutants did not confer protection, whereas FBCC-CC-12K and ALG-15-231 mutants demonstrated variable protection, with ALG-15-231 achieving an RPS of 73.4 in one trial. Notably, protection did not correlate with serum IgM antibody titers, and vaccinated fish frequently exhibited antibody levels comparable to sham-vaccinated fish. Protein profiling revealed conserved antigenic patterns between parent and mutant strains, with subtle alterations in band intensity. Collectively, these findings indicate that the protective efficacy of rifampicin-resistant *F. covae* strains is strain-specific and trial-dependent, with FBCC-CC-12K and ALG-15-231 mutants warranting further investigation and optimization as live-attenuated vaccine candidates.

3.2. Introduction

Catfish aquaculture is the leading sector of the United States aquaculture industry. Production of channel catfish (*Ictalurus punctatus*) and hybrid catfish (♀ *I. punctatus* × ♂ blue catfish, *I. furcatus*) contributed to $480 million in total U.S. sales in 2023 (USDA NASS). The majority of U.S. catfish production occurs in the southern states, including Mississippi, Alabama, and Arkansas. Within these states, commercial catfish production supports local economies by providing a high-quality protein food source and offers employment to rural communities. Although catfish aquaculture productivity has remained stable in recent years, total water surface area used for production has decreased, indicating an intensification of catfish aquaculture (USDA NASS 2023; Engle,

Hanson, and Kumar, 2021). Under these intensified production conditions, stress associated with higher stocking densities combined with suboptimal water quality can increase the risk of pathogen transmission and disease prevalence.

Infectious diseases remain one of the biggest challenges to the profitability of catfish aquaculture. Bacterial pathogens are the leading cause of disease-related losses in catfish aquaculture and contribute millions of dollars in treatment expenditures each year (Abdelrahman et al., 2023; Peterman and Posadas, 2019). Among these, columnaris disease, which was historically attributed to a single species, is now known to be caused by four distinct species of columnaris-causing bacteria (CCB): *F. columnare, F. covae, F. davisii,* and *F. oreochromis* (LaFrentz et al., 2022). Of these, *F. covae* is the predominant species associated with disease outbreaks in the southeastern U.S. catfish industry (LaFrentz et al. 2024).

F. covae is a Gram-negative, yellow-pigmented bacterium believed to be ubiquitous in freshwater environments (Starliper and Schill, 2011; Plumb and Hanson, 2010). Outbreaks can result in significant economic losses due to rapid mortality, reduced feed conversion efficiency, increased labor costs, and treatment expenditures (Peterman and Posadas, 2019). Because columnaris outbreaks frequently occur during periods of elevated water temperature and high stocking density, intensification of production systems may further exacerbate disease severity (Starliper and Schill, 2011).

Historically, management of columnaris disease has relied heavily on antimicrobial therapy. However, concerns regarding antimicrobial resistance and consumer preference for reduced antibiotic usage have increased emphasis on preventative disease control

strategies (Kumar et al., 2024; Abdelrahman et al., 2023). Vaccination represents a promising long-term approach to mitigate columnaris disease. However, the development of an efficacious vaccine has proven challenging. Multiple vaccine approaches, including killed bacterins, recombinant and subunit vaccines, micro- and nanoparticle vaccines, and live-attenuated vaccines, have demonstrated varying degrees of protection under laboratory conditions (Harrison et al., 2025). Nevertheless, reproducible efficacy under production settings has remained limited.

Among the different types of vaccinations, two live-attenuated bacterial vaccines have been developed and approved for use in the U.S. catfish industry, including AquaVac-ESC against *Edwardsiella ictaluri* (Wise et al., 2015), and AquaVac-Col for protection against columnaris disease derived from an *F. columnare* isolate (Shoemaker, Klesius, and Evans, 2011). Both vaccines were developed by creating rifampicin-resistant mutants following a modified protocol described by Schurig et al. (1991). Live-attenuated vaccines, particularly rifampicin-resistant mutants, have shown promise due to their ability to retain broad antigenic repertoires and stimulate strong immune responses following immersion exposure (Mohammed et al., 2013; Zhang et al., 2017). Given that *F. covae* is now recognized as the predominant CCB species affecting channel catfish production in the U.S., evaluation of live-attenuated vaccine candidates derived specifically from *F. covae* isolates may provide improved protection tailored to the primary pathogen and fish host. Therefore, the development of a live-attenuated vaccine candidate generated from a virulent *F. covae* strain could confer protection against columnaris disease in channel catfish.

3.3. Materials and Methods

3.3.1. Catfish Rearing and Husbandry Catfish Rearing and Husbandry

All *F. covae* vaccine candidate strains were tested for vaccine efficacy using juvenile channel catfish (*I. punctatus;* Delta Select strain), with a mean weight between 4 and 20 g, and were housed at the E.W. Shell Fisheries Center at Auburn University (Auburn, AL, USA). Catfish were supplied with heated (up to 22 °C), dechlorinated, and UV-treated municipal water buffered with sodium bicarbonate in a recirculating aquaculture system and were fed 2% of their daily body weight with a commercial diet. All vaccination efficacy trials were performed in accordance with Auburn University IACUC PRN #2022-4056.

3.3.2. Bacterial Strains and Culture Conditions

Parent and rifampicin-resistant mutant strains ALG-00-530, FBCC-CC-12K, ML-17-22A, IPRS-15-49, and ALG-15-231were revived onto modified Shieh agar (MSA; LaFrentz and Klesius, 2009) and grown at 28 °C for 48 h, except for ALG-15-231 mutant, which grew for 96 h. Bacteria were subcultured and incubated for an additional 24 h (72 h for ALG-15-231 mutant) at the same temperature. Between 3-5 pure colonies were then inoculated into 12 mL of MSB and incubated for 12 h with shaking at 175 rpm, then the culture was expanded to 1-1.2 L and incubated for an additional 12 h before vaccination. Mutant strains IPRS-15-49 and ALG-15-231 were incubated in broth culture for 24 h. Parent and mutant strains were adjusted to an optical density (OD_{540}) ranging from 0.48-0.71, with target OD values selected based on preliminary dose optimization to achieve colony-forming unit (CFU) concentrations. Prior to vaccination and efficacy challenges, 1 mL of

OD-adjusted bacterial culture was retained and used for serial dilution for CFU mL^{-1} concentration determination.

3.3.3. Vaccination Efficacy Trials

A summary of vaccination trials experimental design details is outlined in Table 3.6.1. Average fish size across all trials ranged between 5-20 g. Vaccination was trial-dependent, and dose across trials ranged between 4.2×10^6 – 1.4×10^7 CFU mL^{-1}. Vaccination duration (amount of time channel catfish were exposed to the vaccine) ranged between 0.5 – 1 h. Groups of channel catfish were vaccinated (using the mutant strain) or sham-vaccinated (serving as a control group using sterile MSB) via a static immersion bath with aeration. Channel catfish were vaccinated at a density of approximately 105 g L^{-1}. The holding period (amount of time channel catfish were held post-vaccination until being challenged with the virulent parent strain) was 28 days for most trials. In vaccination trials with ALG-15-231 (1a and 1b), the holding period was 41 days and 48 days, respectively. In ML-17-22A and IPRS-15-49 trial 1, channel catfish were reared, vaccinated, and held for 28 days in outdoor raceways supplied with pond water. In all other trials, channel catfish were reared, vaccinated, and held in UV-treated, dechlorinated municipal water. During the vaccination trials, fish were monitored twice daily and fed a commercial diet to satiation. Water temperature and dissolved oxygen was 28.6 ± 0.3 °C and 5.7 ± 0.5 mg L^{-1}, respectively, during the vaccination holding period.

Prior to vaccination efficacy trials with the corresponding virulent parent strain, fish from each vaccine group were transferred to replicate treatment tanks holding 38 L of flow-

through water, wherein fish per tank ranged from 20 – 30 depending on the trial (Table 3.6.1). Each challenge consisted of exposing both vaccinated and control groups of channel catfish to a 0.5 h static immersion bath with aeration. Before exposure to the parent strain, water volume in each tank was dropped to 10 L and water flow was halted. The challenge doses of each parent strain for each trial are listed in Table 3.6.1. Mock tanks that served as negative controls were administered sterile MSB in the same volume given for parent strains. Following the immersion challenge, water flow was restored to 0.4 L min^{-1} and water volume increased back to 38 L for the duration of the 7-day efficacy trial. Average water temperature and dissolved oxygen was 28.2 $\pm$ 0.4 °C and 6.7 $\pm$ 0.5 mg L^{-1}, respectively. During the 7-day efficacy challenge, fish were offered a commercial diet twice per day.

3.3.4. Sampling and Data Collection

Prior to each vaccination, a subsample of channel catfish (5-10 per group) was anesthetized with 100 mg mL^{-1} of tricaine methanesulfonate (MS-222; Syndel, Ferndale, WA, USA) buffered with sodium bicarbonate, and blood was drawn via venipuncture of the caudal vertebral vessel using a 25–27-gauge sterile needle and 1 mL syringe. Blood samples were kept on ice during collection, then allowed to clot overnight at 4 °C. Blood samples were centrifuged at 9,503 $\times$ *g* for 5 minutes to collect sera. Sera samples were also taken from 5 individual fish per treatment group (vaccinated and control) at the end of the vaccination holding period prior to challenge with the parent strain. Daily mortalities were collected and recorded to determine cumulative percent mortality (CPM) at the end

of each vaccine efficacy experiment, along with relative percent survival (RPS; Johnson, Flynn, and Amend, 1982). RPS was determined using the following equation:

RPS = [1- [% mortality of vaccinated fish / % mortality of unvaccinated fish]] x 100

Mortalities were examined for clinical signs of disease during every vaccination trial. Bacterial cultures were taken of the gills and posterior kidney of at least 20% of daily tank mortalities for bacterial re-isolation.

3.3.5. Bacterial DNA Extraction and PCR Confirmation

Reisolated bacterial colonies that were collected from daily mortalities were subcultured into MSB and processed for bacterial DNA extraction for endpoint PCR to confirm bacterial identity. Bacterial DNA was extracted using the Quick-DNA Fungal/Bacteria Miniprep Kit (Zymo Research; Irvine, CA, USA) following the manufacturer's protocol. Quantification of DNA was done spectrophotometrically via Nanodrop One (Thermo Fisher Scientific) and stored at -20 °C until PCR analysis.

Confirmation of re-isolated bacteria recovered from dead fish was performed following the CCB multiplex PCR as described by LaFrentz, Garcia, and Shelley (2019). Positive control samples included *F. columnare* IA-S-4, *F. covae* AL-02-36^{T}, *F. davisii* 90-106^{T}, and *F. oreochromis* Costa Rica 04-02-TN^{T}. Each 25 μL reaction included 12.5 μL of 2X DreamTaq Hot Start Green PCR Master Mix (Thermo Fisher Scientific), 2.0 μL of the primer mix including 0.5 μM of GG-fwd, 0.1 μM of GG1-rev, 0.45 μM of GG2- and GG3-rev, and 0.3 μM of GG4-rev, 5.5 μL of nuclease-free water, and 5.0 mL of DNA template at a concentration of 5 ng/μL. Amplification was performed using the following parameters:

initial denaturation for 5 minutes at 95°C, 40 cycles of 30 seconds at 94°C, 20 seconds at 56°C, and 1 minute at 72°C, then a final cycle of 10 minutes at 72°C. Amplified products were resolved on a 2% agarose gel run at 75V for 1 h. Product sizes were 415, 320, 894, and 659 base pairs (bp) corresponding to bacterial species *F. columnare*, *F. covae*, *F. davisii*, and *F. oreochromis*, respectively.

3.3.6. Whole-Cell Lysate Preparation

F. covae parent and mutant strains were revived onto MSA from -80 °C cryostock and grown for 48 h at 28 °C. Next, 3-5 pure colonies were inoculated into 10 mL of MSB and incubated for 12 hours at 28 °C and 175 rpm. Bacterial cultures were expanded to 200 mL by inoculating 6 mL of 12-h culture into fresh MSB and incubated for 12 h under the same parameters. Cultures were centrifuged at 2,683 × *g* for 10 minutes to obtain a pellet. Pellets were resuspended in 1 mL of Protein grade water (BioRad) and placed on ice. Whole-cell lysates were prepared by sonication at 20% amplitude for 30-second intervals four times. Lysates were cooled on ice between each sonication step. Protein concentration was determined using the Pierce Dilution-Free Rapid Gold BCA Protein Assay (Thermo Fisher Scientific, Waltham, MA, USA).

3.3.7. Characterization of IgM Post-Vaccination

An indirect ELISA was used to measure serum IgM antibodies from channel catfish prior to vaccination, and at 28 – 48 days post-vaccination. Controls for the ELISA included pooled sera from hyperimmune channel catfish (positive) and PBST (negative). Corning 96-

well microplates (Corning Life Sciences, Corning, NY, USA) were coated with 100 μL of 10 μg mL^{-1} of bacterial whole-cell lysate in BupH carbonate-bicarbonate buffer (Thermo Scientific, Rockford, IL) and incubated overnight at 4 °C. Plates were rinsed three times with 300 μL of 1X phosphate-buffered saline with 0.05% Tween 20 (PBST) with a microplate washer (BioTek 405 TS Microplate Washer, BioTek Instruments Inc., USA). Plates were then coated with 100 μL of sera diluted at 1:25 in PBST with 4% non-fat dry milk (NFDM) and serially diluted down the plate and incubated at room temperature for 1 hour. Plates were washed again with PBST, and 100 μL anti-channel catfish IgM monoclonal antibody E8 (Klesius, 1990) was diluted 1:1000 and added to the plate and incubated at room temperature for 1 hour. Plates were washed again three times with PBST and 100 μL of goat anti-mouse HRP-conjugated IgG (Bio-Rad, Hercules, CA, USA) was diluted 1:5000 in PBST with 4% NFDM and incubated for 1 hour at room temperature. Plates were washed three times with PBST and 50 μL of 1-Step Ultra TMB-ELISA (Thermo Fisher Scientific) was added and incubated in the dark for 15 minutes. To stop the substrate solution, 50 μL of 4M sulfuric acid was added to the plate and absorbance read immediately at 450 nm using a BioTek Synergy H1 plate reader (Agilent Technologies, Santa Clara, CA, USA) operated under the Gen5 software. Antibody titers were considered positive if the reciprocal of the highest dilution had an optical density of at least two times greater than the negative control.

3.3.8. Antigen Characterization by Western Blot

Frozen whole cell lysates of parent and mutant *F. covae* strains were thawed on ice and diluted to 1 μg mL^{-1} with protein-grade water. Protein was denatured by mixing lysate 1:1 with Laemmli sample buffer (Bio-Rad) containing β-mercaptoethanol (5%), heated for 5 minutes then cooled on ice. Final protein concentration was 0.5 μg mL^{-1} prior to SDS-PAGE. Protein samples were separated by loading 20 μL of sample and 5 μL of Precision Plus Protein Unstained and All Blue standards (Bio-Rad) onto a 12% precast gel (Bio-Rad) and run at 200 V for 45 minutes with a Mini-PROTEAN Tetra Vertical Electrophoresis Cell (Bio-Rad). Protein samples were transferred to a nitrocellulose membrane using a Trans Turbo Blot system (Bio-Rad) using the 1 Mini-TGX protocol (5-150 MW, kD; 3 min; 2.5 A, up to 25 V), then the membrane was stained with Ponceau S staining solution (Thermo Fisher Scientific) to visualize protein transfer. The membrane was thoroughly rinsed with deionized (DI) water and blocked with PBS with 0.05% Tween in with 4% NFDM for 1 h at room temperature with gentle agitation. Then, the membrane was rinsed 3 times with PBST for 3 minutes. Pooled sera from either channel catfish before vaccination (baseline), control groups (sham-vaccinated at the end of the vaccination period), or vaccinated groups (at the end of the vaccination period) for each vaccination trial was diluted to 1:25 in PBST with 4% NFDM and incubated for 1 hour with agitation The membrane was rinsed again 3 times with PBST for 3 minutes. Anti-channel catfish monoclonal IgM antibody (E8) was added 1:1000 in PBST with 4% NFDM and incubated for 1-h with agitation and following the membrane was rinsed 3 times with PBST. Goat anti-mouse IgG Alkaline Phosphate conjugate (Bio-Rad) was added 1:500 in PBST to the membrane and incubated

for 1-h at room temperature with agitation. The membrane was washed again with PBST 3 times for 5 minutes, and alkaline phosphatase conjugate substrate (Bio-Rad) was added and developed for 15 minutes at room temperature with agitation. Color development was stopped by adding DI water and agitating for 10 minutes.

3.3.9. Statistical Analysis

Statistical analyses were performed using GraphPad Prism (version 11.0.0). Differences in mean CPM between control and vaccinated groups were assessed using an unpaired two-tailed Welch's t-test. Differences among sera IgM antibody levels were assessed using an ordinary one-way analysis of variance (ANOVA) with Tukey's multiple comparison test to evaluate pairwise differences among baseline, control, and vaccinated groups. Probabilities of $P < 0.05$ were considered statistically significant.

3.4. Results

3.4.1. Vaccination Efficacy Trials

Mutant strain ALG-00-530 was tested as a vaccine on a cohort of channel catfish with an average weight of 20 g. Following exposure to the virulent parent strain, results indicated a CPM of 35 ± 11.8 % in vaccinated fish, and 6.5 ± 1.2% in the control fish (sham-vaccinated; Table 3.6.2). Mean CPM did not differ significantly between vaccinated and control groups ($P = 0.137$). Due to the higher CPM in the vaccinated group, the trial was repeated once more in 15 g channel catfish to verify the results. Trial 2 yielded similar

results to Trial 1, with the vaccinated group showing having a CPM of 41.6 ± 17.9% compared to the control group (36.3 ± 26.3%; *P* = 0.875; Table 3.6.2). Not only did vaccination with ALG-00-530 fail to protect against the virulent parent strain, but vaccination with this strain could have adversely affected subsequent challenge susceptibility, resulting in higher CPM of vaccinated fish compared to control fish in both trials. Mortalities from the vaccination efficacy trials exhibited typical signs of columnaris disease, including depigmented skin lesions and necrotic gills by 48 hours post-exposure to the virulent parent strain.

Two more vaccination trials were conducted on a new cohort of channel catfish having an average weight of 8 g. Groups of channel catfish were vaccinated with either ML-17-22A or IPRS-15-49, with each group having a control group that were sham-vaccinated with sterile media. Trial 1 of mutant strain ML-17-22A resulted in high mortality in the vaccinated group ((79.4 ± 2.6%) and control group (87.0 ± 12.2%), with minimal difference in mean CPM (*P* = 0.445; Table 2.6.3). Likewise, mutant strain IPRS-15-49 resulted in both vaccinated and control groups having the same CPM (96.2 ± 2.2% and 96.2 ± 3.8%, *P* = 0.994; Table 3.6.3). Bacterial re-isolation was not attempted for this trial due to the acute mortality observed following exposure to the virulent parent strain. The trial was terminated 3 days post-exposure.

Mutant strain FBCC-CC-12K was tested for vaccine efficacy using a new lot of channel catfish with an average weight of 5.1 g. Two doses (low and high) of the analogous parent strain were utilized to test the efficacy of the mutant strain. Although CPM was not dose-dependent, vaccinated groups had numerically lower CPM and RPS values than

control groups. The vaccinated group exposed to the low dose of the parent strain resulted in 16.0 ± 8.3% CPM and the control group had 26.6 ± 9.6% CPM (RPS = 39.8, *P* = 0.449; Table 3.6.3). At the high dose, vaccinated fish yielded 13.3 ± 3.5% CPM and control fish had 16 ± 5.8% CPM (RPS = 16.9, *P* = 0.856). Mortalities were observed starting at 4 days post-exposure to the parent strain, and fish displayed disease signs such as depigmented skin lesions, frayed fins, and necrotic gills.

FBCC-CC-12K, ML-17-22A, and IPRS-15-49 efficacy trials were repeated. FBCC-CC-12K Trial 2 resulted in vaccinated fish having a mean CPM of 30.8 ± 9.9% and the control fish having a mean CPM of 40.8 ± 8.1% (RPS = 24.5, *P* = 0.454; Table 3.6.3), indicating low protection against the virulent strain. *F. covae* was re-isolated from 92.8% (13/14) of the bacterial isolates recovered from mortalities examined during FBCC-CC-12K Trial 2. Fish displayed typical signs of columnaris disease (saddleback lesions, necrotic gills, and frayed fins). Vaccination with ML-17-22A resulted in low mortality among both vaccinated (10.0 ± 3.1%) and control (6.0 ± 3.1%) groups of fish with minimal difference in mean CPM (*P* = 0.385). A total of 5 bacterial isolates were re-isolated from mortalities, with 2/5 isolates confirmed to be *F. covae*. For IPRS-15-49 mutant strain, vaccination efficacy was evaluated across two replicate trials (2a and 2b). In Trial 2a, mean CPM was 26.0 ± 3.9% for the vaccinated group, and 29.3 ± 5.0% for the control group (*P* = 0.483). Similar results were seen for the replicate trial (2b), with 17.3 ± 1.4% CPM in vaccinated fish and 18.0 ± 2.8% CPM in control fish (*P* = 0.682; Table 3.6.3). *F. covae* was re-isolated from 61.5% (8/13) of bacterial isolates recovered from mortalities. Mortalities were observed

starting at 24 h post-exposure to the parent strain and fish displayed typical signs of columnaris disease.

Vaccination with ALG-15-231 mutant resulted in variable outcomes between replicate trials. In Trial 1a, mean CPM was minimal between vaccinated fish (55.0 ± 16.3%) and control fish (54.2 ± 13.1%; $P = 0.925$). However, in Trial 1b, vaccination resulted in a marked reduction in CPM in vaccinated fish (16.6 ± 4.2%), with the control fish still exhibiting a high CPM (62.6 ± 11.2%), corresponding to an RPS of 73.4. There was a significant difference between the mean CPM of vaccinated and control groups in Trial 1b ($P = 0.007$; Table 3.6.3), indicating strong protection against the parent strain. A total of 14 isolates were recovered from the mortalities, with 100% confirmed as *F. covae*. Mortalities in response to exposure to the virulent parent strain started around 24 h post-exposure, and fish displayed disease signs related to columnaris disease.

3.4.2. Antibody Titer Characterization Titer

Serum antibody titers were compared among sham-vaccinated (control), and vaccinated channel catfish at the end of the vaccination holding period prior to challenge with the parent strain. There were no significant differences in antibody titers among control and vaccinated fish in ALG-00-530 trials 1 and 2 ($P = 0.089$ and 0.361, respectively; Figure 3.7.1). In all other trials with FBCC-CC-12K, ML-17-22A, IPRS-15-49, and ALG-15-231, serum IgM antibody titers did not differ statistically between control and vaccinated fish ($P > 0.05$; Figure 3.7.1). This suggests that IgM antibody titers did not correlate with the protection observed during vaccination trials.

3.4.3. Antigenic Characterization of Parent and Mutant Strains

Whole-cell lysate proteins of parent and mutant isolates were compared by SDS-PAGE. Overall, banding pattern between parent and mutant isolates were conserved, although slight differences were observed between parent and mutant protein profiles. ALG-00-530 mutant (lane 4, Figure 3.7.3), demonstrated minor differences in banding pattern around 70-75 kDa compared to its parent. FBCC-CC-12K parent and mutant protein profiles appeared very similar (lanes 5 and 6, Figure 3.7.3). Lanes 7 and 8, representing ML-17-22A parent and mutant, respectively, showed pronounced differences. Notably, two higher molecular weight bands (~140-150 kDa) were present in ML-17-22A mutant but absent in the parent strain. IPRS-15-49 mutant (lane 10, Figure 3.7.3) appeared to lack one protein around ~100 kDa,, while most lower weight bands remained conserved. Similarly, ALG-15-231 mutant (lane 12, Figure 3.7.3), also appeared to lack one prominent protein around ~100 kDa compared to its parent. Conversely, ALG-15-231 mutant demonstrated more prominent banding in the ~12-60 kDa region relative to its parent. Collectively, results of SDS-PAGE indicate that while overall protein profiles of parent and mutant strains of *F. covae* were generally conserved, several mutants displayed alterations in the presence/absence of specific high and mid-molecular weight proteins.

Western blot of the whole -cell parent and mutant isolates probed with pooled channel catfish sera (n = 5) collected at day 0 (baseline), sham-vaccinated catfish, and vaccinated catfish at the end of the vaccination holding period and corresponding to the strain used for vaccination, revealed similar immunoreactive banding patterns (Figure

3.7.4). Antigenic reactivity was present in pooled baseline sera, suggesting that channel catfish may have had pre-existing antibodies that bind to *F. covae* proteins. Prominent banding was observed in lanes 4 and 5 within the ~75-250 kDa region (FBCC-CC-12K parent and mutant; Figure 3.7.4 A), and lanes 6, 7, 8, 10, and 11, referring to ML-17-22A parent and mutant, IPRS-15-49 parent, and ALG-15-231 parent and mutant, showed a variety of banding over a wide region (~20-100 kDa). Faint banding was seen around the ~30-37 kDa region in IPRS-15-49 mutant (lane 9). No detectable reactivity was seen in ALG-00-530 parent and mutant (lanes 2 and 3, respectively).

Sera collected from sham-vaccinated fish at 4 weeks post-vaccination produced immunoreactive profiles that retained high molecular weight bands within the ~50-250 kDa region (Figure 3.7.4 B). FBCC-CC-12K parent and mutant banding showed increased intensity banding at the same region as the baseline sera group, with an additional faint band ~50 kDa. IPRS-15-49 parent and mutant (lanes 8 and 9) also revealed prominent banding ~250 kDa that was not present with baseline sera. Similarly, ALG-00-530 parent and mutant revealed banding at the ~120 kDa region with 4-week sham-vaccinated sera that was absent with baseline sera. Parent and mutant strain pairs ML-17-22A, IPRS-15-49, and ALG-15-231 had a faint band at the ~75 kDa marker. Similar immunoreactive banding was seen in 4-week post-vaccinated sera (Figure 3.7.4 C), although at a lower intensity as the sham-vaccinated sera.

3.5. Discussion

The current study assessed the efficacy of 5 *F. covae* rifampicin-resistant and confirmed attenuated mutant strains as vaccines against columnaris disease in channel catfish. Variability across trials observed in the present study underlines the challenges associated with developing a protective vaccine against columnaris disease. Across multiple vaccination trials, mutants derived from ALG-00-530, ML-17-22A, and IPRS-15-49 did not provide protection to channel catfish against their virulent parent strain. In contrast, two mutant strains (FBCC-CC-12K and ALG-15-231) demonstrated the potential to provide protection to channel catfish, although results were inconsistent between trials. Among both vaccine trials with FBCC-CC-12K mutant, channel catfish vaccinated with the mutant strain exhibited lower CPM than sham-vaccinated control groups (Table 3.6.2), suggesting further optimization of the vaccine dose, exposure duration, immune status, and optimal fish size at time of vaccination could improve reproducibility. Evaluation of ALG-15-231 mutant revealed variability between replicated trials. In Trial 1a, CPM was high among both vaccinated and control groups (55.0% and 54.2%, respectively), with no protection in the vaccinated group was observed. However, the repeat trial (1b) demonstrated substantial protection to vaccinated fish with an RPS of 73.4 (Table 3.6.2). Although protection was not reproducible, ALG-15-231 mutant remains a potential vaccine candidate. Collectively, vaccine efficacy appeared to be strain-specific and trial-dependent, meaning protective outcomes varied not only among mutant strains, but also between repeated trials using the same strain. This variability may reflect differences in experimental conditions, such as fish size and physiological status, virulent parent strain

challenge dose or vaccination dose, or environmental conditions such as water temperature and dissolved oxygen, the presence/absence of other flavobacteria, and stocking density. These results suggest that although attenuated strains of *F. covae* species were tested as vaccines, in most cases, they did not provide protection to channel catfish against columnaris disease. While FBCC-CC-12K and ALG-15-231 mutants demonstrate potential as vaccine candidates, further optimization of vaccination parameters and standardization of experimental conditions will be necessary to achieve consistent and reproducible outcomes.

Immunogenicity data generated in the present study suggest protective responses to the five *F. covae* vaccine strains could be more complex than measurable serum IgM antibody titers. Although two mutants (FBCC-CC-12K and ALG-15-231) demonstrated potential protection based on mortality and survival, serum IgM antibody titers measured for each vaccination trial revealed no significant difference between control and vaccinated groups. Trial 1b with ALG-15-231 demonstrated substantial protection against the virulent parent strain to channel catfish vaccinated with the mutant stain, yet vaccinated fish did not exhibit significant difference in antibody titers compared to control (sham-vaccinated) fish (Figure 3.7.2 D). Protection in trial 1b may reflect differences in host susceptibility or timing relative to immune development between trials, allowing for conferred protection in trial 1b but not in trial 1a. Taken together, the lack of differentiation between control and vaccinated fish antibody titers suggests that vaccination did not enhance systemic humoral responses beyond background immune variation.

Serum and cutaneous IgM antibodies have been shown to play an important role in the protective immune response of channel catfish (Shelby, Shoemaker, and Klesius, 2007; Shoemaker, Xu, Shelby, and Klesius, 2005). Measurable agglutinating antibody titers have been detected following vaccination or natural infection (Fujihara and Nakatani, 1971), however, protective efficacy has not always accompanied robust systemic antibody production. For example, Leal et al. (2010) demonstrated strong antibody responses following injection of killed *F. oreochromis* in tilapia, but this did not provide protection. Similarly, Shoemaker et al. (2005) reported that antibodies detected in skin explants of vaccinated channel catfish were likely produced locally at mucosal surfaces rather than derived from serum. Collectively, these studies suggest that systemic IgM antibody titers may not reflect the most relevant immune mechanisms involved in resistance to columnaris disease, and therefore future studies should include a closer evaluation of mucosal and cell-mediated immunity.

SDS-PAGE analysis revealed that rifampicin-resistant mutants retained much of the overall banding pattern observed in their respective parent lysates, indicating that attenuation with rifampicin did not dramatically alter the overall protein profile. Subtle strain-specific differences in the presence or absence of select molecular weight bands were observed, indicating that attenuation resulted in modified protein expression. Similar results were seen in SDS-PAGE of parent and rifampicin-resistant mutant pairs of *F. covae* (Olivares-Fuster and Arias, 2011) and *F. psychrophilum* (LaFrentz et al., 2008). Likewise, comparative analyses of *F. columnare* strains demonstrated that attenuated isolates retained many shared protein bands while lacking select bands present in virulent strains,

including differences in the ~33-34 kDa range (Zhang, Arias, Shoemaker, and Klesius, 2006).

Although slight changes were observed between parent and mutant protein profiles in this study, protein identity was not investigated. Proteomic characterization of the sarcosine-insoluble outer membrane fraction of *F. columnare* revealed numerous proteins spanning a broad molecular weight range, including proteins involved in membrane biogenesis, nutrient transport, and host interaction, such as TonB-dependent receptors and other outer membrane-associated proteins (Liu, Nie, Zhang, and Li, 2008). The presence of proteins with diverse functional roles across a wide molecular weight range supports the interpretation that relatively minor differences in SDS-PAGE banding patterns may correspond to biologically meaningful changes in proteins involved in a broad range of functions, like membrane structure, nutrient acquisition, or host-pathogen interactions. Therefore, it would be beneficial to identify the expression and function of unique proteins observed from the SDS-PAGE comparison of parent and mutant strains in this study. Characterization of such proteins could provide insight into the mutant strain phenotype and elucidate their potential role in attenuation and immunogenic function.

Western blot analysis revealed that sera from baseline, sham-vaccinated, and vaccinated fish recognized multiple protein bands across parent and mutant protein lysates. The shared immunoreactive banding patterns between parent and mutant proteins reinforce that antigenic targets were conserved following attenuation. This is further supported by immunoblot analyses demonstrating that, despite variation in SDS-PAGE banding patterns among flavobacterial isolates, many antigenic proteins are

conserved across strains and related genera. For example, whole-cell antigens of *F. columnare* have been shown to produce antibody responses against a broad range of molecular weight proteins, whereas lipopolysaccharide fractions elicit more restricted antigenic profiles, with prominent bands near ~20 kDa (Shelby, Shoemaker, and Klesius, 2007). In addition, shared immunogenic bands have been observed across a broad molecular weight range (~90-250 kDa), including prominent conserved regions near 85, 74, and 35 kDa (Bruce et al., 2020). At the same time, isolate-specific antigenic bands have also been reported, indicating that both conserved and variable protein targets contribute to host immune recognition. These findings indicate that rifampicin-induced attenuation may alter the expression of select proteins associated with virulence and antigenicity while preserving a substantial proportion of shared antigenic determinants. One explanation of the observed alterations could be from transcriptional changes associated with the *rpoB* gene (Jin and Gross, 1988), which could potentially alter the expression of specific immunogenic determinants without substantially altering the overall protein profile.

Another explanation of the presence of antibody recognition in baseline and sham-vaccinated fish could be due to cross-reactivity among CCB isolates due to conserved protein and LPS antigens, which has been noted previously in other CCB species (Zhang et al., 2006). The presence of antibody recognition in baseline and control groups of channel catfish could also mean that fish were previously exposed to CCB species prior to vaccination. Notably, vaccinated sera from vaccinated channel catfish did not demonstrate novel antigen recognition relative to control groups, suggesting that

immersion exposure to live-attenuated strains did not substantially expand the range of detectable systemic antibody targets.

Together, these findings suggest that preservation of antigenicity alone is insufficient to drive protective immunity. Previous transcriptomic studies provide further insight into potential mechanisms. Regulation of rhamnose-binding lectin (RBL) expression and arginine metabolism pathways, including inducible nitric oxide synthase (iNOS), has been linked to host susceptibility and resistance (Sun et al., 2012; Beck et al., 2012; Peatman et al., 2013; Liu et al., 2013). Recently, attenuated *F. covae* strains were shown to induce broader early immune activation in gill tissue compared to virulent strains, including upregulation of chemokines and iNOS (Zhang et al., 2024). These findings suggest that effective live-attenuated vaccines may function by priming early mucosal and innate immune pathways.

In conclusion, targeting the predominant CCB species (*F. covae*) through rifampicin-resistant live-attenuated vaccination did not yield consistent protection in channel catfish. Protective efficacy was strain-specific and trial-dependent and did not correlate with systemic humoral antigenicity. However, rifampicin-resistant strains FBCC-CC-12K and ALG-15-231 provided varying degrees of protection and warrant further investigation and optimization as live-attenuated vaccine candidates. When considered alongside prior immunogenicity and transcriptomic studies, these results support a model in which protective immunity against columnaris disease is multifactorial and likely driven by early mucosal and innate immune priming. Future work with FBCC-CC-12K and ALG-15-231 mutants should focus on optimizing vaccination parameters, including dose, fish size

and immune status, administration of the vaccine (e.g., immersion versus oral), and evaluating these vaccine candidates under standardized conditions to improve consistency and reproducibility. Additionally, incorporation of mucosal antibody assays and transcriptomic profiling may help identify reliable correlates of protection and guide the development of more effective vaccine strategies.

3.6. Tables

Table 3.6.1. Summary of vaccination trials experimental design, including average fish size, vaccination dose, vaccination duration, holding period, challenge dose, replicate tanks, and fish per tank. CFU = colony forming units.

F. covae Strain/Trial	Fish Size (g)	Vaccination Dose (CFU mL^{-1})	Vaccination Duration	Holding Period	Challenge Dose (CFU mL^{-1})	Replicate Tanks	Fish Per Tank
ALG-00-530 Trial 1	20 ± 2.0	1.0×10^7	0.5 h	28 days	1.3×10^6	3	30
ALG-00-530 Trial 2	15 ± 1.8	8.7×10^6	0.5 h	28 days	1.4×10^6	3	30
FBCC-CC-12K Trial 1a	5 ± 1.7	1.2×10^7	1 h	28 days	1.3×10^5	3	25
FBCC-CC-12K Trial 1b					5.5×10^5		
FBCC-CC-12K Trial 2	20 ± 0.7	1.2×10^7	1 h	28 days	3.5×10^6	6	20
ML-17-22A Trial 1	8 ± 0.4	1.3×10^7	0.5 h	28 days	4.5×10^5	3	26
ML-17-22A Trial 2	17 ± 1.0	1.1×10^7	1 h	28 days	1.0×10^5	3	20
IPRS-15-49 Trial 1	8 ± 0.4	1.4×10^7	0.5 h	28 days	1.9×10^6	3	26
IPRS-15-49 Trial 2a	17 ± 1.0	7.4×10^6	1 h	28 days	6.5×10^5	6	20
IPRS-15-49 Trial 2b					6.6×10^5		
ALG-15-231 Trial 1a	20 ± 0.7	4.2×10^6	1 h	41 days	2.1×10^6	6	20
ALG-15-231 Trial 1b				48 days	3.6×10^6		

Table 3.6.2. *Flavobacterium covae* rifampicin-resistant mutant ALG-00-530 vaccination efficacy trials in juvenile channel catfish. Cumulative percent mortality (CPM) ± standard error of the mean (SEM), and p-value of unpaired, two-tailed Welch's t-test are reported.

Trial	Vaccinated CPM (%)	Control CPM (%)	Mock Vaccinated CPM (%)	Mock Control CPM (%)	*P*-value
1	35.0 ± 11.8	6.5 ± 1.2	0.0 ± 0.0	0.0 ± 0.0	0.137
2	41.6 ± 17.9	36.3 ± 26.3	1.3 ± 1.3	1.3 ± 1.3	0.875

Table 3.6.3. *Flavobacterium covae* rifampicin-resistant mutant vaccine efficacy trials in channel catfish and Nile tilapia. Cumulative percent mortality (CPM) ± standard error of the mean (SEM), relative percent survival (RPS), bacterial doses in colony-forming units per milliliter (CFU mL^{-1}), and p-value of unpaired, two-tailed Welch's t-test are reported for all vaccine trials. NA=not available.

Isolate	Trial	Control CPM (%)	Vaccinated CPM (%)	Mock CPM (%)	RPS	*P*-value
FBCC-CC-12K	1a	26.6 ± 9.6	16.0 ± 8.3	0.0 ± 0.0	39.8	0.449
	1b	16.0 ± 5.8	13.3 ± 3.5	0.0 ± 0.0	16.9	0.856
	2	40.8 ± 8.1	30.8 ± 9.9	2.5 ± 2.5	24.5	0.454
ML-17-22A	1	87.0 ± 12.2	79.4 ± 2.6	0.0 ± 0.0	NA	0.445
	2	6.0 ± 3.1	10.0 ± 3.1	0.0 ± 0.0	NA	0.385
IPRS-15-49	1	96.2 ± 3.8	96.2 ± 2.2	0.0 ± 0.0	NA	0.994
	2a	29.3 ± 5.0	26.0 ± 3.9	12.0 ± 0.0	NA	0.483
	2b	18.0 ± 2.8	17.3 ± 1.4	8.0 ± 0.0	NA	0.682
ALG-15-231	1a	54.2 ± 13.1	55.0 ± 16.3	0.0 ± 0.0	NA	0.925
	1b	62.6 ± 11.2 [a]	16.6 ± 4.2 [b]	0.0 ± 0.0	73.4	0.007

Note: Superscript letters represent significance between vaccinated and control mean CPM.

3.7. Figures

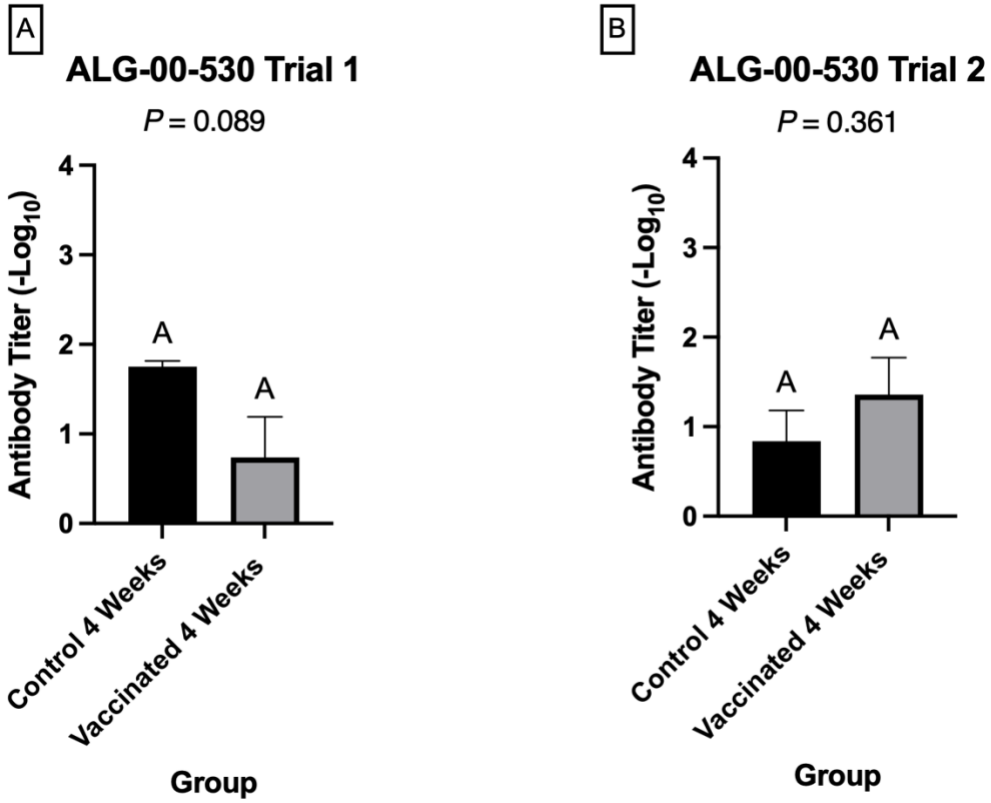

Figure 3.7.1. Mean IgM antibody titer (transformed as $-\log_{10}$) ± standard error of the mean (SEM) of 5 individual channel catfish at 4-weeks post-vaccination with sterile MSB (control) and vaccinated with mutant strain ALG-00-530 (vaccinated).

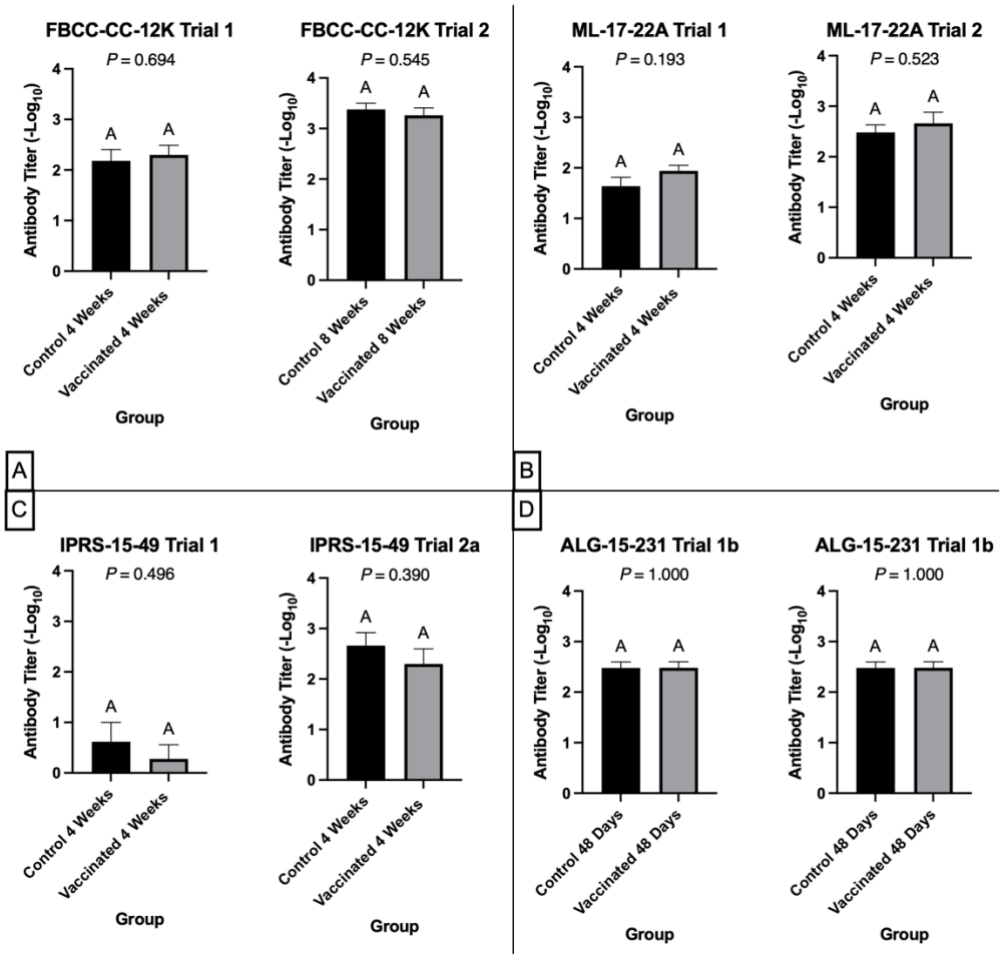

Figure 3.7.2. Mean IgM antibody titer (transformed as -$\log_{10}$) ± SEM of 5 individual channel catfish at 4-weeks post-vaccination with sterile MSB (control) and vaccinated with mutant strain A) FBCC-CC-12K, B) ML-17-22A, C) IPRS-15-49, and D) ALG-15-231.

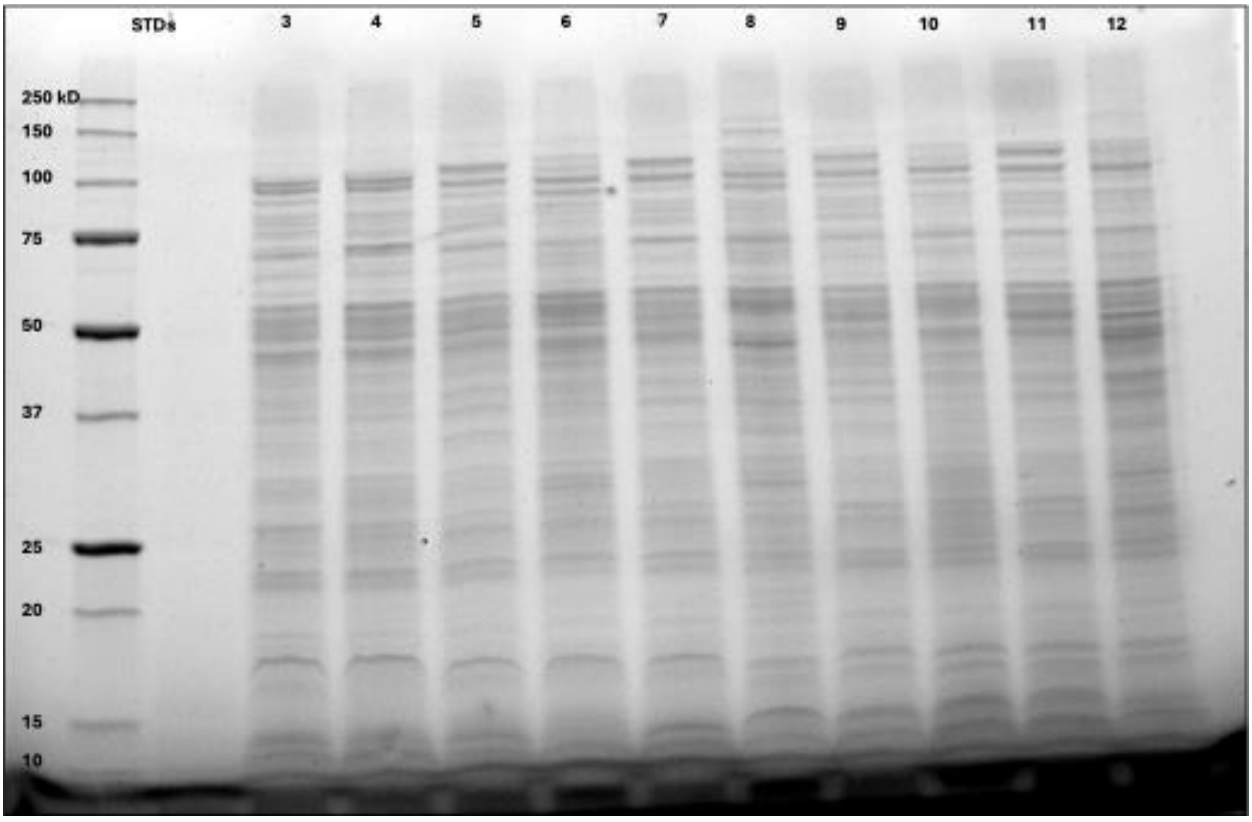

Figure 3.7.3. SDS-PAGE gel (12%; 12-well) profile of *Flavobacterium covae* whole-cell lysates. Lane 1 & 2: Precision Plus Protein Unstained and All Blue Standards (STDs; Bio-Rad); lanes 3 & 4: ALG-00-530 parent & mutant; lanes 5 & 6: FBCC-CC-12K parent & mutant; lanes 7 & 8: ML-17-22A parent and mutant; lanes 9 & 10: IPRS-15-49 parent and mutant; and lanes 11 & 12: ALG-15-231 parent & mutant.

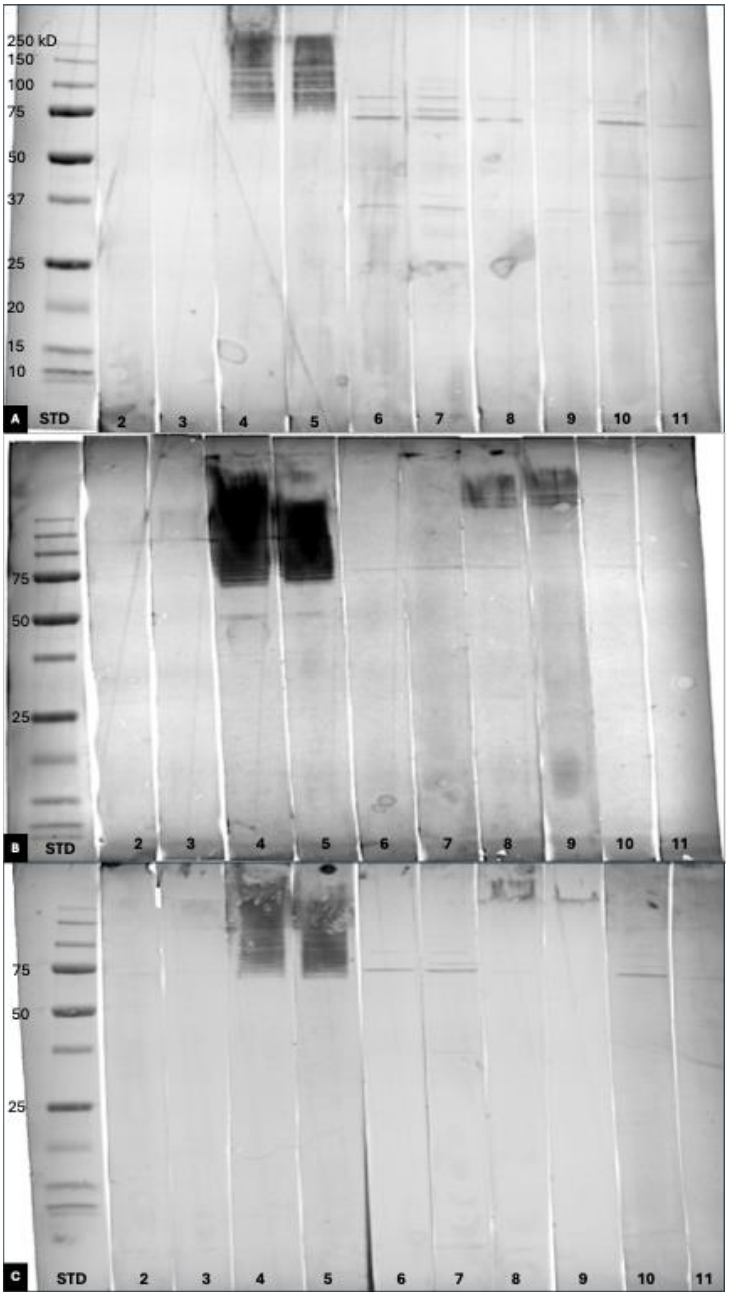

Figure 3.7.4. Western blot of *Flavobacterium covae* parent and mutant strain whole-cell lysates, A) probed with pooled channel catfish sera on day 0 pre-vaccination from ALG-00-530 Trial 2, FBCC-CC-12K Trial 2, ML-17-22A Trial 2, IPRS-15-49 Trial 2a, and ALG-15-231 Trial 1b, B) probed with pooled channel catfish sera at the end of the vaccination period for the same vaccine trials; post-sham-vaccination (control), and C) probed with pooled channel catfish sera at the end of the vaccination period for the same vaccine trials. Lane 1: Precision Plus Protein Unstained Standard (STD; Bio-Rad); lanes 2 & 3: ALG-00-530 parent & mutant; lanes 4 & 5: FBCC-CC-12K parent and mutant; lanes 6 & 7: ML-17-22A

parent and mutant; lanes 8 & 9: IPRS-15-49 parent and mutant; and lanes 10 & 11: ALG-15-231 parent and mutant.

3.8. References

Abdelrahman, H.A., Hemstreet, W.G., Roy, L.A., Hanson, T.R., Beck, B.H. and Kelly, A.M. 2023. Epidemiology and Economic Impact of Disease-Related Losses on Commercial Catfish Farms: A Seven-Year Case Study from Alabama, USA. *Aquaculture*, 566, p.739206. https://doi.org/10.1016/j.aquaculture.2022.739206

Beck, B.H., Farmer, B.D., Straus, D.L., Li, C. and Peatman, E. 2012. Putative Roles for a Rhamnose Binding Lectin in *Flavobacterium columnare* Pathogenesis in Channel Catfish *Ictalurus punctatus*. *Fish & Shellfish Immunology*, 33(4), pp.1008-1015. https://doi.org/10.1016/j.fsi.2012.08.018

Bruce, T.J., Ma, J., Knupp, C., Loch, T.P., Faisal, M. and Cain, K.D. 2020. Cross-Protection of a Live-Attenuated *Flavobacterium psychrophilum* Immersion Vaccine Against Novel *Flavobacterium* spp. and *Chryseobacterium* spp. Strains. *Journal of Fish Diseases*, 43(8), pp.915-928. https://doi.org/10.1111/jfd.13201

Decostere, A., Haesebrouck, F., Turnbull, J.F. and Charlier, G. 1999. Influence of Water Quality and Temperature on Adhesion of High and Low Virulence *Flavobacterium columnare* Strains to Isolated Gill Arches. *Journal of Fish Diseases*, 22(1), pp.1-11. https://doi.org/10.1046/j.1365-2761.1999.00132.x

Engle, C.R., Hanson, T. and Kumar, G. 2022. Economic History of US Catfish Farming: Lessons for Growth and Development of Aquaculture. *Aquaculture Economics & Management*, 26(1), 1-35. https://doi.org/10.1080/13657305.2021.1896606

Fujihara, M. P., and R. E. Nakatani. 1971. Antibody production and immune responses of rainbow trout and Coho salmon to *Chondrococcus columnaris*. *Journal of the Fisheries Research Board of Canada,* 28, 1253–1258. https://doi.org/10.1139/f71-191.

Harrison, C.E., LaFrentz, B.R., Shoemaker, C.A., Lange, M.D., Liles, M.R., Mohammed, H.H., Beck, B.H., Churchman, E.M., Peatman, E. and Bruce, T.J. 2025. An Overview of Vaccine Development Strategies for Columnaris-Causing Bacteria in Cultured Fish. *Journal of Fish Diseases*, 48(8), p.e14155. https://doi.org/10.1111/jfd.14155

Jin, D.J. and Gross, C.A. 1988. Mapping and Sequencing of Mutations in the *Escherichia coli rpoB* Gene that Lead to Rifampicin Resistance. *Journal of Molecular Biology*, 202(1), pp.45-58. https://doi.org/10.1016/0022-2836(88)90517-7

Johnson, K.A., Flynn, J.K. and Amend, D.F. 1982. Onset of Immunity in Salmonid Fry Vaccinated by Direct Immersion in *Vibrio anguillarum* and *Yersinia ruckeri* Bacterins. *Journal of Fish Diseases*, 5(3), pp.197-205. https://doi.org/10.1111/j.1365-2761.1982.tb00474.x

Klesius, P. H. 1990. Effect of Size and Temperature on the Quantity of Immunoglobulin in Channel Catfish, *Ictalurus punctatus*. *Veterinary Immunology and Immunopathology*, 24(2), 187-195. https://doi.org/10.1016/0165-2427(90)90021-j

LaFrentz, B.R., LaPatra, S.E., Call, D.R. and Cain, K.D. 2008. Isolation of Rifampicin Resistant *Flavobacterium psychrophilum* Strains and their Potential as Live Attenuated Vaccine Candidates. *Vaccine*, 26(44), pp.5582-5589. https://doi.org/10.1016/j.vaccine.2008.07.083

LaFrentz, B.R. and Klesius, P.H. 2009. Development of a Culture Independent Method to Characterize the Chemotactic Response of *Flavobacterium columnare* to Fish Mucus. *Journal of Microbiological Methods*, 77(1), pp.37-40. https://doi.org/10.1016/j.mimet.2008.12.011

LaFrentz, B.R., Khoo, L.H., Lawrence, M.L., Petrie-Hanson, L., Hanson, L.A., Baumgartner, W.A., Hemstreet, W.G., Kelly, A.M., García, J.C., Shelley, J.P., Johnston, A.E., Bruce, T.J, and Griffin, M.J. 2024. *Flavobacterium covae* is the Predominant Species of Columnaris-Causing Bacteria Impacting the Channel Catfish Industry in the Southeastern United States. *Journal of Aquatic Animal Health*, 36(1), pp.3-15. https://doi.org/10.1002/aah.10207

LaFrentz, B.R., Królová, S., Burbick, C.R., Alexander, T.L., Phillips, C.W., Griffin, M.J., Waldbieser, G.C., García, J.C., de Alexandre Sebastião, F., Soto, E. and Loch, T.P. 2022. The Fish Pathogen *Flavobacterium columnare* Represents Four Distinct Species: *Flavobacterium columnare*, *Flavobacterium covae* sp. nov., *Flavobacterium davisii* sp. nov. and *Flavobacterium oreochromis* sp. nov., and Emended Description of *Flavobacterium columnare*. *Systematic and Applied Microbiology*, 45(2), p.126293. https://doi.org/10.1016/j.syapm.2021.126293

Leal, C.A.G., Carvalho-Castro, G.A., Sacchetin, P.S.C., Lopes, C.O., Moraes, A.M. and Figueiredo, H.C.P. 2010. Oral and Parenteral Vaccines Against *Flavobacterium columnare:* Evaluation of Humoral Immune Response by ELISA and *In Vivo* Efficiency in Nile Tilapia (*Oreochromis niloticus*). *Aquaculture International*, 18(4), pp.657-666. https://doi.org/10.1007/s10499-009-9287-x

Liu, G.Y., Nie, P., Zhang, J. and Li, N. 2008. Proteomic Analysis of the Sarcosine-Insoluble Outer Membrane Fraction of *Flavobacterium columnare*. *Journal of Fish Diseases*, 31(4), pp.269-276. https://doi.org/10.1111/j.1365-2761.2007.00898.x

Liu, L., C. Li, B. Su, B. H. Beck, and Peatman, E. 2013. Short-Term Feed Deprivation Alters Immune Status of Surface Mucosa in Channel Catfish (*Ictalurus punctatus*). *PLoS One* 8(9), e74581. https://doi.org/10.1371/journal.pone.0074581.

Mohammed, H., Olivares-Fuster, O., LaFrentz, S. and Arias, C.R. 2013. New Attenuated Vaccine Against Columnaris Disease in Fish: Choosing the Right Parental Strain is Critical for Vaccine Efficacy. *Vaccine*, 31(45), pp.5276-5280. https://doi.org/10.1016/j.vaccine.2013.08.052

Olivares-Fuster, O. and Arias, C.R. 2011. Development and Characterization of Rifampicin-Resistant Mutants from High Virulent Strains of *Flavobacterium columnare*. *Journal of Fish Diseases*, 34(5), pp.385-394. https://doi.org/10.1111/j.1365-2761.2011.01253.x

Peatman, E., Li, C., Peterson, B.C., Straus, D.L., Farmer, B.D. and Beck, B.H. 2013. Basal Polarization of the Mucosal Compartment in *Flavobacterium columnare* Susceptible and Resistant Channel Catfish (*Ictalurus punctatus*). *Molecular Immunology*, 56(4), pp.317-327. https://doi.org/10.1016/j.molimm.2013.04.014

Peterman, M.A. and Posadas, B.C. 2019. Direct Economic Impact of Fish Diseases on the East Mississippi Catfish Industry. *North American Journal of Aquaculture*, 81(3), pp.222-229. https://doi.org/10.1002/naaq.10090

Plumb, J.A. and Hanson, L.A. 2010. *Health Maintenance and Principal Microbial Diseases of Cultured Fishes*. John Wiley & Sons. https://doi.org/10.1002/9780470958353

Shelby, R.A., Shoemaker, C.A. and Klesius, P.H. 2007. Passive Immunization of Channel Catfish *Ictalurus punctatus* with Anti-*Flavobacterium columnare* Sera. *Diseases of Aquatic Organisms*, 77(2), pp.143-147. https://doi.org/10.3354/dao01828

Schurig, G.G., Roop II, R.M., Bagchi, T., Boyle, S., Buhrman, D. and Sriranganathan, N. 1991. Biological Properties of RB51; A Stable Rough Strain of *Brucella abortus*. *Veterinary Microbiology*, 28(2), pp.171-188. https://doi.org/10.1016/0378-1135(91)90091-s

Shoemaker, C.A., Klesius, P.H., Drennan, J.D. and Evans, J.J. 2011. Efficacy of a Modified Live *Flavobacterium columnare* Vaccine in Fish. *Fish & Shellfish Immunology*, 30(1), pp.304-308. https://doi.org/10.1016/j.fsi.2010.11.001

Shoemaker, C.A., Xu, D.H., Shelby, R.A. and Klesius, P.H. 2005. Detection of Cutaneous Antibodies Channel Catfish, *Ictalurus punctatus* (Rafinesque). *Aquaculture Research*, 36(8), pp.813-818. https://doi.org/10.1111/j.1365-2109.2004.01291.x

Starliper, C.E. and Schill, W.B. 2011. Flavobacterial Diseases: Columnaris Disease, Coldwater Disease and Bacterial Gill Disease. In *Fish Diseases and Disorders. Volume 3: Viral, Bacterial and Fungal Infections* (pp. 606-631). Wallingford UK: CABI. https://doi.org/10.1079/9781845935542.0606

Sun, F., Peatman, E., Li, C., Liu, S., Jiang, Y., Zhou, Z. and Liu, Z. 2012. Transcriptomic Signatures of Attachment, NF-kB Suppression and ifn Stimulation in the Catfish Gill Following Columnaris Bacterial Infection. *Developmental and Comparative Immunology,* 38(1), pp.169-180. https://doi.org/10.1016/j.dci.2012.05.006

Tongsri, P., Meng, K., Liu, X., Wu, Z., Yin, G., Wang, Q., Liu, M. and Xu, Z. 2020. The Predominant Role of Mucosal Immunoglobulin IgT in the Gills of Rainbow Trout (*Oncorhynchus mykiss*) After Infection with *Flavobacterium columnare*. *Fish & Shellfish Immunology*, 99, pp.654-662. https://doi.org/10.1016/j.fsi.2020.01.044

Wise, D.J., Greenway, T.E., Byars, T.S., Griffin, M.J. and Khoo, L.H. 2015. Oral Vaccination of Channel Catfish Against Enteric Septicemia of Catfish Using a Live Attenuated *Edwardsiella ictaluri* Isolate. *Journal of Aquatic Animal Health*, 27(2), pp.135-143. https://doi.org/10.1080/08997659.2015.1032440

Zhang, D., Zhou, G., Thongda, W., Li, C., Ye, Z., Zhao, H., Beck, B.H., Mohammed, H. and Peatman, E. 2024. Early Divergent Responses to Virulent and Attenuated Vaccine Isolates of *Flavobacterium covae* sp. nov. in Channel Catfish, *Ictalurus punctatus*. *Fish & Shellfish Immunology,* 144:109248. https://doi.org/10.1016/j.fsi.2023.109248.

Zhang, D., Thongda, W., Li, C., Zhao, H., Beck, B.H., Mohammed, H., Arias, C.R. and Peatman, E. 2017. More Than Just Antibodies: Protective Mechanisms of a Mucosal Vaccine Against Fish Pathogen *Flavobacterium columnare*. *Fish & Shellfish Immunology*, 71, pp.160-170. https://doi.org/10.1016/j.fsi.2017.10.001

Zhang, Y., Arias, C.R., Shoemaker, C.A. and Klesius, P.H. 2006. Comparison of Lipopolysaccharide and Protein Profiles between *Flavobacterium columnare* Strains from Different Genomovars. *Journal of Fish Diseases*, 29(11), pp.657-663. https://doi.org/10.1111/j.1365-2761.2006.00760.x

Chapter IV

Identification, Virulence, and Co-Infection of Yellow-Pigmented Bacteria in Juvenile Channel Catfish (*Ictalurus punctatus*)

4.1. Abstract

Yellow-pigmented bacteria (YPB) resembling atypical *Flavobacterium* species other that of columnaris-causing bacteria were isolated from diseased channel catfish (*Ictalurus punctatus*) and hybrid catfish (female *I. punctatus* × male *I. furcatus*). Initial *gyrB* gene sequencing presumptively identified the isolates as members of the genera *Chryseobacterium* and *Flavobacterium*. Whole-genome sequencing using long reads subsequently resolved the identities of the YPB as possible undescribed *Chryseobacterium* species closely related to *C. mucoviscidosis* (n=4), *C. gleum* (n=1), *C. cucumeris* (n=1), *Empedobacter brevis* (n=1), and *Flavobacterium saliperosum* (n=1). High-quality draft genomes were assembled with BUSCO completeness scores ranging from 98.5-100% and a high degree of continuity (1-3 contigs per isolate). Virulence screening revealed cumulative percent mortality (CPM) in channel catfish intraperitoneally (i.p.)-injected with *C. mucoviscidosis* isolates S22-436 (10%) and S22-539 (10%), *C. gleum* S22-0124 (10%), *C. cucumeris* S22-519 (10%), and 70% CPM from *E. brevis* S22-158. Channel catfish i.p.-injected with *C. mucoviscidosis* S22-335 and S22-424, *F. saliperosum* S18-81, and all isolates exposed via immersion exposure resulted in 0% CPM. A larger

virulence assessment of *E. brevis* S22-158 via i.p. injection in channel catfish demonstrated a dose-dependent trend, with CPM ranging from 1.6-90% and the median lethal dose (LD_{50}) estimated to be 1.3×10^8 CFU/fish. Infected fish showed gross signs of disease, including exophthalmia, hemorrhage, and frayed fins. Additionally, *E. brevis* was re-isolated from the kidney and spleen tissue of infected fish, demonstrating experimental pathogenicity. In a co-infection with channel catfish, 1.8×10^8 CFU/fish of *E. brevis* was i.p.-injected, and 1.2×10^6 CFU mL^{-1} of *F. covae* ALG-00-530 was administered via immersion for 30 minutes. The co-infected fish exhibited significantly higher mortality (P = 0.017) than a single exposure to *F. covae* alone. Whereas there was no difference in mortality between the single infection of *E. brevis* and the co-infected group (P = 0.506). This is the first report of pathogenic potential by *C. mucoviscidosis* and *E. brevis* in channel catfish. Collectively, these findings highlight the importance of genome-based bacterial identification for diagnostics and broaden the current understanding of atypical YPB associated with disease in channel catfish aquaculture.

4.2. Introduction

The southeastern United States aquaculture industry primarily produces channel catfish (*Ictalurus punctatus*) and hybrid catfish (female *I. punctatus* bred with male *I. furcatus*). In 2025, the catfish industry had sales of $394 million USD, with Mississippi, Alabama, Arkansas, and Texas accounting for 96% of total sales (USDA NASS, 2026). The catfish aquaculture industry has shifted from historically extensive practices to more intensive systems, including split ponds systems, intensive aeration, and increased

stocking density (Engle, Hansen, and Kumar, 2022). Although intensive systems yield enhanced efficiency and lower production costs, increased stocking density increases the risk of disease outbreak.

Infectious diseases are a critical threat to aquaculture sustainability, especially in high-level production settings. Disease outbreaks result from infectious agents, such as bacteria, viruses, parasites, fungi, and oomycetes. Non-infectious factors, such as poor water quality, toxic algal blooms, handling and crowding stress, and nutritional deficiencies, can stress fish and increase their susceptibility to disease. In catfish aquaculture, bacterial pathogens are the main cause of disease-related losses, resulting in millions of dollars in treatment costs each year (Peterman and Posadas, 2019; Abdelrahman et al., 2023). The leading bacterial pathogens in the southeastern catfish industry include virulent *Aeromonas hydrophila* (motile *Aeromonas* septicemia), *Flavobacterium covae* (columnaris disease), and *Edwardsiella* species, including *E. ictaluri* (enteric septicemia of catfish; ESC; Peterman and Posadas, 2019; Abdelrahman et al., 2023; LaFrentz et al., 2024), and *E. piscicida* (Griffin et al, 2015; Kumar et al, 2024). These infectious bacterial pathogens are harmful on their own, yet they can also occur as co-infections, which can exacerbate disease onset and mortality (Wise et al., 2021a; Wise et al., 2021b; Wise et al., 2023; Wang et al., 2025). Given the potential for co-infections to intensify disease, it is important to consider the role of additional, less-characterized bacterial taxa within disease dynamics in catfish aquaculture.

Chryseobacterium spp. were previously classified in the family *Flavobacteriaceae* (Vandamme, Bernardet, Segers, Kersters, and Holmes, 1994). García-López et al. (2019)

performed a large-scale, genome-based phylogenetic analysis of the phylum *Bacteroidetes*, which resulted in the genus *Chryseobacterium* being reassigned to the Family *Weeksellaceae*. Regardless of the reclassification, *Chryseobacterium* and *Flavobacterium* spp. share several phenotypic and biochemical characteristics. Both genera consist of gram-negative, yellow-pigmented bacilli that produce cytochrome c oxidase and catalase enzymes, are non-fermentative, and aerobic (Bernardet and Bowman, 2015; Hugo, Bernardet, Nicholson, and Kämpfer, 2015). Likewise, both genera have been found in the same habitat, such as soil and marine and freshwater (reviewed in Loch and Faisal, 2015a). These shared traits can make baseline identification challenging. However, *Chryseobacterium* spp. can be distinguished by their darker, opaque yellow-orange pigment and having a strong odor (Kim et al., 2020).

Chryseobacterium spp. have been reported in human infection cases and certain spp., such as *C. indologenes*, are considered emerging (Mukerji, Kakarala, Smith, and Kusz, 2016). Likewise, several spp. of *Chryseobacterium* are also considered emerging fish pathogens. Ilardi, Fernández, and Avendaño-Herrera (2009) isolated *C. piscicola* from diseased rainbow trout (*Oncorhynchus mykiss*) and Atlantic salmon (*Salmo salar)*, *C. balustinum* was isolated from diseased rainbow trout (Mallik et al., 2023), *C. indologenes* was isolated from a co-infection with *Aeromonas dhakensis* in largemouth bass (*Micropterus nigricans*; Yang et al., 2024), Shahi, Sharma, Pandey, Bisht, and Mallik (2018) recovered *C. scophthalmum* from gill lesions in golden masheer (*Tor putitora)*, and several spp. of *Chryseobacterium* were recovered in multiple freshwater fish (de Alexandre

Setastião et al., 2019; Heckman et al., 2023). However, the pathogenicity of *Chryseobacterium* remains largely unknown, particularly in channel catfish.

Fish infected with *Chryseobacterium* spp. display clinical signs similar to bacterial gill disease, which is caused by *Flavobacterium branchiophilum* (Wakabayashi, Huh, and Kimura, 1989), and columnaris disease, which is caused by *F. columnare*, *F. covae, F. davisii, and F. oreochromis* (LaFrentz et al., 2024). Such similar disease signs could potentially lead to misdiagnosis and ineffective treatment. Moreover, *Chryseobacterium* spp. can also cause mortality in fish co-infected with *Flavobacterium*. In one case, rainbow trout (*Oncorhynchus mykiss*) infected with both bacteria displayed indistinguishable disease signs, and co-infection led to increased mortality (Bruce et al., 2020). Therefore, it is imperative to characterize disease signs associated with different genera of yellow-pigmented bacteria and determine their virulence.

A collection of atypical yellow-pigmented bacteria was recovered from multiple diseased channel and hybrid catfish following mortality events. Channel and hybrid catfish, ranging in size and production stages, presented with gross signs of disease resembling either columnaris disease, ESC, or a combination of the two. Based on initial bacterial culture and the presence of disease signs, the yellow-pigmented bacterial colonies were labeled and saved as putative columnaris-causing bacteria (CCB). However, following subculture, many bacterial isolates did not exhibit typical CCB culture characteristics, such as morphology and growth period, and some exhibited a distinct pungent odor leading to a presumptive identification of something other than CCB. Given that these atypical yellow-pigmented bacteria were recovered from diseased catfish spp.,

it was hypothesized that they could potentially contribute to disease either independently or contribute to co-infection. To evaluate this, collected isolates were subjected to molecular identification and *in vivo* virulence assessment in channel catfish. Of the collected isolates, the most virulent isolate identified was then assessed in a co-infection study with *F. covae* to determine its role in co-infection disease dynamics.

4.3. Materials and Methods

4.3.1. Ethics Statement

Procedures involving the handling and treatment of channel catfish used in this study was approved by the Auburn University Institutional Animal Care and Use Committee (AU-IACUC, Protocol #2023-5426) prior to initiation.

4.3.2. Data Availability

Data supporting this study's findings are available from the corresponding author upon reasonable request.

4.3.3. Initial Disease Cases

Channel and hybrid catfish were submitted to the Aquatic Diagnostic Laboratory (ARDL) at the Thad Cochran National Warmwater Aquaculture Center in Stoneville, MS, USA for diagnostic investigation between May – September 2022. Catfish submitted for diagnostics ranged from fingerlings to food size; wherein alive or freshly dead catfish were examined for signs of disease and bacterial re-isolation. Isolates used in this study were

collected from the following disease cases. Isolate S22-0124 was recovered from a case of freshly dead hybrid fingerlings that exhibited columnaris-like lesions on the skin and in the mouth. Isolate S22-158 was recovered from freshly dead hybrid stockers wherein all catfish had columnaris lesions in their mouth, with one fish having columnaris lesions on its skin. One catfish from this case also displayed signs of proliferative gill disease on its gills. Isolate S22-335 was recovered from a case of six freshly dead channel catfish fingerlings. Four of the catfish had lesions suggestive of ESC, and one fish had a columnaris lesion in its mouth. Isolate S22-424 was recovered from a case five freshly dead channel catfish fingerlings, where all five catfish had lesions suggestive of ESC, and one catfish had columnaris lesions in its mouth. Isoalte S22-436 was recovered from a case of five freshly dead channel catfish fingerlings, where all five catfish fish had lesions suggestive of ESC, and two of the five catfishfish had columnaris lesions on the gills. Isolate S22-519 was recovered from live hybrid food size catfish that displayed columnaris lesions on their fins and gills. Isolate S22-539 was recovered from a case of three freshly dead channel catfish fingerlings that exhibited columnaris lesions in their mouth, and two catfish had columnaris lesions on their gills. One fish also exhibited lesions resembling ESC. The last isolate, S18-81, was reisolated from a fin lesion on a catfish that grew on diluted Mueller-Hinton agar and was reported as yellow-pigmented, smooth, and “non-adherent” on the agar.

4.3.4. Initial Bacterial Screening

To identify putative *Chryseobacterium* species, a collection of yellow-pigmented bacteria was retrieved from -80 °C cryostock and revived onto modified Shieh agar (MSA; LaFrentz and Klesius, 2009) and grown for 24 h at 28 °C. Following visual confirmation of purity, one colony was picked and inoculated into 1 mL of MSB and incubated for 12 h at 28 °C and 175 rpm. Bacterial cultures were pelleted by centrifugation for 10 min at 16 000 × *g*. Bacterial DNA was extracted using the PuroSPIN DNA/RNA Purification Kit (Luna Nanotech, Markham, Ontario, Canada). Bacterial DNA was quantified using the Nanodrop One spectrophotometer (Thermo Fisher Scientific, Waltham, MA, USA) and diluted to a final concentration of 10 ng mL^{-1} for *gyrB* PCR analysis.

Amplification and sequencing of the *gyrB* gene was conducted using external primers 40F (5` -AGT ATT CAG GCA TTA GAA GG-3`) and 1763R (5` -TCT CCA AGA CCT TTA TAA CG-3`) and internal sequencing primers 471F (5` -DGA ACC WCC CAT CGG AGA TT-3`) and 1449R (5` -TCC ACG ARA AAG ARC ARA AAT C-3`; Sebastiao et al., 2019). Each reaction consisted of 25 µL of Phusion Green Hot Start II High-Fidelity PCR Master Mix (Thermo Fisher Scientific, Inc.), 2 µL each of forward and reverse primer (10 µM each), 16 µL of nuclease-free water, and 5 µL of DNA template. Amplification consisted of the following cycle: 98 °C for 3 min, followed by 44 cycles of 98 °C for 10 seconds, 52 °C for 10 seconds, and 72 °C for 1 min, and ending at 72 °C for 5 min. Amplified PCR products were visualized on a 2% agarose gel with a ChemiDoc imaging system (Bio-Rad, Hercules, CA, USA). PCR products were purified using the PuroSpin PCR gel extraction kit (Luna Nanotech) and products and the same primers for the *gyrB* gene were submitted to

Eurofins Genomics (Lexington, KY, USA) for Sanger sequencing. Generated sequences were quality-trimmed, and consensus sequences were assembled using Geneious Prime (Version 2026.0.02). Within Geneious Prime, the default *de novo* assembly function was performed on trimmed sequences, followed by MAFFT alignment (Katoh, Misawa, Kuma, and Miyata, 2002; Katoh and Standley, 2013). Generated sequences were queried against the National Center for Biotechnology Information (NCBI, Bethesda, MD, USA) using the BLASTN software for identification.

4.3.5. Whole Genome Sequencing

Based on bacterial identification following *gyrB* sequencing, select YPB isolates S22-335, S22-158, S22-436, S22-424, S22-539, S22-519, S22-0124, and an additional YPB isolate presumptively identified as *Flavobacterium* (S18-81), were retrieved from –80 °C cryostock and revived onto MSA and grown for 24 h at 28 °C. Following visual confirmation of purity, one colony was picked and inoculated into 1 mL of MSB and incubated for 12 h at 28 °C and 175 rpm. Bacterial cultures were pelleted by centrifugation for 10 min at 16 000 × *g*. Genomic DNA (gDNA) was extracted using the Wizard Genomic DNA Purification Kit following the protocol for Gram-negative bacteria (Promega, Madison, WI, USA). Bacterial DNA was quantified using the Qubit Flex Fluorometer (Thermo Fisher Scientific, Inc.) and diluted to 50 ng μL^{-1} prior to library preparation.

The library was prepared using the Rapid Sequencing Barcoding Kit (SQK-RBK114.24) and sequenced on a R10.4.1 FLO-MIN114 flow cell using the GridION X5 (Oxford Nanopore Technologies, Oxford, United Kingdom). Generated reads were re-

basecalled using Dorado 0.5.3, adapter trimming was performed with Porechop (Version 0.2.4), and NanoFilt (Version 2.8.0) was then used to filter out reads < 500 bp, and 10 bp were cropped from the 5' end. Genome assembly (estimated genome size = 4.9 Mb) and polishing (1 iteration) was performed using Flye (Version 2.9.6).

Isolates that were identified as being the same species were submitted to the Type Strain Genome Server (TYGS; DSMZ, Germany) for genome-based species relatedness based on whole genome comparison to type strains. Species delineation was determined using the TYGS pairwise digital DNA-DNA hybridization (dDDH) option to determine overall genome relatedness. Species delineation was calculated using the Genome-to-Genome Distance Calculator (GGDC) and Genome BLAST Distance Phylogeny formulas d_0, d_4, and d_6 formulas. Formula d_0 represents the length of all high-scoring segment pairs (HSPs) divided by the total genome length, d_4 (the most robust of the formulas), represents the sum of all identities found in the HSPs divided by the overall length, and d_6 (a hybrid of d_0 and d_4) is the sum of all identified found in the HSPs divided by the total genome length. Using the 70% threshold established for prokaryotes (Auch, von Jan, Klenk, and Göker, 2010), values below this threshold were considered distinct species.

For added resolution of genomes that initially had low assembly coverage (< 30x) or had ≥ 3 fragments following genome sequencing, isolates S22- 436, S22-424, S22-539, S22-519, and S18-81 were grown to logarithmic phase and pelleted for submission to Plasmidsaurus Inc. (San Francisco, CA, USA) for long-read Oxford Nanopore bacterial whole genome sequencing (Oxford Nanopore). Identification based on most closely-related bacterial species of YPB isolates was performed with Sourmash (Version 4.9.4;

Irber et al, 2024) with searches performed using the default k-mer size of 31 and scaled at 1,000 against the Genome Taxonomy Database RS220.

4.3.6. Preliminary Virulence

The virulence of each YPB isolate was assessed *in vivo* using 18 g $\pm$ 0.2 channel catfish (Delta Select strain). Bacterial isolates were revived from cryostock and grown on MSA for 24 h at 28 °C. Following visual inspection for purity, 1 colony was picked and inoculated into 12 mL of MSB and incubated for 12 h at 28 °C and 175 rpm. The culture was expanded to 250 mL by inoculating 6 mL of the 12-h culture into fresh broth and incubating for an additional 12 h at 28 °C and 175 rpm. The OD_{540} was measured for each culture, and 1 mL was used for a ten-fold serial dilution and spread plating (on MSA) to determine bacterial concentration (Table 4.6.1).

Isolates were tested for virulence in two separate trials, with the first including isolates S22-158, S22-436, S22-424, S22-539, and S22-519, and the second that included S22-335, S22-0124, and S81-18. Two exposure routes were tested for each isolate, including immersion and intraperitoneal (i.p.) injection (e.g., S22-158 was administered to 1 tank of 10 fish for immersion, and 1 tank of 10 fish for i.p.-injection). Tanks (the experimental unit) were not replicated in either trial. Channel catfish were transferred into challenge tanks holding approximately 38 L of dechlorinated, heated (28 °C), and UV-treated water adjusted to 0.4 L min^{-1} with supplemented dissolved oxygen. Channel catfish that were to be injected were anesthetized with 100 μg L^{-1} of Syncaine (tricane methanesulfonate; Syndel, Ferndale, WA, USA) buffered to a neutral pH in system rearing

water, prior to injection of 100 µL of bacterial culture, or phosphate-buffered saline (mock group) of the same volume. Immediately following injection, fish were returned to their respective challenge tanks with oxygen and allowed to recover. Immersion challenges involved exposing channel catfish to 200 mL of bacterial culture in 10 L of static wearing rater for 1 h. While water flow was halted for 1 h during immersion, dissolved oxygen remained. Following immersion, water flow was restored to 0.4 L min^{-1}. Water quality parameters throughout the trial, including temperature and dissolved oxygen, were measured at 27.9 ± 0.3 °C and 8.3 ± 0.1 mg L^{-1}, respectively.

For the duration of the trial, catfish were offered a commercial diet (AquaXcel, Wayzata, MN, USA), twice daily. Mortalities were recorded every 12 h, and 20% of daily tank mortality was examined for signs of disease and bacterial re-isolation to fulfill Koch's postulates (Koch, 1890). Anterior kidney and spleen tissue was swabbed with a sterile 1 mL loop onto MSA for bacterial re-isolation. Cumulative percent mortality (CPM) was determined following 48 h of no observed mortality across all tanks.

4.3.7. Virulence Trial

Isolate S22-158 was utilized for a larger, replicated trial to determine the median lethal dose (LD_{50}). Isolate S22-158 was prepared in the same manner as the preliminary virulence trial. Four doses of YPB S22-158 were tested in channel catfish (Delta Select strain) weighing an average of 20.0 ± 0.3 g. Doses were prepared by making ten-fold serial dilutions of the undiluted culture, which served as the highest dose. The challenge consisted of four doses ranging from 10^5-10^8 CFU mL^{-1}, with each dose having triplicate

tanks holding 20 fish per 38 L tank, including mock tanks. All doses were administered with 100 μL of bacterial inoculum via i.p. injection immediately after fish were anesthetized with Syncaine (100 mg L^{-1}). Fish in mock tanks were given 100 μL of PBS. All fish recovered following injection and were checked every 12 h for mortality monitoring. Daily mortalities were recorded and 20% of daily tank mortality was necropsied and had spleen and kidney tissues swabbed for bacterial re-isolation. Cumulative percent mortality was determined after 7 d post-exposure. The median lethal dose (LD_{50}) of YPB isolate S22-158 was estimated using the method described by Reed and Muench (1938).

4.3.8. Co-Infection Trial

A bacterial co-infection trial was performed to determine the effects on CPM in channel catfish (Delta Select strain; average weight of 21 $\pm$ 0.3 g) following exposure to isolate S22-158 and to another widely known virulent YPB, *F. covae* (ALG-00-530). Isolate S22-158 was prepared in the same manner as the larger virulence trial, but the administered dose was determined based on results of the virulence trial to achieve at least 50% CPM. The ALG-00-530 was revived from cryostock onto MSA and grown for 48 h at 28 °C. Next, 3-5 colonies were inoculated into 12 mL of MSB and incubated for 12 h at 28 °C and 175 rpm. The *F. covae* culture was expanded to 200 mL by inoculating 6 mL of the 12 h culture into MSB and incubating for an additional 12 h at 28 °C and 175 rpm. Following incubation, *F. covae* diluted to an OD_{540} of 0.700 and 1 mL was retained for serial dilution and spread plating.

The co-infection trial consisted of 1 dose per isolate (YPB S22-158 and *F. covae* ALG-00-530), and a co-infection consisting of 65 mL of *F. covae* and 100 µL of YPB S22-158. Each treatment (single pathogen of S22-158, single pathogen of ALG-00-530, and co-infection) was replicated with three tanks holding 20 fish per 38 L tank. Mock-infected tanks (negative controls) were given either 65 mL of sterile MSB or 100 µL of sterile phosphate-buffered saline (PBS). Mock tanks were not replicated, and each of the three mock tanks (single pathogen mocks and co-infection mock) were not replicated. Catfish assigned to the single pathogen group of the S22-158 were anesthetized as before (100 mg L^{-1} of Syncaine), and i.p. injected with 100 µL of bacterial inoculum. Catfish assigned to the *F. covae* ALG-00-530 single pathogen group were exposed to 65 mL of the culture in 10 L of tank water and immersed in a static bath for 30 minutes. Following immersion, water flow was restored to 0.4 L min^{-1}. Catfish in co-infection tanks were i.p. injected with 100 µL of S22-158 and immersed in a static bath containing 65 mL of *F. covae* ALG-00-530 in 10 L of water for 30 minutes. Mock co-infection tanks were treated in the same manner, but sterile MSB (immersion) and sterile saline (i.p. injection of 100 µL) were administered. Water temperature and dissolved oxygen during the trial was 29.1 ± 0.3 °C and 7.0 ± 0.1 mg L^{-1}. The co-infection trial lasted for 7 d, during which catfish were checked every 12 h for mortality. Mortalities were subjected to clinical examination of disease signs, and bacterial cultures of the gill, spleen, and posterior kidney were taken for bacterial re-isolation. Catfish were fed a commercial diet daily at the willingness of the fish.

4.3.9. Bacterial DNA Extraction and Molecular Identification

Bacterial DNA was extracted from the re-isolated bacteria from mortalities using the Quick-DNA Bacteria/Fungal Miniprep Kit (Zymo Research, Irvine, CA, USA) following the manufacturer's instructions. DNA concentration was determined using the Nanodrop One (Thermo Fisher Scientific, Inc.) and diluted to a final concentration of 10 ng μL^{-1} for PCR analysis. Molecular characterization was performed by the amplification of the 16S rRNA gene fragments. PCR of the 16S rRNA gene with 27F (5` -AGA GTT TGA TCC TGG CTC AG-3`) and 1492R (5` -TAC GGY TAC CTT GTT ACG ACT T-3`; Heuer, Krsek, Baker, Smalla, and Wellington, 1997), consisted of 12.5 µL of 2X DreamTaq Green Hot Start PCR Master Mix (Thermo Fisher), 2 µL of the forward and reverse primer, 9.5 µL of nuclease-free water, and 1 µL of DNA template. Amplification parameters included an initial denaturation at 95 °C for 2 minutes, followed by 30 cycles of 95 °C for 30 seconds, 58 °C for 30 seconds, and 72 °C for 50 seconds, ending with a final extension at 72 °C for 5 min. PCR products were purified using the DNA Clean & Concentrator Kit (Zymo Research), and products and the same primers for the 16S rRNA gene submitted to Eurofins Genomics (Lexington, KY, USA) for Sanger sequencing. Generated sequences were quality-trimmed, and consensus sequences were assembled in Geneious Prime (Version 2026.0.02) and queried against the National Center for Biotechnology Information (NCBI) using BLASTN for identification.

4.3.10. Statistical Analyses

Cumulative percent mortality data from the virulence and co-infection trials were analyzed using GraphPad Prism (version 11.0.0). Average CPM between different doses of S22-158 was assessed using a one-way Analysis of Variance (ANOVA), followed by Tukey's HSD multiple comparisons test. Mortality between the single pathogen and co-infection groups in the co-infection trial were assessed using the Kruskal-Wallis test followed by Dunn's multiple comparisons test. Differences in CPM were considered statistically significant at $P < 0.05$.

4.4. Results

4.4.1. Initial Bacterial Screening and Whole Genome Sequencing

Initial *gyrB* sequencing presumptively identified seven isolates, including S22-158, S22-0124, S22-436, S22-335, S22-539, S22-424, and S22-519 as belonging to the genus *Chryseobacterium*. Isolate S18-81 was later added to the collection for downstream molecular analyses and virulence screening. However, subsequent whole genome sequencing demonstrated that the isolates represented multiple genera, including *Chryseobacterium*, *Empedobacter*, and *Flavobacterium*.

Whole genome sequencing of genomic DNA purified from YPB isolates yielded genome assemblies ranging from approximately 2.9-5.4 Mb in total length, with BUSCO completeness scores ranging from 98.5-100% and sequencing coverage ranging from 32× to 253×, indicating high-quality genome assemblies (Table 4.6.1). Genome assemblies were highly contiguous, consisting of 1-3 contigs per isolate with 0% gaps, and several

isolates assembled into single-contig genomes. Genome size ranged from 2.9 - 5.4 Mb (Table 4.6.1). Plasmidsaurus Inc. results provided Bandage visualization of each genome assembly (Version 0.8.1; Wick, Schultz, Zobel, and Holt, 2015). Bandage visualization identified putative plasmid-associated contigs for isolates S22-436, S22-424, S22-539, and S22-519 based on the presence of smaller, circularized or disconnected contigs.

Sourmash was used to determine the closest-related bacterial species. Isolates S22-335, S22-424, S22-436, and S22-539 were identified as potential undescribed *Chryseobacterium mucoviscidosis* isolates, S22-0124 was identified as *Chryseobacterium gleum*, S22-519 as *Chryseobacterium cucumeris*, S22-158 as *Empedobacter brevis*, and S18-81 as *Flavobacterium saliperosum* (Table 4.6.1). Pairwise dDDH analysis of isolates identified as *C. mucoviscidosis* determined if they were correctly identified as the same species when compared to the *C. mucoviscidosis* type strain VT 16-26^{T}. Among the presumptive *C. mucoviscidosis* isolates, isolates S22-539 and S22-436 had a d_4 value (C.I.) of 69.3% (66.3%-72.1%) and 69.2% (66.2%-72.1%), respectively. (Table 4.6.2) Isolate S22-335 had a d_4 value of 67.8% (64.9%-70.7%; Table 4.6.2). Isolates S22-539, S22-436, and S22-335 values were just below the 70% species delineation cutoff threshold, indicating close genetic similarity, however, enough variation to conclude that they are not the same species as *C. mucoviscodosis* VT 16-26^{T}. S22-424 had the lowest d_4 value of the group (47.8%; 45.3%-50.5%), indicating greater genetic variation between the isolate and *C. mucoviscidosis* type strain. Although Sourmash identified all four isolates being closely related to *C. mucoviscidosis*, dDDH results suggest three are closely related to C. mucoviscidosis, while one has greater genetic deviation. This data suggests that these four

species could be undescribed species of *Chryseobacterium* closely related to *C. mucoviscidosis*.

4.4.2. Preliminary Virulence

Preliminary virulence screening was conducted to assess the pathogenic potential of multiple atypical YPB isolates in channel catfish (Table 4.6.3). Following i.p. injection, select isolates caused mortality, with *E. brevis* isolate S22-158 producing the highest CPM (70%). Three isolates, including undescribed *C. mucoviscidosis* isolates S22-436 and S22-539, and *C. gleum* S22-0124, resulted in low mortality (10% CPM). *C. mucoviscidosis* isolates S22-335 and S22-424, and *F. saliperosum* S18-81 did not cause mortality (0% CPM) after both exposure routes. Immersion challenges did not result in mortality for any isolate, despite exposure to doses up to 10^7 CFU mL^{-1}.

Bacteria re-isolated from th preliminary virulence trials were identified by PCR confirmation of *gyrB* and 16S rRNA genes, and Sanger sequencing using primers of those same genes. Only 20% of the re-isolated bacteria was processed for PCR and Sanger sequencing. For the S22-158 i.p.-injection tank, 3/8 isolates were confirmed as *E. brevis* (NCBI BLAST percent identity of 98-99%). The S22-519 i.p. injection tank had 1/4 isolates confirmed as *C. cucumeris* (99%). Only two isolates were recovered from S22-436 and S22-539 i.p.-injected fish, and in both cases, 1/2 isolates were identified as *C. gambrini* (94%).

4.4.3. Virulence Trial

Based on the results from the preliminary virulence screening, *E. brevis* 522-158 was assessed further to determine the median lethal dose via i.p. injection. Channel catfish were exposed to four doses ranging from $4.7 \times 10^5 - 4.7 \times 10^8$ CFU/fish, with the highest dose exhibiting 90 ± 5.0 % CPM, which was significantly greater than all other doses ($P < 0.001$; Figure 4.7.1). Lower doses of *E. brevis* displayed mortality ranging from 1.6-15.0% CPM. One mortality occurred in the mock tank where *Plesiomonas shigelloides* was identified following re-isolation and 16S rRNA gene sequencing. No other bacteria resembling *E. brevis*, or exhibiting yellow pigmentation, was recovered from kidney or spleen tissue from the mortality in the mock tank. A total of 28 bacterial isolates were re-isolated from the mortalities observed during the virulence trial. Only approximately 35% of those isolates were selected at random and identified by 16S rRNA gene sequencing. Of those, the identity of 7/7 isolates were confirmed as *E. brevis* (99%-100% NCBI BLAST percent identity). The LD_{50} of *E. brevis* in channel catfish was estimated to be 1.3×10^8 CFU/fish.

Channel catfish injected with 4.7×10^8 CFU/fish of *E. brevis* exhibited several gross signs of disease, including severe bilateral exophthalmia (Figure 4.7.3 A), multifocal, shallow ulcerations along the ventral region (Figure 4.7.3 B), severe cranial hemorrhage (Figure 4.7.3 C), severe gill pallor with multifocal petechial hemorrhaging, and fin laceration with severe erythema (Figure 4.7.3 D).

4.4.4. Co-Infection Trial

Channel catfish were exposed to either a single dose of *E. brevis* (1.8×10^8 CFU/fish), a single dose of *F. covae* (1.2×10^6 CFU mL^{-1}) or a combination of the two in a co-infection (Figure 4.7.2). The first mortalities were observed at 0.5 days post-infection across all treatment groups. By 24 h post-infection, all replicate tanks of the co-infection group reached 100% CPM. Mortality in the *E. brevis* group also occurred rapidly and reached $86.6 \pm 5.7\%$ CPM by day 3 post-infection, then ceased for the remainder of the challenge. The observed *F. covae* mortality was lower than the other groups tested and reached $31.6 \pm 37.5\%$ CPM by 48 h post-infection. A Kruskal-Wallis test revealed a significant difference in mean CPM among treatments ($P = 0.004$). Dunn's multiple comparisons test indicated that the co-infection group resulted in significantly higher mortality compared to *F. covae* alone ($P = 0.017$), whereas the *E. brevis* group was not significantly different from either *F. covae* alone or the co-infection group ($P = 0.506$; Figure 4.7.2).

During the co-infection trial, a total of 40 bacterial isolates were re-isolated among the treatment groups of fish. In the single pathogen group exposed to *F. covae* ALG-00-530, 2/5 isolates were confirmed as *F. covae* via the columnaris-causing bacteria (CCB) multiplex (LaFrentz, García, and Shelley, 2019). From the single pathogen group i.p.-injected with *E. brevis* S22-158, 11/17 isolates were confirmed as *E. brevis* (99% NCBI BLAST percent identity). In the co-infection group exposed to both *E. brevis* and *F. covae*, 8/18 isolates were confirmed as *E. brevis* (99%-100% NCBI BLAST percent identity). None

of the yellow-pigmented bacterial isolates from the co-infection group were confirmed as *F. covae*.

Catfish exposed to *F. covae* only mostly displayed depigmented skin lesions along the external surface and frayed fins (Figure 4.7.4 A), moderate hemorrhage on the pectoral aspect (Figure 4.7.4 B), and severely necrotic gills, multifocal depigmented skin lesions, and frayed fins (Figure 4.7.4 C). Catfish exposed to *E. brevis* only exhibited multifocal hemorrhage and ulcerations. Catfish exposed to the co-infection of *E. brevis* and *F. covae* displayed gross signs of disease, including multifocal, shallow ulcerations along the ventral region (Figure 4.7.5 A), severe necrotic gill lesions with yellow pigmentation (Figure 4.7.5 B), and frayed dorsal, pelvic, and anal fins (Figure 4.7.5 C), which were present at 48 h post-infection with *E. brevis* and *F. covae*.

4.5. Discussion

Eight atypical YPB isolates recovered from diseased catfish in Mississippi, USA were molecularly identified as members of multiple bacterial genera, including *Chryseobacterium*, *Flavobacterium*, and *Empedobacter*. Several isolates, including select strains of potentially undescribed *C. mucoviscidosis*, *C. gleum*, *C. cucumeris*, and *E.brevis*, demonstrated pathogenic potential in channel catfish following i.p. injection. Among the isolates tested, *E. brevis* 522-158 produced the highest cumulative percent mortality and induced severe gross sign of disease, including exophthalmia, hemorrhage, ulceration, and pale gills. Additionally, co-infection of channel catfish with *E. brevis* S22-158 and *F. covae* ALG-00-530 resulted in increased mortality compared to *F. covae* alone,

suggesting that atypical strains of YPB may contribute to complex disease dynamics in channel catfish aquaculture.

Initial *gyrB* sequencing presumptively identified seven isolates as belonging to the genus *Chryseobacterium*. Following whole genome sequencing, further taxonomic resolution was provided at the species level, revealing isolates belonging to multiple genera, including *Chryseobacterium*, *Empedobacter,* and *Flavobacterium*. This was not surprising, as similar challenges attempting to distinguish *Chryseobacterium* and *Flavobacterium* from diseased fish have been previously reported (Ilardi and Avendaño-Herrera, 2008; Zamora et al., 2012). Additionally, as *Chryseobacterium* and *Flavobacterium* share many phenotypic characteristics and can make baseline identification challenging, clinical presentation of disease signs in fish can further complicate initial identification (Loch and Faisal, 2015b; Sebastião et al., 2019; Heckman et al., 2023). Moreover, there is continuous and increasing diversity within flavobacterial taxa that further complicates identification of these already closely related genera (García-López et al., 2019; LaFrentz et al., 2022; Heckman et al., 2023). These challenges highlight the importance of incorporating genome-based approaches to improve taxonomic resolution for closely-related YPB spp.

Sequencing of *E. brevis* S22-158 positively amplified *gyrB* during preliminary screening of YPB isolates and was presumptively identified as a *Chryseobacterium* sp. However, whole genome sequencing revealed that isolate S22-158 was actually *E. brevis*. Subsequent re-testing of the original S22-158 cryostock and re-isolated bacteria from the *E. brevis* virulence trial failed to amplify the *gyrB* gene. Therefore, primers for the 16S rRNA

gene were used to correctly identify re-isolated bacteria from channel catfish from the *E. brevis* virulence study and further supported the whole genome-based classification of *E. brevis*. Sequencing of the *gyrB* gene was chosen for this study because *gyrB* is generally regarded as having higher evolutionary power compared to the gold standard gene used for bacterial identification, 16S rRNA (Heckman et al., 2023). Additionally, previous studies used the *gyrB* gene for greater resolution of atypical flavobacterial (i.e., *Chryseobacterium* spp.) identification from bacterial isolates recovered from diseased fish (de Alexandre-Sebastião et al., 2019; Heckman et al., 2023). However, a recent assessment of flavobacterial identification approaches revealed that sequencing of the *gyrB* gene correctly identified only 70% of flavobacterial species due to primer binding site mutations (Gélinas, Paquet, Paquet, Vincent, and Charette, 2024). Therefore, it is important to note such limitations when using only the *gyrB* gene for YPB taxonomic identification, especially if *Flavobacterium* or *Chryseobacterium* spp. are suspected (Holmes, Steigerwalt, and Nicholson, 2013; Nicholson et al., 2020). Additionally, other types of genotypic identification should be considered for accurate identification of closely related species (Lin et al., 2017; Muigg et al., 2024).

The pathogenic potential of multiple bacterial isolates spanning several YPB genera was observed during *in vivo* challenges with channel catfish. Notably, mortality was not observed following immersion exposure for any isolate tested, whereas differences in CPM were observed following i.p. injection. These findings suggest that the YPB isolates that caused mortality following i.p. injection may behave as opportunistic pathogens, requiring disruption of host barriers or direct entry into the host to establish infection.

Chryseobacterium spp. isolates have been recovered from diseased fish, and their virulence is often considered opportunistic or facultative (Loch and Faisal, 2015b; de Alexandre Sebastião et al., 2019; Jung et al., 2022; Srinath et al., 2026). Malick et al. (2022) reported *C. gleum* isolates caused mortality ranging from 10-20% CPM and induced disease signs resembling columnaris disease following i.p. injection in *Labeo rohita*, *L. catla*, and *Oreochromis niloticus*. Similarly, *C. gleum* isolate S22-0124 in the current study resulted in 10% CPM in channel catfish. Kim et al. (2020) assessed the pathogenic potential of *C. cucumeris* in pond loaches (*Misgurnus anguillicaudatus*) and reported that immersion exposure did not result in mortality, even after 24 hours of exposure. However, mortality reached 20% CPM when fish were abraded prior to immersion, and i.p.-injected fish displayed dose-dependent mortality (Kim et al., 2020). Similarly, channel catfish in the present study displayed low mortality following i.p. injection with *C. cucumeris* isolate S22-519, with no mortality following immersion exposure. To date, there are no reports of *C. mucoviscidosis* associated with fish disease or mortality, making this the first assessment of its pathogenic potential in channel catfish.

Less is known about the specific pathogenicity of *Empedobacter* spp. in fish. *Empedobacter brevis* was originally classified as *Flavobacterium breve* and belonged to the family *Flavobacteriaceae,* but was later reassigned to *Weeksellaceae* (Vandamme, Bernardet, Segers, Kersters, and Holmes, 1994; García-López et al., 2019). Like *Chryseobacterium*, *Empedobacter* spp. are documented in human clinical cases and are frequently linked to nosocomial infections (Janknecht, Schneider, and Ness, 2002; Basani and Aepala, 2018; D'Ostillo, Stacchiotti, Perilli, Bari, and Amoroso, 2022; Martinez,

Matabang, Miller, Aggarwal, and LaFortune, 2023; Zubova et al., 2025). However, and similar to *Chryseobacterium* spp., *E. brevis* has been isolated from aquatic environments (Isroni, Setyawati, and Maulida, 2019). Additionally, *E. brevis* was identified in a mixed bacterial infection from the gills of diseased gilthead sea brim (*Sparus aurata* L.; Kapetanović et al., 2006). In the present study, *E. brevis* S22-158 demonstrated virulence in channel catfish and caused severe disease signs and high mortality following i.p. injection. Additionally, *E. brevis* was re-isolated from the spleen and kidney tissue of mortalities, demonstrating a systemic infection during the experimental virulence trial. The median lethal dose of *E. brevis* in channel catfish was estimated to be 1.3×10^8 CFU/fish, indicating that relatively high bacterial loads are required to induce mortality. However, mortality was not observed following immersion exposure, further supporting the opportunistic nature of *E. brevis*. Ultimately, this study represents the first report of *E. brevis* causing disease and mortality in channel catfish. These findings expand the current understanding of *Empedobacter* spp., specifically, *E. brevis*, in fish hosts and emphasizes the importance of opportunistic YPB during diagnostic investigation of disease outbreaks in catfish aquaculture.

A co-infection study demonstrated significantly greater mortality in channel catfish exposed to both *E. brevis* and *F. covae* compared with fish exposed to *F. covae* alone. While this is the first time this specific bacterial combination has been assessed, the bacteria appear to demonstrate a synergistic relationship. Disease signs displayed by the co-infection group were more severe than disease signs from the groups exposed to *F. covae* or *E. brevis* alone. Similar results were demonstrated in a co-infection study with

virulent *Aeromonas hydrophila* and *F. covae* in channel catfish. Catfish exposed to *A. hydrophila* and *F. covae* alone resulted in 28.3% and 23.3% CPM, respectively. However, when the bacteria were combined as a co-infection, mortality was significantly higher (98.3%; Wise et al., 2025). Another co-infection study from the same group demonstrated higher mortality in channel catfish exposed to both *F. covae* and *Edwardsiella ictaluri* than fish exposed to either pathogen individually (Wise et al., 2023). The same study also reported a change in disease dynamics during co-infection. Wise et al. (2023) also observed a delay in mortality when fish were exposed to *F. covae* first, followed by *E. ictaluri* 48 h later, compared to when *E. ictaluri* was administered first followed by *F. covae*. Although the same co-infection dynamics were not investigated in the current study, future work should incorporate similar experiments to provide a more comprehensive assessment of co-infections with *E. brevis* and *F. covae*.

Exacerbated disease signs observed in channel catfish infected with *E. brevis* and *F. covae* also supports a synergistic effect in co-infection disease dynamics. Catfish in the co-infection group displayed typical signs of infection with *F. covae*, such as depigmented skin lesions, frayed fins, and necrotic gills. However, catfish also exhibited multifocal hemorrhaging on the external surface of the skin that resembled hemorrhaging observed during the *E. brevis* virulence study. In the co-infection study, disease signs were more severe in the co-infection group compared to the single pathogen-exposed groups. This has been demonstrated before in co-infections with virulent *A. hydrophila* and *F. covae* (Wise et al., 2025), *E. ictaluri* and *F. covae* (Wise et al., 2023), and *E. ictaluri* and *F. oreochromis* (Nhinh et al., 2023). Additionally, *Empedobacter brevis* has been isolated

from a co-infection study where diseased gilthead seabrim displayed necrotic and swollen gills alongside *Stenotrophomonas maltophilia* and *Aeromonas salmonicida masoucida/achromogenes*, indicating its potential role in gill pathology (Kapetanović et al., 2006).

This study highlights the complex nature of bacterial co-infections in channel catfish aquaculture. Under production settings, what may appear to be an acute disease outbreak, could be the result of a secondary pathogen taking advantage of an established infection caused by a primary pathogen, leading to increased morbidity and mortality (Scott and Bollinger, 2014). Such exacerbated clinical presentation of disease signs can make diagnostic investigations and treatment efficacy challenging by concealing the primary pathogen responsible (Wise et al., 2021; Wise et al., 2025). This can also affect proper treatment, as choosing an appropriate treatment strategy can be challenging. Many *Chryseobacterium* and *Flavobacterium* spp. have an inherent resistance to 2/3 of the approved antibiotics approved for use in U.S. aquaculture (oxytetracycline and florfenicol; Heckman et al., 2023). Resistant atypical YPB can further complicate treatment when antibiotics are given, as those resistant species can still persist within the host. Future studies that investigate co-infections should include minimum inhibitory concentration values for all pathogens involved to help guide treatment and prevention strategies.

In conclusion, this study highlights the challenges associated with identifying atypical yellow-pigmented bacterial species related to catfish aquaculture. Incorporating long-read sequencing allowed for greater resolution of taxonomic identification and should be considered as a primary method for identifying genera within the *Bacteroidetes* phylum.

Among the atypical YPB isolates from this study, *E. brevis* S22-158 displayed high mortality upon i.p. injection, marking the first report of its opportunistic virulence in channel catfish. Future work should investigate alternative challenge models to determine its ability to cause infection at varying doses and exposure routes. Channel catfish displayed severe signs of disease and acute mortality following a co-infection with *F. covae* and *E. brevis*, demonstrating an exacerbated effect on mortality and disease. Bacterial load analysis and histopathology of infected fish should be incorporated in prospective research to provide a deeper understanding of the pathogenicity of co-infection dynamics. Continued studies of atypical YPB presence in co-infections will deepen our understanding of complex disease dynamics in catfish aquaculture and will aid producers and researchers in developing effective strategies to control disease outbreaks.

4.6. Tables

Table 4.6.1. Summary of whole genome assembly metrics for isolates recovered from diseased catfish. Data includes total length (base pairs), number of contigs, percent gaps, assembled coverage, BUSCO completeness scores, and species identity based on the Sourmash results.

Isolate	Total Length (base pairs)	Contigs	Percent Gaps	Assembled Coverage	BUSCO Completeness Score	Identity
S22-0124	5,174,208	1	0.0%	68x	100.0%	*Chryseobacterium gleum*
S22-335	4,235,172	1	0.0%	32x	100.0%	*Chryseobacterium mucoviscidosis*
S22-424	4,434,457	2	0.0%	83x	100.0%	*Chryseobacterium mucoviscidosis*
S22-436	4,461,626	3	0.0%	96x	99.9%	*Chryseobacterium mucoviscidosis*
S22-539	4,386,428	3	0.0%	99x	100.0%	*Chryseobacterium mucoviscidosis*
S22-519	5,444,920	2	0.0%	91x	100.0%	*Chryseobacterium cucumeris*
S22-158	3,461,641	2	0.0%	253x	98.5%	*Empedobacter brevis*
S18-81	2,960,960	1	0.0%	108x	100.0%	*Flavobacterium saliperosum*

Table 4.6.2. Pairwise digital DNA-DNA hybridization (dDDH) values and G+C content differences among queried isolates identified as *Chryseobacterium mucoviscodosis* and the subject stain *C. mucoviscidosis* VT 16-26^{T}. Values are provided for Genome-to-Genome Distance Calculator formulas d_0, d_4, and d_6 with associated 95% confidence intervals (C.I.). Formula d_4 represents the most robust formula, with values < 70% denote species delineation.

Query strain	Subject strain	dDDH (d_0, in %)	C.I. (d_0, in %)	dDDH (d_4, in %)	C.I. (d_4, in %)	dDDH (d_6, in %)	C.I. (d_6, in %)	G+C content difference (in %)
S22-539	*C. mucoviscidosis* VT 16-26	85.2	(81.5 – 88.3)	69.3	(66.3 - 72.1)	85.2	(82.0 – 87.9)	0.13
S22-436	*C. mucoviscidosis* VT 16-26	86.1	(82.5 – 89.1)	69.2	(66.2 – 72.1)	86.0	(82.8 – 88.6)	0.25
S22-335	*C. mucoviscidosis* VT 16-26	82.7	(78.9 – 86.0)	67.8	(64.9 - 70.7)	82.8	(79.5 - 85.7)	0.15
S22-424	*C. mucoviscidosis* VT 16-26	64.7	(60.9 – 68.3)	47.8	(45.3 – 50.4)	62.3	(59.0 – 65.5)	0.31

Table 4.6.3. Results of preliminary virulence screening of yellow-pigmented bacterial isolates in channel catfish (*Ictalurus punctatus*), including optical density (OD), exposure route, dose, number of mortalities, and cumulative percent mortality (CPM).

Isolate	OD_{540}	Exposure Route	Dose (CFU mL^{-1})	Mortalities (n)	CPM (%)
S22-335	2.558	Injection	1.2×10^8	0/10	0%
		Immersion	2.4×10^7	0/10	0%
S22-158	2.796	Injection	7.9×10^7	7/10	70%
		Immersion	1.6×10^7	0/10	0%
S22-436	2.241	Injection	5.7×10^7	1/10	10%
		Immersion	1.1×10^7	0/10	0%
S22-424	2.679	Injection	7.8×10^7	0/10	0%
		Immersion	1.6×10^7	0/10	0%
S22-539	1.878	Injection	9.3×10^7	1/10	10%
		Immersion	1.8×10^7	0/10	0%
S22-519	2.428	Injection	4.5×10^7	1/10	10%
		Immersion	9.0×10^6	0/10	0%
S22-0124	2.551	Injection	2.0×10^8	1/10	10%
		Immersion	4.0×10^7	0/10	0%
S18-81	2.672	Injection	3.4×10^8	0/10	0%
		Immersion	6.8×10^7	0/10	0%

4.7 Figures

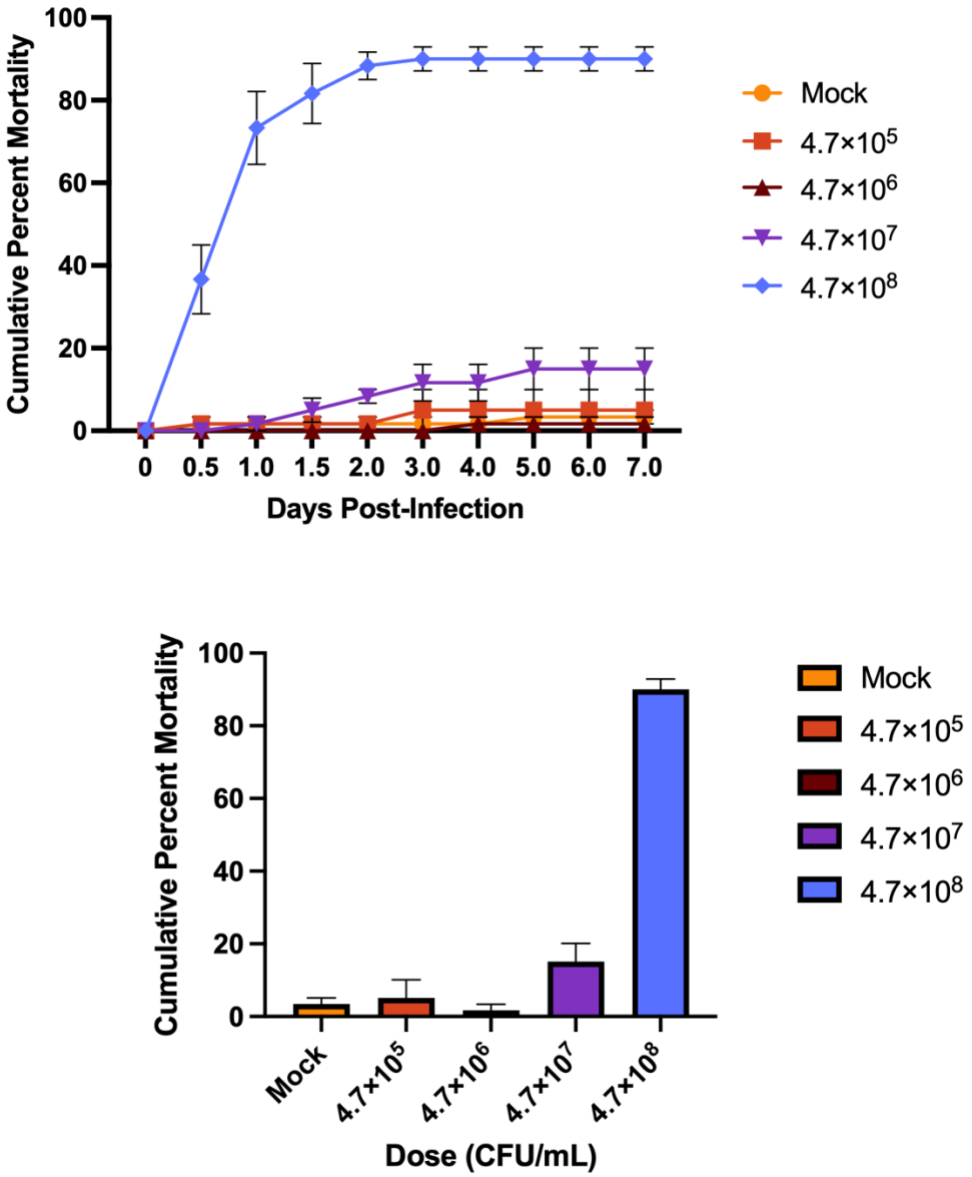

Figure 4.7.1. A) Cumulative percent mortality of channel catfish (*Ictalurus punctatus*) following intraperitoneal injection of *Empedobacter brevis*. B) Bacterial concentrations as colony forming unit per milliliter (CFU/fish). Error bars represent the standard error of the mean (SEM).

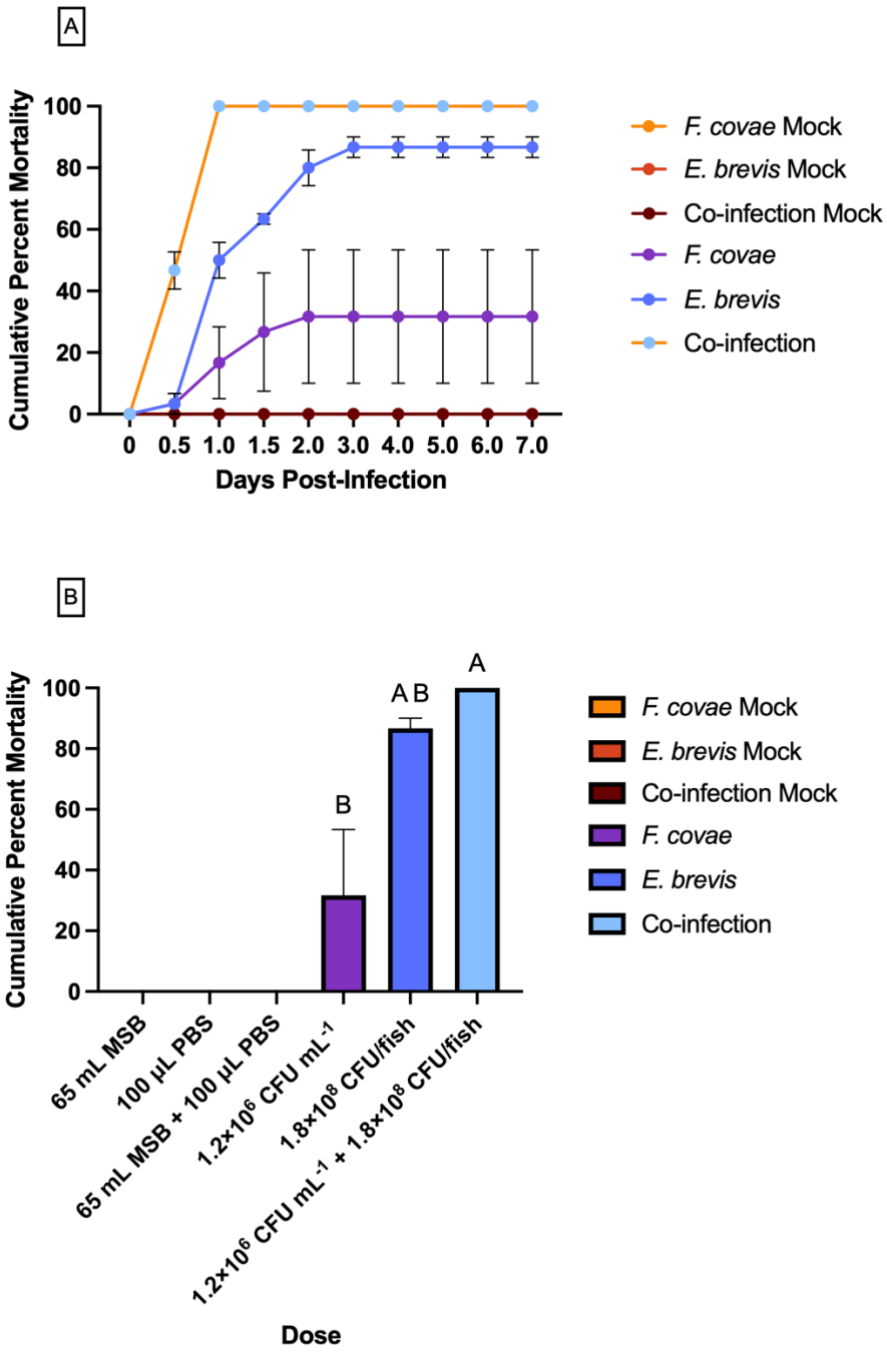

Figure 4.7.2. A) Cumulative percent mortality of channel catfish (*Ictalurus punctatus*) following immersion with *Flavobacterium covae*, intraperitoneal injection with *Empedobacter brevis*, and co-infection with *F. covae* and *E. brevis*. B) Bacterial concentrations as colony forming units per milliliter (CFU mL^{-1}), per fish, and volumes of phosphate-buffered saline (PBS) and sterile media (MSB). Error bars represent the standard error of the mean (SEM).

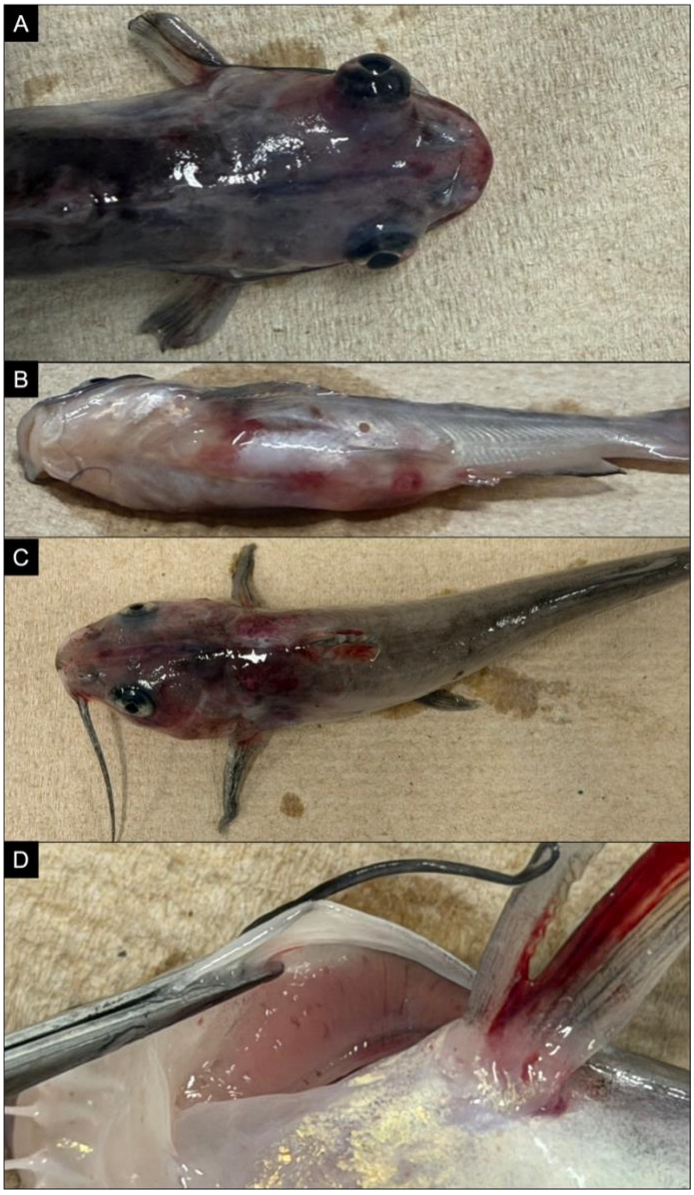

Figure 4.7.3. Gross lesions observed in channel catfish intraperitoneally injected with *E. brevis*: (A) severe bilateral exophthalmia; (B) multifocal hemorrhage and ulcerations along the ventral aspect; (C) severe cranial hemorrhage; and (D) pale gills with multifocal petechial hemorrhage and left pectoral fin laceration and erythema.

Figure 4.7.4. Gross lesions observed in channel catfish following immersion exposure to *Flavobacterium covae*: (A) multifocal depigmented skin lesions, (B) moderate hemorrhage on the pectoral aspect, and (C) severe multifocal skin depigmentation, frayed fins, and severely necrotic gills.

Figure 4.7.5. Gross signs of disease in channel catfish followed by co-infection with *Empedobacter brevis* and *Flavobacterium covae*: (A) multifocal hemorrhage on the ventral aspect, (B) yellow-pigmented and necrotic gill tissue, and (C) frayed dorsal, pelvic, and anal fins.

4.8. References

Abdelrahman, H.A., Hemstreet, W.G., Roy, L.A., Hanson, T.R., Beck, B.H. and Kelly, A.M. 2023. Epidemiology and Economic Impact of Disease-Related Losses on Commercial Catfish Farms: A Seven-Year Case Study from Alabama, USA. *Aquaculture*, 566, p.739206. https://doi.org/10.1016/j.aquaculture.2022.739206

Auch, A.F., von Jan, M., Klenk, H.P. and Göker, M. 2010. Digital DNA-DNA Hybridization for Microbial Species Delineation by Means of Genome-To-Genome Sequence Comparison. *Standards in Genomic Sciences*, 2(1), pp.117-134. https://doi.org/10.4056/sigs.531120

Basani, L. and Aepala, R. 2018. *Empedobacter brevis* Causing Early Onset Sepsis and Pneumonia in a Neonate: Case Report and Review of Literature. *International Journal of Contemporary Pediatrics*, 5(2), p.654. https://doi.org/10.18203/2349-3291.ijcp20180574

Bernardet, J.F. and Bowman, J.P. 2015. *Flavobacterium*. *Bergey's Manual of Systematics of Archaea and Bacteria*, pp.1-75. https://doi.org/10.18203/2349-3291.ijcp20180574

Bruce, T.J., Ma, J., Knupp, C., Loch, T.P., Faisal, M. and Cain, K.D. 2020. Cross-rotection of a Live-Attenuated *Flavobacterium psychrophilum* Immersion Vaccine Against Novel *Flavobacterium* spp. and *Chryseobacterium* spp. Strains. *Journal of Fish Diseases*, 43(8), pp.915-928. https://doi.org/10.1111/jfd.13201

D'Ostilio, A., Stacchiotti, L., Perilli, A., Di Bari, M. and Amoroso, L. 2022. Peritonitis Due to *Empedobacter brevis* in a Patient on Peritoneal Dialysis: An Emerging Pathogen. *Therapeutic Apheresis & Dialysis*, 26(1). https://doi.org/10.1111/1744-9987.13709

de Alexandre Sebastião, F., Loch, T.P., Marancik, D.P., Griffin, M.J., Maret, J., Richey, C. and Soto, E. 2019. Identification of *Chryseobacterium* spp. Isolated from Clinically Affected Fish in California, USA. *Diseases of Aquatic Organisms*, 136(3), pp.227-234. https://doi.org/10.3354/dao03409

García-López, M., Meier-Kolthoff, J.P., Tindall, B.J., Gronow, S., Woyke, T., Kyrpides, N.C., Hahnke, R.L. and Göker, M. 2019. Analysis of 1,000 Type-Strain Genomes Improves

Taxonomic Classification of *Bacteroidetes*. *Frontiers in Microbiology*, 10, p.2083. https://doi.org/10.3389/fmicb.2019.02083

Gélinas, V., Paquet, V.E., Paquet, M.F., Vincent, A.T. and Charette, S.J. 2024. Whole-Genome-Based Taxonomy as the Most Accurate Approach to Identify *Flavobacterium* Species. *FEMS Microbiology Letters*, 371, p.fnae089. https://doi.org/10.1093/femsle/fnae089

Griffin, M.J., Reichley, S.R., Baumgartner, W.A., Aarattuthodiyil, S., Ware, C., Steadman, J.M., Lewis, M., Gaunt, P.S., Khoo, L.H. and Wise, D.J. 2019. Emergence of *Edwardsiella piscicida* in Farmed Channel♀, *Ictalurus punctatus*× Blue♂, *Ictalurus furcatus*, Hybrid Catfish Cultured in Mississippi. *Journal of the World Aquaculture Society*, 50(2), pp.420-432. https://doi.org/10.1111/jwas.12533

Engle, C.R., Hanson, T. and Kumar, G. 2022. Economic History of US Catfish Farming: Lessons for Growth and Development of Aquaculture. *Aquaculture Economics & Management*, 26(1), pp.1-35. https://doi.org/10.1080/13657305.2021.1896606

Heckman, T.I., Yazdi, Z., Pomaranski, E.K., Sebastião, F.D.A., Mukkatira, K., Vuglar, B.M., Cain, K.D., Loch, T.P. and Soto, E. 2023. Atypical Flavobacteria Recovered from Diseased Fish in the Western United States. *Frontiers in Cellular and Infection Microbiology*, 13, p.1149032. https://doi.org/10.3389/fcimb.2023.1149032

Holmes, B., Steigerwalt, A.G. and Nicholson, A.C. 2013. DNA–DNA Hybridization Study of Strains of *Chryseobacterium*, *Elizabethkingia* and *Empedobacter* and of Other Usually Indole-Producing Non-Fermenters of CDC Groups IIc, IIe, IIh and IIi, Mostly from Human Clinical Sources, and Proposals of *Chryseobacterium bernardetii* sp. nov., *Chryseobacterium carnis* sp. nov., *Chryseobacterium lactis* sp. nov., *Chryseobacterium nakagawai* sp. nov. and *Chryseobacterium taklimakanense* comb. nov. *International Journal of Systematic and Evolutionary Microbiology*, 63(Pt_12), pp.4639-4662. https://doi.org/10.1099/ijs.0.054353-0

Hugo, C., Bernardet, J.F., Nicholson, A. and Kämpfer, P. 2015. *Chryseobacterium*. *Bergey's Manual of Systematics of Archaea and Bacteria*, pp.1-107. https://doi.org/10.1002/9781118960608.gbm00301.pub2

Ilardi, P. and Avendaño-Herrera, R. 2008. Isolation of Flavobacterium-Like Bacteria from Diseased Salmonids Cultured in Chile. *Bulletin of the European Association of Fish Pathologists*, 28, pp.176-185.

Ilardi, P., Fernandez, J. and Avendano-Herrera, R. 2009. *Chryseobacterium piscicola* sp. nov., Isolated from Diseased Salmonid Fish. *International Journal of Systematic and Evolutionary Microbiology*, *59*(12), pp.3001-3005. https://doi.org/10.1099/ijs.0.007021-0

Irber et al. 2024. Sourmash v4: A Multitool to Quickly Search, Compare, and Analyze Genomic and Metagenomic Data Sets. *Journal of Open Source Software*, 9(98), 6830. https://doi.org/10.21105/joss.06830

Isroni, W., Setyawati, D. and Maulida, N. 2019. Studi Komunitas Bakteri pada Sistem Resirkulasi pada Budidaya Lele Dumbo (*Clarias gariepinus*). *Journal of Aquaculture and Fish Health*, 8(3), pp.159-166.

Janknecht, P., Schneider, C. and Ness, T. 2002. Outbreak of *Empedobacter brevis* Endophthalmitis After Cataract Extraction. *Graefe's Archive for Clinical and Experimental Ophthalmology*, 240(4), pp.291-295. https://doi.org/10.1007/s00417-002-0435-5

Jung, W.J., Kim, S.G., Giri, S.S., Kim, S.W., Kang, J.W., Kwon, J., Oh, W.T., Lee, S.B., Lee, Y.M., Jo, S.J. and Chi, C. 2022. The Opportunistic Pathogen *Chryseobacterium balustinum* WLT: Pathogenicity and Antibiotic Resistance. *Fishes*, 7(1), p.26. https://doi.org/10.3390/fishes7010026

Katoh, K., Misawa, K., Kuma, K.I. and Miyata, T. 2002. MAFFT: A Novel Method for Rapid Multiple Sequence Alignment Based on Fast Fourier Transform. *Nucleic Acids Research*, 30(14), pp.3059-3066. https://doi.org/10.1093/nar/gkf436

Katoh, K. and Standley, D.M. 2013. MAFFT Multiple Sequence Alignment Software Version 7: Improvements in Performance and Usability. *Molecular Biology and Evolution*, 30(4), pp.772-780. https://doi.org/10.1093/molbev/mst010

Kapetanović, D., Kurtović, B., Vardić, I., Teskeredžić, E. and Teskeredžić, Z. 2006. Gill Disease in a Gilthead Sea Bream (*Sparus aurata* L.). *Medycyna Weter*, 62, pp.1239-1241.

Kim, S.G., Giri, S.S., Kim, S.W., Kwon, J., Lee, S.B. and Park, S.C. 2020. First Isolation and Characterization of *Chryseobacterium cucumeris* SKNUCL01, Isolated from Diseased Pond Loach (*Misgurnus anguillicaudatus*) in Korea. *Pathogens*, 9(5), p.397. https://doi.org/10.3390/pathogens9050397

Koch, R. 1890. Xth International Congress of Medicine, Berlin. https://doi.org/10.1016/s0140-6736(00)64092-8

Kumar, G., Engle, C., Aarattuthodi, S., van Senten, J., Hegde, S., Khoo, L., Hanson, L., Peterman, M. and Dorman, L. 2024. Economic Impact of Edwardsiellosis on the US Catfish Industry. *Aquaculture Economics & Management*, 28(3), pp.415-438. https://doi.org/10.1080/13657305.2024.2319083

LaFrentz, B.R. and Klesius, P.H. 2009. Development of a Culture Independent Method to Characterize the Chemotactic Response of *Flavobacterium columnare* to Fish Mucus. *Journal of Microbiological Methods*, 77(1), pp.37-40. https://doi.org/10.1016/j.mimet.2008.12.011

LaFrentz, B.R., Králová, S., Burbick, C.R., Alexander, T.L., Phillips, C.W., Griffin, M.J., Waldbieser, G.C., García, J.C., de Alexandre Sebastião, F., Soto, E. and Loch, T.P. 2022. The Fish Pathogen *Flavobacterium columnare* Represents Four Distinct Species: *Flavobacterium columnare*, *Flavobacterium covae* sp. nov., *Flavobacterium davisii* sp. nov. and *Flavobacterium oreochromis* sp. nov., and Emended Description of *Flavobacterium columnare*. *Systematic and Applied Microbiology*, 45(2), p.126293. https://doi.org/10.1016/j.syapm.2021.126293

Lin, J.N., Lai, C.H., Yang, C.H., Huang, Y.H., Lin, H.F. and Lin, H.H. 2017. Comparison of Four Automated Microbiology Systems with 16S rRNA Gene Sequencing for Identification of *Chryseobacterium* and *Elizabethkingia* Species. *Scientific Reports*, 7(1), p.13824. https://doi.org/10.1038/s41598-017-14244-9

Loch, T.P. and Faisal, M. 2015a. Emerging Flavobacterial Infections in Fish: A Review. *Journal of Advanced Research*, 6(3), pp.283-300. https://doi.org/10.1016/j.jare.2014.10.009

Loch, T.P. and Faisal, M. 2015b. Polyphasic Characterization Reveals the Presence of Novel Fish-Associated *Chryseobacterium* spp. in the Great Lakes of North America. *Diseases of Aquatic Organisms*, 113(2), pp.113-125. https://doi.org/10.3354/dao02819

Malick, R.C., Das, B.K., Pal, B.B., Bera, A.K., Maurye, P. and Sahoo, A.K. 2022. Molecular Identification, Whole-Cell Protein Profiling, Antibiotics Sensitivity and Pathogenicity of *Chryseobacterium gleum* Recovered from Diseased Fishes of Freshwater Wetlands in India. *Aquaculture*, 559, p.738411. https://doi.org/10.1016/j.aquaculture.2022.738411

Mallik, S.K., Pathak, R., Shahi, N., Kala, K., Chandra, S., Das, P., Singh, B., Singh, M., Giri, A.K., Tandel, R.S. and Sarma, D. 2023. Pathological Analysis and Antimicrobial Susceptibility of *Chryseobacterium balustinum* RTFCP 298 Isolated from Diseased Rainbow Trout, *Oncorhynchus mykiss*. *Scientific Reports*, 13(1), p.13268. https://doi.org/10.1038/s41598-023-40028-5

Martinez, V., Matabang, M.A., Miller, D., Aggarwal, R. and LaFortune, A. 2023. First Case Report on *Empedobacter falsenii* Bacteremia. *Diseases*, 33, p.e01814. https://doi.org/10.1016/j.idcr.2023.e01814

Muigg, V., Seth-Smith, H.M., Adam, K.M., Weisser, M., Hinić, V., Blaich, A., Roloff, T., Heininger, U., Schmid, H., Kohler, M. and Graf, L. 2024. Novel Organism Verification and Analysis (NOVA) Study: Identification of 35 Clinical Isolates Representing Potentially Novel Bacterial Taxa using a Pipeline Based on Whole Genome Sequencing. *BMC Microbiology*, 24(1), p.14. https://doi.org/10.1186/s12866-023-03163-7

Mukerji, R., Kakarala, R., Smith, S.J. and Kusz, H.G. 2016. *Chryseobacterium indologenes*: An Emerging Infection in the USA. *Case Reports*, 2016, p.bcr2016214486. https://doi.org/10.1136/bcr-2016-214486

Nicholson, A.C., Gulvik, C.A., Whitney, A.M., Humrighouse, B.W., Bell, M.E., Holmes, B., Steigerwalt, A.G., Villarma, A., Sheth, M., Batra, D. and Rowe, L.A. 2020. Division of the Genus *Chryseobacterium*: Observation of Discontinuities in Amino Acid Identity Values, a Possible Consequence of Major Extinction Events, Guides Transfer of Nine sSecies to the Genus *Epilithonimonas*, Eleven Epecies to the Genus *Kaistella*,

and Three Species to the Genus *Halpernia* gen. nov., with Description of *Kaistella daneshvariae* sp. nov. and *Epilithonimonas vandammei* sp. nov. Derived from Clinical Specimens. *International Journal of Systematic and Evolutionary Microbiology*, 70(8), pp.4432-4450. https://doi.org/10.1099/ijsem.0.003935

Nhinh, D.T., Hoa, D.T., Giang, N.T.H., Van Van, K., Dang, L.T., Crumlish, M., Dong, H.T. and Hoai, T.D. 2023. Synergistic Infection of *Edwardsiella ictaluri* and *Flavobacterium oreochromis* in Cage Cultured Tilapia (*Oreochromis* sp.). *Journal of Fish Diseases*, 46(10), pp.1125-1136. https://doi.org/10.1111/jfd.13832

Peterman, M.A. and Posadas, B.C. 2019. Direct Economic Impact of Fish Diseases on the East Mississippi Catfish Industry. *North American Journal of Aquaculture*, 81(3), pp.222-229. https://doi.org/10.1002/naaq.10090

Reed, L.J., Muench, H. 1938. A Simple Method of Estimating Fifty Percent Endpoints. *The American Journal of Hygiene*, 27(3):493-497. https://doi.org/10.1093/oxfordjournals.aje.a118408

Scott, S.J. and Bollinger, T.K. 2014. *Flavobacterium columnare*: An Important Contributing Factor to Fish Die-Offs in Southern Lakes of Saskatchewan, Canada. *Journal of Veterinary Diagnostic Investigation*, 26(6), pp.832-836. https://doi.org/10.1177/1040638714553591

Shahi, N., Sharma, P., Pandey, J., Bisht, I. and Mallik, S.K. 2018. Characterization and Pathogenicity Study of *Chryseobacterium scophthalmum* Recovered from Gill Lesions of Diseased Golden Mahseer, *Tor putitora* (Hamilton, 1822) in India. *Aquaculture*, 485, pp.81-92. https://doi.org/10.1016/j.aquaculture.2017.11.018

Srinath, R., Sudhagar, A., Dharmaratnam, A., Satkar, S.G. and Basheer, V.S. 2026. Emerging Pathogen *Chryseobacterium* sp. Isolated from Diseased Goldfish *Carassius auratus*: Antimicrobial Susceptibility and Pathology. *Diseases of Aquatic Organisms*, 166, pp.1-12. https://doi.org/10.3354/dao03910

USDA NASS United States Department of Agriculture (USDA), Released 9 February 2026 by the National Agriculture Statistics Service (NASS). Available online: https://esmis.nal.usda.gov/sites/default/release-files/795763/cfpd0226.pdf

Vandamme, P., Bernardet, J.F., Segers, P., Kersters, K. and Holmes, B. 1994. New Perspectives in the Classification of the Flavobacteria: Description of *Chryseobacterium* gen. nov., *Bergeyella* gen. nov., and *Empedobacter* nom. rev. *International Journal of Systematic and Evolutionary Microbiology*, 44(4), pp.827-831. https://doi.org/10.1099/00207713-44-4-827

Wakabayashi, H., Huh, G.J. and Kimura, N. 1989. *Flavobacterium branchiophila* sp. nov., a Causative Agent of Bacterial Gill Disease of Freshwater Fishes. *International Journal of Systematic and Evolutionary Microbiology*, 39(3), pp.213-216. https://doi.org/10.1099/00207713-39-3-213

Wick, R.R., Schultz, M.B., Zobel, J. and Holt, K.E. 2015. Bandage: Interactive Visualization of *De Novo* Genome Assemblies. *Bioinformatics*, 31(20), pp.3350-3352. https://doi.org/10.1093/bioinformatics/btv383

Wise, A.L., LaFrentz, B.R., Kelly, A.M., Khoo, L.H., Xu, T., Liles, M.R. and Bruce, T.J. 2021. A Review of Bacterial Co-Infections in Farmed Catfish: Components, Diagnostics, and Treatment Directions. *Animals*, 11(11), p.3240. https://doi.org/10.3390/ani11113240

Wise, A.L., LaFrentz, B.R., Kelly, A.M., Liles, M.R., Griffin, M.J., Beck, B.H. and Bruce, T.J. 2023. The Infection Dynamics of Experimental *Edwardsiella ictaluri* and *Flavobacterium covae* Coinfection in Channel Catfish (*Ictalurus punctatus*). *Pathogens*, 12(3), p.462. https://doi.org/10.3390/pathogens12030462

Wise, A.L., LaFrentz, B.R., Kelly, A.M., Liles, M.R., Griffin, M.J., Beck, B.H. and Bruce, T.J. 2025. Coinfection of Channel Catfish (*Ictalurus punctatus)* with Virulent *Aeromonas hydrophila* and *Flavobacterium covae* Exacerbates Mortality. *Journal of Fish Diseases*, 48(8), p.e13912. https://doi.org/10.1111/jfd.13912

Yang, Q., Tu, Y.Y., Zhang, N., Miao, B., Zhang, Y.Z., Deng, X.T., He, T., Su, S.Q., Lin, L.Y. and Zhu, S. 2024. Co-Infections of *Aeromonas dhakensis* and *Chryseobacterium indologenes* in Largemouth Bass (*Micropterus salmoides*). *Aquaculture*, 579, p.740259. https://doi.org/10.1016/j.aquaculture.2023.740259

Zamora, L., Vela, A.I., Palacios, M.A., Domínguez, L. and Fernández-Garayzábal, J.F. 2012. First Isolation and Characterization of *Chryseobacterium shigense* from Rainbow

Trout. *BMC Veterinary Research*, 8(1), p.77. https://doi.org/10.1186/1746-6148-8-77

Zubova, K.V., Kuznetsova, V.A., Kanevsky, M.V., Kondratenko, O.V., Glinskaya, E.V., Nechaeva, O.V. and Afinogenova, A.G. 2025. Biological Properties and Pathogenetic Potential of *Weeksellaceae* Family Bacteria. *Russian Journal of Infection and Immunity*, 15(3), pp.505-516. https://doi.org/10.15789/2220-7619-bpa-17859

Chapter V

Growth and Proteomic Responses of Virulent *Aeromonas hydrophila*, *Flavobacterium covae*, and *Edwardsiella ictaluri* in Co-Culture

5.1. Abstract

Virulent *Aeromonas hydrophila*, *Flavobacterium covae*, and *Edwardsiella ictaluri* are the three predominant bacterial pathogens affecting the U.S. catfish industry. Individually, these pathogens cause serious disease outbreaks annually, resulting in major economic losses. Co-infection of these same pathogens can worsen disease outbreaks under production settings. *In vivo* co-infection assessment of these same pathogens revealed cooperative and competitive behaviors that exacerbated mortality. However, the mechanisms underlying these bacterial interactions have yet to be investigated. Co-culture (Co) combinations of virulent *A. hydrophila* (vAh), *F. covae* (Fc), and *E. ictaluri (*Ei) were grown for *in vitro* assessment of their bacterial growth and extracellular protein secretion. Co-culture of Ei and Fc exhibited cooperative growth dynamics, with both bacteria increasing the carrying capacity, maximum growth rate, and total growth of one another. Comparative secretome analysis of the Ei + Fc co-culture revealed substantial remodeling of secreted protein abundance, where 25 unique virulence-associated proteins displayed significant differential abundance relative to monocultures (FDR ≤ 0.05). In contrast, the co-culture of vAh + Fc revealed slight competitive growth dynamics,

however comparisons were not statistically significant (FDR > 0.05). A secretome analysis revealed 17 unique virulence-associated proteins with significant relative abundance (FDR ≤ 0.05). Growth assessment of vAh + Ei in co-culture also indicated competition, with a significant interaction between bacterial strain and culture condition ($P \leq 0.001$). Collectively, these findings reveal species-specific interactions in growth and in the abundance of differentially secreted proteins under co-culture conditions.

5.2. Introduction

Catfish aquaculture is the largest aquaculture industry in the United States and produces both channel (*Ictalurus punctatus*) and hybrid catfish (female *I. punctatus* ´ male *I. furcatus*). In rural communities in the southeast, particularly in Mississippi, Alabama, and Arkansas, catfish aquaculture contributes approximately $1.91 billion annually (Engle, 2003; Hegde et al., 2022). Despite its success, the industry faces significant economic pressure from competing foreign imports, rising feed and energy costs, and infectious diseases (Peterman and Posadas, 2019; Hedge et al., 2022; Abdelrahman et al., 2023). Among these, infectious diseases pose a significant threat to the catfish industry by limiting profitability due to fish mortality, reduced production efficiency, and the high cost of treatment (Peterman and Posadas, 2019).

Of the infectious diseases disrupting the catfish industry, bacterial pathogens are the leading cause of disease and mortality. A recent epidemiological study of the Alabama catfish industry reported that bacterial infections were responsible for more than 83% of disease-related losses (Abdelrahman et al., 2023). Among these bacterial pathogens,

three are primarily responsible for substantial economic losses; virulent *Aeromonas hydrophila*, *Flavobacterium covae*, and *Edwardsiella ictaluri* (Wagner, Wise, Khoo, and Terhune, 2002; Peterman and Posadas, 2019; Abdelrahman et al., 2023). While each pathogen can cause detrimental disease outbreaks on its own accord, each possesses the ability to co-infect and lead to substantial mortality. For example, a co-infection of *E. ictaluri* and *F. covae* resulted in exacerbated mortality among juvenile channel catfish, with mortality resembling that of a single infection of *E. ictaluri* (Wise et al., 2023). Additionally, fish exposed to *E. ictaluri* exhibited increased immune activity, suggesting that *E. ictaluri* was the primary driver of disease progression. In contrast, another co-infection with *F. covae* and virulent *A. hydrophila* demonstrated significant mortality among channel catfish in co-infection groups compared to single-pathogen exposed groups, indicating the bacteria worked in tandem to increase disease severity and mortality (Wise et al., 2024). Given that bacterial co-infections produce dynamic and complex interactions within the host, it is imperative to understand specific mechanisms underlying these bacterial interactions.

While bacterial-host interactions of virulent *A. hydrophila*, *E. ictaluri*, and *F. covae* have been investigated during *in vivo* challenges (Wise et al., 2023; Wise et al., 2025), their specific physiological interactions when grown as co-culture *in vitro* has yet to be investigated. The advent of relevant technology that allows contact-independent bacterial interactions mediated by diffusible molecules has presented an attractive application for observing these interactions in real time (Moutinho et al., 2017). Moreover, this application allows for the collection of rapid optical density measurements and generation of bacterial

growth curves, allowing quantitative comparisons of co-culture and monoculture growth metrics.

While bacterial growth metrics can provide valuable insight into bacterial proliferation, they do not reveal the mechanisms underlying these interactions. Identifying and characterizing the extracellular proteins produced by bacteria in co-culture, specifically those associated with virulence, could offer insight into how bacterial pathogens influence one another during disease progression. Proteomic investigations have identified virulence factors associated with disease in virulent *A. hydrophila* (Pridgeon et al., 2013; Wang et al., 2019; Zhang, Xu, and Beck, 2019; Barger, Liles, and Newton, 2020; Barger, Liles, Beck, and Newton, 2021), columnaris-causing bacteria (Thunes et al., 2022; Sayed et al., 2023), and *E. ictaluri* (Dumpala, Lawrence, and Karsi, 2009; Dubytska, Rogge, and Thune, 2016; Akgul, Akgul, Lawrence, and Karsi, 2018; Kalindamar et al, 2023). However, it remains unclear whether the production and abundance of these virulence-associated proteins are altered under co-culture conditions.

Given the severity of mortality in co-infections, and the ability of bacteria to compete or cooperate, it is essential to elucidate the mechanisms underlying these interactions. Therefore, virulent *A. hydrophila*, *F. covae*, and *E. ictaluri* were evaluated *in vitro* under co-culture conditions to characterize their interactions. Additionally, the secreted extracellular product profile (secretome) of each bacterium in monoculture and co-culture were analyzed to identify changes in protein abundance between monoculture and co-culture over time. Finally, virulence-associated secreted proteins were identified to determine whether co-culture altered the abundance of factors involved in pathogenicity.

5.3. Materials and Methods

5.3.1. Bacteria and Culture Conditions

Virulent *A. hydrophila* (ML09-119), *E. ictaluri* (S97-773), and *F. covae* (ALG-00-530), were revived from -80 °C storage onto optimal growth media, including tryptic soy agar (TSA; Becton, Dickinson and Company, Sparks, MD, USA), brain heart infusion agar (BHI; Becton, Dickinson and Company) and modified Shieh agar (MSA; LaFrentz & Klesius, 2009), respectively. *E. ictaluri* and *F. covae* were incubated for 48 h at 28 °C, while *A. hydrophila* was incubated for 24 h at the same temperature. Following primary growth, approximately 1-3 colonies of bacteria were individually inoculated into 12-20 mL of broth and according to their co-culture pairing (*E. ictaluri* and *A. hydrophila* were grown in BHI broth, *F. covae* and *E. ictaluri* were grown in MSB, and *F. covae* and *A. hydrophila* were grown in MSB). All bacteria were incubated at 28 °C and 175 rpm for 12 h, then expanded to fresh 20 mL of broth and incubated for another 12 h under the same conditions.

5.3.2. Bacterial Growth Curves

Growth curves of monoculture and co-cultures were created using the Duet Co-Culture System (Cerillo, Charlottesville, VA, USA). Bacterial cultures were prepared as described above and diluted to an optical density (OD) measured at 600 nm of 0.01 for standardization (OD_{600} = 0.01). Each well of the Duet Co-Culture System was inoculated with a total volume of 800 μL. Individual co-culture combination plates included three replicates of the following: monoculture A, monoculture B, co-culture (A + B), blank, and

monoculture A + blank, and monoculture B + blank. Plates were covered with a Breathe-Easy sealing membrane (Diversified Biotech, Dedham, MA, USA) before transferring the plate to the Optical Density Microplate Reader (Cerillo) inside of an incubator set at 28 °C. The microplate reader was placed on a magnetic shaker set to 175 rpm. The OD_{600} was recorded every 30 mins for a 36-h period using the Canopy Wireless Accessory Package (Cerillo), and the growth curve and raw data was generated using the Labrador Software (Cerillo).

5.3.3. Growth Metric Analysis

Bacterial growth metric analysis of co-culture interactions was done using R (Version 2026.05.0). Raw OD_{600} measurements were used to assess monoculture and co-culture growth metrics, including carrying capacity (K), instantaneous growth rate (m), maximum specific growth rate (m_{max}), doubling time (t_d), time to 10% carrying capacity (t_{10K}), and total growth estimated as area under the curve (AUC). These parameters are commonly used to describe bacterial growth curves (Zwietering et al., 1990; Kahm et al., 2010; Hall et al., 2014; Sprouffske and Wagner, 2016). Raw OD_{600} values were blank-corrected and smoothed using a three-point moving average to reduce reading noise. Smoothed OD_{600} values above the minimum OD threshold (i.e., the average blank value), were natural log transformed, and the instantaneous growth rate was calculated as the change in the natural log of OD over time. Final growth density was estimated as the median of the smoothed OD_{600} over the final 3 h of incubation, and area under the curve was calculated using the trapezoidal rule. Co-culture effects were calculated as

proportional changes in each growth metric relative to the corresponding mono-culture condition to describe strain-specific interaction effects in mixed culture (Ram et al., 2019; Schmitz et al., 2024).

5.3.4. Secretome Preparation

Bacterial growth was performed as described previously with minor adjustments to the second broth culture. Following 12 h of incubation, both monocultures were diluted to an OD_{600} of 0.1 to standardize the starting bacterial concentrations, then 125 μL of monoculture was added to 100 mL of broth in a baffled 250 mL flask, whereas 125 μL of each monoculture (125 μL of monoculture A + 125 μL of monoculture B) was added to 100 mL of broth for co-culture for each combination. Mock control flasks were inoculated with 125 μL of sterile media. Each experiment included four treatments: monoculture A, monoculture B, co-culture (A + B), and mock (sterile media), and two timepoints (12-h and 24-h), consisting of 24 flasks total for each experiment. All 24 flasks were incubated at 28 °C and 175 rpm.

Following 12 h post-inoculation, flasks designated for the 12-h timepoint were removed from the incubator, and a 1 mL sample from each flask was taken, and OD_{600} was measured and recorded. Another 1 mL sample from one replicate flask was obtained for ten-fold serial dilution and spread plating to determine bacterial concentration. Pierce protease and phosphatase inhibitor (Thermo Fisher Scientific, Waltham, MA, USA) was added to each flask at a concentration of 1% v/v and mixed by swirling. The entire 100 mL cultures were then transferred to 250 mL ultracentrifuge tubes and pelleted at 20,000 $\times g$

for 15 minutes at 4 °C. The supernatant was decanted directly into a .45 μM vacuum filter, and the filtrate was collected. Remaining cells were removed from the collected filtrate by passing through a 0.22 μM vacuum filter. Secreted proteins were precipitated from the cell-free supernatant by adding 41.1 g of ammonium sulfate to achieve 65% saturation and incubated at 4 °C on a rotary platform shaker with gentle mixing (100 rpm) for 24 h. Precipitated proteins were pelleted by centrifugation at 30,000 × *g* for 45 minutes at 4 °C and dissolved in 10 mL of cold 20 mM Tris-HCl (pH = 7.6). Proteins were dialyzed twice; first for 18 hours, then for 12 h, against the same Tris-HCl buffer using a 10K MWCO Slide-A-Lyzer G3 dialysis cassette (Thermo Fisher Scientific). Protein concentration was determined using the Pierce Dilution-Free Rapid Gold BCA Protein Assay (Thermo Fisher Scientific).

5.3.5. Protein Digestion and Mass Spectrometry

Secreted proteins at a concentration of 50 μg were precipitated with ice-cold acetone and allowed to dry in a fume hood. Protease max surfactant (0.01%) was added to the precipitated protein and incubated for 10 minutes, followed by 40 μL of ammonium bicarbonate. Cysteines were reduced with 0.5 μL of 250 mM DTT and incubated for 20 minutes at 57 °C, then 0.6 μL of 550 mM iodoacetamide was added and incubated in the dark for 20 minutes. Trypsin at 1 μg μL^{-1} was added at a ratio of 1:50, then samples were incubated at 37 ° for 3 h. Samples were cleaned with acidic reverse-phase Stage-Tips (Rappsilber, Mann, and Ishihama et al., 2007).

Samples were analyzed on an Orbitrap Exploris 240 mass spectrometer equipped with an UltiMate 3000 RSCLnano including binary pump, column compartment, and autosampler. The column is an EASY-Spray PepMap RSLC C18 2 μm, 100 Å 50 μm × 15 cm column with an Acclaim PepMap 100 Å C18 3 μm trapping column. The gradient solvent system consists of 0.1% (v/v) Formic Acid (FA) in water (buffer A) and 0.1% (v/v) FA in 80% acetonitrile and 20% water (buffer B). Peptide samples were separated at a flow rate of 300 nL min^{-1} with a segmented gradient: 3.5% (v/v) buffer B for 5 minutes linear gradient to 36% buffer B at 40 minutes, to 60% buffer B at 45 minutes, 98% buffer B at 48 minutes and held for 6 minutes, to 3.5% buffer B for 1 minute, and 5-minute re-equilibration at 3.5% buffer B.

Full mass spectrometry scans were acquired with a m/z range of 375-1500 and mass resolution of 120,000, with advanced peak width determination enabled and RunStartEasyIC in peptide application mode. The normalized automatic gain control (AGC) target was set to 300%, and the RF lens was set to 70%, with 1 microscan. MS/MS acquisition was performed in top 10 mode. The charge state filter was set to 2-5, the dynamic exclusion was set to on after 1 time with a 10-ppm tolerance for 45 seconds, and the intensity filter was set to a minimum of 5,000. The resolved fragments were scanned at a mass resolution of 30,000 standardized AGC and a normalized fixed HCD collision energy of 30%. The isolation window was 1.6 m/z. Mass spectrometry data were analyzed using Proteome Discoverer software (Version 2.3) and the Sequest search engine.

5.3.6. Secreted Protein Abundance Processing

Protein abundance values generated from mass spectrometry was separated from sample metadata and values were transformed using a log10 transformation in R. Values of zero or missing values were defined as "NA". Protein filtering was performed by keeping proteins only if they were present in at least 50% of all samples and in at least 2/3 replicates in at least two experimental groups.

5.3.7. Statistical Analyses

Differences between interaction effects of growth metric data (K, μ_{max}, and AUC) was assessed by a two-way Analysis of Variance (ANOVA) evaluating the effects of bacterial strain, culture condition, and their interaction. When a significant interaction was detected, pairwise comparisons of estimated marginal means of each bacterial strain under each culture condition was performed. A Tukey adjustment was made for multiple comparisons. Statistical significance was defined as $P < 0.05$. Differential abundance analysis was performed using the limma package in R (Version 3.68.4; Ritchie et al., 2015). Following protein filtering, abundance values were log2-transformed and fit to a linear model. Pairwise comparisons were performed for treatment and time combinations to assess differential abundance among co-culture, monoculture, and mock control at each time point, as well as temporal changes within each culture group. Variance estimation was performed using the Empirical Bayes method (Smyth, 2004; McCarthy and Smyth, 2009; Phipson, Lee, Majewski, Alexander, and Smyth, 2016), and *P*-values adjusted for multiple testing using the Benjamini-Hochberg false discovery rate (FDR; Benjamini and

Hochberg, 1995). Protein abundance with FDR < 0.05 were considered significantly differentially abundant.

5.3.8. Annotation of Virulence-Associated Secreted Proteins

Significantly differentially abundant secreted proteins identified by limma were annotated using UniProtKB (UniProt Consortium, 2015) accession assigned by the Proteome Discoverer software to retrieve gene amino-acid sequence, protein name, and validated source organism. Amino acid sequences were searched using BLASTP (NCBI Protein BLAST; Altschul et al., 1997) against the Virulence Factors of Pathogenic Bacteria (VFDB; Chen et al., 2005) Set A (protein sequences of core dataset).

5.4. Results

5.4.1. Growth Metrics

Bacterial growth metrics were assessed for each co-culture combination. Growth curves of all culture conditions are shown in Figure 5.7.1A. In the experiment assessing growth metrics of *E. ictaluri* and *A. hydrophila* in co-culture, a significant interaction between bacterial strain and culture condition was detected for carrying capacity (K; P = 0.001), maximum specific growth rate (μ_{max}; $P < 0.001$), time to 10% carrying capacity (t_{10K}; $P = 0.019$), and total growth (AUC; $P < 0.001$; Table 5.6.1). In co-culture, *E. ictaluri* had significantly higher K ($P = 0.005$), μ_{max} ($P < 0.001$), and AUC ($P = 0.001$) than in monoculture. In co-culture, *A. hydrophila* had significantly lower μ_{max} ($P = 0.003$) and AUC ($P = 0.011$) than in monoculture. In monoculture, *E. ictaluri* had significantly lower t_{10K} ($P = 0.001$) than

Ei monoculture + blank. Culture condition had a significant effect on μ_{max} ($P = 0.011$), t_{10K} ($P < 0.001$), and AUC ($P = 0.013$; Table 5.6.1). Interaction effects indicated that *A. hydrophila* had a positive effect on *E. ictaluri* K (94.2%), μ_{max} (65.1%), and AUC (84.1%), whereas *E. ictalrui* had a negative effect on those same growth metrics for *A. hydrophila* (-32.6%, -34.7%, and -36.2%, respectively; Figure 5.7.1B). This suggests that *E. ictaluri* and *A. hydrophila* demonstrate a competitive growth relationship in co-culture.

In the growth experiment assessing *F. covae* and *A. hydrophila*, the two-way ANOVA detected a significant effect in bacterial strain, culture condition, and their interaction in nearly every growth metric ($P < 0.05$; Table 5.6.3). However, bacterial strain had no significant effect on t_d ($P = 0.124$). No significant difference was detected when comparing growth of *F. covae* and *A. hydrophila* in co-culture to their growth in monoculture ($P > 0.05$; Table 5.6.4). However, significant differences in culture condition were detected across all growth metrics in comparisons between *A. hydrophila* in monoculture and monoculture + blank ($P < 0.005$). The μ_{max} of *F. covae* was significantly higher in *F. covae* monoculture compared to monoculture + blank ($P = 0.017$), however, t_{10K} was significantly lower in the F. *covae* monoculture compared to monoculture + blank ($P < 0.001$). Interaction effects indicated that *F. covae* had a positive effect on *A. hydrophila* K (13.0%), μ_{max} (3.7%), and AUC (9.2%), whereas *A. hydrophila* had a negative effect on the same growth metrics for *F. covae* (-19.0%, -12.2%, and -25.3%, respectively; Figure 5.7.2B). This data also suggests that *F. covae* and *A. hydrophila* demonstrate a competitive relationship when grown in co-culture.

The two-way ANOVA revealed that bacterial strain and culture condition had a significant effect on K and AUC ($P < 0.05$; Table 5.6.5) when assessing the growth metrics of *F. covae* and *E. ictaluri*. The K of *F. covae* was significantly higher in *F. covae* monoculture compared to monoculture + blank ($P = 0.026$), and AUC of *F. covae* was also significantly higher in monoculture compared to monoculture + blank ($P = 0.003$; Table 5.6.6). Interaction effects indicated that *F. covae* had a positive effect on *E. ictaluri* K (20.1%), μ_{max} (6.8%), and AUC (32.4%) while grown in co-culture (Figure 5.7.3B). Likewise, *E. ictalrui* also had a positive effect on *F. covae* K (11.0%), μ_{max} (6.5%), and AUC (3.2%). Collectively, this data suggests that *F. covae* and *E. ictaluri* behave cooperatively in co-culture.

5.4.2. Secretome Growth

Optical density measurement and bacterial concentration was determined and recorded at 0, 12, and 24 h post-inoculation during each individual secretome preparation experiment to align with sampling timepoints. Aligning with the Cerillo co-culture growth metric assessment, *E. ictaluri* + *A. hydrophila* was prepared in BHI broth, while *F. covae* + *A. hydrophila* and *F. covae* + *E. ictaluri* were prepared using MSB. During the *E. ictalrui* + *A. hydrophila* secretome sampling, *A. hydrophila* grew well as a monoculture, yielding high OD_{600} > 3.0 and concentration of 9.6×10^8 and 6.5×10^8 CFU mL^{-1} at 12 and 24 h post-inoculation, respectively (Figure 5.7.4A). Between the 0 and 12 h sampling timepoints, *A. hydrophila* monoculture was in exponential growth, and by 24 h reached death phase as CFU mL^{-1} decreased. However, *E. ictaluri* did not grow as monoculture, with OD_{600} reaching

0.073 by 24 h and concentration consistently below detectable limits on spread plate at both sampling timepoints (Figure 5.7.4A). Therefore, growth of the co-culture was primarily driven by *A. hydrophila* and cannot be interpreted as proliferation of both bacterial species.

During secretome sampling for *F. covae* and *A. hydrophila*, both monocultures grew well, making interpretation of the co-culture possible. The optical density and bacterial concentration of *F. covae* monoculture increased from OD_{600} = 0.207 to 0.586 and 1.5×10^8 to 3.7×10^8 CFU mL^{-1}, respectively (Figure 5.7.4B), indicating slow and consistent growth throughout the sampling timepoints. Monoculture of *A. hydrophila* had higher overall growth than the monoculture of *F. covae*, with OD_{600} increasing slightly from 2.649 to 2.802 and concentration being 2.2×10^9 CFU mL^{-1} from 12 – 24 h post-inoculation (Figure 5.7.4B), indicating *A. hydrophila* likely began stationary phase at 12 h. Optical density of co-culture of *F. covae* and *A. hydrophila* increased from 2.76 to > 3.0, whereas bacterial concentration decreased from 2.5×10^9 to 1.8×10^9 CFU mL^{-1} (Figure 5.7.4B), indicating that exponential growth likely occurred before 12 h, and bacterial cells likely began dying before or during the 24 h sampling timepoint. Upon inspection of colony morphologies, only 1 morphology representing *A. hydrophila* growth was observed on co-culture spread plates. Colonies representative of *F. covae* were not observed on co-culture spread plates. Therefore, bacterial concentration of the co-culture condition represents *A. hydrophila* growth only.

In the secretome analysis involving *F. covae* and *E. ictaluri*, the OD_{600} for the *F. covae* monoculture increased from 0.328 to 0.626, *E. ictaluri* monoculture increased from 0.143 to 0.835, and co-culture increased from 0.588 to 1.361 between the 12 h to 24 h

timepoints (Figure 5.7.4C). The monoculture of *E. ictaluri* grew the most by 24 h, reaching 1.4×10^9 CFU mL^{-1}, followed by *F. covae* in co-culture (6.8×10^8), *E. ictaluri* in co-culture (5.6×10^8) and *F. covae* in monoculture (4.2×10^8; Figure 5.7.4C). Due to the last sampling timepoint being 24 h post-inoculation, it is uncertain whether all three cultures reached stationary phase, as OD and CFU measurements displayed a slower, continuous growth.

5.4.3. Differential Abundance Analysis of Secreted Proteins

Due to *E. ictaluri* not growing in monoculture, in which the same culture was used to inoculate the co-culture (*E. ictaluri* + *A. hydrophila*), full interpretation of the secreted proteins from the secretomes was limited. Additionally, no *E. ictaluri*-associated proteins were present in any secretome of the co-culture dataset. Following protein filtering, a total of 35 proteins were analyzed. Pairwise comparison between *E. ictlauri* (12 h and 24 h), and Mock (12 h and 24 h), revealed no significant difference in protein abundance ($P > 0.05$; Table 5.6.4). Likewise, comparison of co-culture and *A. hydrophila* at 12 h and 24 h, yielded no significant proteins ($P > 0.05$), further confirming the absence of *E. ictaluri* growth in monoculture and co-culture. Moreover, comparisons between co-culture and *E. ictaluri* at 12 h, and co-culture and Mock at 12 h were identical (14/35 significant proteins; 40.0%; 13 proteins highly abundant, and 1 protein of low abundance; $P < 0.001$;Table 5.6.4). Secreted proteins that were more abundant in co-culture included a hemolysin, two aerolysin, flagellin, S8 family serine peptidase, a chitin binding protein, two ornithine carbamoyltransferase, an extracellular serine protease, a major outer membrane lipoprotein, chitinase, GlyGly-CTERM sorting domain-containing protein, and a

carbohydrate binding domain protein. One secreted protein has significantly low abundance (bifunctional metalloprotease). Co-culture versus *E. ictaluri* at 24 h exhibited 3/35 significant proteins (8.6%), with one protein being more abundant in co-culture (carbohydrate binding domain protein) and two being less abundant (bifunctional metalloprotease and lipase). Co-culture versus Mock at 24 h showed slight differences, with 6/35 proteins significant (17.1%), 3 more abundant, including a carbohydrate binding protein, a chitin binding protein, and ornithine carbamoyltransferase, and 3 less abundant in co-culture (lipase, serine proteinase, and bifunctional metalloprotease; Table 5.6.4). The secretome of co-culture differed in protein abundance by 31.4% (11/35 significant proteins) from 12 h – 24 h, wherein all 11 proteins were significantly reduced (Table 5.6.4).

A total of 348 proteins were assessed for differential abundance from monocultures of *F. covae*, *A. hydrophila*, co-culture, and sterile MSB representing a negative control (Mock) group. Of the 348 proteins, 4 belonged to *A. hydrophila*, 328 were *F. covae*, and 16 were unknown. The monoculture of *A. hydrophila* had no significant difference in secreted protein abundance from 12 h – 24 h ($P = 0.199$; Table 5.6.5). Therefore, the secreted protein profile of *A. hydrophila* in monoculture was consistent throughout the 24 h culture. Additionally, no significant difference in abundance was detected for co-culture at 12 h compared to vAh at 12 h (0/348; $P = 0.250$), and only 2 proteins that were significantly abundant at 24 h (0.6%; $P = 0.028$), indicating that the overall profile is the same in co-culture and *A. hydrophila* at 12 h. Comparing abundance of co-culture versus *F. covae* at 12 h and 24 h, secreted proteins significantly changed in co-culture at both timepoints (29.3% and 71.8%; $P < 0.001$; Table 5.6.5), indicating proteins were less abundant in co-

culture. There was a significant difference in the abundance of secreted proteins in co-culture compared to Mock at 12 h (6.9%; $P < 0.001$) and 24 h (4.0%; $P = 0.002$), with the most significant proteins being reduced. Significant proteins in *F. covae* monoculture changed by half (50.9%) at 24 h, with 159 proteins increasing, and 18 decreasing ($P < 0.001$; Table 5.6.5). This result shows that the *F. covae* secretome in monoculture changes drastically over time. In comparison, a small shift in abundance of secreted proteins in co-culture (2.3%, $P = 0.013$), and Mock (0.6%; $P = 0.018$) was observed (Table 5.6.5).

Significant differences in abundance of secreted proteins in the secretome of Fc, Ei, and Co (Fc + Ei) were detected and ranged from 36.1% – 68.6% ($P < 0.001$; Table 5.6.6). A total of 592 secreted proteins were assessed. Of those, 284 were associated with *F. covae*, 118 were *E. ictaluri*, and 190 were unknown. Pairwise comparison between co-culture and *F. covae* at 12 h indicated 334/592 secreted proteins were more abundant in co-culture than *F. covae* (56.4%), however, at 24 h, there was a 41.6% significant difference in co-culture compared to *F. covae* (Table 5.6.6). A similar trend was displayed when comparing co-culture and *E. ictaluri* at 12 h (52.7%) and 24 h (68.6%; Table 5.6.6). Within the comparisons of each monoculture versus co-culture, at 12 h, significant proteins were more abundant in co-culture, but at 24 h, significant proteins were significantly reduced in co-culture compared to *E. ictaluri* and *F. covae* (Table 5.6.6). Temporal comparison within each monoculture further reflected this trend, with *F. covae* and *E. ictaluri* exhibiting an abundance of significant proteins at 24 h (53.2% and 59.3%m respectively) then at 12 h. Additionally, secreted proteins in co-culture were significantly reduced by 36.1% at 24 h (Table 5.6.6). This suggests that over time, both *F. covae* and *E. ictaluri* cultures actively

modify their secretome, while the co-culture secretome becomes depleted. At 12 h, 396/592 (66.9%) differed significantly in co-culture compared to Mock, with the majority of significant proteins being higher in co-culture (383). Likewise, at 24 h, co-culture differed significantly from Mock (53.2%), with most significant proteins being greater in co-culture (Table 5.6.7). Lastly, comparison between Mock at 12 h and 24 h indicated no significant difference in protein abundance (0%; $P = 0.073$).

5.4.4. Analysis of Virulence-Associated Secreted Proteins

Analysis of putative virulence-associated secreted proteins was performed following limma differential abundance analysis for the secretome of all bacterial cultures. Annotation and virulence screening of significant differentially abundant proteins of the *E. ictaluri* + *A. hydrophila* secretome identified 1 unique secreted protein, GbpA, which is associated with adherence (Figure 5.7.5). In co-culture, GbpA was significantly higher compared to *E. ictaluri* monoculture at 12 h, Mock at 12 h, and Mock at 24 h (FDR < 0.05). The absence of secreted proteins of *E. ictaluri* origin was suspected, as *E. ictaluri* in culture did not grow.

Within the *F. covae* + *A. hydrophila* secretome, a total of 17 unique secreted proteins with association to virulence were significantly differentially abundant (FDR < 0.05; Figure 5.7.6). A total of 5 *A. hydrophila*-associated proteins associated with enzyme function (HAP), effector delivery system (LasB), and adherence (GbpA, Hsp60, and GroEL) displayed significant relative abundance. HAP and LasB were significantly higher in co-culture compared to *F. covae* monoculture at 12 h, and GbpA was significantly higher in

co-culture compared to *F. covae* monoculture at 24 h. A significant reduction in relative abundance was detected for Hsp60 and GroEL in co-culture compared to Mock at 12 h, *F. covae*-associated proteins with significant relative abundance in co-culture represented virulence factors related to immune modulation, stress survival, effector delivery system, adherence, and nutritional/metabolic factors. An LPS gene (*kdsA*) was identified to have significantly lower abundance in co-culture than *F. covae* monoculture at 12 h. Compared to *F. covae* monoculture at 24 h, the following *F. covae* virulence proteins/genes were identified to have significantly lower abundance (FDR < 0.05) in co-culture: SodA, SodB, T4SS secreted effectors, LPS, KatAB, KatG, T9SS, ClpP, *purCD*, and GuaA (Figure 5.7.6).

The *E. ictaluri* + *F. covae* secretome was enriched with an abundance of significant virulence-associated proteins compared to both monocultures and Mock (Figure 5.7.7). *E. ictaluri* had a total of 14 unique virulence-associated proteins showing temporal significant relative abundance. These virulence-associated proteins are involved in diverse functions, including immune modulation (PGI, BpIF, GmhA, GmhA2, GmhA. LpcA, KdsB), biofilm (LuxS), stress survival (ClpP), motility (NueA), invasion (KpsU), adherence HtpB and GroEL), and some represented effector delivery system (CBU_0270 and LPG_RS00105; Figure 5.7.7). All but LPG_RS00105 had significantly higher abundance in co-culture at 12 h post-inoculation but decreased in abundance in co-culture by 24 h (Figure 5.7.7). *F. covae* had 11 unique virulence-associated proteins with significant differential relative abundance in co-culture compared to monocultures and Mock. F. covae-associated virulence proteins represented immune modulation (KdsA and LPG_RS03745), stress survival (SodB, SodA, KatG, KatB, KatA, and ClpP), nutritional/metabolic factor (PurCD),

and adherence (TufA; Figure 5.7.7.) These *F. covae*-secreted virulence factors were significantly higher in co-culture compared to monocultures and Mock at 12 and 24 h post-inoculation. However, all of them showed significant reduction in abundance in *F. covae* monoculture at 24 h. This information suggests that both *E. ictlauri* and *F. covae* actively respond to one another when grown in co-culture and modify their secretome over time in response.

5.5. Discussion

To date, attention has been increasingly given to understanding bacterial co-infections in channel catfish aquaculture; by demonstrating the severity of mortality (Mohammed and Peatman, 2018; Wise et al., 2021), elucidating bacterial interactions within the host (Wise et al., 2023; Wise et al., 2025) and investigating alternative methods for disease management (Oladipupo et al., 2026). These reports have provided valuable insight into bacterial-host dynamics, however, bacterial-bacterial interactions remain largely understood. Whether bacterial pathogens exhibit competitive or cooperative behavior in co-culture can provide a more comprehensive understanding of bacterial co-infections. For example, Kluge, Hoffman, Benndorf, Rapp, and Reichl (2012) demonstrated that *Pseudomonas aeruginosa* displayed antagonistic growth behavior in co-culture with *Staphylococcus aureus,* wherein *S. aureus* growth was inhibited. Another study involving different closely-related bacterial species grown in mixed culture acquire mutations that can alter antagonistic effects of vesicle-enriched secretomes (Warsi, Gedda, Edwards, and Andersson, 2023).

In vitro co-culture of *E. ictaluri* and *F. covae* revealed cooperative growth and secretome remodeling. Growth metric analysis showed that *E. ictaluri* and *F. covae* had a positive interaction on one another in co-culture, demonstrating mutual growth promotion. A potential mechanism that could explain the cooperative growth demonstrated by *E. ictaluri* and *F. covae* could be from bidirectional metabolite cross-feeding (Mataigne, Vannier, Vandenkoornhuyse, and Hacquard, 2021). The co-culture system used in this study allowed fluidic contact between bacterial cultures, therefore secreted compounds like metabolites (≤ 0.2 μM) could be passed through a semi-permeable membrane. One hypothesis is that *E. ictaluri* and *F. covae* engaged in bidirectional metabolite cross-feeding during co-culture, which could have resulted in reciprocal growth enhancement of co-culture compared to their growth in monoculture.

Changes observed in abundance of secreted proteins further support the possibility that active physiological interactions occurred between *E. ictaluri* and *F. covae* in co-culture. Differential abundance analysis of secreted proteins showed a significant enrichment in abundance within co-culture relative to respective monocultures at 12 h post-inoculation. However, a shift was observed at 24 h, with the co-culture showing a significant reduction in secreted proteins. These observations indicate that co-culture of *E. ictaluri* and *F. covae* secretome underwent secretion remodeling over time, perhaps as a result of their transition into later stages of growth leading to reduced metabolic activity and nutrient depletion. Collectively, these findings suggest that the interaction between *E. ictaluri* and *F. covae* extend beyond just coexistence and provide evidence of active and complex physiological interactions that could affect bacterial fitness and behavior.

An objective of the current study was to identify, if any, secreted virulence-associated proteins in secretomes and compare their abundance between co-cultures and monocultures. Co-culture of *E. ictaluri* and *F. covae* exhibited significant enrichment of virulence-associated secreted proteins relative to monocultures. The virulence-associated proteins represent diverse functions, including immune modulation, biofilm formation, motility, invasion, adherence, stress survival, effector delivery system, and nutritional/metabolic factors. However, a temporal shift in abundance was observed between 12 h – 24 h in co-culture compared to monoculture and Mock, which suggests that the bacteria in co-culture experienced a change in secreted protein production in response to their interaction. While virulence was not assessed in the current study, previous studies have demonstrated virulence associated with the same bacteria. Dong et al. (2015) demonstrated that an immersion of co-infection with *E. ictaluri* and *F. columnare* resulted in significantly greater mortality in striped catfish (*Pangasianodon hypophthalmus*) compared to single infection of *E. ictaluri* or *F. columnare*. Interestingly, Wise et al. (2023) demonstrated that mortality patterns in co-infection groups involving immersion with *E. ictaluri* and *F. covae* in channel catfish followed suit with mortality exhibited in single-infection with *E. ictaluri*, while single-infection with *F. covae* resulted in low mortality. Given the strong positive effect of *F. covae* on *E. ictaluri* growth metrics, and vice versa, along with numerous *E. ictalurid* and *F. covae*-associated virulence-related secreted proteins in the co-culture secretome throughout the 24-h experiment, it can be speculated that *F. covae* and *E. ictaluri* may positively influence the growth and extracellular activity of one another. Therefore, in co-culture with *F. covae*, *E. ictaluri* could

have an advantage in early disease establishment. This interpretation of *E. ictaluri* and *F. covae* interaction aligns with the findings of Wise et al. (2023), where mortality was primarily driven by *E. ictaluri*. However, the current study demonstrated an abundance of significant virulence-associated proteins within the co-culture at 24 h, indicating that both bacteria can actively secrete virulence-associated proteins at 24 h. Future proteomic studies involving this bacterial co-culture combination should establish a timepoint threshold for secreted virulence-associated proteins.

Co-culture of *F. covae* and *A. hydrophila* demonstrated antagonistic growth and secretome dynamics. Although no statisticaly significant difference in growth was detected in co-culture, *A. hydrophila* had a negative growth effect on *F. covae*. Conversely, interaction with *F. covae* in co-culture seemed to benefit *A. hydrophila* growth. Differential abundance of the co-culture secretome revealed no significant change compared to *A. hydrophila* secretome at 12 h, and overall, very little change between 12 h – 24 h, while a significant reduction in abundance was observed at 12 h and 24 h when compared to *F. covae*. *A. hydrophila*-associated LasB (effector delivery system) and Hap (enzyme) was significantly abundant in co-culture at 12 h, while most *F. covae*-associated virulence-related secreted proteins were significantly reduced over time. Collectively, these results show that *in vitro*, *A. hydrophila* was antagonistic in co-culture with *F. covae*. This finding is interesting, as a previous *in vivo* co-infection with the same isolates demonstrated higher mortality among co-infected channel catfish compared to single-infection groups, suggesting the two bacteria act synergistically (Wise et al., 2025). Although *A. hydrophila* suppressed *F. covae* growth and secreted virulence proteins *in vitro*, host-associated

factors may have altered this interaction during infection and contributed to enhanced disease severity *in vivo*.

Growth metric analysis of *A. hydrophila* and *E. ictaluri* using the Cerillo Duet co-culture system revealed a competing interaction between the two bacteria. In co-culture, *E. ictaluri* displayed significantly increased growth compared to monoculture, whereas *A. hydrophila* showed reduced growth. This suggests that *A. hydrophila* may have supported *E. ictaluri* growth, while *A. hydrophila* growth was suppressed, indicating competition between the two bacteria in co-culture. However, this pattern was not observed in the secretome analysis, in which *E. ictaluri* failed to achieve sufficient growth as a monoculture. Because the monoculture of *E. ictaluri* was used to inoculate the co-culture, the resulting secretome was driven by the extracellular activity of *A. hydrophila*, which was supported by the absence of *E. ictaluri*-associated secreted proteins.

Although the growth metric and secretome experiments used OD-standardized starting inocula, successful growth of *E. ictaluri* in the Cerillo microplate format did not translate to the scaled-up secretome format. Various factors could have contributed to this discrepancy in *E. ictaluri* growth between experiments. For example, differences in starting culture volume (André, Doulcier, Brenner, and Rainey, 2022), aeration (Mitchell and Goodwin, 2000), and reliance on optical density alone to standardize starting inocula (Mira, Yeh, and Hall, 2022) could have disproportionately affected *E. ictaluri* growth. Additionally, *E. ictaluri*'s established growth rate differs from that of *A. hydrophila*, wherein *E. ictaluri* requires longer incubation compared to *A. hydrophila* (Wise et al., 2023; Wise et al., 2025). Additionally, the monoculture of *E. ictaluri* grew well in MSB during the

secretome experiment but grew poorly using the same media during the Cerillo microplate growth experiment. Future experiments involving *E. ictaluri* for secretome analysis should consider adjusting inoculum ratios, staggering inoculation times so that both bacteria reach comparable growth phases, selecting the optimal growth medium for both bacteria, and ensuring viable cell counts of the starting inoculum.

Proteomics has become a useful application for investigating bacterial co-infection dynamics. While conventional growth metrics provide useful information on bacterial proliferation, analysis of secreted extracellular profiles offers mechanistic insight into potential virulence-related factors. Pridgeon et al. (2013) identified shared toxic extracellular products among strains of virulent *A. hydrophila* by mass spectrometry and confirmed toxicity of those fractions via intraperitoneal injection in channel catfish. Barger et al. (2021) utilized mass-spectrometry to examine virulent *A. hydrophila* secretome remodeling in biofilm versus planktonic growth of the bacterium. The study demonstrated that secretome profiles can change drastically in response to environmental conditions. Results were validated with functional assays including protease, elastase, hemolysis, and *in vivo* fish challenges, to demonstrate the biological consequences of changing protein secretion. The current study observed temporal changes within co-culture and monoculture secretomes and identified changes in the abundance of virulence-associated proteins and their interaction in co-culture. Both studies represent the value of mass spectrometry-based proteomics for identifying mechanistic changes that are otherwise masked from bacterial growth metrics alone. The integration of proteomics with

conventional microbiological assays can provide a comprehensive understanding of bacterial pathogenesis and identify mechanisms responsible for disease progression.

Findings from this study have important implications for disease diagnostics, treatment, and management in the commercial catfish industry. Results from growth metric and secretome analysis reveal that bacterial co-cultures can alter bacterial growth dynamics and virulence-associated protein secretion. When investigating disease outbreaks, the potential presence of co-infection should be considered, as understanding whether pathogens exhibit cooperative or competitive behaviors could influence appropriate treatment strategies. From a management perspective, the ability to identify and characterize secreted virulence-associated proteins, like ones highlighted in the current study, can provide targets for future diagnostic assays and vaccine development.

5.6. Tables

Table 5.6.1. Two-way Analysis of Variance (ANOVA) evaluating the effects of bacterial strain (*Edwardsiella ictaluri* or virulent *Aeromonas hydrophila*), culture condition (monoculture, co-culture, and monoculture + blank), and their interaction (strain × condition) on select growth metrics. K = carrying capacity, μ_{max} = maximum specific growth rate, t_d = doubling time, t_{10K} = time to 10% carrying capacity, and AUC = total growth (area under the curve).

Metric	Effect	*P*-value
K	Bacterial Strain	0.160
	Culture Condition	0.063
	Strain × Condition	0.001
m_{max}	Bacterial Strain	0.208
	Culture Condition	0.011
	Strain × Condition	<0.001
t_d	Bacterial Strain	0.813
	Culture Condition	0.142
	Strain × Condition	0.804
t_{10K}	Bacterial Strain	0.057
	Culture Condition	<0.001
	Strain × Condition	0.019
AUC	Bacterial Strain	0.119
	Culture Condition	0.013
	Strain × Condition	<0.001

Table 5.6.2. Pairwise comparisons of estimated marginal means for growth metrics of each bacterial strain (*Edwardsiella ictaluri* and virulent *Aeromonas hydrophila*) under monoculture, monoculture + blank, and co-culture conditions. Tukey adjustment was made for multiple comparisons. Statistical significance is defined as $P < 0.05$. Ei = *E. ictaluri*, vAh = virulent *A. hydrophila*, Co = co-culture, Mono = monoculture, SEM = standard error of the mean.

Metric	Strain	Comparison	Mean Difference	SEM	*P*-value
K	Ei	Co vs Mono_Ei	0.98	0.25	0.005
m_{max}	Ei	Co vs Mono_Ei	0.69	0.13	<0.001
t_d	Ei	Co vs Mono_Ei	-0.26	0.57	0.890
t_{10K}	Ei	Co vs Mono_Ei	-1.50	1.46	0.575
AUC	Ei	Co vs Mono_Ei	23.21	4.90	0.001
K	vAh	Co vs Mono_vAh	-0.60	0.25	0.075
m_{max}	vAh	Co vs Mono_vAh	-0.56	0.13	0.003
t_d	vAh	Co vs Mono_vAh	0.23	0.57	0.913
t_{10K}	vAh	Co vs Mono_vAh	1.92	1.46	0.415
AUC	vAh	Co vs Mono_vAh	-17.26	4.90	0.011
K	Ei	Mono_Ei vs Ei_blank	0.19	0.25	0.735
m_{max}	Ei	Mono_Ei vs Ei_blank	0.21	0.13	0.278
t_d	Ei	Mono_Ei vs Ei_blank	-0.53	0.57	0.635
t_{10K}	Ei	Mono_Ei vs Ei_blank	-6.92	1.46	0.001
AUC	Ei	Mono_Ei vs Ei_blank	6.25	4.90	0.435
K	vAh	Mono_vAh vs vAh_blank	0.35	0.25	0.360
m_{max}	vAh	Mono_vAh vs vAh_blank	0.30	0.13	0.093
t_d	vAh	Mono_vAh vs vAh_blank	-0.95	0.57	0.254
t_{10K}	vAh	Mono_vAh vs vAh_blank	-3.42	1.46	0.088
AUC	vAh	Mono_vAh vs vAh_blank	11.60	4.90	0.084

Table 5.6.3. Two-way Analysis of Variance (ANOVA) evaluating the effects of bacterial strain (*Flavobacterium covae* or virulent *Aeromonas hydrophila*), culture condition (monoculture, co-culture, and monoculture + blank), and their interaction (strain × condition) on select growth metrics. K = carrying capacity, μ_{max} = maximum specific growth rate, t_d = doubling time, t_{10K} = time to 10% carrying capacity, and AUC = total growth (area under the curve).

Metric	Effect	*P*-value
K	Bacterial Strain	<0.001
	Culture Condition	<0.001
	Strain × Condition	<0.001
μ_{max}	Bacterial Strain	0.001
	Culture Condition	<0.001
	Strain × Condition	0.005
t_d	Bacterial Strain	0.124
	Culture Condition	0.004
	Strain × Condition	0.021
t_{10K}	Bacterial Strain	<0.001
	Culture Condition	<0.001
	Strain × Condition	<0.001
AUC	Bacterial Strain	<0.001
	Culture Condition	<0.001
	Strain × Condition	<0.001

Table 5.6.4. Pairwise comparisons of estimated marginal means for growth metrics of each bacterial strain (*Flavobacterium covae* and virulent *Aeromonas hydrophila*) under monoculture, monoculture + blank, and co-culture conditions. Tukey adjustment was made for multiple comparisons. Statistical significance is defined as $P < 0.05$. Fc = *F. covae*, vAh = virulent *A. hydrophila*, Co = co-culture, Mono = monoculture, SEM = standard error of the mean.

Metric	Strain	Comparison	Mean Difference	SEM	*P*-value
K	vAh	Co vs Mono_vAh	0.22	0.12	0.194
μ_{max}	vAh	Co vs Mono_vAh	0.06	0.10	0.824
t_d	vAh	Co vs Mono_vAh	-0.02	0.38	0.999
t_{10K}	vAh	Co vs Mono_vAh	0.33	1.07	0.948
AUC	vAh	Co vs Mono_vAh	3.71	2.57	0.349
K	Fc	Co vs Mono_Fc	-0.11	0.12	0.615
μ_{max}	Fc	Co vs Mono_Fc	-0.16	0.10	0.266
t_d	Fc	Co vs Mono_Fc	0.09	0.38	0.970
t_{10K}	Fc	Co vs Mono_Fc	0.33	1.07	0.948
AUC	Fc	Co vs Mono_Fc	-2.89	2.57	0.516
K	vAh	Mono_vAh vs vAh_blank	0.83	0.12	<0.001
μ_{max}	vAh	Mono_vAh vs vAh_blank	0.66	0.10	<0.001
t_d	vAh	Mono_vAh vs vAh_blank	-1.76	0.38	0.002
t_{10K}	vAh	Mono_vAh vs vAh_blank	-3.33	1.07	0.023
AUC	vAh	Mono_vAh vs vAh_blank	19.82	2.57	<0.001
K	Fc	Mono_Fc vs Fc_blank	0.08	0.12	0.799
μ_{max}	Fc	Mono_Fc vs Fc_blank	0.31	0.10	0.017
t_d	Fc	Mono_Fc vs Fc_blank	-0.27	0.38	0.759
t_{10K}	Fc	Mono_Fc vs Fc_blank	-11.25	1.07	<0.001
AUC	Fc	Mono_Fc vs Fc_blank	2.31	2.57	0.650

Table 5.6.5. Two-way Analysis of Variance (ANOVA) evaluating the effects of bacterial strain (*Flavobacterium covae* or *Edwardsiella ictaluri*), culture condition (monoculture, co-culture, and monoculture + blank), and their interaction (strain × condition) on select growth metrics. K = carrying capacity, μ_{max} = maximum specific growth rate, t_d = doubling time, t_{10K} = time to 10% carrying capacity, and AUC = total growth (area under the curve).

Metric	Effect	*P*-value
K	Bacterial Strain	<0.001
	Culture Condition	0.013
	Strain × Condition	0.105
μ_{max}	Bacterial Strain	0.616
	Culture Condition	0.116
	Strain × Condition	0.505
t_d	Bacterial Strain	0.921
	Culture Condition	0.109
	Strain × Condition	0.422
t_{10K}	Bacterial Strain	0.564
	Culture Condition	0.430
	Strain × Condition	0.691
AUC	Bacterial Strain	<0.001
	Culture Condition	<0.001
	Strain × Condition	0.119

Table 5.6.6. Pairwise comparisons of estimated marginal means for growth metrics of each bacterial strain (*Flavobacterium covae* and *Edwardsiella ictaluri*) under monoculture, monoculture + blank, and co-culture conditions. Tukey adjustment was made for multiple comparisons. Statistical significance is defined as $P < 0.05$. Fc = *F. covae*, Ei = *E. ictaluri*, Co = co-culture, Mono = monoculture, SEM = standard error of the mean.

Metric	Strain	Comparison	Mean Difference	SEM	*P*-value
K	Ei	Co vs Mono_Ei	0.07	0.08	0.660
m_{max}	Ei	Co vs Mono_Ei	0.11	0.62	0.983
t_d	Ei	Co vs Mono_Ei	-0.03	0.06	0.909
t_{10K}	Ei	Co vs Mono_Ei	0.42	0.97	0.905
AUC	Ei	Co vs Mono_Ei	2.37	1.29	0.199
K	Fc	Co vs Mono_Fc	0.07	0.08	0.654
m_{max}	Fc	Co vs Mono_Fc	0.11	0.62	0.982
t_d	Fc	Co vs Mono_Fc	-0.03	0.06	0.901
t_{10K}	Fc	Co vs Mono_Fc	0.75	0.97	0.728
AUC	Fc	Co vs Mono_Fc	0.41	1.29	0.946
K	Ei	Mono_Ei vs Ei_blank	0.01	0.08	0.981
m_{max}	Ei	Mono_Ei vs Ei_blank	-1.37	0.62	0.110
t_d	Ei	Mono_Ei vs Ei_blank	0.15	0.06	0.078
t_{10K}	Ei	Mono_Ei vs Ei_blank	-1.33	0.97	0.387
AUC	Ei	Mono_Ei vs Ei_blank	1.31	1.29	0.583
K	Fc	Mono_Fc vs Fc_blank	0.24	0.08	0.026
m_{max}	Fc	Mono_Fc vs Fc_blank	-0.46	0.62	0.747
t_d	Fc	Mono_Fc vs Fc_blank	0.05	0.06	0.739
t_{10K}	Fc	Mono_Fc vs Fc_blank	-0.50	0.97	0.866
AUC	Fc	Mono_Fc vs Fc_blank	5.43	1.29	0.003

Table 5.6.7. Limma differential abundance analysis of secreted proteins from *Edwardsiella ictaluri* (Ei), virulent *Aeromonas hydrophila* (vAh), Co-culture of Ei + vAh (Co), and negative control (Mock) at 12 and 24 h post-inoculation. The number and percentage of proteins with significant differential abundance (FDR < 0.05) among pairwise comparison, percent significance, and number of proteins with significantly higher (↑) or lower (↓) abundance in the first group relative to the second group.

Comparison	Significant/Total	Percent Significant	Higher/Lower	Minimum FDR
Co vs Ei 12 h	14/35	40.0%	13 ↑, 1 ↓	<0.001
Co vs Ei 24 h	3/35	8.6%	1 ↑, 2 ↓	0.004
Co vs vAh 12 h	0/35	0.0%	N/A	0.178
Co vs vAh 24 h	0/35	0.0%	N/A	0.086
Co vs Mock 12 h	14/35	40.0%	13 ↑, 1 ↓	<0.001
Co vs Mock 24 h	6/35	17.1%	3 ↑, 3 ↓	0.018
Ei 24 h vs 12 h	0/35	0.0%	N/A	0.937
vAh 24 h vs 12 h	0/35	0.0%	N/A	0.862
Co 24 h vs 12 h	11/35	31.4%	11 ¯	0.009
Mock 24 h vs 12 h	0/35	0.0%	N/A	0.993

Table 5.6.8. Limma differential abundance analysis of secreted proteins from *Flavobacterium covae* (Fc), virulent *Aeromonas hydrophila* (vAh), Co-culture of Fc + vAh (Co), and negative control (Mock) at 12 and 24 h post-inoculation. The number and percentage of proteins with significant differential abundance (FDR < 0.05) among pairwise comparison, percent significance, and number of proteins with significantly higher (↑) or lower (↓) abundance in the first group relative to the second group.

Comparison	Significant Proteins	Percent Significant	Direction	FDR
Co vs Fc 12 h	102/348	29.3%	6 ↑, 96 ↓	<0.001
Co vs Fc 24 h	250/348	71.8%	5 ↑, 245 ↓	<0.001
Co vs vAh 12 h	0/348	0.0%	N/A	0.250
Co vs vAh 24 h	2/348	0.6%	2 -	0.028
Co vs Mock 12 h	24/348	6.9%	2 ↑, 22 ↓	<0.001
Co vs Mock 24 h	14/348	4.0%	5 ↑, 9 ↓	0.002
Fc 24 h vs 12 h	177/348	50.9%	159 ↑, 18 ↓	<0.001
vAh 24 h vs 12 h	0/348	0.0%	N/A	0.199
Co 24 h vs 12 h	8/348	2.3%	2 ↑, 6 ↓	0.013
Mock 24 h vs 12 h	2/348	0.6%	1 ↑, 1 ↓	0.018

Table 5.6.9. Limma differential abundance analysis of secreted proteins from *Flavobacterium covae* (Fc), *Edwardsiella ictaluri* (Ei), Co-culture of Fc + Ei (Co), and negative control (Mock) at 12 and 24 h post-inoculation. The number and percentage of proteins with significant differential abundance (FDR < 0.05) among pairwise comparisons, percent significance, and number of proteins with significantly higher (↑) or lower (↓) abundance in the first group relative to the second group.

Comparison	Significant Proteins	Percent Significant	Direction	FDR
Co vs Fc 12 h	334/592	56.4%	331 ↑, 3 ↓	<0.001
Co vs Fc 24 h	246/592	41.6%	51 ↑, 195 ↓	<0.001
Co vs Ei 12 h	312/592	52.7%	255 ↑, 57 ↓	<0.001
Co vs Ei 24 h	406/592	68.6%	135 ↑, 271 ↓	<0.001
Co vs Mock 12 h	396/592	66.9%	383 ↑, 13 ↓	<0.001
Co vs Mock 24 h	315/592	53.2%	282 ↑, 33 ↓	<0.001
Fc 24 h vs 12 h	351/592	59.3%	337 ↑, 13 ↓	<0.001
Ei 24 h vs 12 h	388/592	65.5%	385 ↑, 2 ↓	<0.001
Co 24 h vs 12 h	214/592	36.1%	54 ↑, 160 ↓	<0.001
Mock 24 h vs 12 h	0	0.0%	N/A	0.073

5.7. Figures

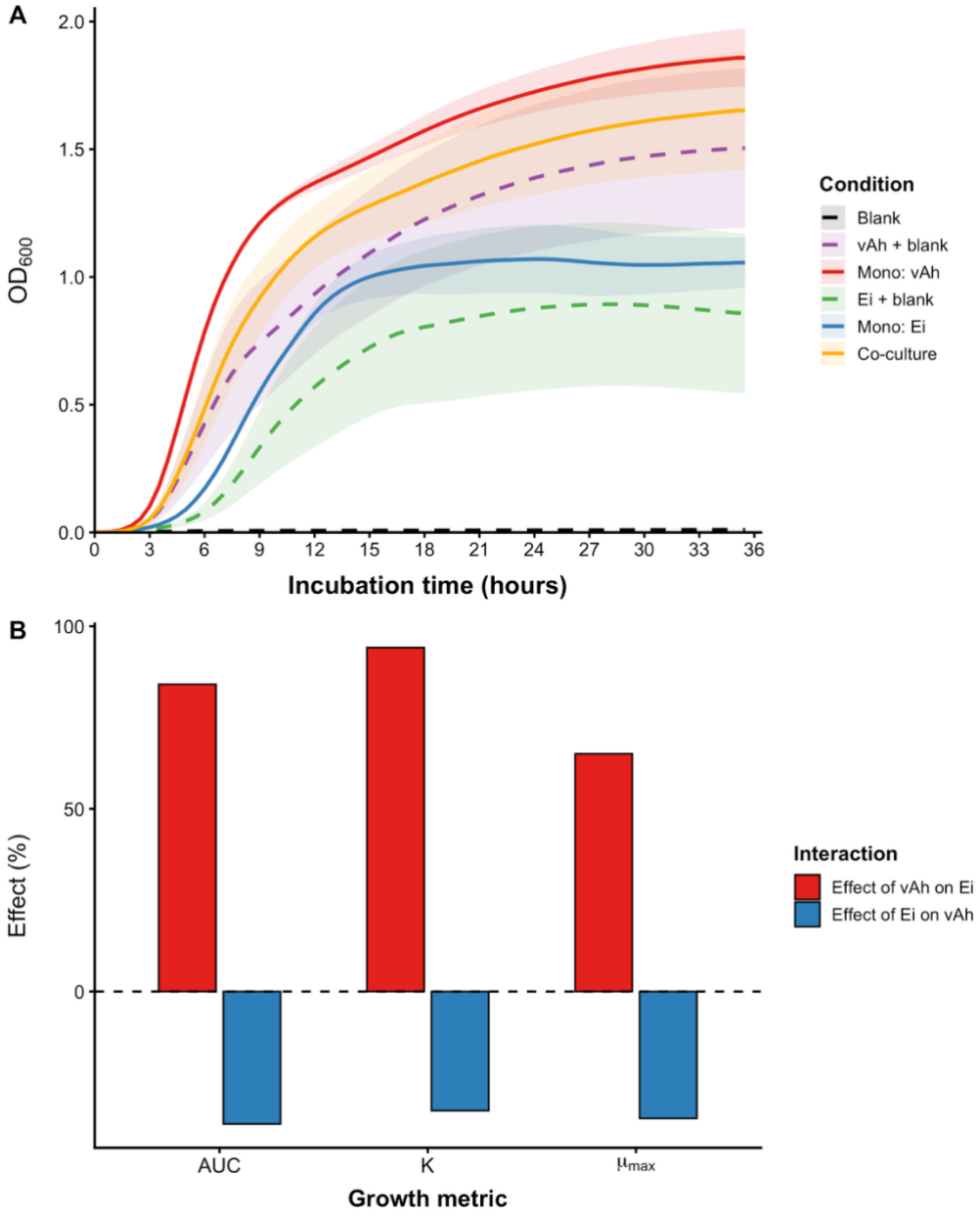

Figure 5.7.1. Growth metrics of virulent *Aeromonas hydrophila* (vAh) and *Edwardsiella ictaluri* (Ei) measured using the Cerillo microplate reader, showing monoculture co-culture responses over a 36-h incubation period. (A) Growth curves over time; (B) relative interaction effects between co-cultured bacteria expressed as % change in growth metrics.

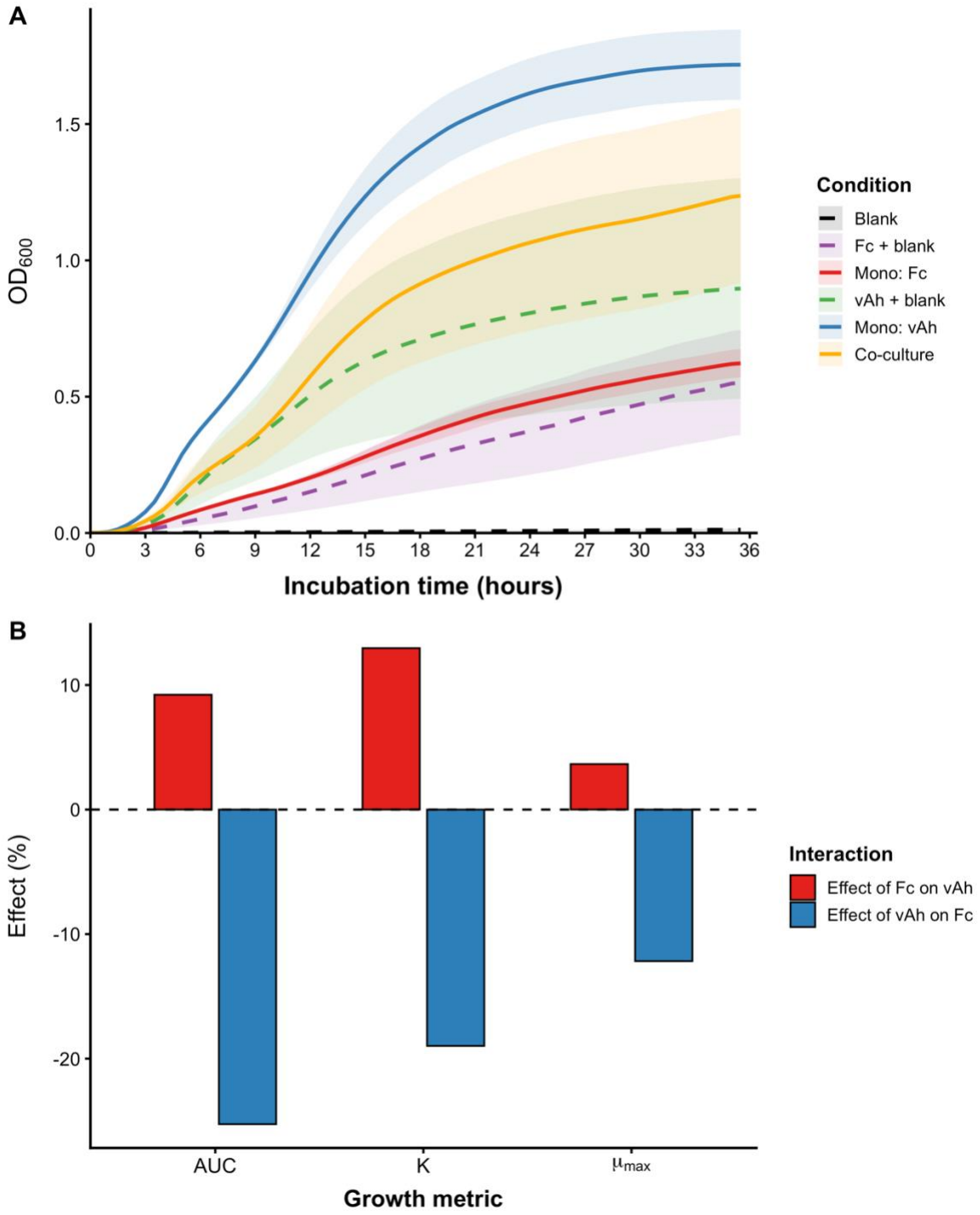

Figure 5.7.2. Growth metrics of *Flavobacterium covae* (Fc) and virulent *Aeromonas hydrophila* (vAh) measured using the Cerillo microplate reader, showing monoculture, monoculture + blank, co-culture, and blank responses over a 36-h incubation period. (A) Growth curves over time; (B) Relative interaction effects between co-cultured bacteria expressed as % change in growth metrics.

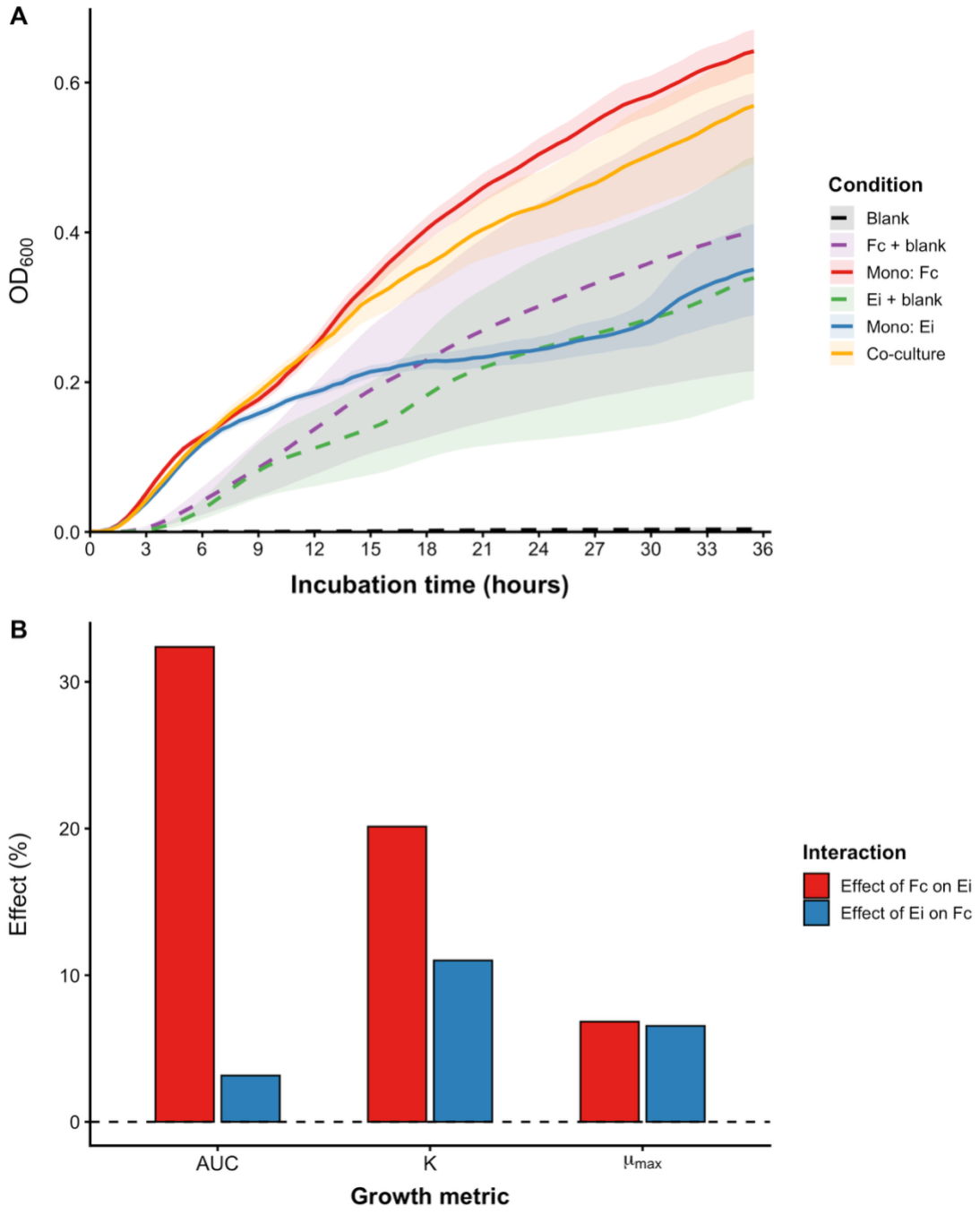

Figure 5.7.3. Growth metrics of virulent *Flavobacterium covae* (Fc) and *Edwardsiella ictaluri (*Ei) measured using the Cerillo microplate reader, showing monoculture and co-culture responses over a 36-h incubation period. (A) Growth curves over time; (B) relative interaction effects between co-cultured bacteria expressed as % change in growth metrics.

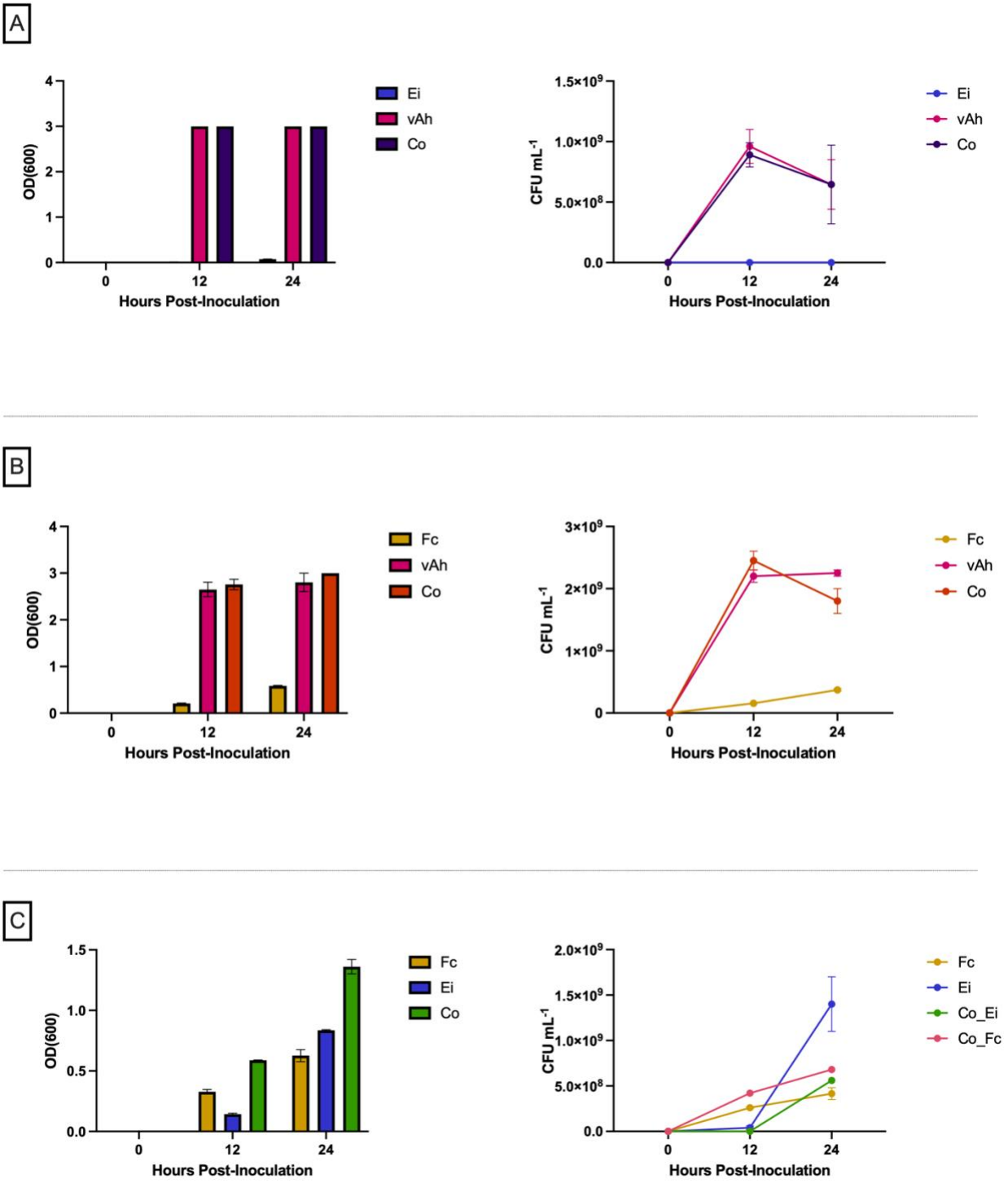

Figure 5.7.4. Optical density read at 600 nm (OD_{600}) and bacterial concentration as colony-forming units per milliliter (CFU mL^{-1}) for A) *Edwardsiella ictaluri* (Ei) and virulent *Aeromonas hydrophila* (vAh), B) *Flavobacterium covae* (Fc) and vAh, and C) Fc and Ei. Optical density and bacterial concentrations were taken twice over a 24 h period.

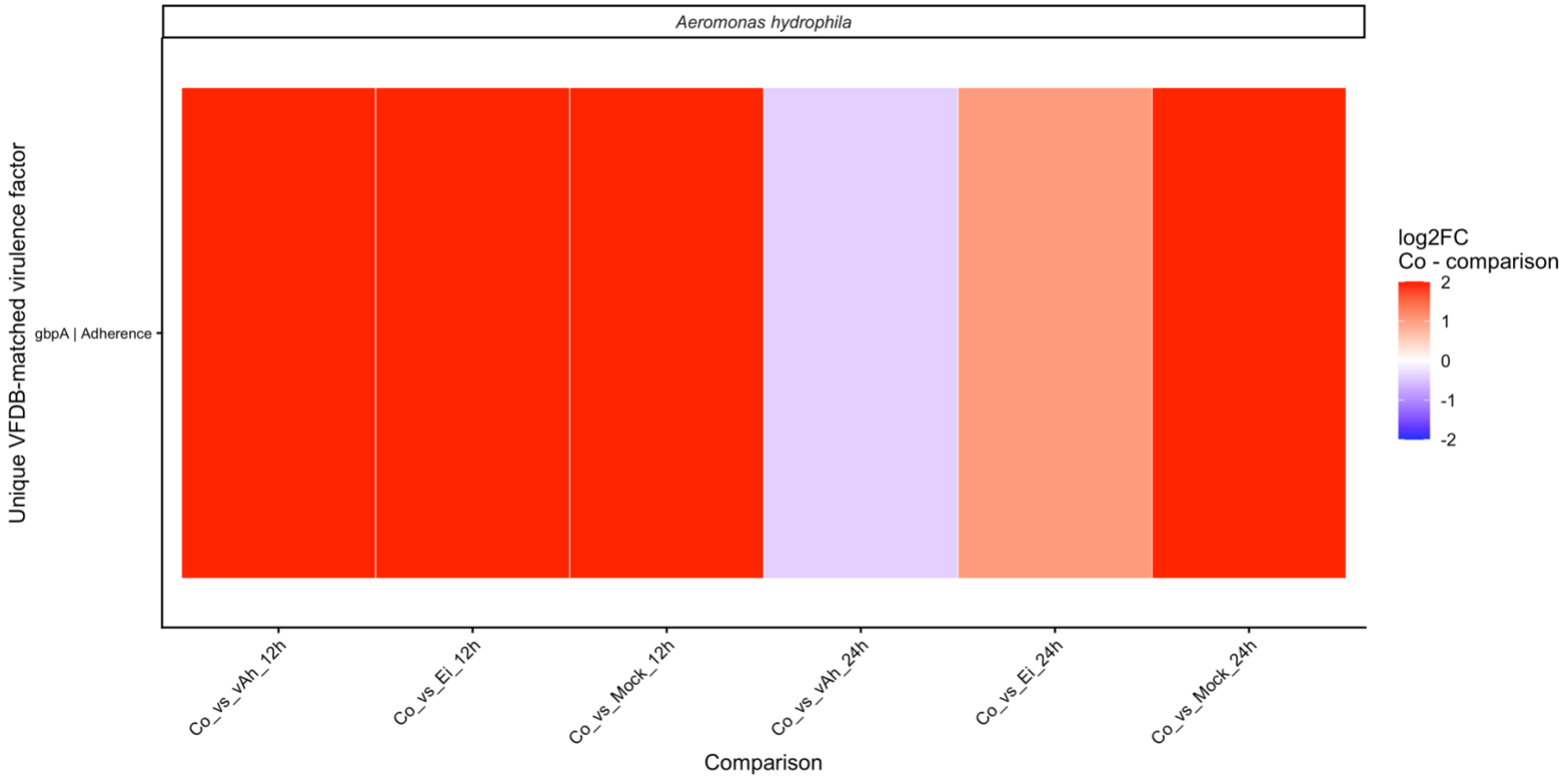

Figure 5.7.5. Differential protein abundance of unique virulence-associated secreted proteins identified by the Virulence Factors Database (VFDB) between virulent *Aeromonas hydrophila* (vAh), *Edwardsiella ictaluri* (Ei), Co-culture of vAh and Ei (Co), and Mock groups at 12 and 24 h post-inoculation. Proteins are displayed by their bacterial origin (*Aeromonas hydrophilia*).

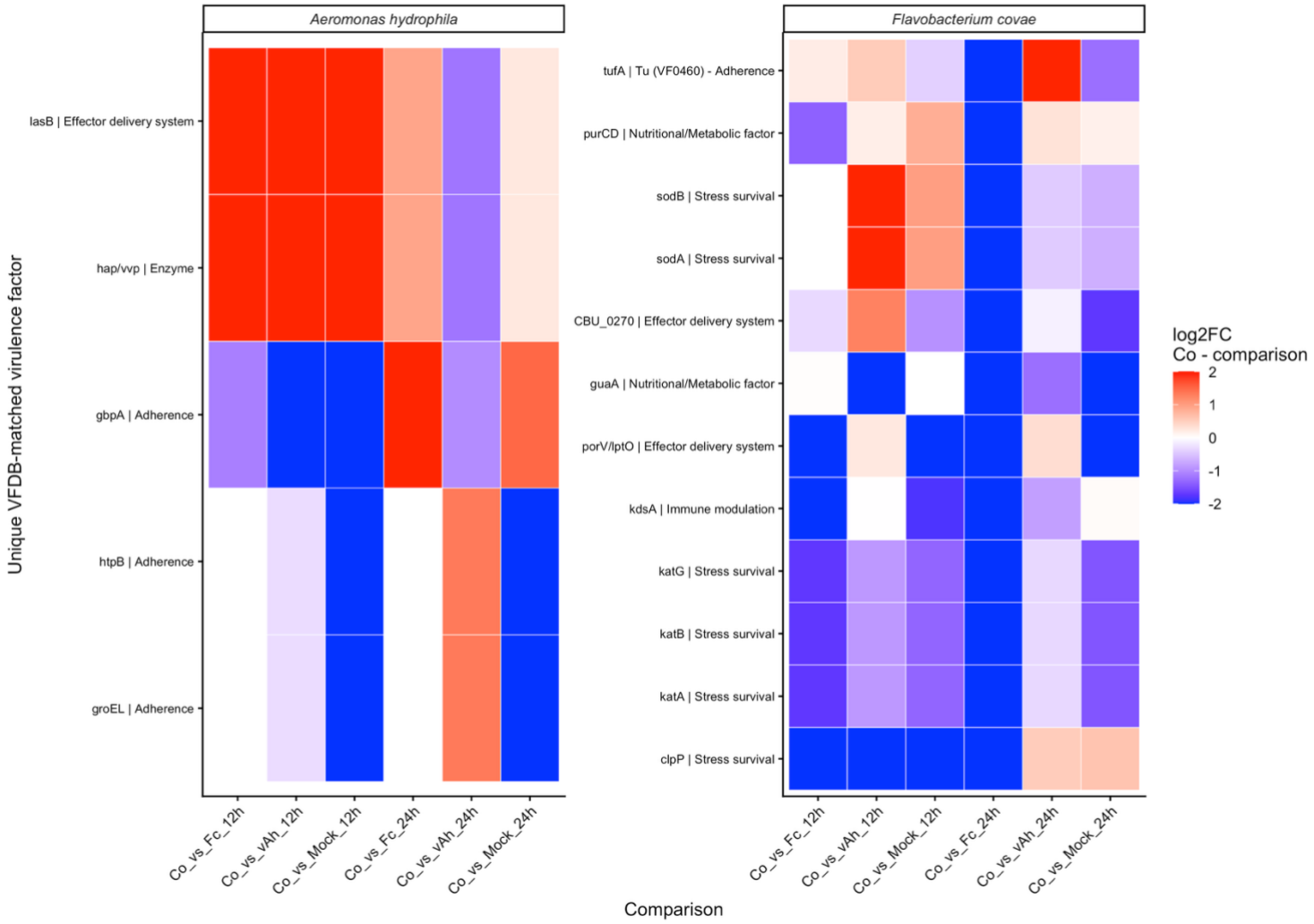

Figure 5.7.6. Differential protein abundance of unique virulence-associated secreted proteins identified by the Virulence Factor Database (VFDB) between virulent *Aeromonas hydrophila* (vAh), *Flavobacterium covae* (Fc), Co-culture of vAh and Fc (Co), and Mock groups at 12 and 24 h post-inoculation. Proteins are separated by their bacterial origin (*Aeromonas hydrophila* or *Flavobacterium covae*).

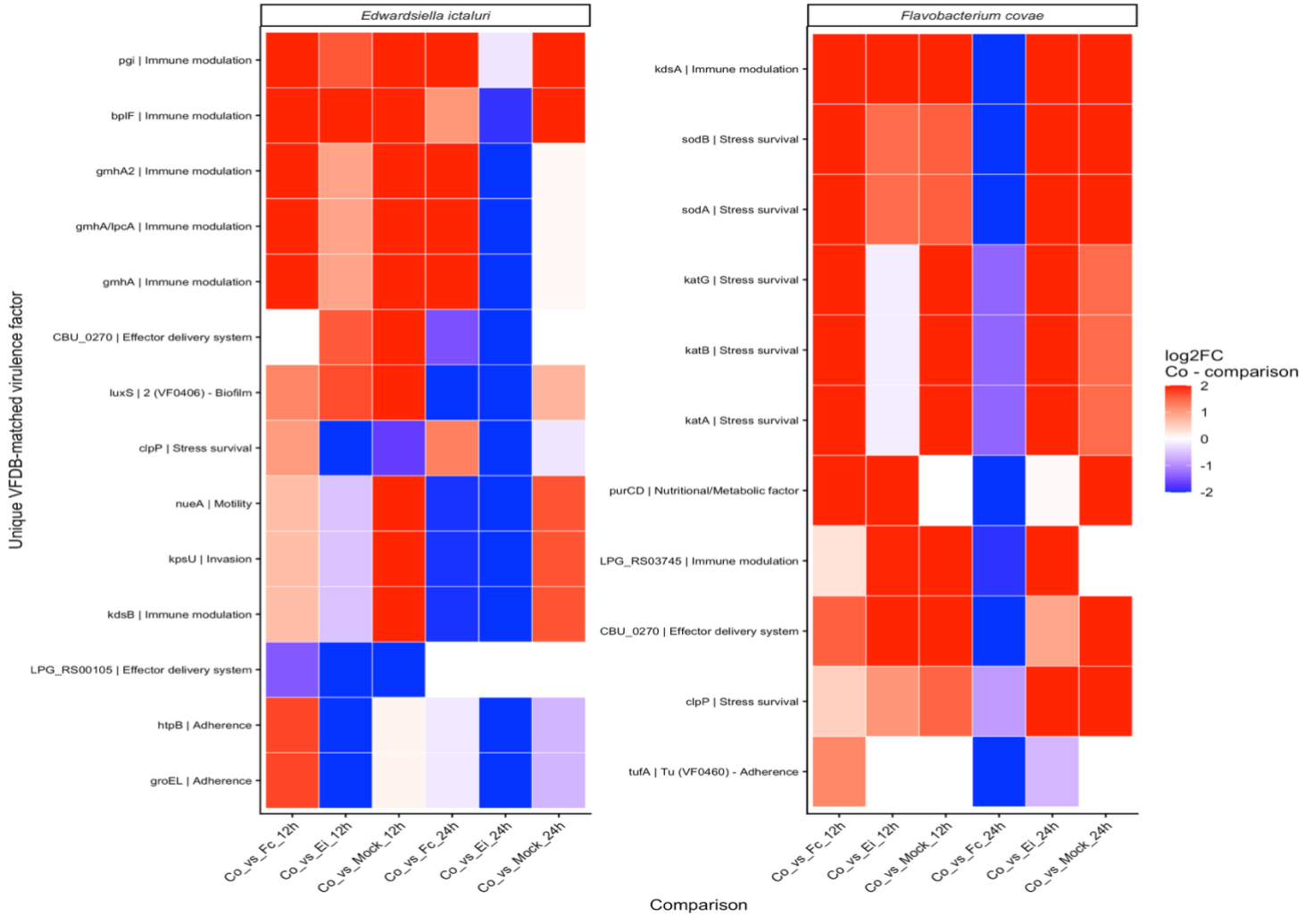

Figure 5.7.7. Differential protein abundance of unique virulence-associated secreted proteins identified by the Virulence Factor Database (VFDB) between *Edwardsiella ictaluri* (Ei), *Flavobacterium covae* (Fc), Co-culture of Ei and Fc (Co), and Mock

groups at 12 and 24 h post-inoculation. Proteins are separated by their bacterial origin (*Edwardsiella ictaluri* or *Flavobacterium covae*).

5.8. References

Abdelrahman, H.A., Hemstreet, W.G., Roy, L.A., Hanson, T.R., Beck, B.H. and Kelly, A.M. 2023. Epidemiology and Economic Impact of Disease-Related Losses on Commercial Catfish Farms: A Seven-Year Case Study from Alabama, USA. *Aquaculture*, 566, p.739206. https://doi.org/10.1016/j.aquaculture.2022.739206

Altschul, S.F., Madden, T.L., Schäffer, A.A., Zhang, J., Zhang, Z., Miller, W. and Lipman, D.J. 1997. Gapped BLAST and PSI-BLAST: A New Generation of Protein Database Search Programs. *Nucleic Acids Research*, 25(17), pp.3389-3402. https://doi.org/10.1093/nar/25.17.3389

Akgul, A., Akgul, A., Lawrence, M.L. and Karsi, A. 2018. Stress-Related Genes Promote *Edwardsiella ictaluri* Pathogenesis. *PLoS One*, 13(3), p.e0194669. https://doi.org/10.1371/journal.pone.0194669

Ardré, M., Doulcier, G., Brenner, N. and Rainey, P.B. 2022. Interaction Among Bacterial Cells Triggers Exit from Lag Phase. *BioRxiv*. https://doi.org/10.1101/2022.01.24.477561

Barger, P.C., Liles, M.R. and Newton, J.C. 2020. Type II Secretion is Essential for Virulence of the Emerging Fish Pathogen, Hypervirulent *Aeromonas hydrophila*. *Frontiers in Veterinary Science*, 7, p.574113. https://doi.org/10.3389/fvets.2020.574113

Barger, P.C., Liles, M.R., Beck, B.H. and Newton, J.C. 2021. Differential Production and Secretion of Potentially Toxigenic Extracellular Proteins from Hypervirulent *Aeromonas hydrophila* Under Biofilm and Planktonic Culture. *BMC Microbiology*, 21(1), p.8. https://doi.org/10.1186/s12866-020-02065-2

Benjamini, Y. and Hochberg, Y. 1995. Controlling the False Discovery Rate: A Practical and Powerful Approach to Multiple Testing. *Journal of the Royal Statistical Society: Series B (Methodological)*, 57(1), pp.289-300. https://doi.org/10.1111/j.2517-6161.1995.tb02031.x

Chen, L., Yang, J., Yu, J., Yao, Z., Sun, L., Shen, Y. and Jin, Q. 2005. VFDB: A Reference Database for Bacterial Virulence Factors. *Nucleic Acids Research*, 33(suppl_1), pp.D325-D328. https://doi.org/10.1093/nar/gki008

Dong, H.T., Nguyen, V.V., Phiwsaiya, K., Gangnonngiw, W., Withyachumnarnkul, B., Rodkhum, C. and Senapin, S. 2015. Concurrent Infections of *Flavobacterium columnare* and *Edwardsiella ictaluri* in Striped Catfish, *Pangasianodon hypophthalmus* in Thailand. *Aquaculture*, 448, pp.142-150. https://doi.org/10.1016/j.aquaculture.2015.05.046

Dubytska, L.P., Rogge, M.L. and Thune, R.L. 2016. Identification and Characterization of Putative Translocated Effector Proteins of the *Edwardsiella ictaluri* Type III Secretion System. *MSphere*, 1(3), pp.10-1128. https://doi.org/10.1128/msphere.00039-16

Dumpala, P.R., Lawrence, M.L. and Karsi, A. 2009. Proteome Analysis of *Edwardsiella ictaluri*. *Proteomics*, 9(5), pp.1353-1363. https://doi.org/10.1002/pmic.200800652

Engle, C. 2003. The Evolution of Farm Management, Production Efficiencies, and Current Challenges to Catfish Production in the United States. *Aquaculture Economics & Management*, 7(1-2), pp.67-84. https://doi.org/10.1080/13657300309380332

Hall, B.G., Acar, H., Nandipati, A. and Barlow, M. 2014. Growth Rates Made Easy. *Molecular Biology and Evolution,* 31(1), pp.232-238. https://doi.org/10.1093/molbev/mst187

Hegde, S., Kumar, G., Engle, C., Hanson, T., Roy, L.A., van Senten, J., Johnson, J., Avery, J., Aarattuthodi, S., Dahl, S. and Dorman, L. 2022. Economic Contribution of the US Catfish Industry. *Aquaculture Economics & Management*, 26(4), pp.384-413. https://doi.org/10.1080/13657305.2021.2008050

Kahm, M., Hasenbrink, G., Lichtenberg-Fraté, H., Ludwig, J. and Kschischo, M. 2010. Grofit: Fitting Biological Growth Curves with R. *Journal of Statistical Software*, 33, pp.1-21. https://doi.org/10.18637/jss.v033.i07

Kalindamar, S., Abdelhamed, H., Kordon, A.O., Tekedar, H.C., Pinchuk, L. and Karsi, A. 2023. Characterization of Type VI Secretion System in *Edwardsiella ictaluri*. *PLoS One*, 18(12), p.e0296132. https://doi.org/10.1371/journal.pone.0296132

Kluge, S., Hoffmann, M., Benndorf, D., Rapp, E. and Reichl, U. 2012. Proteomic Tracking and Analysis of a Bacterial Mixed Culture. *Proteomics*, 12(12), pp.1893-1901. https://doi.org/10.1002/pmic.201100362

LaFrentz, B.R. and Klesius, P.H. 2009. Development of a Culture Independent Method to Characterize the Chemotactic Response of *Flavobacterium columnare* to Fish Mucus. *Journal of Microbiological Methods*, 77(1), pp.37-40. https://doi.org/10.1016/j.mimet.2008.12.011

LaFrentz, B.R., Khoo, L.H., Lawrence, M.L., Petrie-Hanson, L., Hanson, L.A., Baumgartner, W.A., Hemstreet, W.G., Kelly, A.M., García, J.C., Shelley, J.P. and Johnston, A.E. 2024. *Flavobacterium covae* is the Predominant Species of Columnaris-Causing Bacteria Impacting the Channel Catfish Industry in the Southeastern United States. *Journal of Aquatic Animal Health*, 36(1), pp.3-15. https://doi.org/10.1002/aah.10207

Mataigne, A., Vannier, N., Vandenkoornhuyse, P. and Hacquard, S. 2021. Microbial Systems Ecology to Understand Cross-Feeding in Microbiomes. *Frontiers in Microbiology*, 12, p.780469. https://doi.org/10.3389/fmicb.2021.780469

McCarthy, D.J. and Smyth, G.K. 2009. Testing Significance Relative to a Fold-Change Threshold is a TREAT. *Bioinformatics*, 25(6), pp.765-771. https://doi.org/10.1093/bioinformatics/btp053

Mira, P., Yeh, P. and Hall, B.G. 2022. Estimating Microbial Population Data from Optical Density. *PLoS One*, 17(10), p.e0276040. https://doi.org/10.1371/journal.pone.0276040

Mitchell, A.J. and Goodwin, A.E. 2000. The Isolation of *Edwardsiella ictaluri* with a Limited Tolerance for Aerobic Growth from Channel Catfish. *Journal of Aquatic Animal Health*, 12(4), pp.297-300.

Moutinho Jr, T.J., Panagides, J.C., Biggs, M.B., Medlock, G.L., Kolling, G.L. and Papin, J.A. 2017. Novel Co-Culture Plate Enables Growth Dynamic-Based Assessment of Contact-Independent Microbial Interactions. *PLoS One*, 12(8), p.e0182163. https://doi.org/10.1577/1548-8667(2000)012%3C0297:tioeiw%3E2.0.co;2

Oladipupo, A.A., Kelly, A.M., LaFrentz, B.R., Davis, D.A., Roy, L.A., Beck, B.H. and Bruce, T.J. 2026. Effects of Supplemental Dietary Blend of Humic Substances and Butyric Acid Plus Yeast Cell Walls on Immunity and Resistance to Bacterial Coinfection in Juvenile Channel Catfish. *Journal of Aquatic Animal Health*, 38(1), pp.37-56. https://doi.org/10.1093/jahafs/vsag002

Mohammed, H.H. and Peatman, E. 2018. Winter Kill in Intensively Stocked Channel Catfish (*Ictalurus punctatus*): Coinfection with *Aeromonas veronii*, *Streptococcus parauberis* and *Shewanella putrefaciens*. *Journal of Fish Diseases*, 41(9), pp.1339-1347. https://doi.org/10.1111/jfd.12827

Peterman, M.A. and Posadas, B.C. 2019. Direct Economic Impact of Fish Diseases on the East Mississippi Catfish Industry. *North American Journal of Aquaculture*, 81(3), pp.222-229. https://doi.org/10.1002/naaq.10090

Phipson, B., Lee, S., Majewski, I.J., Alexander, W.S. and Smyth, G.K. 2016. Robust Hyperparameter Estimation Protects Against Hypervariable Genes and Improves Power to Detect Differential Expression. *The Annals of Applied Statistics*, 10(2), p.946. https://doi.org/10.1214/16-AOAS920

Pridgeon, J.W., Klesius, P.H., Song, L., Zhang, D., Kojima, K. and Mobley, J.A. 2013. Identification, Virulence, and Mass Spectrometry of Toxic ECP Fractions of West Alabama Isolates of *Aeromonas hydrophila* Obtained from a 2010 Disease Outbreak. *Veterinary Microbiology*, 164(3-4), pp.336-343. https://doi.org/10.1016/j.vetmic.2013.02.020

Ram, Y., Dellus-Gur, E., Bibi, M., Karkare, K., Obolski, U., Feldman, M.W., Cooper, T.F., Berman, J. and Hadany, L. 2019. Predicting Microbial Growth in a Mixed Culture from Growth Curve Data. *Proceedings of the National Academy of Sciences*, 116(29), pp.14698-14707. https://doi.org/10.1073/pnas.1902217116

Rappsilber, J., Mann, M. and Ishihama, Y. 2007. Protocol for Micro-Purification, Enrichment, Pre-Fractionation and Storage of Peptides for Proteomics Using StageTips. *Nature Protocols*, 2(8), pp.1896-1906. https://doi.org/10.1038/nprot.2007.261

Ritchie, M.E., Phipson, B., Wu, D.I., Hu, Y., Law, C.W., Shi, W. and Smyth, G.K. 2015. Limma Powers Differential Expression Analyses for RNA-Sequencing and

Microarray Studies. *Nucleic Acids Research*, 43(7), pp.e47-e47. https://doi.org/10.1093/nar/gkv007

Sayed, M., Narayanan, L., Essa, M., Lawrence, M., Karsi, A. and Abdelhamed, H. 2023. Secreted Extracellular Products of *Flavobacterium covae* as Potential Immunogenic Factors for Protection Against Columnaris Disease in Channel Catfish (*Ictalurus punctatus*). *Pathogens*, 12(6), p.808. https://doi.org/10.3390/pathogens12060808

Schmitz, D.A., Wechsler, T., Mignot, I. and Kümmerli, R. 2024. Predicting Bacterial Interaction Outcomes from Monoculture Growth and Supernatant Assays. *ISME Communications*, 4(1), p.ycae045. https://doi.org/10.1093/ismeco/ycae045

Smyth, G. K. 2004. Linear Models and Empirical Bayes Methods for Assessing Differential Expression in Microarray Experiments. *Statistical Applications in Genetics and Molecular Biology*, Volume 3, Article 3. http://www.statsci.org/smyth/pubs/ebayes.pdf

Sprouffske, K. and Wagner, A. 2016. Growthcurver: An R Package for Obtaining Interpretable Metrics from Microbial Growth Curves. BMC Bioinformatics, 17(1), p.172. https://doi.org/10.1186/s12859-016-1016-7

Thunes, N.C., Conrad, R.A., Mohammed, H.H., Zhu, Y., Barbier, P., Evenhuis, J.P., Perez-Pascual, D., Ghigo, J.M., Lipscomb, R.S., Schneider, J.R. and Li, N. 2022. Type IX Secretion System Effectors and Virulence of the Model *Flavobacterium columnare* Strain MS-FC-4. *Applied and Environmental Microbiology*, 88(3), pp.e01705-21. https://doi.org/10.1128/aem.01705-21

UniProt Consortium. 2015. UniProt: A Hub for Protein Information. *Nucleic Acids Research*, 43(D1), pp.D204-D212. https://doi.org/10.1093/nar/gku989

Wagner, B.A., Wise, D.J., Khoo, L.H. and Terhune, J.S. 2002. The Epidemiology of Bacterial Diseases in Food-Size Channel Catfish. *Journal of Aquatic Animal Health*, 14(4), pp.263-272. https://doi.org/10.1577/1548-8667(2002)014%3C0263:teobdi%3E2.0.co;2

Wang, Y., Wang, X., Ali, F., Li, Z., Fu, Y., Yang, X., Lin, W. and Lin, X. 2019. Comparative Extracellular Proteomics of *Aeromonas hydrophila* Reveals Iron-Regulated Secreted

Proteins as Potential Vaccine Candidates. *Frontiers in Immunology*, 10, p.256. https://doi.org/10.3389/fimmu.2019.00256

Warsi, O.M., Gedda, L., Edwards, K. and Andersson, D.I. 2023. Vesicle-Enriched Secretomes Alter Bacterial Competitive Abilities and are Drivers of Evolution in Microbial Communities. *FEMS Microbiology Ecology*, 99(12), p.fiad141. https://doi.org/10.1093/femsec/fiad141

Wise, A.L., LaFrentz, B.R., Kelly, A.M., Liles, M.R., Griffin, M.J., Beck, B.H. and Bruce, T.J. 2025. Coinfection of Channel Catfish (*Ictalurus punctatus*) with Virulent *Aeromonas hydrophila* and *Flavobacterium covae* Exacerbates Mortality. *Journal of Fish Diseases*, 48(8), p.e13912. https://doi.org/10.1111/jfd.13912

Wise, A.L., LaFrentz, B.R., Kelly, A.M., Liles, M.R., Griffin, M.J., Beck, B.H. and Bruce, T.J. 2023. The Infection Dynamics of Experimental *Edwardsiella ictaluri* and *Flavobacterium covae* Coinfection in Channel Catfish (*Ictalurus punctatus*). *Pathogens*, 12(3), p.462. https://doi.org/10.3390/pathogens12030462

Wise, A.L., LaFrentz, B.R., Kelly, A.M., Khoo, L.H., Xu, T., Liles, M.R. and Bruce, T.J. 2021. A Review of Bacterial Co-Infections in Farmed Catfish: Components, Diagnostics, and Treatment Directions. *Animals*, 11(11), p.3240. https://doi.org/10.3390/ani11113240

Zhang, D., Xu, D.H. and Shoemaker, C. 2016. Experimental Induction of Motile *Aeromonas* Septicemia in Channel Catfish (*Ictalurus punctatus*) by Waterborne Challenge with Virulent *Aeromonas hydrophila*. *Aquaculture Reports*, 3, pp.18-23. https://doi.org/10.1016/j.aqrep.2015.11.003

Zwietering, M.H., Jongenburger, I., Rombouts, F.M. and Van't Riet, K.J.A.E.M. 1990. Modeling of the Bacterial Growth Curve. *Applied and Environmental Microbiology*, 56(6), pp.1875-1881. https://doi.org/10.1128/aem.56.6.1875-1881.1990

Chapter VI

Conclusions and Future Research

6.1. Conclusions

6.1.1. Overall Conclusions

Disease management is a critical component to sustainable catfish production. Bacterial pathogens are the primary cause of disease outbreaks and mortality, and catfish producers rely heavily on effective strategies such as good management practices and vaccines for the management and prevention of bacterial diseases. Outcomes from individual studies in this dissertation provide insights for the development of effective vaccination against columnaris disease, demonstrated useful tools for bacterial identification and improving bacterial diagnostics, and gained a deeper understanding of bacterial co-culture dynamics affecting the catfish industry.

Chapter II described the development of multiple rifampicin-resistant strains of CCB to be tested as live-attenuated vaccine candidates. Mutants were derived from three CCB species; though the rate at which resistance was achieved was variable and strain-specific. Confirmation of attenuation was demonstrated in all species, but the level of attenuation varied. Comparisons of cumulative percent mortality provided evidence of attenuation for most strains, although some parent strains exhibited low mortality (*F. davisii* TN-3-2012 and ARS-15-12) and comparisons could not be assessed at the time.

When whole genomes sequences between parent and mutant were compared, predicted deleterious mutations were identified within the rifampicin resistance-determining region of *rpoB*, indicating the selected method of attenuation (rifampicin) successfully altered the bacterial genome (the beta subunit of RNA polymerase) of multiple CCB strains. These findings suggests that rifampicin can be used as a mechanism to attenuate multiple virulent strains of CCB that span multiple species. However, one strain was predicted to have a neutral effect on *rpoB* function (*F. davisii* TN-3-2012 mutant), although the strain displayed reduced virulence in channel catfish. This discovery suggests that though rifampicin caused a mutation in the *rpoB* gene, it may not have affected the function. Additional mutations were discovered throughout mutant genomes that could also explain reduced virulence, which leans towards an explanation of additional mutations generated by serial passage may have a cumulative effect on the mutants; thus, having reduced virulence in channel catfish.

Chapter III assessed the efficacy of five *F. covae* rifampicin-resistant strains as live-attenuated vaccines in channel catfish. Findings from this study revealed that vaccination efficacy was strain-specific and trial-dependent. The mutant strain FBCC-CC-12K offered low to moderate protection in channel catfish; although the level of protection was not consistent, protection was afforded in every trial. The mutant strain ALG-15-231 offered the highest level of protection among all strains, but protection was not reproducible. Serum IgM antibody titers suggested that protection was not conferred by humoral immunity. SDS-PAGE comparisons of the parent and mutant protein profiles revealed that mutation did not dramatically alter mutant proteins profiles, and western blot revealed

that serum antibodies from vaccination trials recognized the same antigenic regions. These discoveries reinforce the notion that vaccination with the live-attenuated mutants did not stimulate a specific antibody response against antigens of the parent and mutant bacterial strains.

Chapter IV emphasized the importance of molecular identification of bacterial isolates for routine diagnostics. Yellow-pigmented bacterial isolates resembling *Flavobacterium* spp. were sequenced using the *gyrB* primers, and a subset were preliminarily identified as *Chryseobacterium*. Following whole genome sequencing of the same isolates, it was determined that they encompassed several different genera, including *Chryseobacterium* spp., *Flavobacterium*, and *Empedobacter*. The newly-identified isolates were then used in an experimental study to determine their virulence in channel catfish by i.p. injection and immersion. None of the isolates caused mortality by immersion. However, by i.p. injection, three *Chryseobacterium* spp. (*C. mucoviscidosis*, *C. gleum*, and *C. cucumeris*) elicited low mortality and *Empedobacter brevis* resulted in high mortality. The mortality observed in the virulence study was reproduced in a replicated study with *E. brevis*, and the median lethal dose by i.p. injection was determined to be 1.3×10^7 CFU/fish. This study also highlighted exacerbated mortality disease signs of bacterial co-infection with *Flavobacterium covae* and *E. brevis*. Channel catfish that were exposed to the bacteria as a co-infection showed significantly higher mortality than fish exposed to a single dose of *F. covae*. This experiment also demonstrated the opportunistic nature of *E. brevis* by causing substantial mortality with i.p. injection and no mortality with

immersion. This finding established that *E. brevis* must enter the host and break the protective barrier of the skin to cause disease.

Chapter V assessed the growth and proteomic responses of three major bacterial pathogens affecting channel catfish, *in vitro*. Co-culture of *Edwardsiella ictaluri* and virulent *Aeromonas hydrophila* exhibited competitive growth, with *E. ictaluri* performing better in co-culture than *A. hydrophila*. It was also determined that *E. ictaluri* suppressed the growth of *A. hydrophila* in co-culture. Although not to the same magnitude, co-culture of *Flavobacterium covae* and *A. hydrophila* also exhibited competitive growth, wherein *A. hydrophila* grew slightly better than *F. covae* in co-culture. Cooperative behavior was displayed by *F. covae* and *E. ictaluri* in co-culture, and this behavior was reflected in the secretome. Virulence-associated proteins were differentially abundant in co-culture of *F. covae* and *E. ictaluri*, with many *F. covae* and *E. ictaluri* proteins actively changing their abundance over time. These findings suggest that virulence associated with co-infection with *F. covae* and *E. ictaluri* could be exacerbated at early timepoints during disease progression. Virulence-associated proteins in co-culture of *F. covae* and *A. hydrophila* showed significant difference in abundance, where *A. hydrophila* proteins were more abundant, and most *F. covae* proteins were suppressed. These results suggest that virulence may be regulated by *A. hydrophila* during co-infection with *F. covae*.

Collectively, the studies comprising this dissertation provide important considerations to bacterial disease management of channel catfish production. While columnaris disease is an ongoing threat to production sustainability, especially disease outbreaks caused *Flavobacterium covae*, outcomes of the first two chapters provide two

promising candidates for further investigation and optimization of a live-attenuated vaccine. Molecular tools for bacterial identification, such as whole genome sequencing, can be utilized during diagnostic investigations to distinguish typical from a-typical, yellow-pigmented bacteria. Considerations of the presence of bacterial co-infections and species-specific behaviors can help producers mitigate disease outbreaks and determine the appropriate treatment. Ultimately, these discoveries can aid in the advancement of mitigating bacterial diseases affecting channel catfish.

6.1.2. Limitations and Future Directions

Although results of this dissertation have provided beneficial information to improve aspects of bacterial disease management in the channel catfish industry, some limitations should be considered. In chapter II, the effect on protein function was predicted for variants by computational means. Although results gave insight into the mechanisms of attenuation, future studies should incorporate molecular techniques to definitively conclude loss of protein function. Targeted mutagenesis of the *rpoB* gene that mimics variants detected in the virulent strains used in this study could determine if those same mutations are responsible for reduced virulence. This approach could also be used for any of the predicted deleterious mutations found within this study. Likewise, gene knockout experiments could also help distinguish whether mutations identified in this study are responsible for the observed phenotypes or repressed secondary mutations accumulated during rifampicin attenuation. Future studies should also evaluate the stability of the attenuated strains identified in this study.

In chapter III, attenuated strains of *F. covae* were evaluated for efficacy as live-attenuated vaccines in channel catfish. Immune response was measured by serum IgM titers, wherein they did not correlate with protection offered by select mutant strains. A limitation of this study was not investigating mucosal immune responses in vaccinated and sham-vaccinated channel catfish. Because live-attenuated vaccines can stimulate humoral and cellular immune responses and given that the vaccines in this study were administered via immersion, it's possible that protective immunity is mediated by mucosal immune responses. Gene expression of IgM, IgD, relevant cytokines, complement, antimicrobial peptides, mucins, and inflammatory markers within the mucus, skin, and gills could help pinpoint immune pathways generated by the mutant strains in this study. Another limitation of this study was not demonstrating colonization of the mutant strains post-vaccination. It would be worthwhile to know if mutant strains generated from this dissertation can colonize the skin and gills of vaccinated fish. Future work should with vaccine candidates should consider tissue sampling immediately following vaccination and throughout the vaccination period to determine bacterial persistence (colonization) and localization. Histopathology paired with *rpoB* sequencing and quantitative PCR of bacterial loads from tissue samples could detail whether or not vaccine strains invade host tissue; this is something the current study did not address.

In chapter V, the biggest limitation was the poor growth of *Edwardsiella icaluri* during the secretome experiment. Had *E. ictaluri* growth been optimized and reproduced prior to the experiment initiation, we would have been able to determine secreted protein responses in co-culture with virulent *Aeromonas hydrophila*. Likewise, we would have

been able to make comparisons of co-culture growth with differential protein abundance of the co-culture secretome. Future studies could expand the bacterial growth and *in vitro* secretome findings by incorporating proteomic approaches to tissues collected during concurrent experimental *in vivo* infection of the same bacterial species in mono- and co-culture. Tissue samples could be collected over time and analyzed by mass spectrometry to determine whether virulence-associated proteins identified in co-culture are also detectable during infection. This would provide valuable information on whether secretome changes observed *in vitro* correlate to bacterial activity and disease progression *in vivo*.